FATIGUE PERFORMANCE OF SEALS

by

Romei Christeline Cloete

*Thesis presented in fulfilment of the requirements
for the degree of Master of Science in the Faculty of Engineering
at Stellenbosch University*

Supervisor:
Professor Kim J. Jenkins
SANRAL Chair in Pavement Engineering
Faculty of Engineering
Department of Civil Engineering

December 2015

DECLARATION

By submitting this thesis electronically, I declare that the entirety of the work contained therein is my own, original work, that I am the sole author thereof (save to the extent explicitly otherwise stated), that reproduction and publication thereof by Stellenbosch University will not infringe any third party rights and that I have not previously in its entirety or in part submitted it for obtaining any qualification.

Signature: …………………………

Date: 25 November 2015

i

ABSTRACT

Thin bituminous surfacings, in particular sprayed seals, are used quite extensively in various countries because they provide a low cost alternative to conventional asphalt. Seals furthermore provide an acceptable wearing course which guards the underlying pavement layers from the harsh effects of traffic and the environment by preventing ingress of moisture. Seals also provide a safe road environment by offering adequate skid resistance and noise reduction during its lifetime.

Evaluating the fatigue performance of thin surfacings is a challenging and complex task. Back calculation of the modulus of a thin surfacing layer has always been difficult because the deflections measured at various distances of the load centre and in the load centre contained little to no information on the deformation of the thin top layer itself.

The main objective of this research study is to characterize the fatigue performance of various types of seals sampled from existing road pavements across South Africa, taking into account different variables such as ages, climatic zones and traffic history. The characterisation of the fatigue of these sampled seals was carried out by developing a bi-layer system consisting of the sampled seal and a fast-cast polyurethane composite beam and subjecting to flexural bending in the four point bending beam apparatus, following the guideline for fatigue testing of Hot Mix Asphalt (HMA).

The test parameters and results are analysed in terms of fatigue and master curves obtained. It is understood that the apparatus affords an insight on the mechanism of fatigue failure of beam specimens by carrying out bending tests with alternating strain and stress amplitudes. The test approach yielded fatigue results for the composite system, which required a direct beam theory solution set-up in MATLAB, to extract the fatigue results of only the seals.

It was found that the conventional fatigue test criterion of fifty (50) percent reduction in initial flexural stiffness was only applicable for Single Seals, after various fatigue criteria were investigated. For Cape Seals the fatigue criteria was defined as fourty (40) percent reduction in initial flexural stiffness, whereas for Double Seals this failure criteria was significantly lower at twenty (20) percent reduction in initial flexural stiffness.

It was furthermore found that Single and Cape Seals imitated the behaviour of a uniform mix, similar to HMA and hence failed at a higher fatigue criterion. Double Seals however had a less uniform mix behaviour which subscribed to a reduced or lower fatigue criterion.

The influence of the variables on the outcome of fatigue was investigated by considering the effect of the single variables, combination of variables and the interaction between variables. For Single Seals it was found that the thickness of the seal, the applied loading strain and the age provided most significance on the outcome of fatigue. Similarly, for Cape Seals, the thickness and age provided most significance, but with the added significance of climate. For Double Seals the environment of the seals provided most significance on the outcome of fatigue.

OPSOMMING

Dun bitumineuse oppervlaktes, in besonder oppervlak seëls, word omvattend baie gebruik in verskeie lande, omdat hulle 'n lae koste alternatief bied teenoor konvensionele asfalt oppervlaktes, oppervlak seëls voorsien 'n aanvaarbare dra laag wat die onderliggende plaveisel lae beskerm teen die negatiewe gevolge van die verkeer en die omgewing deur die instroming van vog te voorkom. Seëls bied ook 'n veilige pad omgewing deur voldoende slip weerstand te voorsien en geraas te verminder.

Die evaluering van die vermoëings geaardheid van dun oppervlaktes is 'n uitdagende en komplekse taak. Terug berekening van die oppervlak laag was nog altyd moeilik, want die gemeete defleksies op verskillende afstande vanaf die las middle punt en in die las middle punt vervat min tot byna geen inligting oor die vervorming van die boonste laag nie.

Die hoof doel van hierdie navorsing studie is om die vermoëings geaardheid van verskillende tipes oppervlak seëls monsters wat uit bestaande paaie regoor Suid Afrika geneem was te kenmerk, met die inagneming van verskillende veranderlikes, soos ouderdom, klimaatsones en verkeer geskiedenis. Die kenmerk van die vermoëings geaardheid van hierdie seël monsters is uitgevoer deur die ontwikkeling van 'n twee-laag stelsel wat bestaan uit die gemonsterde seël en 'n vining-giet poliuretaan saamgestelde balk wat onderwerp was aan buig in die vier punt buig balk apparat, na aanleiding van die riglyn vir die vermoëings toets vir Warm Gemengde Asfalt.

Die toets parameters en resultate was ontleed in terme van vermoëings en meester kurwes. Dit word verstaan dat dié apparaat 'n insig bied oor die meganisme van mislukte vermoëings geaardhede van balk toets monsters deur hulle te onderhewing aan buig toetse met afwisselende vervorming en spanning amplitudes. Dié toets benadering het wel vermoëings resultate gelewer vir die saamgestelde stelsel en die toepassing van direkte balk teorië was nodig om slegs die resultate van die seëls te bekom.

Daar was gevind dat die konvensionele vermoëings toets maatstaf van vyftig (50) present vermindering in die aanvanklike buig styfheid was net van toepassing vir Enkel Seëls, nadat verskeie vermoëings kriteria ondersoek was. Vir Kaapse Seëls was die vermoëings kriteria gedefinieër as veertig (40) present vermindering in die aanvanklike buig styfheid, terwyl vir Dubbel Seëls was hierdie kriteria aansienlik laër op twinting (20) present vermindering in die aanvanklike buig styfheid.

Dit was verder bevind dat Enkel en Kaapse Seëls 'n meer eenvormige mengsel gedrag naboots, soortgelyk aan Warm Gemengde Asfalt en dus op 'n hoër vermoëings maatstaf misluk. Dubbel Seëls het egter 'n minder uniform mengsel gedrag wat by 'n laer vermoëings maatstaf misluk.

Die invloed van die veranderlikes op die uitslag van vermoëing was ondersoek deur die oorweging van die uitwerking van enkele veranderlikes, kombinasie van veranderlikes en die interaksie tussen veranderlikes. Vir Enkel Seëls was bevind dat die dikte van die seëls, die toegepaste vervorming las en die ouderdom die meeste betekenisvolle uitkoms van vermoëing gelewer het. Net so, vir Kaapse Seëls, het die dikte en ouderdom die meeste betekenisvolle uitkoms van vermoëing verskaf, maar met di bykomende belang van klimaat. Vir Dubbel Seëls het die omgewing van die seëls die meeste belang gedra, in terme van die uitkoms van vermoëing.

ACKNOWLEDGEMENTS

Lao Tzu once said that the journey of a thousand miles begins with the first step. I am grateful for the opportunity that I was given to take that first step towards completing my master's degree and for every person that supported me during the journey. My sincere appreciation and gratitude go to:

- My Heavenly Father for His relentless love, favour and protection.
- My beloved family for their love, sacrifices and guidance that have given me wings to fly.
- My supervisor, Professor Kim Jenkins for his guidance and support.
- Dr. Breda Strassheim for his assistance with the MATLAB solution.
- Professors Martin van de Ven and André Molenaar, for their input and guidance.
- Mrs Chantal Rudman, Messrs Gerrie Van Zyl and Steph Bredenham for their advice and good insight.
- Mrs Janine Myburgh, Messrs Collin and Gavin for their assistance.
- My fellow research colleagues; Miss Annie and Messrs LeRiche, Achille, Pius, Nathan, Danny, Alex, Johan, Fabrice and Eben for their camaraderie, assistance and insight.
- Namibia Power Corporation (Nampower) Pty (Ltd), the South African Roads Agency (SANRAL) and my current employer, Burmeister & Partners Pty (Ltd) for their financial assistance.
- My friends of whom I cannot mention all the names.

Table of Contents

List of Figures

List of Tables

List of Abbreviations

4PB	Four Point Bending
SAPDM	South African Pavement Design Method
MATLAB	Matrix Laboratory Software
WMA	Warm Mix Asphalt
ANOVA	Analysis of Variance
AADT	Average Annual Daily Traffic
ARRB	Australian Road Research Board
TRH	Technical Recommendations for Highways
TRB	Transport Research Board
SAPEM	South African Pavement Engineering Manual
NCHRP	National Cooperative Highway Research Programme
ALD	Average Least Dimension
SABITA	South African Bitumen Association
ACV	Aggregate Crushing Value
10% FACT	Ten Percent Fines Aggregate Crushing Test
SANS	South African National Standards
CSRA	Committee of State Road Authorities
PSV	Polished Stone Value
SMA	Stone Mastic Asphalt
ASTM	American Society for Testing and Materials
PAH	Polycyclic Aromatic Hydrocarbons
SARA	Saturates, Aromatics, Resins and Asphaltenes
SOL	Solution
GEL	Gelatinous
RC	Rapid-Curing
MC	Medium-Curing
TG	Technical Guideline
SAM	Stress Absorbing Membrane
RPF	Road Pavements Forum

SBS	Styrene Butadiene Styrene
SBR	Styrene Butadiene Rubber
RTFOT	Rotating Thin Film Oven Test
RCAT	Rotating Cylinder Ageing Test
EN	European Standards
SHRP	Strategic Highway Research Programme
PAV	Pressure Ageing Vessel
HiPAT	High Pressure Ageing Test
PMB	Polymer Modified Bitumen
BRRC	Belgian Road Research Centre
NRB	National Research Bureau
TMH	Technical Methods for Highways
ELV	Equivalent Light Vehicles
HVS	Heavy Vehicle Simulator
COLTO	Committee of Land Transport Officials
HCV	Heavy Commercial Vehicle
ESA	Equivalent Standard Axle (80kN)
Im	Moisture Index
CAM	Crack-Activity Meter
CMS	Crack-Movement Simulator
2PB	Two Point Bending
SCB	Semi-Circular Bending
NAT	Circular Bending
ITT	Indirect Tensile Test
DR	District Road
MR	Main Road
TR	Trunk Road
N	National Road
R	Regional Route
RNIS	Road Network Information System
GPS	Global Positioning System
CSIR	Council of Scientific and Industrial Research

IWT	Inner Wheel Track
SHDR	Shoulder
OWT	Outer Wheel Track
BWT	Between Wheel Tracks
MMLS	Multi Modal Loading Simulation
CDAS	Control and Data Acquisition System
LVDT	Linear Variable Differential Transformer
BFA	Beam Fatigue Apparatus
FTS	Fatigue Testing System
WLF	Williams-Landel-Ferry Model
MANOVA	Multivariate Analysis of Variance
SPSS	Statistical Package for the Social Sciences
SST	Total Sum of Squares
SSR	Regression Sum of Squares
SSE	Error Sum of Squares
dF	Degree of Freedom

1. Introduction

1.1. Overview

Fatigue is one of the main failure modes of the bound layers in pavement structures, which results in degradation of the pavement materials and eventually the entire pavement structure. Bituminous materials in roads, experience short term loading each time a vehicle passes. With sufficiently high loading, loss of rigidity of the material occur and with long term accumulation, failure results.

Seals play a vital part in the pavement structure as they serve as wearing courses that protect the base from direct tyre contact and from moisture entering and migrating through to the rest of the pavement structure. To understand failure in the pavement structure it is therefore important to understand failure in its protecting surface, the seal.

Fatigue of seals is the stage at which the seal failed to perform any one of its functions due to a reduction in its service life occurs. At this point maintenance intervention is required. What causes the seal to successfully carry out its purpose is a combination of a well thought out seal design, use of quality construction material favourable climatic conditions, proper construction and supervision of the site. Each one of these factors however are governed by their own set of dynamics that in themselves are susceptible to influence, both internal and external, which in turn can have varying effects on how the seal performs and when failure is reached.

1.2. Problem Statement

The challenge with evaluating seal fatigue from specimens sampled from an existing road is that the specimens have a complex history, which makes fatigue characterisation challenging. Fatigue or ageing of seals is dependent on the components that make up the seal structure, the underlying pavement layers, the physical environment and applied traffic loading.

Bituminous binders age with time and lose their relaxation capacity as a result. Furthermore when hardening reaches a critical viscosity level (dependent on the local climate), the bituminous surfacing becomes more prone to cracking or losing its surface integrity. At this stage a certain level of fatigue (ageing) has occurred and some form of surface maintenance intervention may be required to maintain the level of service for users of the road.

Furthermore the effects of traffic constantly impose flexural stresses on the seal structure. Lastly, moisture ingress into the base through micro-cracks in the surfacing layer softens the base and increases deflections and strains in the sprayed seal.

Evaluation of pavements with thin surfacings has been proven to be complex. Back calculation of the modulus of a thin top layer is difficult because the deflections measured at various distances from the load centre and in the load centre contain little to no information on the deformation of the thin top layer.

It is for this reason that Four Point Bending (4PB) tests of seals have been proposed. The challenge with the proposed method of laboratory testing was the geometry of test specimen (400 x 65 x 50mm) that the 4PB test apparatus required. This was solved by creating a

beam composite of a sprayed seal from an existing road, with a fast-cast polyurethane as the base of the specimen.

In addition, the seal surfacing plays an important role in waterproofing the pavement structure. The integrity of the sprayed seal, i.e. its resistance to cracking, is an important consideration as it defines the time during which water can penetrate the base layer and impair its bearing capacity.

1.3. Objective of Study

The main objective of this study was to develop fatigue relations as part of the overall mechanistic empirical pavement modelling in South African Pavement Design Method (SAPDM) of seals. This would be used to identify when surface maintenance is required. This is necessary because bituminous surfacings overlying flexible pavement bases have a finite life because bitumen hardens (ages) through reaction with oxygen in the air.

To reach the main objective the following were done:

- Four Point Bending tests were carried out on full scale seals taken from the South African road network comprising of different types, ages, climatic zones and traffic history.
- Wohler's classical approach was used for fatigue characterisation of tested specimens.
- The outputs of these fatigue analyses were used to develop relationships between surface deflection and pavement lives for different types of seals used in South Africa.

1.4.   Outline of Study

Chapter 1 introduces the reader to the complexity of evaluating thin surfacing layers in a pavement structure, defined as the research problem and states the objectives that are desired for the research study, as well as the outline that was followed in carrying out the research project.

Chapter 2 forms the basis of this study since it focuses on the 3 main components investigated in this project. These being the road seal, polymer (polyurethane) and fatigue performance. Backgrounds on the different components that make up road seals are discussed, as well as their performance characteristics within the seal structure. This section also discusses the sprayed seal unit itself and highlights what essentially causes the seal to successfully carry out to its function as a wearing course.

This section furthermore focuses on the fundamentals of fatigue performance for bituminous mixtures. The fatigue fundamentals of seals are discussed in relation to the similarities that exist between thin asphalt surfacings and seals. Lastly this section studies the various approaches used in characterizing and analyzing fatigue of and the vital importance of relating laboratory performance to actual field performance.

Chapter 3 provides a detailed description of the research approach that was followed. It starts by drawing the background of the research study in relation to the scope of work that made up the revision of the SAPDM.

It proceeds with the concept of retrieving seal samples from existing roads, taking into account different variables (seal type, age, climate, binder type, previous traffic). It then describes the concept of analyzing remaining fatigue life of the sampled seals, by developing a bi-layer seal beam, consisting of a sprayed seal and polyurethane from the polymer class, and subjecting the composite to flexural bending in the 4PB Beam Apparatus. This section also explains how the direct beam theory for non-homogenous beams was used in the Matrix Laboratory (MATLAB) software to extract data for the seal component of the tested composite beam. The test parameters and results are analyzed in terms of fatigue and master curves data obtained.

The method of developing a fatigue testing system for seals is then explored by a series of investigations. These included comparisons between Warm Mix Asphalt (WMA) and composite WMA-polyurethane beams and seal-polyurethane and only polyurethane beams. Investigations into applicable strain levels were carried out through trial testing, testing beams upside down and considering both sinusoidal and haversine waveform loading. The fatigue testing system used in the 4PB beam machine is also elaborated upon in terms of the flexural stiffness and master curves calculation that is used to obtain the fatigue data.

This section also presents the statistical analysis that was followed by means of linear regression relationships and an Analysis of Variance (ANOVA).

Lastly this section presents the research design that was followed.

Chapter 4 presents the findings of the research study. It starts by highlighting the relationship between the effective thickness of the sprayed seal and the reduction of flexural stiffness during the loading time in the laboratory and the significance it is on the outcome of fatigue. This section then presents the response of the seals to the frequency sweep and fatigue testing was were carried out. A classical fatigue characterisation was followed considering the possibility of redefining the fatigue criteria. This section also presents the results from the statistical analysis that was followed.

The section thereafter concludes the research by interpreting the analyzed data in terms of seal type and binder, age, traffic (AADT and % Heavies) and climate. This section presents the results for the various investigations carried out; the responses of the seals to frequency sweep testing at medium strain and low strain levels as well as the fatigue testing performed at low strain and high strain levels. A thorough statistical analysis is also presented, highlighting the effect of different fatigue (failure) criteria on the different types of seals, the variables, combination of variables and the interaction between variables.

Chapter 5 presents the findings of the research study for the different types of seals and the variables that influence the outcome of fatigue. The section also discusses the various challenges experienced during the investigation of the research problem and concludes with conclusions and recommendations for future work on fatigue testing of surfacing seals.

Chapter 6 documents the references used in this research study.

Chapter 7 presents the appendices of the research study.

2. Literature Study

2.1. Overview of Seals

A Sprayed Seal (also known as a "Chip Seal") consists of a single layer of bituminous binder that is sprayed as a hot liquid and directly followed by the application of a single layer of crushed aggregate which can be stone or sand (Austroads, 2009). The aggregate is applied immediately and rolled with a pneumatic tyre (Neaylon, 2013) to ensure good adhesion between the aggregate and binder layer (TRH 3, 2007). Figure 2-1 below shows a typical sealed pavement in Namibia.

Figure 2-1: National B1 Road in Namibia (Tumblr, n.d.)

Countries such as South Africa, Namibia, Australia, New Zealand, United Kingdom (UK) and United States of America (USA) have used seals extensively because they are a low cost alternative to asphalt surfacing and have shown success in providing an acceptable wearing course by (TRB, 2005 and Austroads, 2009):

- Guarding the underlying pavement layers (in particular the base) from the harsh effects of traffic by providing a flexible surface that can sustain deflection from traffic volume and the environment by preventing moisture from entering into the pavement structure.
- Offering a long-lasting (durable), safe and dust-free surface.
- Reducing the rate at which the pavement wears out, which is directly linked to the support it lends against the impact of traffic and environmental factors and furthermore impacts the whole of life maintenance costs.
- Offering adequate skid resistance and noise reduction over the life of the surfacing.

In South Africa seals are applied for new construction or as maintenance treatments (SAPEM, 2013) and have gained wide popularity. This is partly due to the ease at which they are placed and maintained, as well as the durability it holds when properly constructed. More importantly though, is that seals provide a cheaper alternative to asphalt surfacing (Marais, 1979). For a developing country like South Africa this is a substantial motivation. So much

4

so, that eighty (80) percent of the country's 150 000 km of surfaced pavement network is surfaced or resealed with seals in rural areas with fairly low volume of traffic. The remaining twenty (20) percent being surfaced with hot mix asphalt in urban areas (SAPEM, 2013 and Milne, 2004), since asphalt can sustain higher traffic loading commonly found in urban zones.

Different viewpoints exist regarding sprayed seal applications in the global road industry. A survey conducted in 2005, by the Transport Research Board (TRB) resulting in the National Cooperative Highway Research Program (NCHRP) Synthesis: Chip Seal Best Practices found that a certain view exists, in some departments of transport, that sprayed seal application is an art and not a science and can possibly explain why these agencies do not employ chip sealing in their pavement preservation programs. The study furthermore noted that certain agencies, North America in particular, were of the opinion that chip sealing can only be applied to low volume roads, despite evidence to the contrary.

This can be understood to some extent though, since chip seal design technology as they knew it, ceased in 1970 in North America, due to the introduction of the McLeod method, which was subsequently adopted by the Asphalt Institute and as such no further development occurred in the sprayed seal design field. The seal design technology largely relied on qualitative design input and adjustments to the rates of binder and aggregate used in the field. This approach required experienced team members and hence added additional variability into an already highly variable technology. When correcting poorly constructed seals, many agencies believe the only effective solution is to mill and overlay the surface. This explains why some countries have chosen to abandon the technology altogether.

In South Africa however, the view is that seals can be an effective pavement technique and the success of the technology is further believed to be largely influence by the extent to which the guideline, Technical Recommendations for Highways: Design and Construction of Surfacing Seals, TRH 3, is understood and correctly applied and the design and construction that subsequently follows. Also, noteworthy is recognising the importance of traffic volumes, climate and the efficiency of the engineering team as highlighted by Judd and Bester in 2007.

2.2. History and Development of the Seal Design Technology

The theory of constructing a thin layer of hot bitumen and a clean single sized aggregate that was not immersed in the binder developed only around the 1930s. Before that bituminous surfacing was achieved by either mixing aggregate and binder or by means of simple sealing methods that involved spraying liquid binder (road oil) and scattering graded aggregate to soak up the oil and create a bituminous bound layer (Austroads, 2009).

Around the 1930s F.M. Hansen of New Zealand developed a design process for seals (Hansen, 1935). His theory was based on partially filling the air voids of an aggregate with binder related to traffic volume (TRH 3 Working Group, 2007 and Austroads, 2009). The aggregate air voids is a function of the average least dimension (ALD) of the aggregate, which is the arithmetic mean of the smallest perpendicular distance between two parallel plates, through which the particle will pass.

From this the first seal design followed (Hansen, 1934-1935, New Zealand). A second seal design arose from the work of Kearby in 1953 in Texas (Kearby, 1953). These two seal design technologies ultimately paved the way for more research in the 1970s with the focus on relating embedment of aggregate into the underlying base to ball penetration tests carried out in the field. The focus was also on rationalizing the seal design method which implied a shift from qualitative to quantitative data input. This swiftly brought to the front the strengths

and opportunities within the sprayed seal and caused it to grow in its newfound status as an accepted science.

If it is a science, then it must surely be governed by principles or standards, in order for it to be recognised by the pavement community at large. In South Africa this was brought about when acceptable standards for low volume roads were established (Sabita, 1993). Soon after Technical Recommendations for Highways (TRH 3) for the design and construction of surfacing seals was produced to serve as guidance for the selection, design and construction of surfacing seals in South Africa. TRH 3 (2007) recommends the allowable traffic range that can be supported by a sprayed seal to be between 125-20 000 equivalent light vehicles (elv), yet state that good performance was reported for seals carrying up to 60 000 elv's, but does not provide further exploration. At this stage the guideline only recommends asphalt surfacing for high traffic volumes.

Some exploration was undertaken by Judd and Bester (2007) and they argued that there is merit in sealing heavily trafficked roads when this application is triggered by crack activity and deflections small enough to be rectified by a sprayed seal. This is a step in answering questions on extending the limits and application of seals, but this seems to only shed light on resealing applications and leaves the potential for new seals still unanswered.

2.3.   Functions of Seals

Seals used as a pavement preservation technology, has a functional as well as a structural role to play in the performance of the road (TRH 3, 2007), although seals are not expected to contribute to the structural capacity of the pavement. Seals are therefore not applied on pavements with severe defects (Moulthrop, 2003).

A functional role of seals is to provide skid resistance, by providing and maintaining the required micro and macro texture required by the road to be slip resistant. With time the macro texture diminishes due to embedment of surfacing aggregate, wear of surfacing aggregate and upward movement of bituminous binder, also referred to as "flushing" (SAPDM Inception Design Report, 2010). With time the aggregate becomes polished and wears out and together with the flushing of bituminous binders cause the micro texture to reduce.

Seals also play a role in wet water visibility, which is primarily cause by water spray. Water spray is caused by traffic type, traffic volume, shape of road, macro texture and interconnecting voids in the seal itself (SAPDM Inception Design Report, 2010).

Another functional role of seals is its influence on noise levels. Road noise levels in turn are influences by vehicle type, vehicle volumes, macro texture and interconnecting voids in the seal itself (SAPDM Inception Report, 2010).

The structural role of sprayed seal is to protect the underlying base from moisture and from direct tyre pressure from traffic. This role is carried out by limiting moisture ingress into the base either by maintaining low permeability in the sprayed seal itself or by slowing down the growth of structural cracking.

The sprayed seal is believed to be fatigued, worn-out or reached the end of its service life when any one of the above mentioned roles are not met to the desired level. This would then require either some maintenance procedure, replacing of the seal or rehabilitation of the entire pavement structure.

6

2.4. Sprayed Seal Components Influencing Performance

From above mentioned roles of seals, it is evident that fatigue performance is dependent on the service life and the degree to which the functional and structural roles are fulfilled. Oliver (1999) summarised the following factors that influence the service life the most. These are (in descending order):

- Designed rate of application
- Traffic
- Quality of binder
- Process of construction
- Time of construction
- Physical environment (climate)
- Maintenance priorities

Each one the sprayed seal factors are ruled by their own set of dynamics and the investigation when maintenance intervention is required. The next sections will explore these factors that are believed of these can ultimately shed light on how seals perform and when they reach failure, i.e. to make a successful seal in terms of what is known through literature and how this bears relevance on answering what causes a seal to fatigue.

During the design phase attention should be given to all the possible situations that may arise on a particular road. In order to do this, the pre-design examination of the road is of utmost importance as it provides valuable information for input into the design and for optimum seal performance. Designs can be revised during construction, if conditions change or new, improved information become available.

Roque et., al (1989) disclosed that over the years, less consideration has been given to traffic control, materials used in construction and construction itself, emphasizing that design procedures have always been the focus. This can be agreed with to a point, since the design process aims to set the length of the seals' service life through careful selection of the desired application rates, but more often though, it has been a combination of design, good material, favourable climatic conditions, proper construction and supervision of the site, that has ultimately determined the sprayed seal life.

2.4.1. Aggregate and Rock Source

2.4.1.1.   Definition

Aggregates are described as an arrangement of minerals that can be separated by mechanical means. In the road construction context, aggregate is composed of hard material which is obtained from the crushing of solid rock or boulders.

Aggregate can also be obtained from mine waste fields, from some combustion ashes or from crushing slags, such as those formed during the manufacture of steel, ferrochrome and

ferromanganese, (SAPEM, 2013). Aggregates' mineralogical composition is dependent on their rock origin, which are linked to igneous, sedimentary or metamorphic rock formations.

2.4.1.2.   Rock Origin

Igneous rocks forms from magma, which is molten rock found in the earth's crust. Igneous rocks are classified as intrusive when the molten rock is forced or thrust into an existing formation under the earth's surface and extrusive when the magma is ejected to the surface, which result in volcanic eruptions, followed by lava flow.

Sedimentary rocks are formed when weathered rock materials are settled and allowed to accumulate on the surface of the earth or within bodies of water. The last rock formation, metamorphic rock, is composed of igneous and sedimentary rocks, whose nature and original state have been drastically altered by heat and pressure in the earth's crust (Blatt et al., 2006).

2.4.1.3.   Classification of Rock Groups

South Africa has an ample quantity of hard rock, which can be obtained either by quarrying naturally occurring deposits of hard rock, or by utilising the rock from mine dumps, which is a more sustainable practice. Technical Recommendations for Highways: Guidelines for Road Construction Materials (TRH 14) provides the classification of hard rock into various groups based on their engineering geological properties.

In South Africa, the most commonly crushed rock groups and their respective types are (SAPEM, 2013):

Basic Crystalline:

Table 2-1: Basic Crystalline Crushed Rock Group (Weinert, 1980)

Rock Origin	Sub Group	Characteristic Minerals	Typical Rock
Igneous	Basic	Ortholase, Amphibole	Dolerite, Norite
		Pyroxene, Plagiodase	Gabbro
		Plagioclase, Feldspar, Pyroxene, Oliviae	Basalt

- Dolerite – Simple igneous rock that are obtained as intrusions in the form of dykes and sills. Present in many parts of South Africa.
- Gabbro and Norite - Found in Limpopo and North West Provinces.
- Basalt – Found in central, northern and eastern parts of South Africa.

8

| Dolerite | Norite | Gabbro/Basalt |
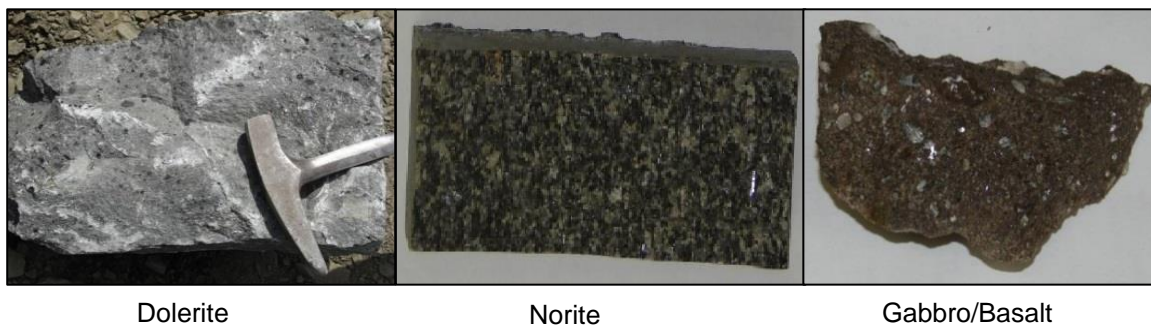
Figure 2-2: Basic Crystalline Crushed Rock Group (SAPEM, 2013)

Acid Crystalline:

Table 2-2: Acid Crystalline Crushed Rock Group (Weinert, 1980)

Rock Origin	Sub Group	Characteristic Minerals	Typical Rock
Igneous	Acidic	Quartz, Orthoclase, Mica, Amphibole	Granite
Metamorphic		Quartz, Orthoclase, Mica (Occasionally)	Gneiss

- Granite and Gneiss – These types occur widespread and are usually used in granular bases and sub-bases once crushed. They are also used extensively in concrete. Granite has a glassy texture that can prevent adhesion between aggregate and bitumen.

| Granite | Gneiss |
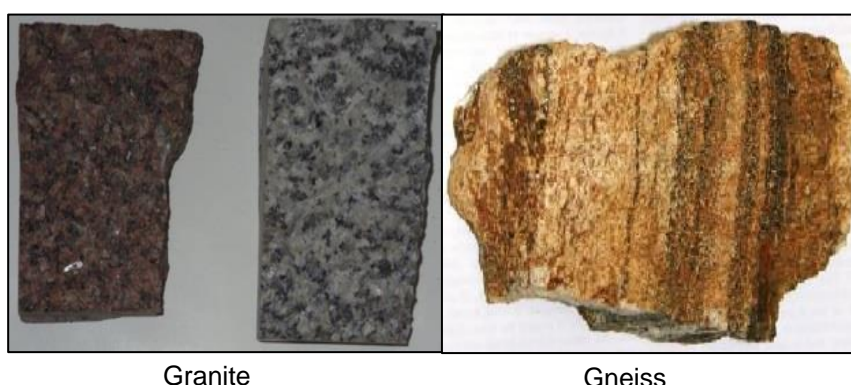
Figure 2-3: Acid Crystalline Crushed Rock Group (SAPEM, 2013)

9

High Silica:

Table 2-3: High Silica Crushed Rock Group (Weinert, 1980)

Rock Origin	Sub Group	Characteristic Minerals	Typical Rock
Metamorphic	Silica	Amorphous Silica, Quartz, Various Others	Hornfels
		Quartz	Quartzite

- Hornfels – This rock type is used most in the Western Cape.
- Quartzite – Obtained all over South Africa, after sandstone re-crystallizes under excessive pressure. The result being an aggregate with improved quality. Quartzite also has a glassy texture causing adhesion problems with bitumen.
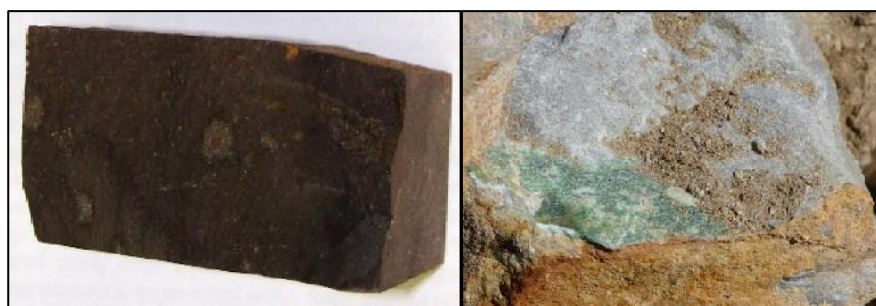
Hornfels   Quartzite

Figure 2-4: High Silica Crushed Rock Group (SAPEM, 2013)

Diamictites:

Table 2-4: Diamictites Crushed Rock Group (Weinert, 1980)

Rock Origin	Sub Group	Characteristic Minerals	Typical Rock
Sedimentary	Clastic	Quartz, Clay Minerals, Others	Tillite

- Tillite – Tillite is produced from glacial rubble and consists of many rock types that are bound together in a clayey matrix. For this reason, tillite has variable quality. They are used more extensively in Kwazulu-Natal and Southern Cape.

Tillite

Figure 2-5: Diamictites Crushed Rock Group (SAPEM, 2013)

Key performance indicators of aggregates linked to sprayed seal performance are discussed in the section that follows.

2.4.1.4.   Performance of Aggregates

Aggregates used in the construction of seals play an important role in the life of the sprayed seal structure by:

- Resisting abrasive forces that cause degradation and polishing.
- Promoting adhesion in the aggregate-bitumen system.
- Supporting the visco-elastic and impermeable binder.
- Assisting in load transfer.
- Providing stability in the seal system.
- Providing a skid resistant surface.

Resisting abrasive forces that cause degradation and polishing:

Aggregates must be tough and abrasion resistant to prevent crushing, degradation, and disintegration when stockpiled, fed through an asphalt plant (for asphalt mixes), placed with a paver (for seals), compacted with rollers, and subjected to traffic loadings. These properties are especially critical in influencing when the fatigue characteristics of seals and open or gap graded (porous) asphalt mixtures which do not benefit from the cushioning effect of the fine aggregate and where coarse particles are subjected to high contact stresses.

Aggregates are broken down (crushed) during the construction stage of seals, when steel wheel rollers are used instead of the preferred pneumatic-tyred rollers and exert a crushing mechanism on the aggregate. This causes a change in the grading of the aggregate because there is an increase in the finer fractions, as well as the shape and angularity. A mechanical interlock between the aggregate particles essentially keep them in place or immersion in the binder film, so it can be deduced that a reduction of voids will cause either the overall size of the original particles to be reduced or the voids to be filled (Milne, 2004)

11

and be detrimental to the integrity of the seal as a whole. The effect of crushing is ultimately dependent on the crushing process and the rock type (mineralogy) which provides resistance against polishing and wearing.

Mineral rocks derive their strength from a combination of hard constituent minerals, the interlock of particles and, where applicable, the cementitious nature of any intergranular matrix. Minor degrees of decomposition along intergranular boundaries can reduce significantly the strength of a rock. Depending on the rock mineralogy, strong and tough rock when first quarried may deteriorate considerably on exposure to open surface conditions if any one of the components, present in even a moderate amount, becomes unstable and weakens under those conditions, causing a weaker sprayed seal with a reduced service life. The most important minerals found in aggregates are silica minerals, feldspars, ferromagnesian minerals, carbonate minerals and clay minerals (Austroads. 2008).

The indication from the Aggregate Crushing Value (ACV) and the 10% FACT of an aggregate ultimately determines the change, if any, to the dimension of the aggregate. The ACV is defined in the South African National Standards (SANS) 3001- AG10 as the percentage of fines that will result from a prescribed 400kN load, whereas the 10% FACT gives an indication of the load that will be required to produce 10% fines. The ACV is mainly used as an indication for the strength of strong aggregate, whereas the 10% FACT is mainly used as an indication for the strength of weaker aggregate. The figures below depict the apparatus' used in the determination of the ACV and the 10% FACT, respectively.

Figure 2-6 A and : ACV and 10% FACT Apparatus (SAPEM, 2013)

Lastly aggregates should resist polishing, when subjected to abrasion from traffic. This resistance to polishing is dependent on the constituent minerals' hardness of the aggregate. CSRA, (1985) showed that quarts is the hardest rock-forming mineral, the other aggregates were strikingly softer. For this reason, road chips containing quarts is a sought after in the road construction industry.

This hardness within the mineral component is not the absolute hardness, but a resistance to polishing, that is attained from a particular distribution of minerals in the aggregate that provides the texture able to resist abrasion. Acidic rocks (quartzitic), has a high resistance to

12

polishing whereas all of the basic crystalline rocks have a very low resistance to polishing. When high silica rocks are used they will polish slower than the binder's degradation, because the high silica content provides great strength.

A smooth, polished surface results in loss of frictional resistance to the road surface and can cause the sprayed seal to not effectively perform its function. The resistance to polishing is determined by the Polished Stone Value (SANS, Section AG11). This polished stone value (PSV) test is applicable to aggregates used for rolled-in chips for asphalt surfacing and for spray seals. It is also applicable to asphalt surfacing where the polishing properties of the aggregate play a major role in the macro surface texture, such Stone Mastic Asphalt (SMA), open-graded or semi open-graded mixes, and to a lesser extent, continuously graded asphalt mixes (SAPEM, 2013).

Specimens containing samples of the candidate aggregate are subjected to accelerate polishing in a specialised polishing machine using emery abrasive powders and water, as can be seen in Figure 2-7 A. Replicate polishing is also carried out on samples of PSV control aggregate. Both candidate specimens and specimens of the control aggregate are subjected to testing with a pendulum friction tester, as can be seen in Figure 2-7 B.
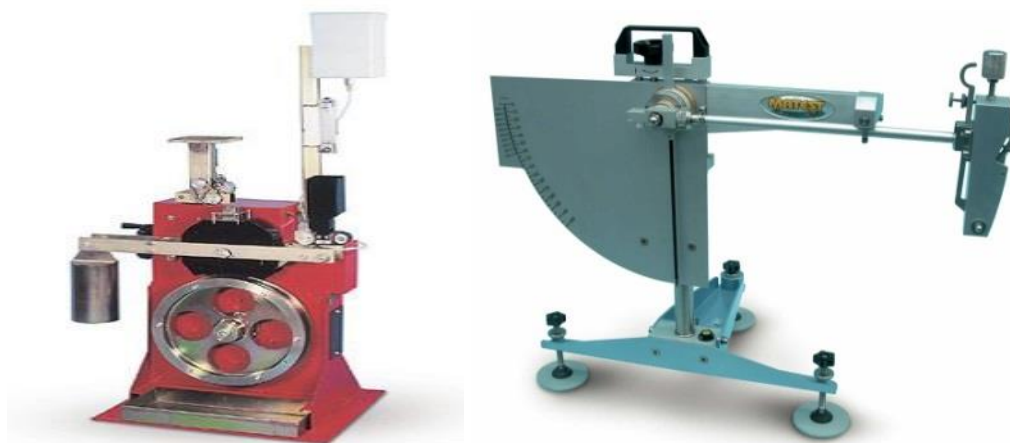
Figure 2-7 A and B: Accelerated Aggregate Testing Machines (Capco, n.d. and JetMaterials, n.d.)

Promoting adhesion in the aggregate-bitumen system:

ASTM D907 defines adhesion as "the state in which two surfaces are held together by valence forces or interlocking forces, or both". Four main adhesion theories exist, namely:

A. Chemical Reaction Theory

After coating aggregate with bitumen, adsorption (adhesion) of bitumen chemical active components on the surface of aggregates takes place.

13

B. Molecular Orientation Theory

Functional groups of both bitumen and aggregate cause the adhesive bond. Bitumen functional groups migrate and aim towards the aggregate surface, resulting from the elastic field caused by the dipole charges of the functional groups on the aggregate surface.

C. Mechanical Theory

Main assumption is that during coating, bitumen enters present pores, holes, cracks and unevenness in the aggregate surface texture (exudation).

D. Thermodynamic Theory

Adhesive bond strength between bitumen and aggregate is based on the surface energy of the bitumen after coating the aggregates. This theory combines elements of chemical reaction and molecular orientation theory.

Hooiberg, (1965) stated that the mineralogical composition and structure of the stone is the biggest contributor to adhesion with bitumen. The mineralogical composition of the aggregate affects the relative affinity between water and bitumen at the interface and for this reason it causes great distress for the sprayed seal, in the form of stripping, which is described as the detachment of bitumen from aggregate. Stripping has subsequently been studied as one of the main factors affecting adhesion. When considering that the phenomenon of stripping occurs when two different entities (aggregate and bitumen), each influenced differently, experience interfacial tension, in the presence of water one cannot simply conclude that moisture damage is attributed to a single mechanism as Little and Jones (2003) also pointed out.

The chemical composition of aggregate affects adhesion of bitumen onto the aggregate surface. Acidic aggregates such as granite and quartzite, which constitute a very large proportion of aggregates used in road construction in southern Africa, are negatively charged, providing good adhesion to the positively charged bitumen in a cationic emulsion. Consequently, in spray seal applications where there is direct contact between the binder and the aggregate cationic emulsions are more widely used as they have superior adhesive properties to a range of mineral aggregates.

Good adhesion is also achieved between anionic emulsions and positively charged aggregates such as dolomite and limestone. If an anionic emulsion is however used with granite or quartzite, effective adhesion is only obtained after the water has evaporated (Sabita, 2011), from this therefore motivation why seals should not be placed during the winter months. In the case, where the aggregates have been pre-coated with a bituminous pre-coating fluid, thus preventing direct contact between the emulsion and the aggregate surface, these restrictions generally do not apply. In general, pre-coated aggregates have indicated higher adhesion bond strength than non-precoated aggregates (Twagirimana, 2014).

After coating the aggregate with bitumen, the bitumen will harden and will also be chemically bonded with the aggregate surface as a result from chemical reactions in the interface. It is

argued that the level of acidity of the aggregates also has a strong influence on these chemical reactions. Arenacious acidic aggregates are considered to be hydrophilic. Hydrophilic (water loving) aggregates have a greater affinity for water than for a bitumen coating. So if such an aggregate, coated with bitumen, is immersed in water the aggregate tends to have a stronger attraction to the water molecules than to its bitumen layer. This can be problematic for the sprayed seal, especially if water passes through cracks and reaches the bitumen-aggregate interface. The bitumen might be 'stripped' from the surface of the aggregate and replaced by the water in time, signifying failure for the seal.

Hydrophobic (oil loving) and basic aggregate appear to have a better adhesion with the bitumen coating, and have a little more resistance to stripping. In most studies this has been confirmed, but not in all. It is found that the presence of some metal components on the aggregate surface could be beneficial to adhesion and the presence of some metal components could be detrimental. Iron, calcium, magnesium and to a certain extend aluminium on the aggregate surface is sometimes beneficial. Alkali metals like potassium and sodium are considered to be detrimental. No aggregate surface is totally acidic or basic; the aggregate surface is always to some extend acidic and to some extend basic. Basic parts of the surface could become positively charged in water and acidic parts positively charged.

Aggregates at the surface, containing the minerals silica could also become negatively charged, whereas minerals containing the metals iron, calcium, magnesium and aluminium could become positively charged. The reason for this is that with the presence of both positively and negatively charged minerals present on the surface, a possibility exists to form salts with the bitumen functional groups. Insoluble salts in water give a better adhesive bonding, whereas soluble salts present on the aggregate surface weaken the adhesive bond. This is because soluble salts are the result of a reaction of acidic functional groups in the bitumen with potassium and sodium, hence when the salts dissolve, the adhesive bond also fades.

Aggregates are however, never totally acidic or basic. The aggregate surface is always to some extend acidic and to some extend basic. In 1968, Majidzadeh and Brovold made a classification based on the silica (SiO_2) content of the aggregate to determine the dominance of acidic or basic properties, as can be seen in the Table 2-5 below.

Table 2-5: Classification of rocks based on silica content (Majidzadeh and Brovold, 1968)

Definition	Percentage SiO_2
Acidic Rocks	> 65
Intermediate Rocks	52-65
Basic Rocks	<52

The surface energy is directly related to the chemical and mineralogical composition of the aggregates. The intermolecular forces at the surface of the aggregates are able to interact with the molecules from the bitumen resulting in an adhesive bond. Different chemicals have different kinds of bonding mechanisms for interaction with the molecules in the bitumen. For

instance the polar molecules on the surface of the aggregates are more able to interact with the functional groups in the bitumen. Non-polar molecules at the surface are more able to interact with non-polar molecules in the bitumen.

The surface energy also influences the wettability of the aggregate, which is the ability of bitumen to wet the aggregate surface, and is dependent on the surface energy of the bitumen and aggregate. The potential of wettability of a surface is described by the contact angle, which is the solid/liquid interface measured from the side of the liquid, as can be seen in Figure 2-8 below. A lower contact angle is associated with increased wettability.
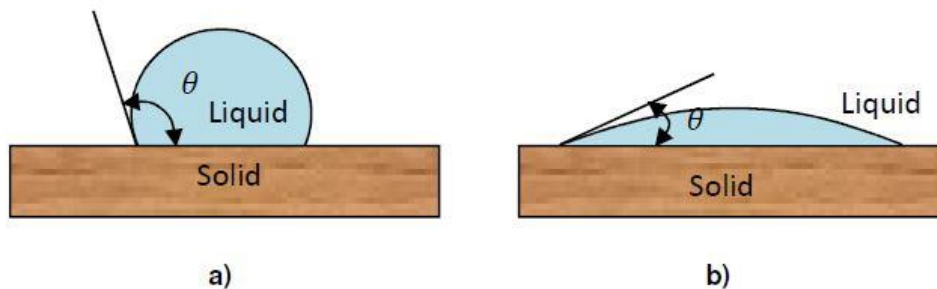
Figure 2-8: Measuring contact angle to determine wettability potential (adapted from NDT Resource Center n.d.)

If the bitumen (emulsion) molecules have a stronger attraction to each other than to the surface of the aggregate, the bitumen beads-up and does not wet the aggregate surface (NDT Resource Center n.d.). Bahia, Jenkins and Hanz (2008) state that aggregate has a higher affinity to water than bitumen and therefore would have a tendency to form bonds with water rather than bitumen as the emulsion breaks and cures. Appropriate selection of 'surfactant can remedy this issue by displacing the water from the aggregate surface hence allowing strong aggregate-bitumen adhesive bonds to develop' (Hanz, Arega and Bahia 2008, p.9).

The magnitude of adhesion in the aggregate-binder system is an important consideration in resisting ravelling (loss of aggregate) and keeping the sprayed seal intact. Ravelling might be caused by cohesive failure of the bituminous mortar or by adhesive failure in the adhesive zone (Mo et al., 2009). Loss of aggregate is considered as the dominant defect type of noise reduction of seals and similarly porous asphalt surfaces and in turn ensuring an adequate service life. The service life for seals and similarly for porous asphalt is limited by the ravelling of the surface. Dense asphalt however, has a higher service life when compared.

With time aggregates wear out, depending on their chemical and mineralogical composition. Some research has already been done on relating weathering to adsorption of bitumen and surface energy of the aggregate, but no clear results were found. Generally it is thought that some aggregates tend to weather more quickly than others and weathering has a negative effect on the adhesion between bitumen and aggregate surface. It is thought that freshly sawed aggregate surfaces have more polar active sites to interact with the bitumen functional groups. Weathering occurs to different extents.

When aggregates are stored outside under rain, frost and sunlight disintegration can take years or even months (Roberts et al., 1998). When aggregates are protected from direct sunlight, frost and rainfall this weathering process will almost not occur. Only a quick ageing of the freshly sawed surface of the aggregate under influence of the air occurs. Some

aggregate ageing effects, such as atmosphere contaminants accumulation and oxidation of organic debris, occur within few seconds after sawing (Little and Bashin, 2006).

During the mixing of bituminous mixes, surface texture influences the extent of coating of the aggregate with bitumen binder. A smooth surface texture is understood to be easier to coat with a proper binder film, but the mechanical bond is less in comparison to a rougher surface texture. A rougher surface however, has a larger surface area per unit mass (specific surface area) resulting in stronger adhesive bonding and a stronger sprayed seal unit.

However when the aggregate is too rough it is possible that not the whole surface of the aggregate is coated. Then the contact area between the bitumen and aggregate is decreased resulting in a weaker adhesive bond. Most natural aggregates are composed of a combination of different minerals. In addition, sharp points on aggregate can result in stress concentrations in the binder, causing the binder to shear and pierce through.

The shape of the aggregates affects the coating process of the bitumen binder onto the aggregates in the asphalt mixture during mixing. Rounder aggregate particles, such as most natural river gravels and sands, are coated easier with a bitumen binder than angular shaped aggregates. During the service life angularity may offer good points of anchoring for the bitumen binder to improve adhesion. It is known however that an increased angularity also increases the probability of puncturing the bitumen film. In this way water can easier penetrate the layer of adhesive bonding and possibly cause stripping (detachment) as illustrated in Figure 2-9 below.
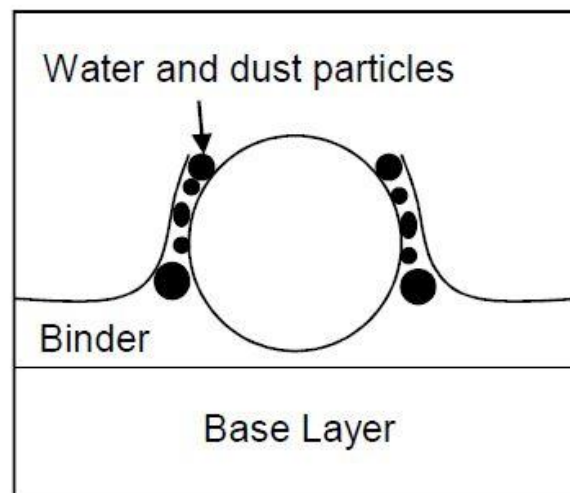
Figure 2-9: Illustration of puncturing of the bitumen film (Whiteoak and Read, 2003)

Furthermore the mineralogical composition affects the surface texture of the aggregate. Many minerals show different kinds of texture when fractured. Quartz has a conchoidal fracture. This fracture has the appearance of series or arcs. Native metals such as copper have a hackly fracture. Other kinds of fractures are even and uneven fracture (Pearl, 1955).

Surface texture is furthermore influenced by the pore size distribution, if many pores are located at the surface of the aggregate, a rougher surface texture will develop and also a

larger surface area per unit mass to ensure stronger adhesive bonding (Van Lent, 2008). Figure 2-10 below illustrates pore size and fracture respectively.
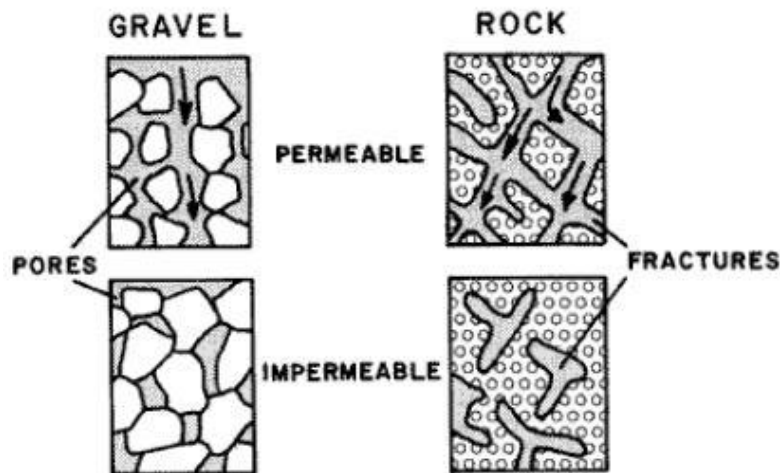
Figure 2-10: Illustration of pore size and fracture (USGS, 1993)

Aggregate particles for road construction in bituminous mixtures are normally smaller than 22 mm. For reasons of processability and aggregate shape, the maximum size of aggregate is limited. The size of crushed stone is limited to 19 mm for surface layers (TRH 3, 2007) and the size is limited to 22 mm for intermediate and lower layers. The finest aggregate particles, the filler, may approach sizes smaller than 2 µm. For seals with larger aggregate sizes the surface texture must therefore increase to ensure that a good adhesive bond is obtained for such a surface area per unit mass.

Adhesion of the binder to the aggregate can further be affected by the presence of contaminants such as dust, mud, oil and fuel. Substantial stone loss may occur if only 1% of dust is present. Adhesion is also negatively affected by moisture, except for emulsion and where aggregates are pre-coated with a high viscosity binder, to improve adhesion. If this cannot be obtained the result will be an unstable seal. Deleterious materials on the surface of aggregate affect to some extent the adhesion between bitumen and aggregate.

These surface impurities include clay, dust (e.g. from aggregate crushing), coal, shale, free mica, salts and vegetation. These impurities can inhibit direct bonding between aggregate and bitumen binder. In this way no proper adhesive bond is ensured. Another property of the deleterious material that affects adhesion in asphalt mixtures is the tendency to attract water. By attracting more water the probability of stripping increases. Deleterious materials may also result in channels and trapped air on the aggregate surface causing water to penetrate more easily, disintegrating the sprayed seal unit.

The possible effect of exudation (absorption) is also an important consideration for the adhesion between the aggregate and bitumen, especially if high porosity is found at the surface. When absorbed bitumen is forced into the pores, it will be locked in, causing an even stronger adhesive bond. The drawback however is that the amount of bitumen available for proper coating of the exterior of the aggregate is reduced. This amount could be compensated with an extra amount of bitumen added during application.

A too high porosity of the stone can however cause a disadvantage. With a too high porosity of the stone not all pores might be able to adsorb the bitumen. Exudation is however not only dependent on the aggregate, but also on the type of binder and its characteristics, as illustrated in the penetration grade Qualagon of Shell, see Figure 2-11 below.
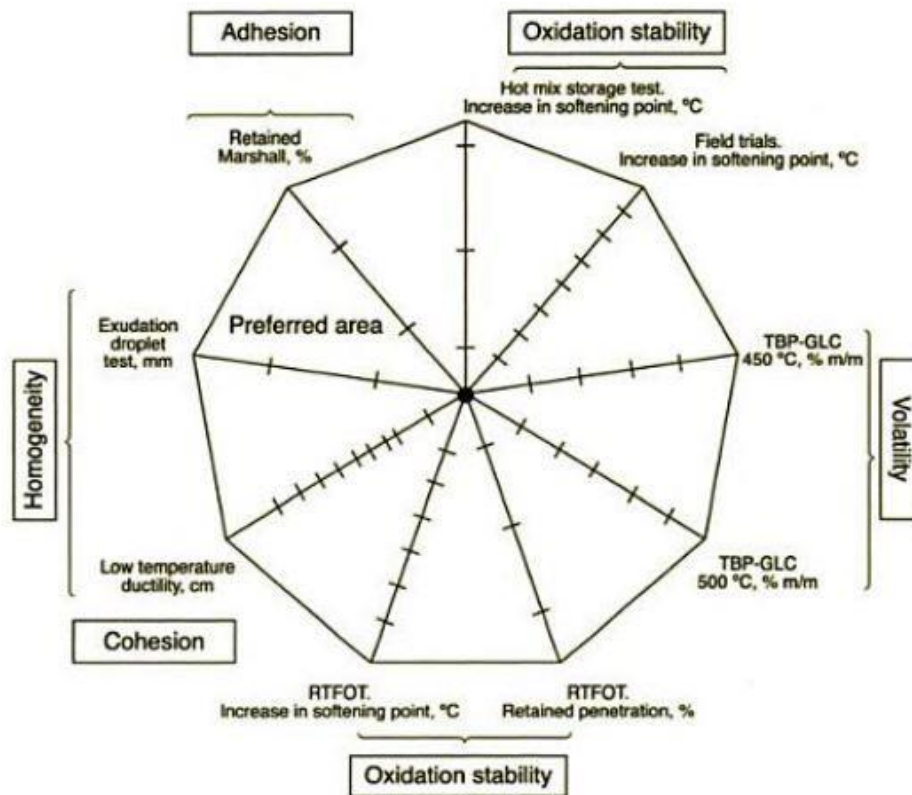
Figure 2-11: Penetration Grade Qualagon (Whiteoak and Read, 2003)

Supporting the binder structure:

Aggregates protect the visco-elastic and impermeable binder structure and should therefore have sufficient texture (or voids) to prevent flushing (Milne, 2004) and keep it intact or embedded in the binder film. Ideally, aggregate should not be too angular, to prevent puncture of the bitumen film.

Assisting in load transfer:

An ideal aggregate packing is when a uniformly mosaic cover of the aggregates are achieved, with aggregate positioned shoulder-to-shoulder, in a single film and in a firmly joined pattern. This is achieved by choosing an ideal aggregate spread rate, measured in cubic metres per square metres (TRH3, 2007). The binder need to be protected from the ultra-violet (UV) damage of the sun, therefore this pattern should not be too loose. In the case where it is too tight, the aggregates may be crushed. The packing of this pattern is greatly influenced by the gradation of aggregate.

Single sized stone provide for better aggregate interlock, but also optimum contact between tyre and road, ensuring better ride-ability. Loads are better distributed as a result, with the

effect that less abrasion and polishing will occur, leading to higher skid resistance. Load transfer mechanism is thus developed when shear stresses from the applied traffic load are carried by the aggregate-binder interface. Aggregate interlock, embedded in the tack coat is important. Chip Seal Best Practices (TRB, 2005) discussed that the angularity of aggregates furthermore play a role in the aggregate interlock. Cubical aggregate tend to lock better together and provide better long term retention and stability.

Providing stability in the seal system:

As discussed above a mosaic of aggregate interlock provide stability. Another important contributor to the stability of the seal structure is the shape of the aggregate, since the shape of an aggregate influence the void content and displacement of water, as well as the interlock of the compacted layer. Aggregates with small stone size have fewer voids and can result in possible bleeding. Larger stone sizes have the advantage that they are less vulnerable to flushing (Ball and Owen 1998). Similarly, larger aggregate sizes have less of an influence on the application rate, causing them to be preferred for the construction of seals.

Providing a skid resistant surface:

Skid resistance (friction) is extremely important for road safety, as it assists to reduce accident risk. Various countries use a friction threshold to measure an acceptable friction level. If the measured value is less than the threshold value, accident risk is considered high for that particular road. In 1966, Krummer composed the following table listing various factors influencing skid resistance.

Table 2-6: Factors influencing road surface friction (Krummer, 1966)

Road	Contaminant (Fluid)	Tyre
Macrotexture	Chemical structure	Tread pattern design
Microtexture	Viscosity	Rubber composition
Uneveness/ Megatexture	Density	Inflation pressure
Chemistry of materials	Temperature	Rubber hardness
Temperature	Thermal conductivity	Load
Specific heat	Specific heat	Sliding velocity
Thermal conductivity	Film thickness	Temperature
		Thermal conductivity
		Specific heat

Of all the road factors, aggregate texture contributes the most to skid resistance, since it provides a high degree of friction at the road surface. For good skid resistance, a good micro texture (grinding paper texture) is required. For this reason, the Netherlands prefers aggregate with both soft as well as hard parts, once the soft parts are removed, the hard

20

parts remain and the micro texture is retained as well. Furthermore, seals and similarly porous asphalt provide significant reduction in splash and spray in wet weather conditions.

2.4.2. Bituminous Binders

2.4.2.1.   Definition

Many definitions exist for bitumen. Sabita (2012) provides the following definition:

"Bitumen is a dark brown to black viscous liquid or solid, consisting essentially of hydrocarbons and their derivatives. It is soluble in trichloroethylene, is substantially non-volatile, and softens gradually when heated. Al though solid or semi-solid at normal temperatures, bitumen may be readily liquefied by applying heat, by dissolving it in petroleum solvents, or by emulsifying it in water. Bitumen is obtained by refining petroleum crude oil, although it is also found as a naturally occurring deposit."

2.4.2.2.   Bitumen Origin and Composition

In South Africa all bitumen used in road construction is processed at oil refineries in Cape Town, Durban and Sasolburg, where imported crude oils are refined to produce petrol, diesel fuel and other petroleum based products. The crude oil is heated and delivered to an atmospheric distillation column, where the lighter fractions are vaporised and drawn off, leaving a residue of heavy oil. This residue is processed, by further distillation under vacuum, into "vacuum bottoms". Treatment under vacuum enables oil fractions to be drawn off in vapour form at relatively low temperatures. These "vacuum bottoms" are used to produce straight-run bitumen.

Sometimes it is further treated by air blowing to produce harder bitumen such as 40/50 penetration grade. The vacuum bottoms not used in bitumen manufacture are further processed to produce marine or furnace fuel oil (Sabita, 2012). The diagram below shows the production of bitumen from the refining process of crude oil.
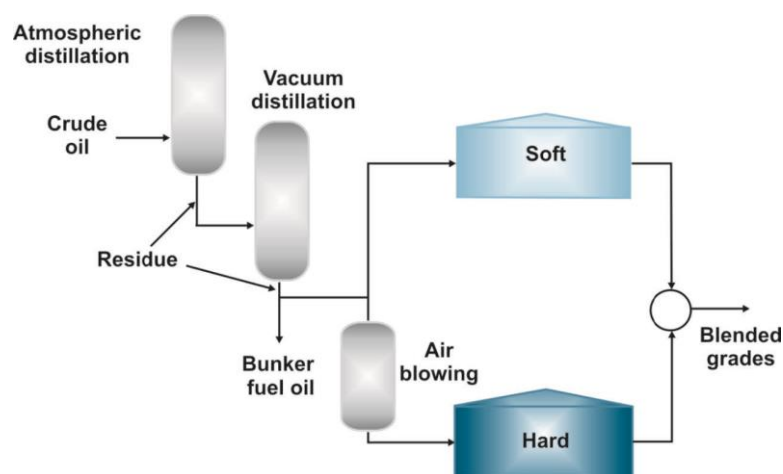
Figure 2-12: Production of Bitumen (Sabita, 2007)

Bitumen is a complex combination of hydrocarbons with small quantities of sulphur, oxygen, nitrogen and trace quantities of metals such as vanadium, nickel, iron, magnesium and calcium. Crude oils normally contain small quantities of polycyclic aromatic hydrocarbons (PAH's), a portion of which ends up in bitumen. Some of these PAH's are suspected of causing cancer in humans. However, the concentrations of these carcinogens are extremely low, and no causal link to cancer in humans has been established. Most bitumen manufactured from a range of crude oils contain 82-88% Carbon, 8-11% Hydrogen, 0-6% Sulphur, 0-1.5% Oxygen and 0-1% Nitrogen.

Rheology is the science that deals with the flow and deformation of material and constitutes a fundamental engineering property of bitumen. The rheological characteristics of bitumen at a particular temperature are determined by both the chemical composition and structure or physical arrangement of the molecules in the material. Therefore to understand the rheology of bitumen, it is essential to understand how the constitution and structure of bitumen interact to influence the rheology (Read & Whiteoak, 2003).

The precise composition of bitumen varies according to the source of crude oil used in the manufacture, the manufacturing processes adopted by a particular refinery and during in-service ageing. The chemistry of bitumen is complex, and for descriptive purposes has been divided into components derived through chemical separation techniques. It is convenient to separate bitumen into two broad chemical groups, called asphaltenes and maltenes. Maltenes are further subdivided into saturates, aromatics and resins (See Figure 2-13). These fractions are commonly referred to as SARA (saturates, aromatics, resins and asphaltenes).
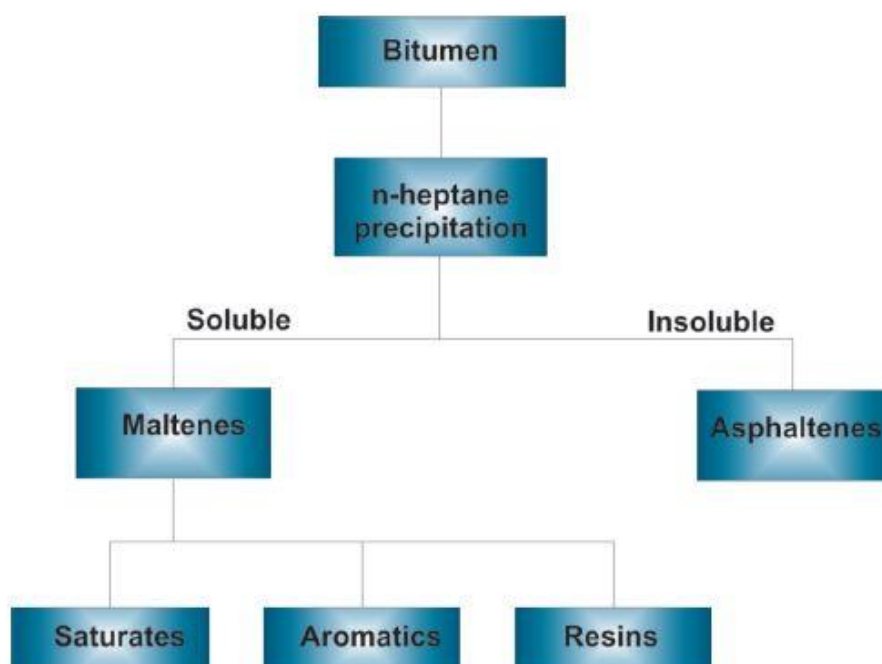
Figure 2-13: Chemical Composition of Bitumen (Sabita, 2007)

Asphaltenes

Asphaltenes are fairly high molecular weight, polar n-heptane in soluble solids that are black and glassy, and they make up 5 - 25% of the bitumen. They contain carbon, hydrogen, some nitrogen, sulphur and oxygen. The asphaltene content has a significant influence on the

22

rheological properties of the bitumen. Increasing the asphaltene content produces a harder, more viscous binder.

Maltenes

Maltenes are the n-heptane soluble phase of the bitumen, and can be further separated into components broadly based on molecular mass and polarity.

Figure 2-14: Asphaltenes and Maltenes (Molenaar, 2013)

Resins are largely composed of hydrogen and carbon with small amounts of oxygen sulphur and nitrogen, making up 30 - 50% of the total bitumen. These dark brown solids or semi-solids act as a dispersing (peptising) agent for the asphaltenes. Being polar in nature, they are strongly adhesive.

Figure 2-15: Maltene Fractions (Molenaar, 2013)

The molecules in the bitumen further fall into two functional categories:

- Polar molecules
- Non-polar molecules

23

Polar molecules form the network of the bitumen and provide the elastic properties, whereas non-polar molecules provide the body of the bitumen and its viscous properties. These two categories of molecules co-exist, forming a homogeneous mixture. Their weak interaction results in the Newtonian behaviour of bitumen at high temperatures, where the viscosity change is directly proportional to the temperature change.

The non-polar molecules (saturates and aromatics) form a carrier for the polar molecules (asphaltenes and resins). In the presence of sufficient quantities of resins and aromatics of adequate solvating capacity, the asphaltenes are fully dispersed, or peptised, and the resulting micelles have good mobility within the bitumen. In such a case the bitumen is known as a "Solution" (SOL) type, as illustrated in Figure 2-16.
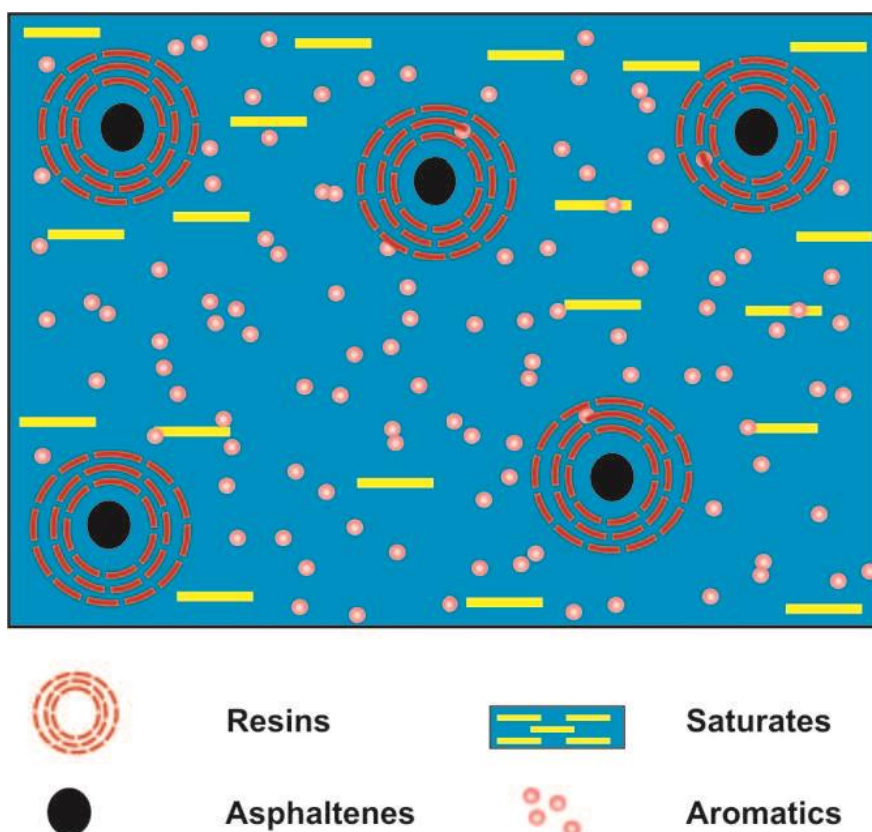
Figure 2-16: Sol Type Bitumen (Sabita, 2007)

If the aromatic or resin fraction is not present in sufficient quantities to peptise the micelles, or has insufficient solvating capacity, the micelles can associate together. This leads to structures of linked micelles, and these types of bitumen are known as "Gelatinous" (GEL) types as illustrated in Figure 2-17.

24
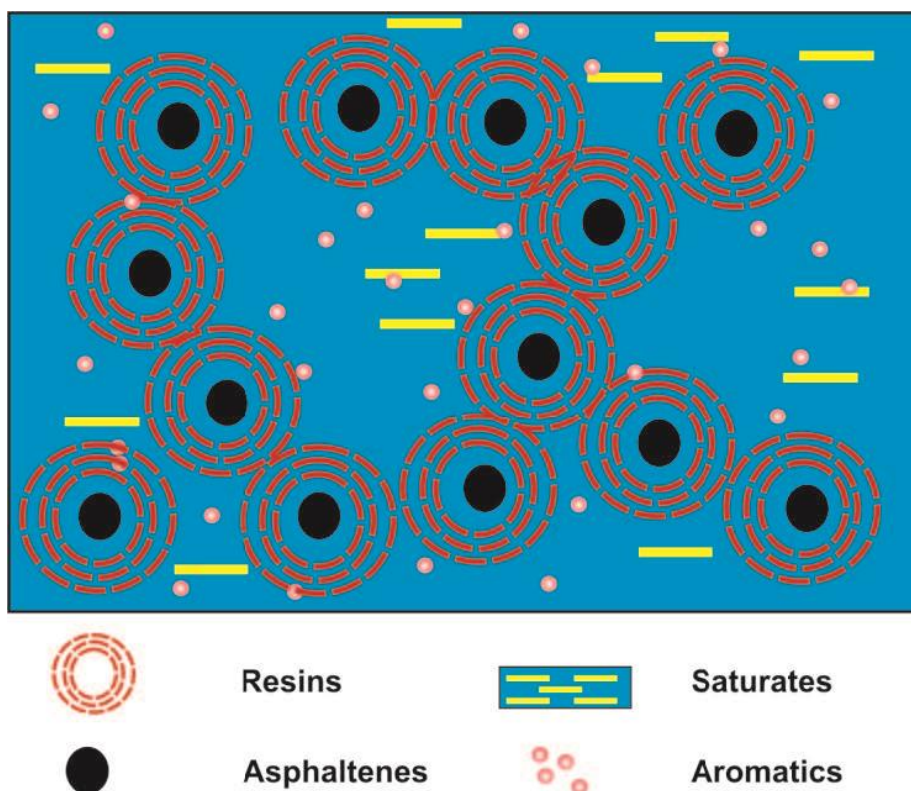
Figure 2-17: Gel Type Bitumen (Sabita, 2007)

2.4.2.3.   Behaviour of Bitumen

Bituminous binders have visco-elastic behaviour, meaning their behaviour varies when subjected to different loading and temperature settings. When bitumen is subjected to low temperature and a short loading time, it will become an elastic solid which will return to its original position once the load is removed. If the temperature is excessively low for a prolonged time and the loading time is rapid, then the bitumen may become brittle and crack.

When subjected to higher temperatures and extended periods of loading, bitumen will however become a viscous liquid. It will undergo plastic deformation i.e. the deformation is not reversible. Flow takes place as adjacent molecules slide past each other, the resulting friction or resistive force being related to the relative velocity of sliding.

The relationship of this resistive force and the relative velocity (of sliding) is termed "viscosity". Under conditions of elevated temperature, pavements bound with bitumen will tend to rut under repeated applications of wheel loads, and the rutting will occur at a rate dependent on the temperature and rate of loading. This plastic behaviour of the bitumen at high temperatures can be offset by the interlocking action of the aggregate, which serves to resist permanent deformation.

In the intermediate range the bitumen will have both elastic and viscous properties which can be represented by a combination of a spring and a dashpot. The so called Burgers model (Figure 2-18) represents all these three different deformation patterns.
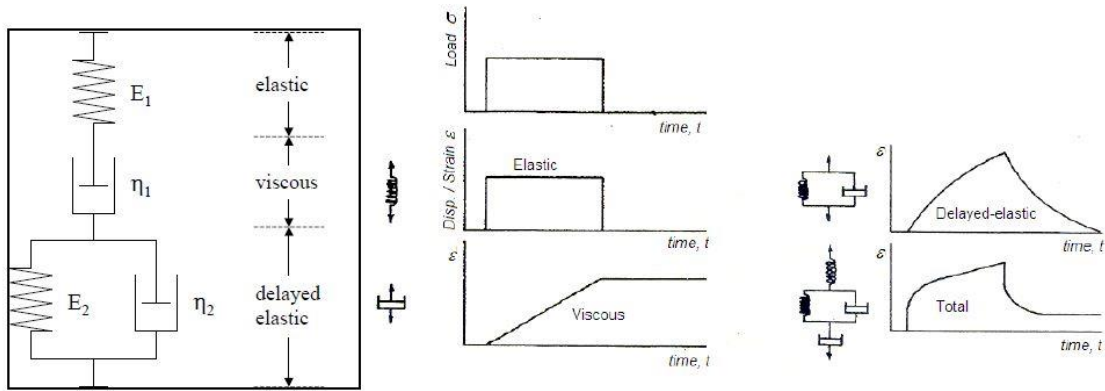
Figure 2-18: Generalized Burgers model illustrating the visco-elastic properties of bitumen and response of various factors

Figure 2-19 shows what the stiffness of bitumen implies when it is subjected to different loading times. Stiffness (S) is defined as the ratio of applied stress (σ) over resulting total strain (ε). Depending on the loading time and temperature at which the stiffness was determined, stiffness can imply elastic stiffness (low temperatures, short loading times), which can be represented by means of spring, or viscosity (high temperatures, long loading times), which can be represented by means of a dashpot.
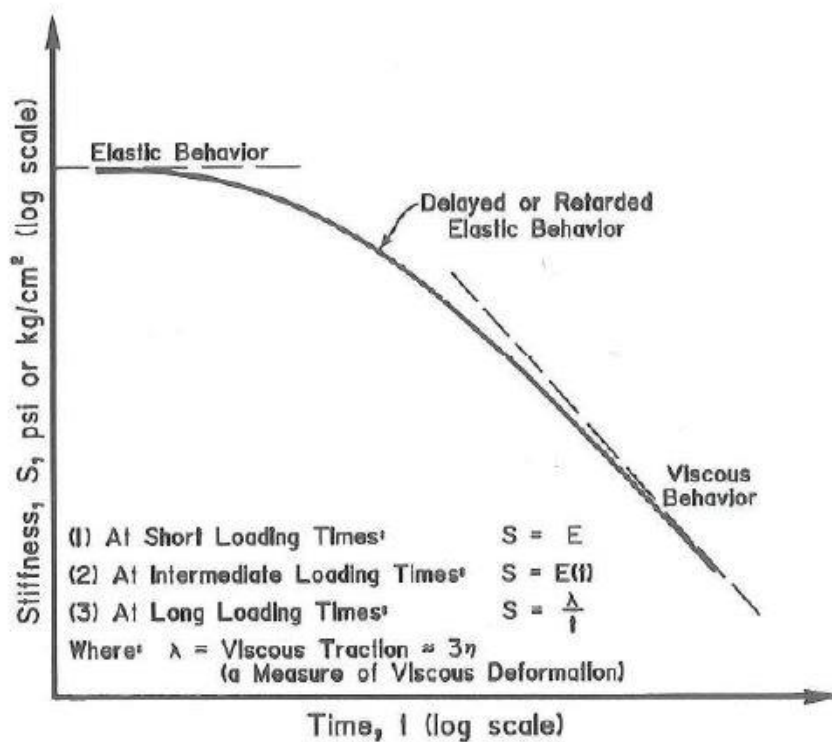
Figure 2-19: Stiffness of Bitumen in Relation to Loading Time (Robert et al., 1966)

2.4.2.4.   Characterisation of Different Bitumen Products

Bituminous binders are used in many ways. They are used in surface treatments such as in seals, prime coats or tack coats. They are also used in asphalt; in hot mix asphalt consisting of hot bitumen or in cold mix asphalt consisting of emulsions or cutbacks. Several types of binders are used in seals.

These are conventional binders, which comprise of penetration grade bitumen, cut-back bitumen and bitumen emulsions, and modified binders, which include hot modified binders and modified emulsions.

- Conventional Binders

Penetration Grade Bitumen

In order to choose the most suitable grade of conventional binder, consideration is given to the anticipated climatic conditions during construction and the way in which the binder will perform over a long term at ambient temperatures (TRH 3, 2007).

Each specific grade is described by the temperature/ viscosity relationship that governs it and has an ideal range for spraying, storage, mixing or pumping. In order to achieve ideal performance from the binder the viscosity needs to be kept within the limits of this range when spray applications are carried out. A specific temperature/ viscosity curve is normally used to define the applicable temperature range for the spray application.

Cut-back Bitumen

Cut-back bitumen emulsions are categorized according to their kinematic viscosity (m^2/s) and similarly to penetration grade bitumen, temperature/ viscosity curves also exist for each grade (TRH 3, 2007). Cutback bitumen is a blend of penetration grade bitumen and petroleum solvents. The choice of solvent determines the rate at which the bitumen will cure when exposed to air. A rapid-curing (RC) solvent will evaporate more quickly than a medium-curing (MC) solvent.

The viscosity of the cut back bitumen is determined by the proportion of solvent added - the higher the proportion of solvent, the lower is the viscosity of the cutback. The solvent used in cutback bitumen is sometimes also referred to as the "cutter" or "flux". When the solvent has evaporated, the binder reverts to the original penetration grade.

The advantage of cutback bitumen is that it can be applied at lower temperatures than penetration grades because of its lower viscosity. A disadvantage is that cutback bitumen consumes non-renewable energy resources which are ultimately lost through evaporation (SABITA, 2012).

27

Bitumen Emulsion

Emulsions are defined in terms of the percentage by mass of the penetration grade bitumen that is found in the emulsion (TRH 3, 2007). A further classification is the presence of a steadying positive charge (cationic) or a steadying negative charge (anionic) that was imparted by the emulsifying agent. Adequate adhesion is often achieved between cationic emulsions and most types of aggregates. Anionic emulsions are however not suitable with certain granites and quartzites. Table 2-7 below indicates which aggregate types are compatible with the two different emulsion types.

Table 2-7: Compatibility of emulsion type with aggregate type (Sabita, 2011):

Aggregate Type	Compatibility	
	Anionic Emulsion	Cationic Emulsion
Dolerite	√	√
Quartzite	x	√
Hornfels/Greywacke	√	√
Dolomite	√	√
Granite	x	√
Andesite	√	√
Tillite	Variable	√
Basalt	√	√
Sandstone	x	√
Rhyolite	x	√
Marble/Norite	√	√
Syenite	X	√
Amphibole	√	√
Felsite	x	√

- Modified Binders

Polymer modified binders behave very similarly to conventional binders, because their properties are also largely influenced by the temperature, viscosity and phase transition of the bitumen and its environment. A polymer added to conventional binders will primarily modify the range in which bitumen can be stiff or elastic, depending on the type of modifying agent and its concentration (TG1, 2008). Table 2-8 shows the different compositions of modified bitumen.

The thermoplastic modifier can be either a plastomer or an elastomer. Plastomers improve the viscosity of the bitumen, while elastomers increase the strength and elastic properties of a binder. The resultant modified binder will thus have improved or enhanced visco-elastic properties, making it ideal to be used in environments where the uses of conventional binders are limited (TG1, 2008).

Modified binders are used mostly in highly stressed areas where high traffic volumes are found and also at intersections, steep inclines and sharp curves. They are also preferred in areas where large daily or seasonal variations in temperature or extended periods of high ambient temperatures occur. Furthermore they are used to seal cracks of up to 3mm, using Stress Absorbing Membrane (SAM), in heavy duty application of slurry seals (for example correcting rutting) and also in remote areas where a higher durability is desired (TG1 ,2007).

Modified binders have a higher resistance to in-service ageing, are less sensitive to temperature influences, have improved consistency, cohesion, stiffness, flexibility, toughness and resilience. They also provide better adhesion between the binder and aggregate (TG1, 2007).

Table 2-8: Composition of Bitumen Modifiers (TG1, 2008)

Type of Modifier	Classification	
Homogenous (Thermoplastic polymers)	Elastomeric	Styrene-Butadiene-Rubber (SBR)
		Styrene-Butadiene-Styrene (SBS)
		Natural Rubber
	Plastomeric	Ethylene-Vinyl-Acetate (EVA)
Non-Homogenous	Bitumen Rubber, recycled from tyres	
Naturally Occuring Hydrocarbons	North American Asphaltum	
	South American Asphaltum	
High Molecular Weight Waxes	Fischer-Tropsch (F-T) wax	

2.4.2.5. Availability and Distribution of Binders Used in South Africa

In 2013, Sabita listed the following diagram indicating the bituminous binders that can be found in South Africa.
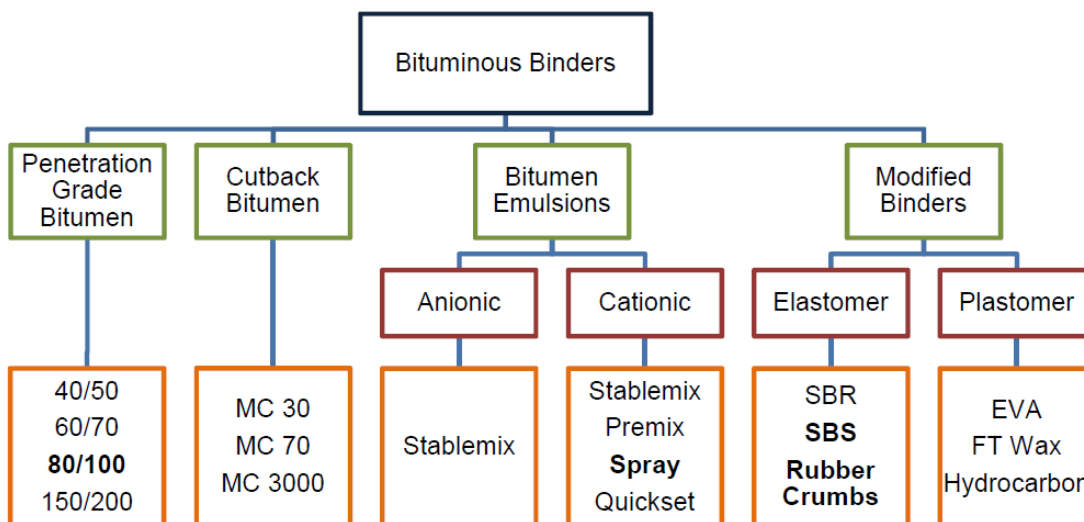
Figure 2-20: Available Bitumen Binders in South Africa (Sabita, 2013)

Distin in 2008 presented the following distribution of bituminous binders used seals in South Africa.
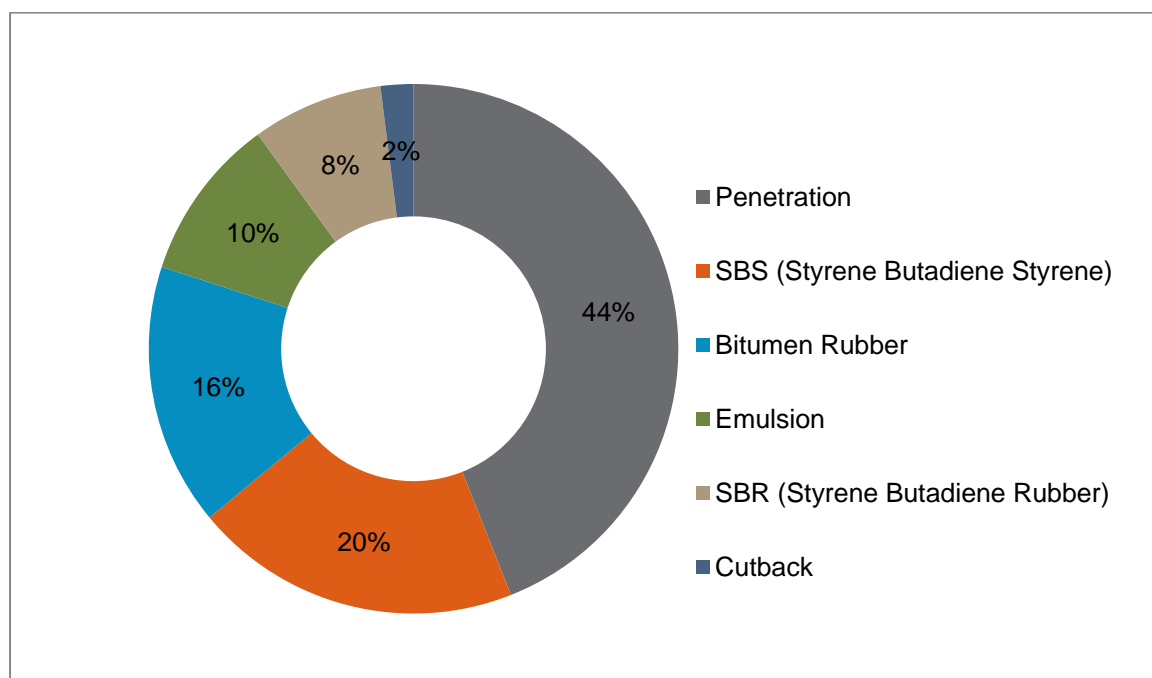
Figure 2-21: Binder proportional distribution in South Africa (Distin, 2008a)

Distin estimation that 40% of the binders used in seals were, due to the desired performance of these binders when high traffic needs are reported. Furthermore, noted that the sprayed seal industry generally favours the use of hot binders more than emulsion or cutback bitumen, because they favour higher sealing production rates (Distin, 2008a).

2.4.2.6. Performance of Binder

Bitumen and modified bitumen are used in the construction of seals due to their qualities of durability, waterproofing, strength and adhesion. Considerations for bitumen is important when considering the performance of the sprayed seal, because it is affected differently by different temperatures and loading conditions.

The binder ultimately binds the seal aggregate to the pavement structure and keeps the aggregate from being pulled out by the force of wheel loads. They also give durability and flexibility to the seal structure and most importantly waterproofs the pavement so that water cannot enter and weaken the underlying structural layers (CSRA, 1997 and TRH 3, 2007).

Bitumen used in road construction play an important role in the life of the structure by:

- Developing adhesive strength between binder, aggregate and road surface and prevent aggregate whip-off.
- Developing cohesive strength, in order to behave reliably in a visco-elastic mode.
- Behaving flexibly and resilient, in order to recover from deformation from applied loads.
- Add to the safety and structural performance of the surfacing layer.
- Waterproofing the pavement structure.
- Providing durability, through resisting ageing.

Developing adhesive strength between binder, aggregate and road surface and prevent aggregate whip-off:

Adhesion is the measure of the stresses required to break the bonds between the bituminous binder and mineral aggregate. It is largely dependent on the physical chemistry as well as the chemical nature of the bituminous binder and aggregate type when combined for application. The rheology of bitumen plays an important role in adhesion. As temperature increases the viscosity of bitumen reduces, due to its visco-elastic properties.

When the temperature of the pavement rises after rain has fallen, blistering and pitting may occur. Bitumen creeps up the edges of the water droplets to form a blister. As the temperature further increases the blister expands, leaving a hollow pit which allows water to access the surface of the aggregate (Whiteoak and Read, 2003), causing adhesion failure, as illustrated in Figure 2-22 and Figure 2-23.

31
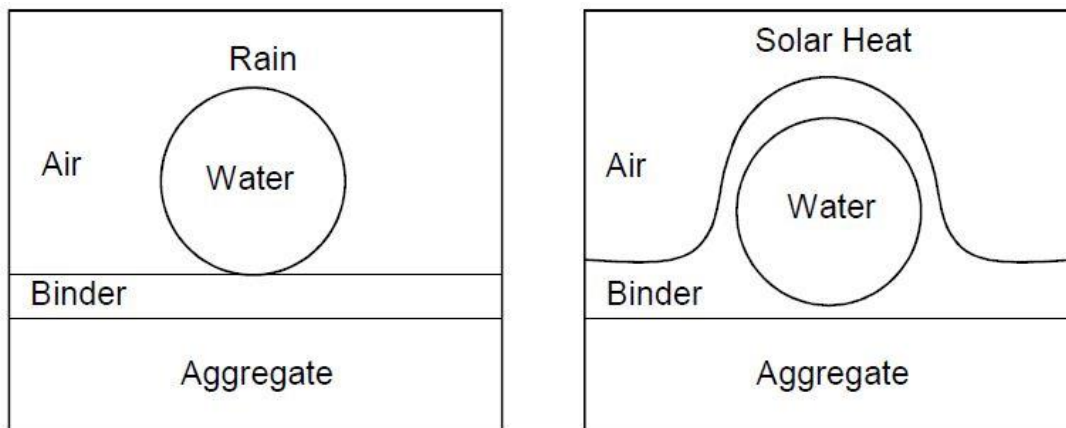
Figure 2-22: Illustration of blistering when viscosity of bitumen increases (Whiteoak and Read, 2003)
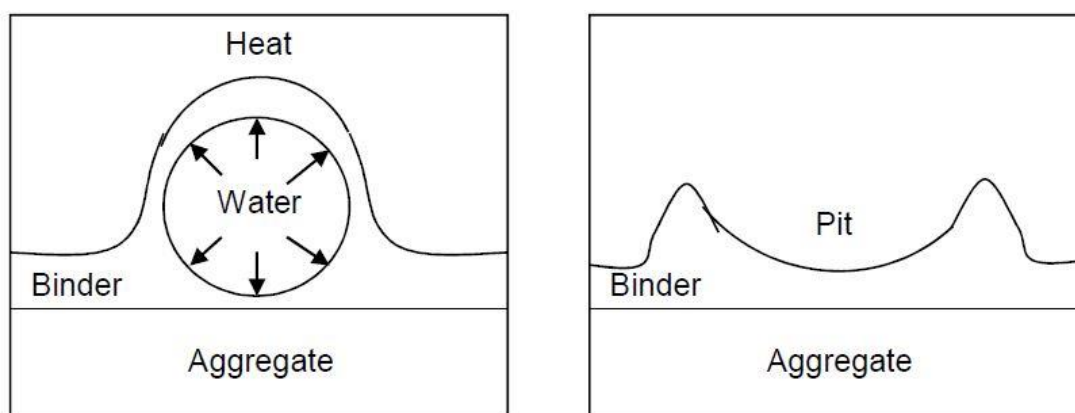
Figure 2-23: Illustration of pitting when viscosity of bitumen increases (Whiteoak and Read, 2003)

Lombard (2014) found that the temperature of the binder had the greatest influence on adhesion failure. Temperature related adhesion failures of surfacing seals are typically associated with two factors. For homogenous modified binders, the higher the level of modification, the higher the risk of adhesion failure due to decreased wetting ability and increased stiffness. At colder temperatures, the higher stiffness of the binder results in a decreased adhesion (TG1, 2008).

By increasing the film thickness of the binder layer the adhesion is improved. The film thickness of the binder layer can be increased by:

- Reducing the time-lag between the binder application and the stone application in surfacing seals.
- Using pre-coated stone.
- Using emulsion cover (fog) sprays to increase or correct the final binder application rate.
- Pre-blending an adhesive agent with the modified binder prior to spraying (TG1, 2008).

The constitution of bitumen furthermore affects adhesion in the bitumen-aggregate system, since it is the asphaltene content that provides adhesion. The level of modification that influences the viscosity of bitumen which in turn affects the wetting ability or time to coat the road stone with bituminous binder. Wetting is an instantaneous process but if the viscosity of

modified binder is too high during application, wetting takes longer and poor adhesion can be expected.

Temporary reduction of the viscosity by the addition of cutters during colder weather conditions also improves the adhesion properties. However, care should be taken in areas with hot humid climates and/or heavy traffic conditions. It should also be noted that different types of aggregates exhibit different adhesion behaviour depending on the chemical nature of the parent rock in terms of its hydrophilic (water-attractive) or oleophobic (oil-repelling) nature. Depending on the chemistry of the parent rock, the nature of the aggregate could vary. However, bitumen is oleophilic (oil-attracting) or hydrophobic (water-repelling).

Therefore, based on the inherent character of the aggregate it may or may not react (form chemical, charge-related bonds) with water but the presence of water will have a negative influence on the adhesion properties and it will repel the bitumen. Acidic aggregates are more hydrophilic than basic aggregates. Acidic aggregates will therefore have poor adhesion properties in the presence of water. Cationic spray grade emulsion overcomes this tendency when the free electrons on the aggregate form physical/electrical bonds with the positively charged bitumen and SBR latex droplets as shown if Figure 2-24.
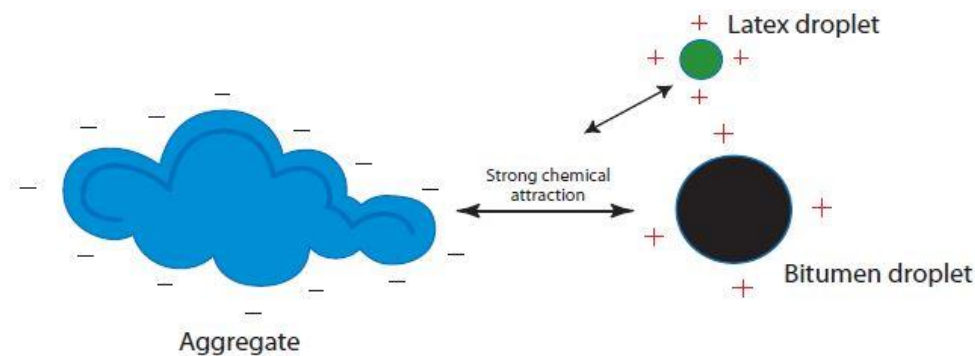
Figure 2-24: Adhesion characteristics of latex modified emulsion (TG1, 2008)

Similarly and, especially in high risk applications and under difficult construction conditions, surface active chemicals in commercially approved adhesion promoters and pre-coating fluids have been used effectively to improve the adhesion properties. However, if these are used in conjunction with bitumen emulsions in the construction of a surfacing seal, they are known to retard the breaking characteristics of the emulsion.

The electrical polarity of the binder also has an influence on adhesion. Bitumen is comprised of non-polar hydrocarbons; it is possible that heteroatoms such as nitrogen (N), sulfur (S), and oxygen (O) may also be form part of these molecules. Furthermore, trace portions of metals also exist and are deemed to be "fingerprints' of the crude source (Robertson, 2000). These atoms introduce polarity into bitumen molecules and although only present in small amounts, have a controlling effect on the properties of the bitumen and its interaction with aggregate surfaces (Petersen et al., 1982).

Petersen (1986) has identified polar, strongly associated functional groups in bitumen. Figure 2-25 shows the chemical structures of important functional groups in natural bitumen including those formed during oxidation.
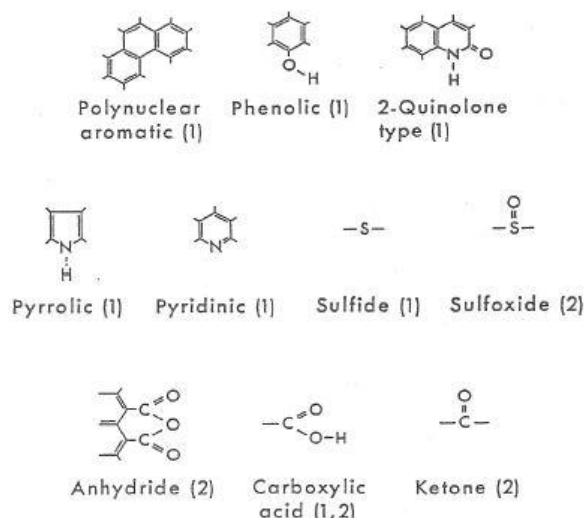
Figure 2-25: Important chemical functional groups that are naturally occurring and formed on oxidative ageing (Petersen 1986)

Benzene-like, unsaturated ring structures are common hydrocarbon compounds in crude oil, and along with alkanes, are typical constituents in the molecular make-up of bitumen (McMurry, 2000). According to the historical micellar model, resins and ultimately asphaltenes represent the more polar fractions in bitumen. These fractions are also the higher molecular weight, or larger molecular size fractions.

Petersen and Plancher (1998) showed that the two chemical functionalities, carboxylic acids and sulfoxides, account for almost half of the total chemical functionality in the strongly adsorbed fractions. These compounds are both hydrophillic (water loving), with aliphatic structures (zigzag chains as opposed to aromatic ring structures) with no other polar functional groups on the same molecule (mono-functional as opposed to poly-functional). This may contribute to their ease of displacement by water.

Developing cohesive strength, in order to behave reliably in a visco-elastic mode:

Cohesion is a measure of the tensile stress required to break the bond between molecules of the bituminous binder. The inherent strength, tenacity and toughness of the bituminous binders are improved by modification with thermoplastic polymers and rubber crumbs. Hence, a greater force or tensile stress is required to break the molecular bonds of modified binders and cause failure compared with a lower tensile stress required to break the bonds of conventional binders.

A force-ductility test is used to determine the cohesive strength of a modified binder and involves the elongation of a sample with the force measured at very small elongation intervals (TG1, 2007), as illustrated in Figure 2-26.
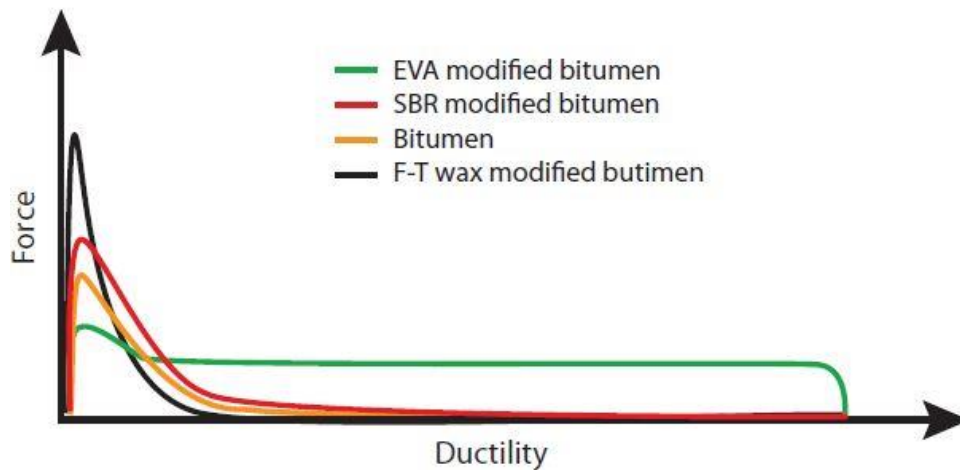
Figure 2-26: Force-ductility of modified bitumen (TG1, 2007)

In the figure above the maximum force is reached early in the elongation process. The elastic phase is represented by the area before the initial peak and the total area under the curve can be used to calculate toughness. This is a good indication of the energy required to extend the binder and therefore provides a good estimation of resistance to cracking. The energy required to elongate elastomeric modified binders is generally significantly more than that for conventional binder. Plastomeric modified binders will impart stiffness to the bituminous binders but not necessarily improve its cohesive nature. Such modified binders may well perform in a brittle manner in tension.

The cohesive properties of modified binders provides guidance to practitioners related to how soon after construction a seal could be opened to traffic as well as providing an assessment of the ability of the binder to withstand shear stresses imparted by heavy traffic.

During construction the binder develops adhesive and cohesive strength. Initially it's a liquid that facilitates the placing and wetting of the stone and then it quickly becomes hard. The binder plays an important role as it provides adhesion between the stone and the road surface. Upon opening the road to traffic the cohesive forces prevent the stone from being pulled from the surface (TRH 3, 2007).

Consistency in the spraying of bituminous binder is dependent on its viscosity, which changes with change in temperature. As discussed previously, each grade of binder has its own unique temperature/ viscosity relationship that determine ideal viscosity needed for optimum spray applications (TRH 3, 2007). If this relationship is not adhered to, streaking is most likely to occur, when the binder becomes too cold and stiffens up. The binder can also break down, run off on steep gradients (seen in the application of emulsions) and become an increase fire hazard if weather conditions become too hot.

Behaving flexibly and resilient, in order to recover from deformation from applied loads:

The Asphalt Institute's Asphalt Surface Treatments-Construction Techniques (1998) requires a bitumen used in seals to not bleed during application at suitable rates. The binder must also be sufficiently fluid to cover the surface and at the same time be sufficiently viscous not to run off, during time of application. It is important for binders to be flexible when exposed to

different temperatures. Upon heating binders become soft and start to flow, whereas when cooled they become rigid and hard.

A suitable binder should therefore be able to withstand high temperatures to prevent stone loss due to flushing from moving traffic and also remain flexible when colder to prevent moisture entering the base, accommodate road deflection and prevent reflection cracking. The most suitable binder is therefore one that is durable and flexible under various climatic conditions.

In 1997, Muthen and Bergh, made the following comparisons between bitumen binders, based on the differences in their composition, working temperature and ageing properties:

- Penetration grade binders retain their flexibility for 2 to 3 years and become brittle at low temperatures (about 5°C).
- Modified bitumens remain flexible for 5 to 17 years, depending on the modifier. Bitumen rubber however retains flexibility for up to 15 years only and when temperatures are -5°C.

Add to the safety and structural performance of the surfacing layer, by limiting the flushing potential and extent:

Flushing on seals is caused by the upward migration of binder which results in full or partial covering of surface aggregate. This creates a smooth surface with low skid resistance. As a result, flushing causes major problems in terms of both safety and structural performance of the pavement surface. In New Zealand, flushing of seals has been recognized as one of the key reasons for resurfacing on national roads (Koddipily et al., 2010), which could be explained by the excessive binder quantities that result from the build-up of sprayed seal layers, a practise that is common in New Zealand (See *Section 2.5.4.. Seal Design* for further discussion).

There are various factors of the binder that influence the potential and extent of flushing of the sprayed seal. The binder susceptibility to temperature and loading plays an important role in the potential and extent of flushing. When exposed to high temperature and short loading period the viscosity of bitumen will reduce, resulting in an increased embedment of aggregate into the substrate. Additionally, when bitumen occupies the voids in the sprayed seal it can also lead to flushing (Lawson and Senadheera, 2009). Flushing due to the occupation of voids by the bitumen is also dependent on water vapour or large amounts of fines, which can similarly occupy the voids and cause the bitumen to migrate upwards.

The reduction of binder application rates is one of the measures taken in the current sprayed seal industry to minimise flushing and to achieve sufficient texture. Sand texture for the flushing potential is quantified by the sand patch test as well as the mean of aggregate profile depths as illustrated in Figure 2-27.
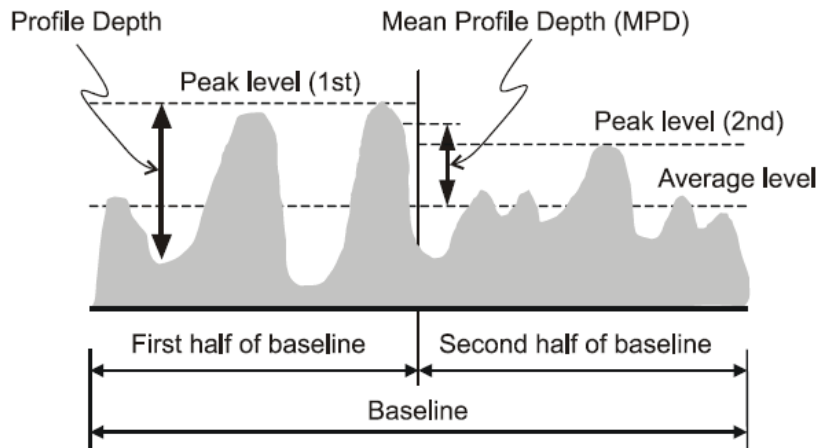
Figure 2-27: Determination of mean profile depth (Flintsch et al., 2003)

Reducing the application rates however can create additional surfacing problems such as increased aggregate loss, which is another reason for resurfacing. Although there are various criteria that aid in selecting acceptable binder grades, the success of such a selection is still greatly influenced by experience of the designer and as such it is still challenging to estimate the future performance of binders (TRH3, 2007).

Ball and Patrick (1998) found that the harder bitumen grades, such as 80/100 pen bitumen or 130/150 pen caused a delay in flushing and considerably increased the life of the sprayed seal, when compared to a 180/200 pen bitumen, since the former binders have higher softening points that ensure that the binder will not flow in service. The softening point is also related to the ageing of bitumen, since a loss of volatiles in the binder occurs over time, resulting in a low softening point, which ultimately yields a softer (less stiff) binder that has a higher flushing potential.

Flushing however is not only influenced by the binder properties but also by the frequency of load application (Ball and Patrick, 1998), tyre pressures and different mechanisms of moisture ingress (Ball et al., 1999) and the extent of aggregate embedment in the wheel path as opposed to between the wheel paths (Alderson and Oliver, 2008).

Waterproofing the pavement structure in order to protect the underlying pavement structure:

Bitumen waterproofs the pavement structure in order to prevent the underlaying support layers including the subgrade from becoming saturated through moisture ingress. When saturated, the structural layers below lose their ability to adequately support the applied axle loads, which will lead to premature failure of the pavement.

Providing durability, through resisting ageing:

Bitumen and asphalt mixtures are not only affected by temperature but also by oxygen and UV radiation. UV radiation and especially the influence of oxygen will cause ageing of bitumen and asphalt mixtures. Ageing causes bitumen and asphalt mixtures to be stiffer and

37

more brittle. Bituminous materials are losing their flexibility due to the combined effects of oxygen, UV radiation and temperature.

Ageing has a significant effect on the characteristics of the bitumen. Ageing occurs during production, storage and transportation of the hot mix to the construction site, also known as short term ageing. During that period some of the volatiles will evaporate making the bitumen harder. But also during the lifetime of the pavement, significant ageing can occur because of the influence of temperature, oxygen and UV radiation. Figure 2-28 below shows how this long term ageing can change the bitumen characteristics.
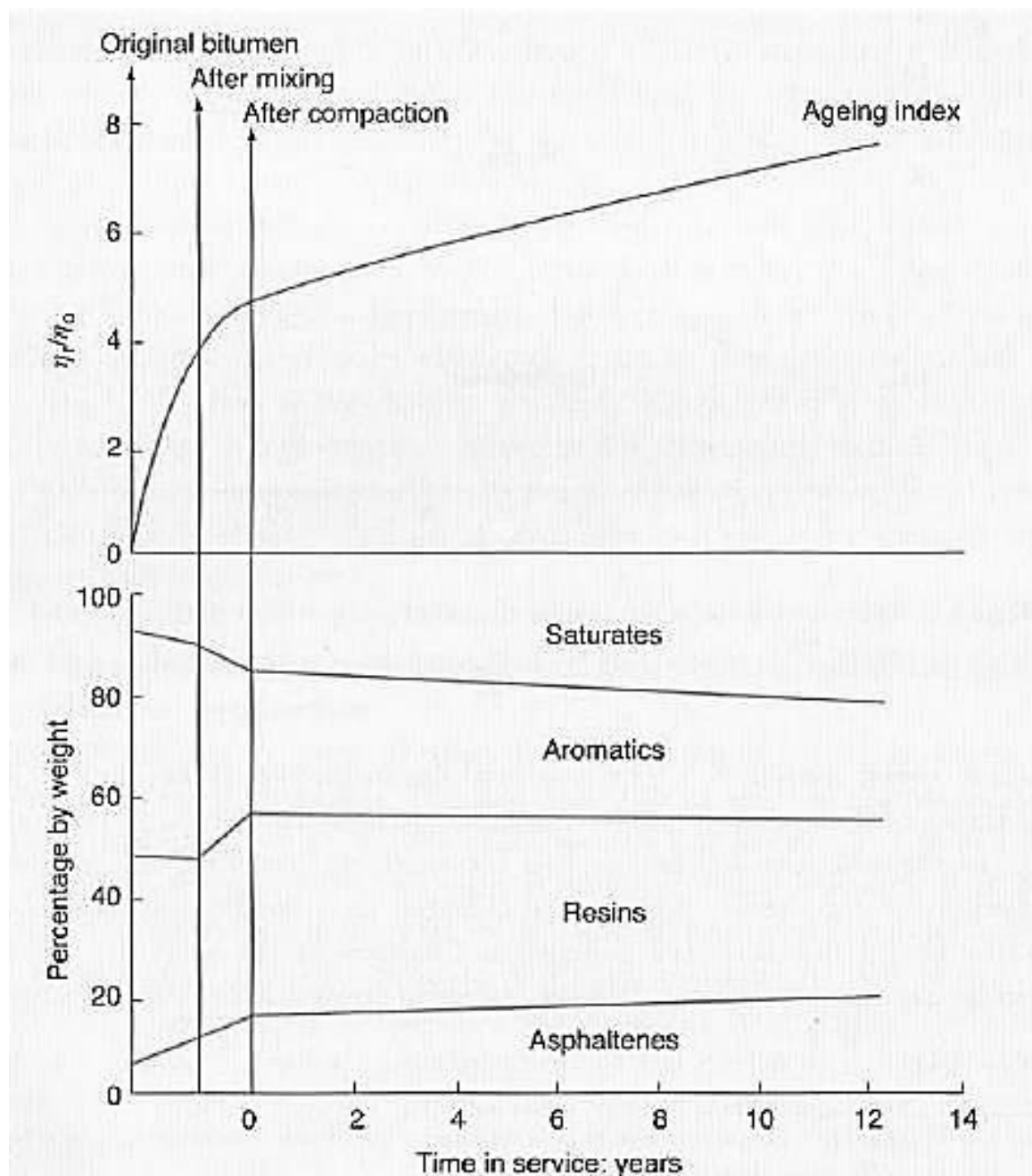
Figure 2-28: Changes in bitumen composition over time (Whiteoak and Read, 2003)

Simulating the ageing that occurs during the production and laying of asphalt mixtures is relatively simple. One just has to subject the material to the same temperature regime and during the same period of time as occurs in practice (mixing + storage + transportation + laying and compacting). However, simulating in the laboratory the ageing that occurs in practice in the road is a delicate task. Ageing in the road is a relatively slow process but the amount of time that is needed to age bitumen in the road is not available when evaluating materials in the laboratory. For practical reasons we like to reduce the ageing period in the laboratory to e.g. one week (Molenaar, 2013).

This means that one has to accelerate ageing and usually this achieved by subjecting the bitumen to elevated temperatures, pressure and a flow of air or oxygen. By doing so it is indeed possible to achieve penetration and ring and ball temperatures of the artificially aged binder which are comparable to the values which would be obtained from bitumens that are aged in the road. The question however is whether the material aged in the lab still has the same chemical characteristics as the material which is aged in the field.

Short term ageing implies the loss of volatiles while long term ageing implies the formation of oxides called ketones and solfoxides (oxides of carbon and sulfur). Short term ageing is usually performed in the laboratory using the following tests:

- RTFOT (EN 12607-1): Rotating Thin Film Oven Test
- RCAT163 (draft NEN-EN 15323): Rotating Cylinder Ageing Test

Table 2-9: Laboratory test conditions for short term ageing of bitumen

Test Conditions	RTFOT	RCAT163
Temperature (°C)	163	163
Duration (min)	75	235
Amount of bitumen (g)	8 bottles x 35g	500g

The Rolling Thin Oven Test (RTFOT; ASTM D 2872, EN 12607-1) shown in figure 2-29 is used as a standard test under the SHRP binder specification to simulate ageing in hot-mix asphalt plant. The ageing test is conducted by placing 50 g of bitumen in cylindrical bottles that have an opening at one end (there are 8 bottles in total). The bottles are placed in oven at 163°C for 75 min (85 min in the case of SHRP specification). The bottles rotate in a carousel, and fresh hot air is periodically injected into the bottles.
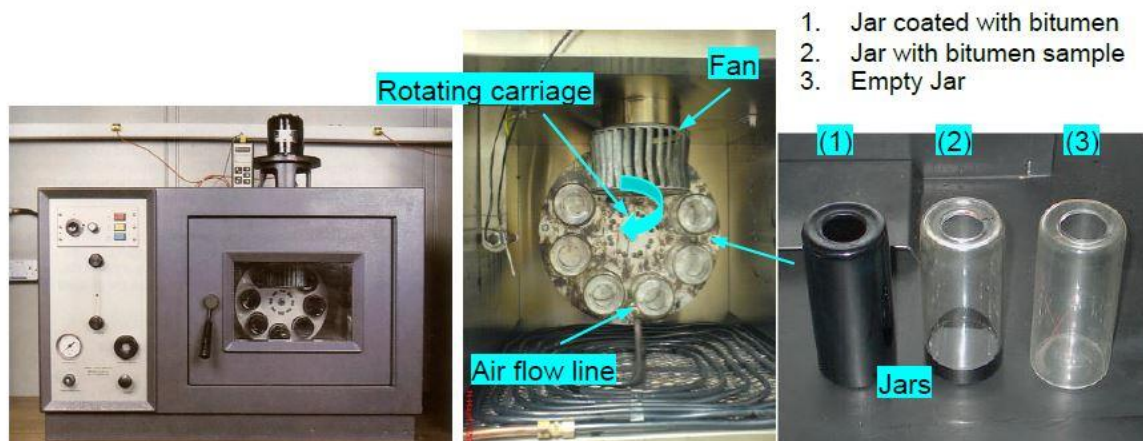
Figure 2-29: Rotating Thin Film Oven Testing Apparatus (RTFOT) for short term ageing of bitumen (Molenaar, 2013)

The % mass loss is determined. The effect of hardening is determined on the basis of the change in mass loss (expressed as a percentage) and/or as a change in the binder property, such as penetration (EN1426), softening point (EN 1427) or dynamic viscosity (EN 12596), before and after oven ageing.

As mentioned before, long term Ageing refers to the ageing of bitumen during the service period of an asphalt pavement. The laboratory accelerated ageing method which is used in a number of European countries to simulate long term Ageing of bitumen is the RCAT90 (Rotating Cylinder Ageing Test). This test is performed based on the standard test for RCAT90 test (draft NEN-EN 15323) after the binder has been exposed to short term ageing.

The Pressure Ageing Vessel (PAV, SHRP test method B-005, EN 14769) is a SHRP ageing method used to simulate the oxidation process that takes place during the service life of the pavement. The binder is firstly aged for short term using either TFOT or RTFOT (SHRP standard test) method. In the standard PAV test (Figure 2-30) 50 g of binder is poured into preheated 140 mm diameter pan (the binder film thickness will be approximately 3.2 mm) and is placed in a shelf rack with a capacity of 10 pans. The temperature of the Ageing vessel is maintained at 85 ° C (PAV 85), 90°C (PAV 90), 100°C (PAV 100), or 110°C (PAV 110) and at a pressure of 2.1 MPa during the Ageing process that is run for 20 hours.
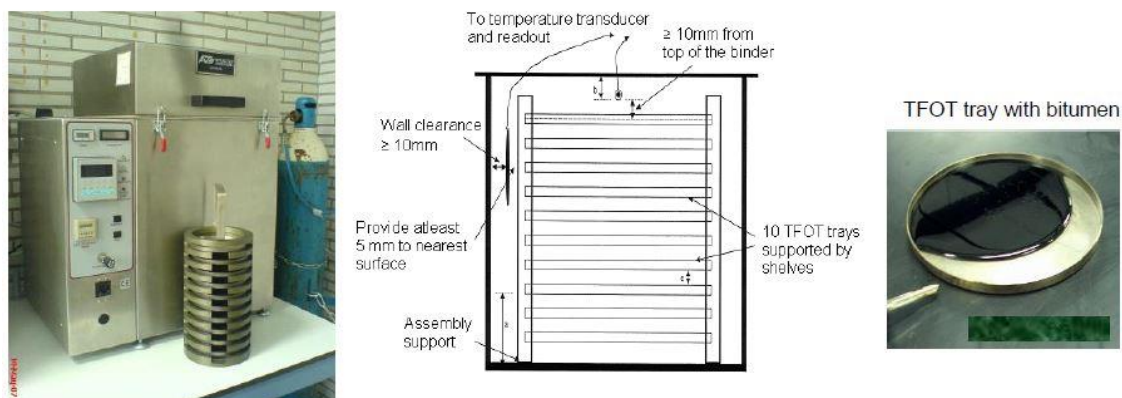
Figure 2-30: Pressure Ageing Vessel (PAV) apparatus and tray assembly inside the PAV (Molenaar, 2013)

Ageing temperatures below 100°C are generally recommended in order to achieve similar chemical changes as in field ageing. The HiPAT (High Pressure Ageing Test) is another long

40

term testing method which is performed using the PAV equipment at a lower operating temperature and a longer Ageing time. The HiPAT Ageing test is conducted at 85°C for 65 hours under 2.1 MPa air pressure. For a constant temperature, ageing with application of different pressures will result in different degrees of hardening of the binder. Furthermore one should be aware of the fact that the rate of increase in binder ageing is not only pressure dependant, but also geometry, temperature and time dependant.

It is claimed that the PAV ageing method accelerates the binder ageing without destroying the integrity of the binder. The ageing of bituminous materials according to this procedure was introduced to model field ageing and predict performance. Researchers debate however that accelerated ageing tests conducted at elevated temperature above the actual pavement temperatures may result in a change of binder properties different from reality.

A major criticism of researchers to the PAV ageing technique is that it is a static test and the diffusion of oxygen is inhomogeneous leading to differences in ageing between the surface and the bulk of the sample. It has been shown that polymer migration occurs in the PAV ageing of PMB materials by investigating the top and bottom parts of the aged specimens. Nevertheless, it is possible that the ageing process in the road is also similar to the static Ageing which substantiates the PAV ageing procedure for simulating long term Ageing. The PAV aging procedure however has a drawback of only simulating a few years, ageing for 10 years and beyond is yet to be simulated (Glover et al., 2005).

The Rotating Cylinder Ageing Test (RCAT), figure 2-31, is an accelerated ageing test developed by the Belgian Road Research Centre (BRRC) to simulate both the short and the long-term ageing of binders.
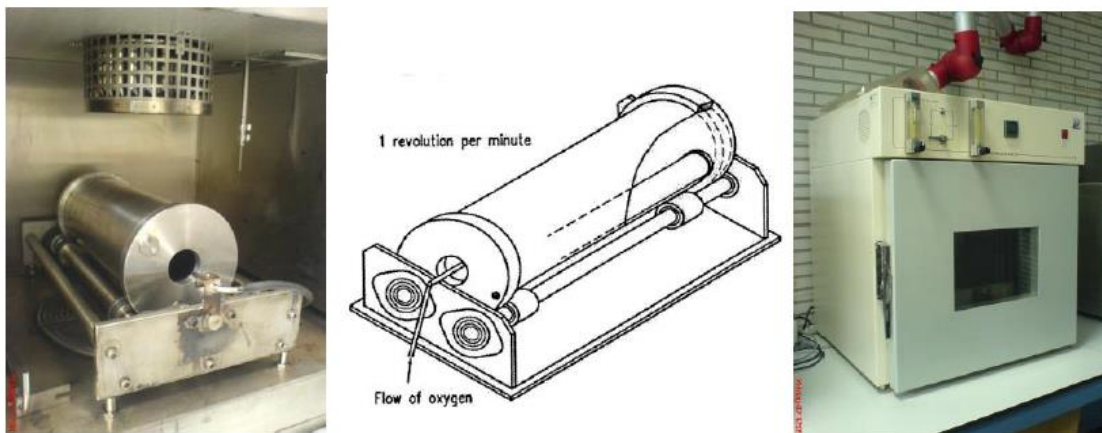
Figure 2-31: RCAT apparatus used for accelerated testing of bitumen

The test is dynamic, ageing of binder is uniform, and the amount of aged binder is sufficient for further testing to characterize the bitumen. Despite the long duration of testing, which is a major disadvantage, it has the advantage of monitoring the development of ageing on the properties of the binder at various intervals of time (reaction time) during the testing process.

Table 2-10: The laboratory test conditions for long term ageing of bitumen

Test Conditions	RCAT90
Temperature (°C)	90
Duration (min)	185*
Amount of bitumen (g)	500g

*The long term ageing time of bitumen in the standard test is specified as 140 hours. An ageing time of 185 hour is often used to account for the high amount of ageing of porous asphalt mixtures, with a void content greater than 20%.

Another major advantage of the RCAT test is that it is possible to combine short-term (RTFOT-type) ageing test and long-term (PAV-type) ageing for the same sample and with the same equipment, which reduces intermediary sample handling operations. It has been shown that the long term ageing procedure using the RCAT method produces good correlation with recovered binder samples from porous asphalt pavements.

This may be explained by the relatively slow ageing process, prevention of skin formation and uniform ageing of the binder compared to PAV ageing which is also conducted at the same temperature.

2.5. Sprayed Seal Unit Influencing Performance

2.5.1. History and Development as a Wearing Course

The design of a sprayed seal involves calculating accurate quantities of a bituminous binder together with corresponding volume of aggregate that will be placed over a unit area of pavement surface (NCHRP, 2005).

In 1935 New Zealander, F.M Hanson presented the first ever design procedure for seals in his paper *"The bituminous surface treatment of rural highways"* to the Conference of NZ Society of Civil Engineers (Hanson, 1935). The National Roads Board 1968 *"Manual of sealing and paving practice"* provided the following synopsis of his theory and can be seen in Figure 2-32:

- When aggregate is placed on a bituminous binder, a single layer thick in shoulder to shoulder contact, the void percentage of the initially loosely placed aggregate is nearly 50%. During construction this is lessened to 30% due to rolling effects and to 20% later as a result of traffic compacting the aggregate further.

42

- A relationship exists between the quantity of required binder and the volume of stone aggregate. It was understood that 65-70% of the voids, after compaction, be filled with binder.

- After construction and traffic compaction, the average depth of embedded stone aggregate is roughly equivalent to the average least dimension (ALD) of the stone aggregate used.
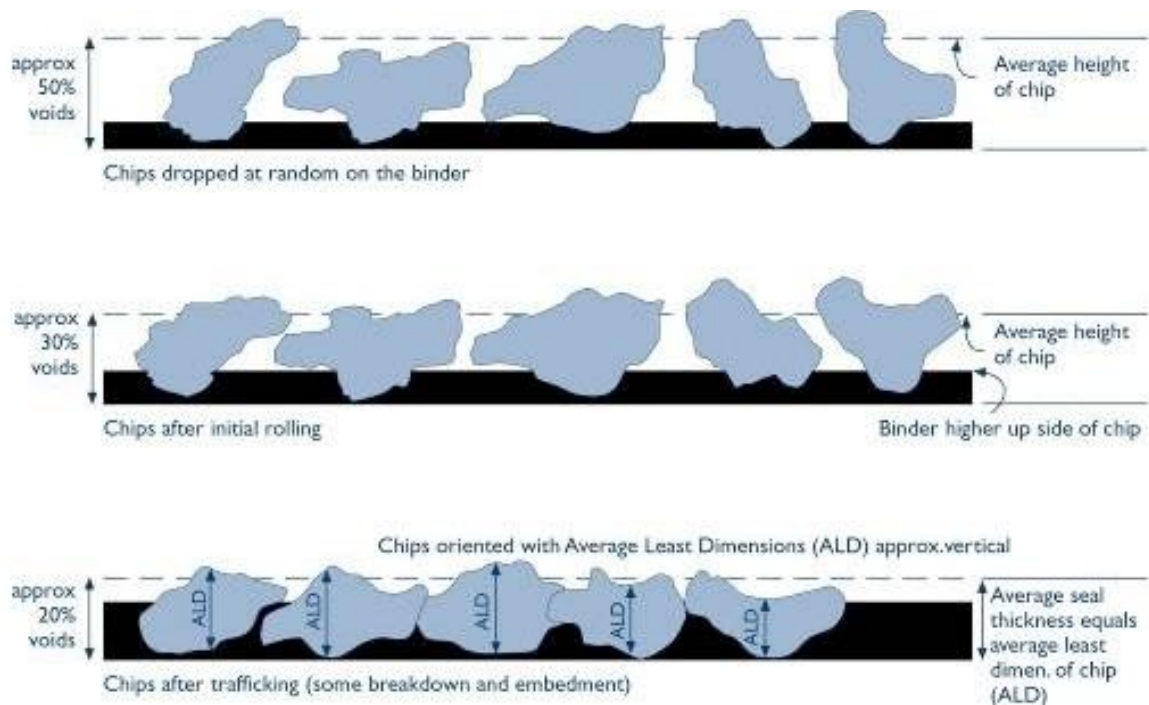
Figure 2-32: Levels of embedment of aggregate in binder (NRB Manual, 1968)

Hanson based his whole theoretical approach on the ALD of the stone aggregate that is placed on the pavement surface. Marais (1979) similarly found, through his observations, that when a coat of bituminous binder is uniformly distributed over a pavement and embedded with a single sized stone aggregate, only one layer of stone stays bonded with the pavement, following the removal of excess chips by traffic. The bonded aggregate adjust their position to a close-packed mosaic structure. Stone aggregates end up lying with their ALD in vertical direction.

SANS 3001-AG3 defines the ALD as the average of the least dimensions of all particles in which the least dimension of a single aggregate particle is the smallest perpendicular distance between two parallel plates through which the particle will just pass. It furthermore relates the grading obtained from the particle size analysis to the shape of the aggregate (flakiness index) as can be seen in Figure 2-33 below.
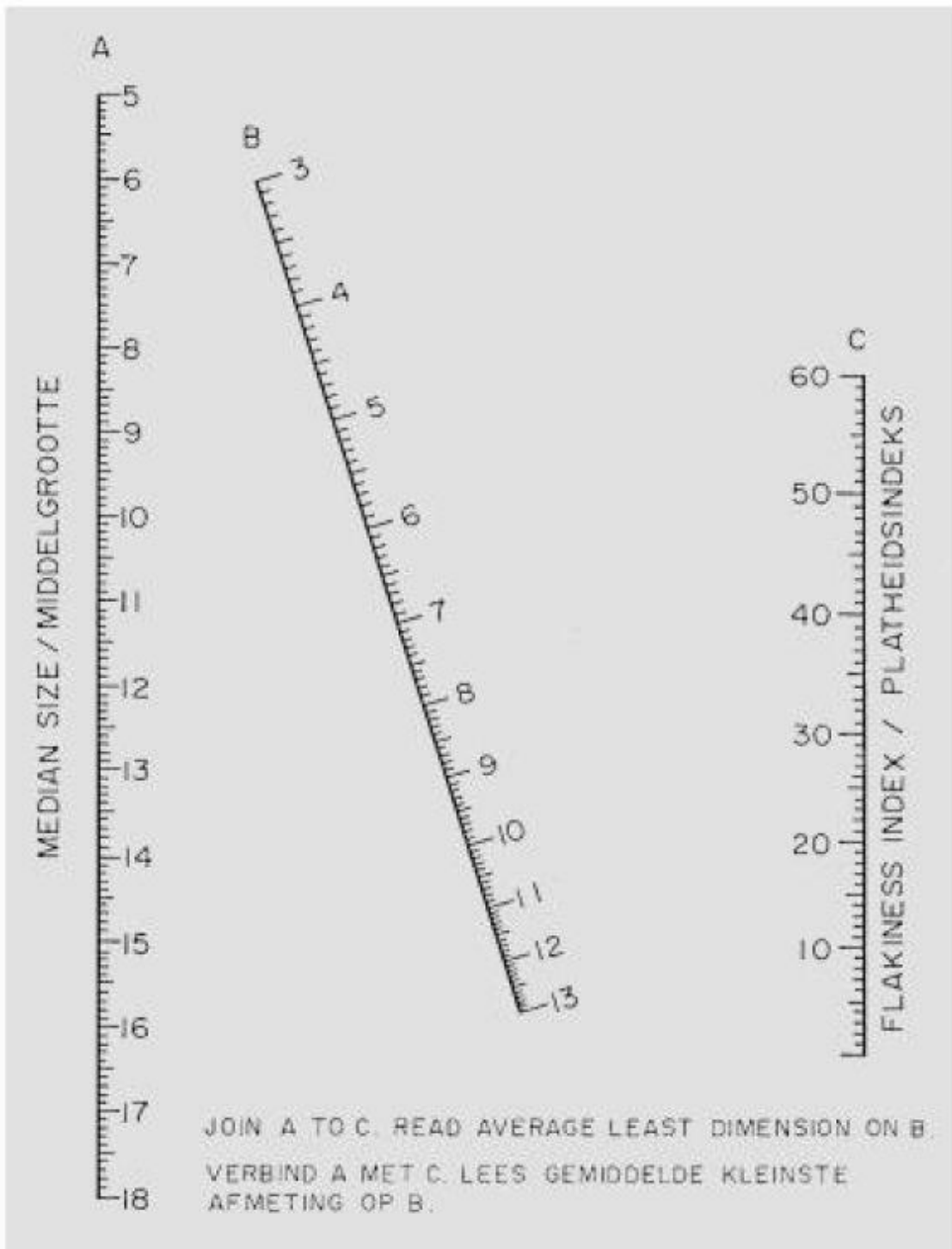
Figure 2-33: Determination of ALD using Median Size and Flakiness Index (TMH1, 1986)

Marais (1979) was convinced that the majority of defects and failures occurring in seals were due to unsatisfactory attention given to embedment. Marais found that the amount of expected embedment couldn't be precisely predicted in practice. An idea of embedment can however be deduced from the type and intensity of traffic, which are predominantly responsible.

Texture depth/ voids reduce after a short period of time (the first three months), with it steadying after roughly three years. A further factor affecting embedment is surface temperature; higher surface temperatures cause greater embedment. Marais (1979) attempted to measure the expected embedment and consequently, the lessening of voids/ surface texture, by using the Ball Penetration Test, as can be seen in Figure 2-34 below.
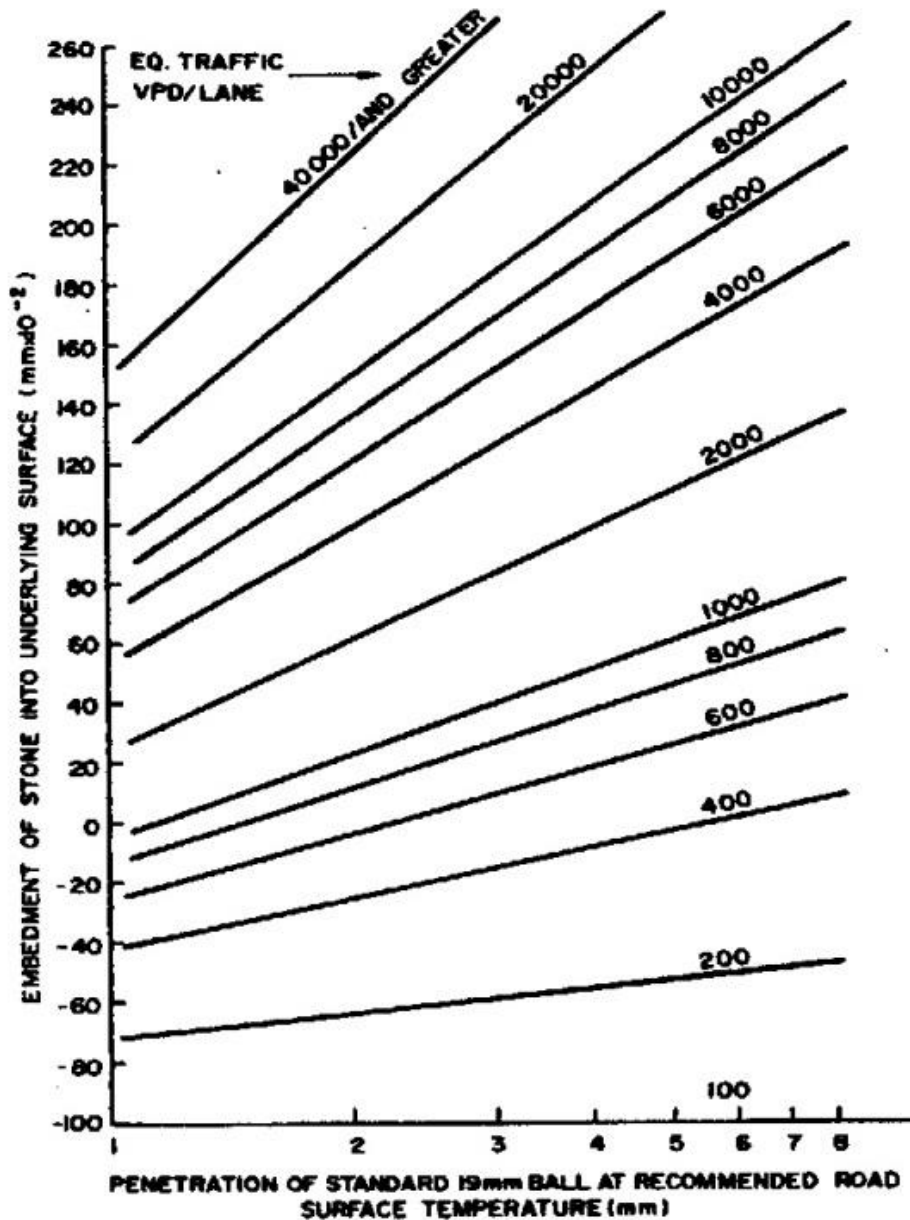
Figure 2-34: Link between penetration of standard ball, traffic and equilibrium embedment of aggregate into surface (Marais, 1979)

2.5.2. Type of Seals

2.5.2.1. Single Seals

Seals are generally assumed to be single seals unless otherwise stated but can encompass a large range of aggregate and binder types (Figure 2-35).

Choice of aggregate size, binder type and the design of aggregate and binder application rates are important factors in the selection of single seals for a particular application.
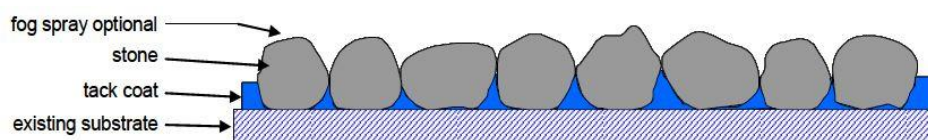
Figure 2-35: Single Seal Structure (TRH 3, 2007)

Of all the sprayed seal types, the single seal is the most "unforgiving" due to the limited amount of voids available. A small error in the aggregate and binder application rates can cause a significant error on the percentage of voids that are available to be filled with bitumen. In the case where smaller aggregates are used in single seals, this is particularly true. Aggregate loss may be substantial, but can be prevented, to a certain extent, by using pre-coated aggregates.

The aggregate spread rate therefore becomes the most influential factor, as the available voids are limited. For this reason, it is important to ensure that aggregate particles are orientated in a tight fitting mosaic pattern, to guarantee a shoulder to shoulder interlock pattern of aggregates, embedded in the binder layer (TRH3, 2007). Careful rolling and brooming are thus important construction factors to take into account.

Single seals are also unforgiving with regards to the completed base layer. Since these seals are relatively thin, any imperfections in the base will be mirrored through to the surface and have a negative effect on the riding quality for the road user.

2.5.2.2. Double Seals

A double sprayed seal is applied by spraying a layer of binder, spreading the large sized aggregate and, after trafficking and/or suitable rolling, spraying another low application of binder followed by the spreading of a layer of smaller aggregate. The smaller aggregate fits into the spaces between the larger aggregate and locks it into place (Figure 2-36).
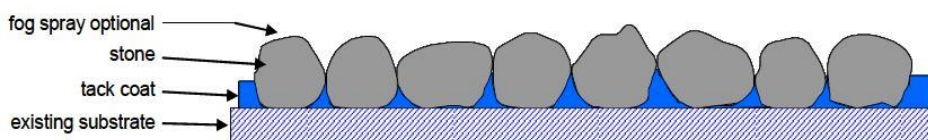
Figure 2-36: Double Seal Structure (TRH 3, 2007)

Double seals are used when:

- Additional waterproofing must be ensured
- The traffic noise from a single application (single/single) is unacceptable
- A fine texture is required (parking areas, residential streets, footpaths, etc).
- In areas subject to high shear loading compared to single application (single/single) seals.

Double seals are also commonly used in geotextile reinforced seals as they provide a more robust treatment with better resistance to turning traffic than single/single seals.

In remote areas the second application of a double seal has been used to protect the binder in the bottom layer from extreme climatic conditions and dust, resulting in an increase in the life of the sprayed seal. Table 2-11 show double sprayed seal combinations in South Africa and Australia, respectively.

Table 2-11: Double Sprayed Seal Combinations

In South Africa (TRH3, 2007)	In Australia (Austroads, 2009)
13.2mm with 6.7mm	10mm with 5mm
19mm with 6.7mm	14/16mm with 5/7mm
19mm with 9.5mm	20mm with 7/10mm

The double seals (together with the Cape Seal) normally give better performance results when compared to the single seals, since these seals have better aggregate retention. Application of the binder can be up to three applications, which causes the lower layer of aggregate to be wedged or filled in by the aggregate layer that follows, thus improving stone retention.

The use of pre-coated aggregate or the application of a fog spray can further enhance this retention of aggregate in a double sprayed seal (TRH3, 2007). Double seals are also less permeable than single seals, since they have binder content that far exceeds that of single seals, as more voids can be filled.

In Australia and New Zealand, in addition to the double seals, a racked-in sprayed (also known as a single/double) seal is also used, which is a variation to the double seal. It is constructed by spraying a single layer of bitumen, spreading the large-sized aggregate at less than the normal spread rate and, after suitable rolling, spreading another layer of smaller aggregate. The smaller aggregate fits into the spaces between the larger aggregate and is locked into place by a small amount of bitumen (from the first spray). In a racked-in seal, the second aggregate application is a permanent and integral part of the seal (Austroads, 2009).

2.5.2.3.   Cape Seals

Cape seal was developed and first used in Cape Province, South Africa. It is constructed by applying a single seal to the pavement (usually using a size 13mm or 19 mm aggregate) followed by a slurry surfacing that can either partially fill the void space between the bitumen and the top of the aggregate, or completely cover the top of the aggregate (Figure 2-37). This is achieved by either a single or double application of slurry.
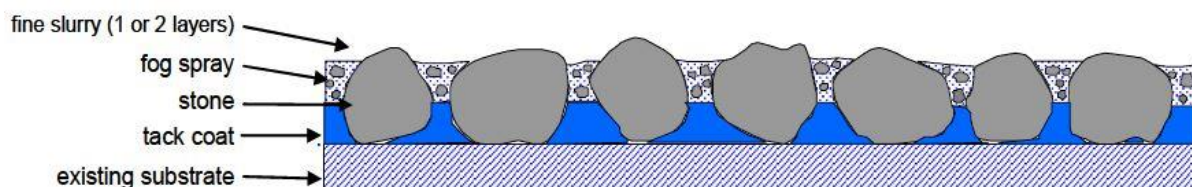
Figure 2-37: Cape Seal Structure (TRH 3, 2007)

The binder is split in two applications, as follows:

- Tack coat applied with either a hot binder or bitumen emulsion.
- Penetration coat applied as a mixture comprising of 60% stable grade emulsion and water applied at recommended/ nominal rate.

This type of sprayed seal provides a very robust surfacing and the surface characteristics are substantially those of slurry. It has been used in rural areas to provide a surfacing with high shear resistance, comparable to that of asphalt, but in areas where asphalt is not economically available.

The prevailing temperatures affect to a greater extent the choice of grade of bitumen and its application rate and to a lesser extent the type of sprayed seal. Care should however be given to the selection of the sprayed seal in wetter regions. In such cases, water ingress into the structural layers below (base and sub-base) and binder stripping from the surfacing, should be avoided by selecting a sprayed seal that is not permeable. The Cape Seal is usually selected in such instances.

Cape seals have various advantages. They are relatively easy to build and user friendly. Secondly, the application rates of the binders used are not critical as regards under application, since the slurry will rectify any error in under application (TRH3, 2007). Cape seals furthermore perform better than double seals, since they can carry higher traffic volumes and have a higher life expectancy.

The disadvantage of cape seals is that they are relatively expensive.

2.5.2.4.   Slurry Seals
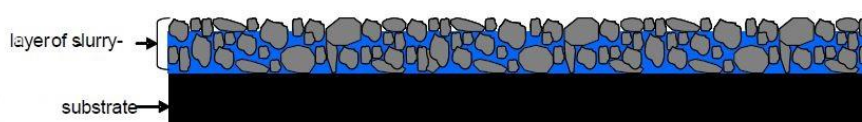
Figure 2-38: Slurry Seal Structure (TRH3, 2007)

2.5.2.5.   Sand and Grit Seals
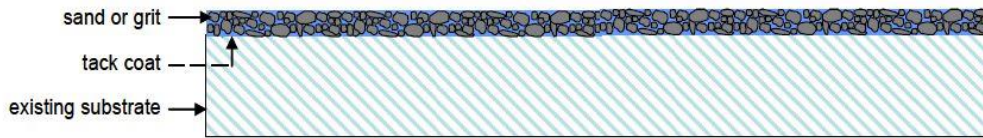
Figure 2-39: Sand and Grit Seal Structure (TRH3, 2007)

2.5.2.6.   Inverted Double Seals
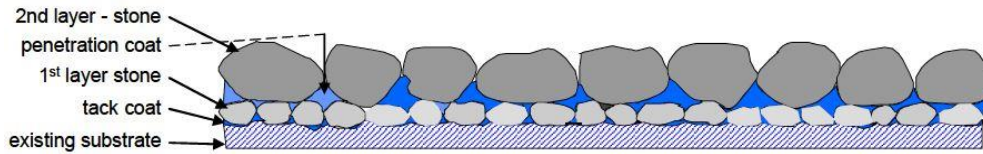
Figure 2-40: Inverted Double Seal Structure (TRH3, 2007)

2.5.2.7.   Graded Aggregate Seals (Otta)
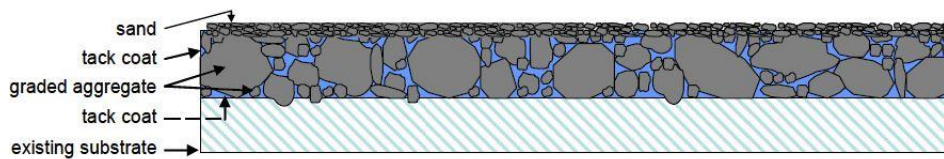
Figure 2-41: Otta Seal Structure (TRH3, 2007)

2.5.2.8.   Other Less Frequently used Seals
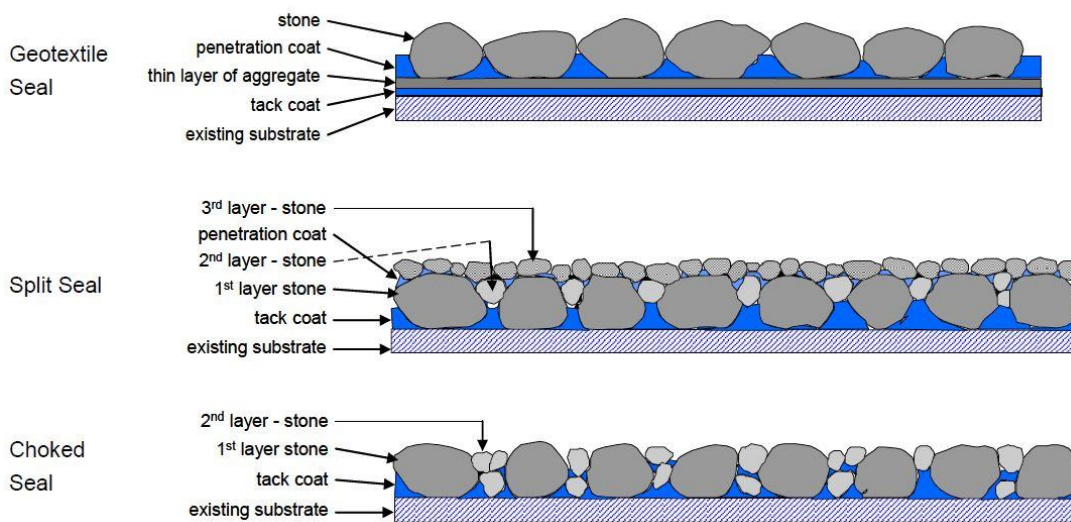
Figure 2-42: Less frequently used seals (TRH3, 2007)

2.5.3. Resistance to Shear Forces

Each type of sprayed seal has a different measure of resistance to shear forces. Factors that contribute to the development of horizontal stresses in sprayed seal surfacings are:

- The motion of the wheel (braking, accelerating, turning)
- Wheel loading, tyre type, inflation pressure
- The coefficient of friction between the pavement surface and the tyre rubber.

Regardless of the motion of the vehicle (braking, acceleration or turning action), these three factors control the level of the horizontal stress. In each of these driving actions, a limiting force and thus stress results from tyre slippage (skidding). Braking sometimes leads to slippage; acceleration rarely results in slippage; but turning (for a multi-wheel multi-axle assembly) always results in slippage where the turning circle is reduced to the point where the capacity of the tyre tread and side-wall compliance to accommodate the developed strain is reached. Tyre pressure affects the compliance of the tyre wall and therefore the tyre's capacity to accommodate this movement. Surfacing stress resulting from the action of turning vehicles is thought to be a major cause of distress in bituminous surfacings.

Resistance to shear forces can be an important factor in selection of surfacing type. A guide to typical relative resistance to shear stress of various surfacing types is provided in Table 2-12.

Table 2-12: Typical Relative Resistance to Shear Forces (Austroads, 2009)

Relative Resistance	Type of Seals
Greatest	Cape Seal
	Double Seal (including geotextile reinforced double seals)
	High Stress Seal (including single seal with polymer modified binder)
	Fibre Reinforced Seal
	Slurry Seal
Least	Single Seal (conventional binder)

2.5.4. Seal Design

The main factors that influence the selection of a sprayed seal as an initial surfacing is traffic volume, traffic actions, gradient, maintenance capability, required surface texture and construction techniques (TRH 3, 2007).

An initial surfacing is termed that because it is the first surfacing layer on a newly built road. The following seal type description is used in TRH 3:

S1   = Single seal

S2 (9)   = Double seal with 9.5mm stone aggregate and sand

S2 (13)   = Double seal with 13.2mm stone aggregate and sand

S2 (13/6) = Double seal with 13.2mm stone aggregate followed by 6.7mm

S2 (19/9) = Double seal with 19mm stone aggregate followed by 9.5mm

S2 (19/6) = Double seal with 19mm stone aggregate followed by 6.7mm

S3   = Sand seal

S4 (13)   = Cape seal with 13.2mm stone aggregate and one layer of slurry seal

S4 (19)   = Cape seal with 19mm stone aggregate and one layer of slurry seal

S7   = Course slurry seal

AC   = Asphalt

2.5.4.1.   Traffic Considerations

Traffic Volume

Embedment, wearing and polishing of the seal aggregate is significantly influenced by the amount (volume) of traffic. Voids in the seal reduce as a result, causing flushing of aggregate and poorer skid resistance. But, it is also assumed that for a seal with a conventional binder, a minimum of 50 vehicles per day is required to keep the binder soft and flexible (TRH3, 2007).

For polymer modified bitumen this required volume is higher. In discussions it has been the understanding that this volume is needed to disintegrate large chain hydrocarbons that are created from oxidation and also to remove bulky oxidized matter by the abrasive action of traffic (Milne, 2004). Care should be given to this value as some justification states that 25 vehicles per day are acceptable for a single seal (SABITA, 1992, Manual 10).

Equivalent light vehicles (ELV), as defined in South Africa, are equivalent to L+40HV. Seals are mostly used on roads carrying 125 – 20 000 ELV per lane per day. Roads carrying more than this traffic volume will require an asphalt surfacing (TRH 3, 2007). Table 2-13 below displays the recommended sprayed seal types with their allowable range of traffic volume.

A single seal is mostly placed for normal conditions where no special attention is required, with a traffic volume up to 2000 ELV.

Table 2-13: Recommended sprayed seal types with corresponding allowable traffic volume (TRH 3, 2007)

Traffic Volume (ELV/lane/day)	S3	S7	S1	S2 (9)	S2(13)	S4(13)	S2(13/6)	S4(19)	S2(19/9) S2(19/6)	AC
< 750	√	√	√	√	√	√	√	√	√	√
750-2000	x	√	√	√	√	√	√	√	√	√
2000-5000	x	x	√a	√a	√a	√	√	√	√	√
5000-10000	x	x	x	x	√a	√	√	√	√	√
10000-20000	x	x	x	x	x	√a	√	√	√	√
20000-40000	x	x	x	x	x	x	√a	√a	√	√
>40000	x	x	x	x	x	x	x	√a	√a	√

Note:

√ - Recommended

x - Not recommended

a – Several cases have been observed that showed good performance. Modified binders and trials on site can possibly lessen associated risks of loss of skid resistance and bleeding

Heavy Vehicle Concept

More stone will be embedded in the existing surface with heavy axle loads than with lighter ones. The increase of tyre pressure is another factor influencing seal performance. Tyre inflation pressures contribute to bleeding and certain vertical stresses here can be lower than on the surface (TRH3, 2007). Through Heavy Vehicle Simulator (HVS) tests it was found that more flushing of aggregate occurred on segments trafficked with similar wheel loads but with greater inflation pressures.

Tandem or tridem axles harm the surface when turning into/from access roads or at intersections. The road surface experiences high shear loads and raveling, debonding or

slippage may result. Furthermore the speed of the vehicle also plays a role in causing damage to the seal. It is found that for slow-moving vehicles (less than 40km/hr), seals experience more damage because of the prolonged period of loading, fuel spillage and higher horizontal stresses induced by traction.

Excessive movements of traffic in a specific wheel path (e.g. narrow roads) will severely influence the performance of seals. The same can be said for roads opened to traffic prematurely, when the binder is still soft or roads exposed to cold temperatures, when the binder is brittle (TRH 3, 2007).

Traffic plays a role in determining the volume of binder required to embed the stone aggregate (NCHRP, 2005). The percentage of heavy vehicles needs to be included in the design procedure as well when traffic is considered as an input design parameter. Higher traffic amounts lessen bituminous binder application rates (*Seal Coat and Surface Treatment Manual* 2003); due to heavy traffic causing more embedment once traffic is allowed on the sprayed seal. This incorporation of heavy traffic is achieved by calculating annual daily traffic (ADT) and adding an adjustment factor for heavy vehicles (TRB, 2005) or by using an equivalent heavy vehicle concept (TRH 3, 2007; Austroads 2002; Transit New Zealand et al., 2005).

In South Africa the amount of heavy vehicles are changed to equivalent light vehicles (ELV). Total ELV/ lane /day is calculated as (SANRAL, 2007; TRH 3, 2007):

*Total ELV/lane/day = Total light vehicles + Total heavy vehicles * 40*   Equation (1)

This adjustment factor used to be 20 in previous years (COLTO, 1998), but increase in tyre pressure and axle load demanded a higher value. Holtrop 2008a anecdotally stated that this number is no longer adequate and a revision should be considered.

In New Zealand, this heavy vehicle model was introduced in 1993, as a derivation from the South African TRH3 guideline. A Heavy Commercial Vehicle (HCV) was deemed equal to 10 light vehicles. HCV is labelled as a vehicle over four tonnes gross weight (Arnold et al., 2005). The increase in mass limits necessitates the need to revise the Equivalent Standard Axles (ESA). New Zealand practitioners currently assume that one HCV is equal to one ESA, hence:

1 ESA = 10 ELV*   Equation (2)

Speed

An increase in a vehicle's speed rapidly reduces the skid resistance of surfaces, particularly fine-textured (smooth) surfaces, which is necessary for road safety. For this reason it is desirable to design and construct coarse-textured (rough) surfaces for rural high speeds and the opposite for urban roads. As the operating speed increase, so would the required texture depth. A texture depth exceeding 0.7mm would be required for operating speeds faster than 80km/hr (TRH 3, 2007).

Speed also has an effect on the potential fattiness/bleeding of the binder. This particular defect was observed with the speed and profiles of heavy vehicles and should be taken into account when designing the sprayed seal (See Section 2.5.4.2.Road Geometry). Reduction of the binder application rates would be required for speeds less than 40km/hr.

Seals under lower operating speeds furthermore tend to perform weaker than those under higher operating speeds, due to the extended period of traffic induced loads and the increased horizontal stresses that result from the subsequent traction, mostly from the braking and accelerating of heavy vehicles and from oil and fuel spillage (TRH 3, 2007).

Care should be given to the operating speeds within urban drainage areas. This is due to the road carrying stormwater and subsequently moving soil particles and/or detergents in suspension, that increase the rate of erosion/ degradation of the sprayed seal. Single seals, thin sand seals and slurry seals should therefore not be designed and constructed in urban drainage environments or on steep gradients (TRH 3, 2007).

Once opened to traffic, the operating speed should be controlled to allow the sprayed seal to settle, particularly for the bitumen to develop adequate cohesion to hold the aggregate under traffic. This is normally achieved with proper traffic accommodation of the construction site, either by enforcing an operating speed of 60km/hr or by delaying opening the road section to traffic (TRH 3, 2007).

Traffic Actions

Table 2-14 below shows the seals most suitable with combinations of traffic and road types. These recommended allowable combinations have been based on experience on South African roads (TRH 3, 2007).

Table 2-14: Recommended sprayed seal types with corresponding allowable traffic and road type combinations (TRH 3, 2007)

Turning Actions	S3	S7	S1	S2 (9)	S2(13)	S4(13)	S2(13/6)	S4(19)	S2 (19/9) S2(19/6)	AC
Rural with occasional heavy vehicles	√	√a	√	√	√	√	√	√	√	√
Residential - developed	x	√a	√b	√	√	√	√	√	√	√
Residential - developing	x	√a	x	x	x	√	x	√	x	√
Urban with occasional heavy vehicles	x	√a	x	x	x	√	√b	√	x	√
Urban with many heavy vehicles	x	x	x	x	x	x	x	x	x	√

Note:

√ - Recommended

a – Only thick slurries (> 10mm)

x - Not recommended

b-Preferably blinded with coarse sand

2.5.4.2. Road Geometry

Steep gradients cause an increase in the traction force of tyres. This then leads to debonding, slippage or flushing of aggregate. On inclines and declines construction becomes challenging and adversely affects the seal performance. Inclines causes traffic to move slower and this result in flushing due to the extended loading period. Water diverted in a canal flow down declines and erodes the seal stone. This is aggravated in cases of roads with kerbs in hilly and wet locations.

Vehicles induce high horizontal stresses on the road surface when at sharp curves, resulting in slippage and ravelling of the seal. On lower volume roads these vehicles "cut" corners, causing stone loss as the outer part of the road become brittle and dry. Cambers on curves cause higher loads to be conveyed to the inner part of the bend, causing fattiness. In cases where surplus binder "ran-off" during construction and accumulated at these locations, the situation is amplified (TRH 3, 2007)

At intersections deceleration forces cause excessive horizontal shear stresses which result in slippage. In these areas the binder softens due to oil spillage. Fattiness in the wheel paths may also result because of concentrated traffic movements on narrow paths. This also creates a brittle zone between the wheel track and in edge breaks.

Earlier versions of TRH 3 and South African provincial design manuals recommended an adjustment of binder application rates at steep gradients, but practitioners within the sprayed seal industry agree that fattiness/ bleeding does not automatically correspond with steep gradients. The presence of this defect is mostly observed with the speed and profiles of heavy vehicles (Van Zyl, 2008) and is illustrated in Figure 2-43 below.
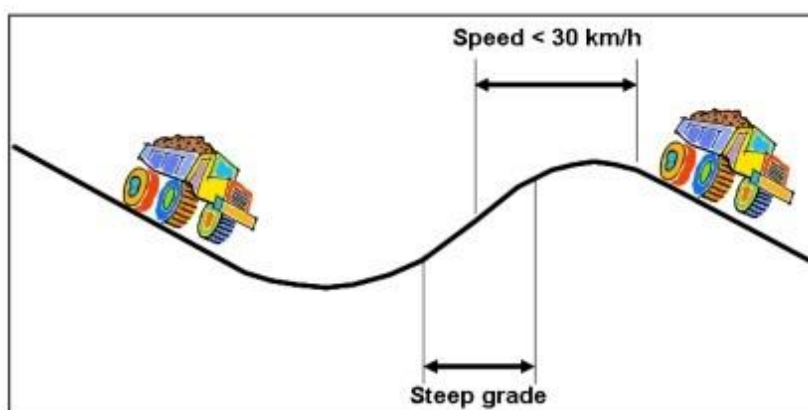
Figure 2-43: Correlation between speed of heavy vehicles and road gradient (Van Zyl, 2008)

Van Zyl (2008) observed that on short steep gradients following long down hills fattiness rarely occur, but have noted fatty surfaces on long up hills, even with gradients of 5%. This defect has also been noted on winding down hills, due to the effects of heavy vehicles braking and down gearing. A speed less than 30 and 40km/hr is most likely responsible for a fatty surface, but this also depends on the tyre pressures present.

Assimwe (2013) found that the application spray rate of the binder during construction had the highest influence on bitumen emulsion run-off, followed by texture depth and gradient.

Table 2-15 shows the TRH 3 (2007) recommendation for sprayed seal types with their corresponding allowable road gradient categories.

Table 2-15: Recommended sprayed seal types with corresponding allowable road gradient categories (TRH 3, 2007)

Gradient	S3	S7	S1	S2 (9)	S2(13)	S4(13)	S2(13/6)	S4(19)	S2(19/9) S2(19/6)	AC
< 6%	√	√	√	√	√	√	√	√	√	√
6 - 8%	b,c	a,d	b,c,d	c,d	a,c,d	d	c,d	d	c,d	√
8 -12%	a,b,c	x	x	c,d,e	a,c,d,e	d,e	c,d,e	d,e	c,d,e	√
12 - 16%	x	x	x	x	a,c,d	a,d	a,c,d	a,d	a,c,d	√
> 16%	x	x	x	x	x	x	x	x	x	x

Note:

√ - Recommended

a – Not recommended on stabilized base-courses built with fine material

b – Not recommended if channelling of water is expected due to soil wash, which is common in developing areas

c – Not recommended if urban drainage systems (kerbs) are present

d - Not recommended if communal water systems are present, as these cause wash up of detergents into the road that leads to erosion of the bituminous binder

e - Not recommended on gradients above 10 % if channelling of flow is expected due to soil wash, which is common in developing and hilly terrain

x - Not recommended

2.5.4.3.   Physical and Social Environment

The environment in which the sprayed seal will be placed greatly affects its performance. When climatic conditions are incorrectly evaluated it often times result in inappropriate grade and type of binder (TRH3, 2007). Examples are ultrav-voilet rays of the sun that can cause the ageing of the binder to accelerate, extremely high temperatures that can reduce cohesion and cold temperatures which can cause the binder to become brittle, loose aggregate and crack.

South Africa's TRH 3 uses the Weinert (1980) macro-climatic regions of southern Africa in its climatic design considerations (Figure 2-44). There exists three basic climatic regions for South Africa, namely; wet, moderate and dry. A wet climatic region corresponds to a Weinert N value of less than 2, a moderate region ranges between 2 and 5 and a dry region has a Weinert N value greater than 5. Weinert number is related to temperature and humidity in the following correlation:

$$N = 12 * \frac{E_j}{P_a}$$

Equation (3)

Where:

E_j = The calculated evaporation during January

P_a = The total annual precipitation
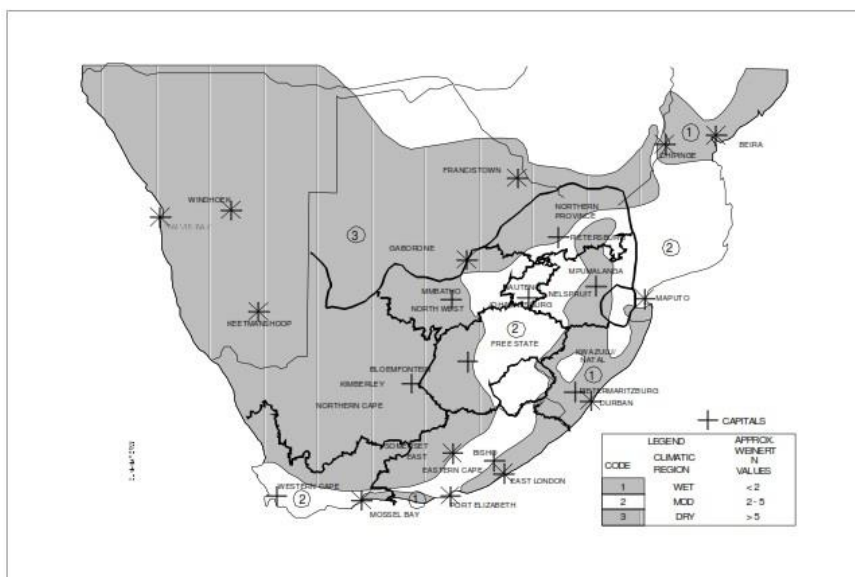
Figure 2-44: Macro-climatic regions of southern Africa (adapted from Weinert, 1980)

This Weinert N value is used to make adjustments to the binder application rates (TRH 3, 2007), when conventional binders are used. In dry areas (Weinert N value > 5), 10 per cent is added to the minimum application rates, whereas in wet or humid areas (Weinert N value < 2), 10 per cent is subtracted from minimum application rates.

The Thornthwaite Index (Im) has however recently been used to describe the various climatic regions. Im defines the aridity or humidity of the soil and climate of a region. It is calculated from the various influence of evatranspiration, precipitation, soil water storage, run-off and moisture deficit (Austroads, 2010).

$$M = Ih - 0.6 * Ia$$ Equation (4)

Where:

Ih = Index of humidity

Ia = Index of aridity

Or

$$M = \frac{100\alpha - 60\beta}{\gamma}$$ Equation (5)

Where:

α = Water surplus

β = Water deficiency

γ = Water need or potential evatranspiration

Recent work by Leyland and Paige Green (2010) provide revised climatic zones for South Africa, namely (see Figure 2-45), Humid Areas (Im>20), Moist subhumid areas (0<Im>20), Dry subhumid areas (-20<Im>0), Semiarid (-40<Im>-20) and Arid (Im< -40), as can be seen in Figure 2-45.
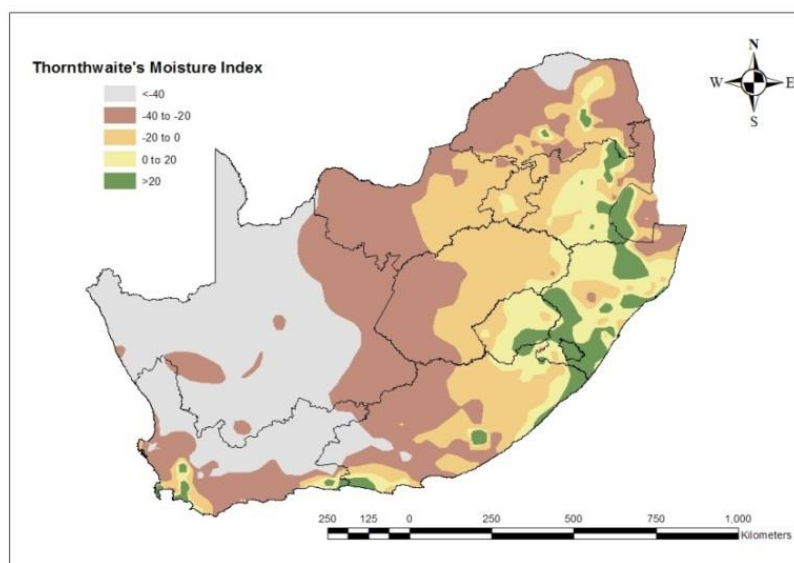
Figure 2-45: Revised Thornthwaite's Map (CSIR, 2010)

2.5.4.4. Existing Substrate

The seal type and design will be determined by the condition of the underlying surface. This condition is assessed by measuring the surface texture depth and unevenness, permeability, expected embedment of stone and visual assessment of defects (e.g. cracking). The following factors should be taken into account when selecting the most suitable pre-treatment, size of stone, seal type, type of binder and amount of binder:

1. Texture depth
2. Permeability
3. Degree and extent of cracking
4. Expected embedment

Pre-treatment of the underlying surface is needed to correct variations in texture depth, permeability, degree and extent of cracking. This is achieved by adding extra binder. With high expected stone seal embedment it is found that the new seal will have a low number of voids. Ball-penetration tests provide useful information on this expected stone seal embedment, but do not consider the softening of the underlying binder by the new, at times oily and very hot binder used in resealing. The degree and extent of cracks on the surface point to the possible reflection of these cracks to the new surface or indicates the loss of flexibility or relative brittleness of the current surface.

A comparison was made between seals positioned on worn surfaces and seals positioned on new or leveled surfaces (Roque et al., 1989). It was found that the seals maintained the highest mean texture depth on worn surfaces. These surfaces were harder as they had better compaction under traffic load than new or leveled surfaces. In resealing attempts

leveling courses should therefore not be applied unless rutting of the existing surface was severe. If this is the case, additional emulsion needs to be added for aggregate retention, because of the porosity of the seal and because older surfaces generally have lower mean texture depth due to flushing of aggregate.

The existing texture is an indication of the condition of the core surface and the materials used in its building (TRH 3, 2007). The existing substrate is made up of the existing texture depth, permeability potential, expected embedment and degree and extent of cracking (TRH 3, 2007). Surface texture is a quantity that determines the nominal size of stone aggregate used in seals. It ultimately influences the material application rates, skid resistance and road noise (NCHRP, 2005). Countries such as South Africa, New Zealand, Australia and the United Kingdom use the sand patch test together with visual assessment to describe existing surface texture. These countries furthermore distinguish between different surface hardness and link it to expected embedment depth into core surface.

Sand Patch Method

This test is also known as the sand circle test. ASTM E965 describes this test as a procedure to establish surface macro texture through the distribution of a set volume of sand or glass beads to a set area. It proceeds then to calculate the volume that fills the surface voids, higher volume implies a greater texture depth and volume of material lost in the surface texture.

Visual Assessments

In South Africa, TMH 9 is used to perform visual assessment of the existing texture. This can be used to calculate the required binder application rates but it is very subjective as there are inconsistencies in terminology used within organizations and between them.

The main purpose of the surfacing seal is to serve as a wearing course and prevent moisture entering the pavement. In order for the seal to perform as desired the pavement need to be structurally adequate.

The flexural characteristics of the pavement surface and structure will also reduce with time due to fatigue from the buildup of deflection damage. Distresses such as raveling and cracking of the surface also occur with time. These become intensified when oxidation and cold temperatures are present, also if the seals are rigid. Seals should therefore be chosen to fit well with the behavioural characteristics of the pavement.

Another distress is reflective cracking, caused by the magnitude and frequency of the crack walls moving due to increased load applications, chemical reactions, and moisture or temperature changes. If this crack movement increases significantly, crack reflection will be the result. Rust and Hugo (1988) also detailed that reflection cracks occur because of the influences of wheel loads and thermal changes. They've suggested, as a preventative measure against the recurrence of reflective cracking, the use of inventive materials such as low viscosity bitumen, rubber bitumen and geo-fabrics. These materials essentially provide a maximum reflection of cracks through the surface.

They also developed the Crack-Activity Meter (CAM) to record the vertical and horizontal crack activity relative to the position of the wheel load. From the CAM they were able to predict the field performance of different binders and different spray rates. A moving wheel load created a greater horizontal crack movement than vertical crack movement. These

fatigue properties were then further explored in the laboratory using a Crack Movement Simulator (CMS).

2.5.4.5. Maintenance capability

In areas where routine maintenance won't be regularly possible, it is advisable to advocate for a more expensive sprayed seal type, for instance a larger sized aggregate, double, Cape Seal or asphalt, to ensure that the surface will last longer. Table 2-16 below displays the recommended sprayed seal selection when considering the maintenance capability of the road authority of the area.

Table 2-16: Sprayed seal selection base on maintenance capability (TRH 3, 2007)

Maintenance Capability of Road Authority	S3	S7	S1	S2 (9)	S2(13)	S4(13)	S2(13/6)	S4(19)	S2(19/9) S2(19/6)	AC
High (Can perform any type of maintenance whenever needed)	√	√	√	√	√	√	√	√	√	√
Medium (Routine maintenance, patching and crack sealing on regular basis, but no MMS#)*	x	a	c	b	b	√	√	√	√	√
Low (Patching done irregularly, no committed team, no inspection system)	x	a	x	x	x	√	c	√	c	√
None	x	x	x	x	x	x	x	x	x	√

Note:

√ - Recommeded

a – Only thick slurries (> 10mm)

b – Only rural areas

c – Performance of these types of seals are sensitive to design and construction procedures

- It is not essential to have maintenance management system (MMS), but its existence is indicative of a certain level of capability and sophistication

x - Not recommended

The lifetime of seals and pavement structures can be extended greatly by timeous maintenance (TRH 3, 2007).

Potholes, sub-failures, poorly constructed patches and active or wide cracks need to be repaired in time to prevent defects reflecting through (TRH 3, 2007).

Poor construction of seals, insufficient supervision during construction or lack of attention to detail often result in seals performing poorly (TRH 3, 2007). Binder and stone application rates need to be applied consistently, as well as the rolling and brooming that follows. Plant equipment need to be correctly calibrated and operated.

2.5.4.6.   Construction and Supervision

The initial and long term performance of the seals is also affected by the preparation of the surface, pre-treatment applied on time and the repair maintenance performed before the sprayed seal is constructed (TRH 3, 2007).

Pre-treatment and Condition of base

Pre-treatment of the road is essential to eradicate non-uniformity (transverse and longitudinal) of the existing road surface. Transverse non-uniformity being the variation in surface texture in the wheel track, outside the wheel track and between the wheel track, longitudinal non-uniformity being the variation in surface texture along the road (NCHRP, 2005). In new construction the type of base affects the degree of compaction and the aggregate resistance to penetrate into the base.

Figure 2-46: Compacted base layer before prime application

Shortly after construction the surface aggregates will become more embedded into the base, reducing the amount of voids in the seal, creating a bleeding or fatty surface. This may also result in loss of skid resistance.

Application of pre-coated and clean aggregate

A clean, solid road surface is required for a good bond between the placed seal and the underlying surface. This will reduce potential aggregate loss or embedment of the seal into the base, causing loss of skid resistance.

Pre-coating the aggregates are preferred as it protects the aggregate against dust and other contaminants as well as enhances adhesion between the aggregate and the base.

Figure 2-47: A and B: Application of pre-coated aggregate

Rolling of surface after application

Rolling after application of the pre-coated aggregate is essential for embedment of aggregate into surface.

Figure 2-48: Rolling of surface after application

Opening of road section to traffic

Once opened to traffic, the operating speed should be controlled to allow the sprayed seal to settle, particularly for the bitumen to develop adequate cohesion to hold the aggregate under traffic. This is normally achieved with proper traffic accommodation of the construction site, either by enforcing an operating speed of 60km/hr or by delaying opening the road section to traffic (TRH 3, 2007) as indicated in Figure 2-49.

62

Figure 2-49: Road closed for traffic

Type of and application of bituminous binder

Binder Application Rate

The correct binder application rate is required to prevent fattiness of the surface, which can cause loss of skid resistance, as more aggregates will be embedded in the surface. Figure 2-50 shows a typical binder application on site.

Figure 2-50: Application of prime binder to base

Required binder application rate as discussed in TRH 3 (2007) is calculated from design charts (see Figure 2-51) that integrate aggregate spread rate, traffic volume and aggregate ALD. TRH 3 uses correction factors to adjust binder application rates when polymer modified binders are used, due to a change in aggregate orientation when compared with compared to conventional binders (NCHRP, 2005).
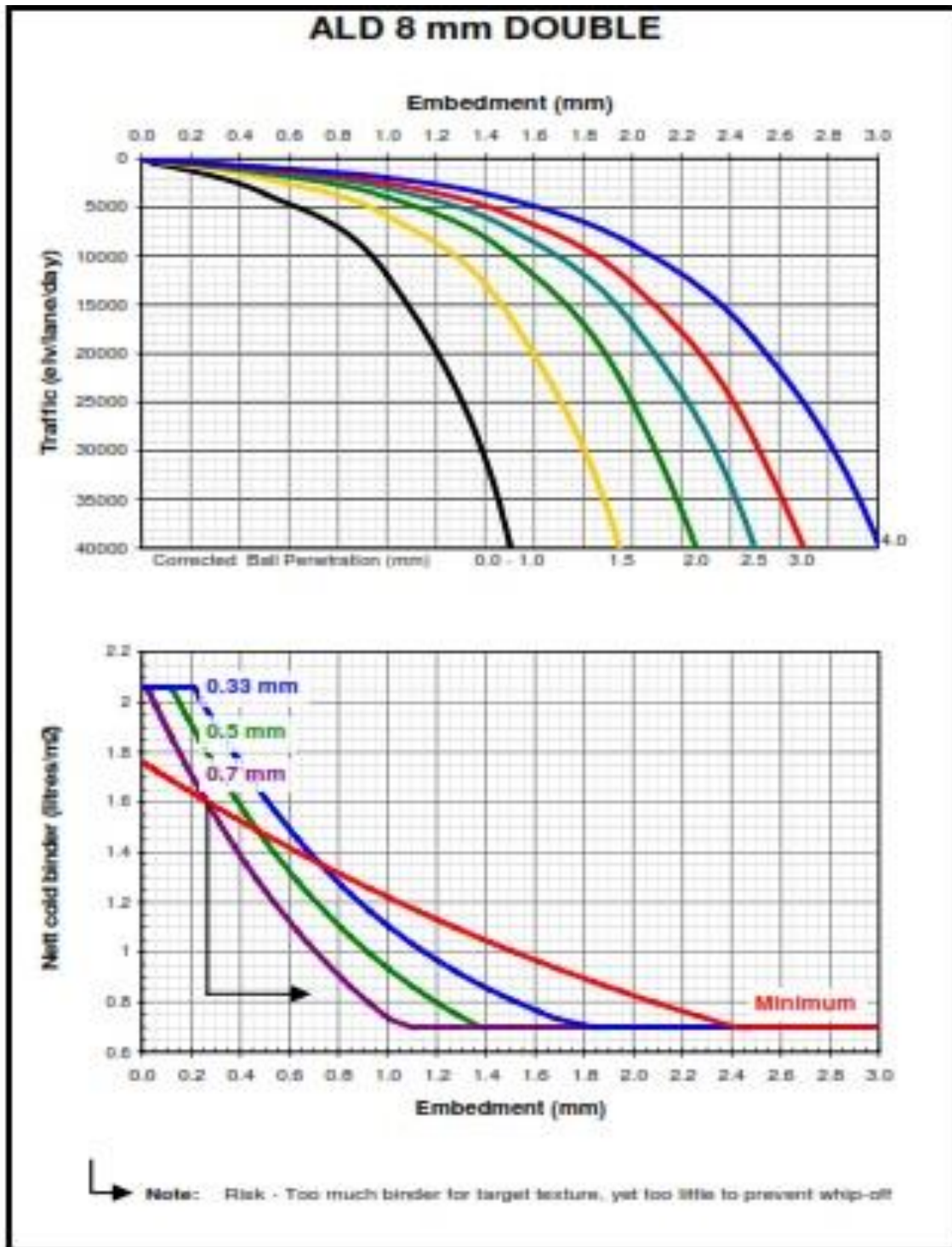
Figure 2-51: Design charts to determine minimum binder application rate (TRH 3, 2007)

The determination of binder application rates attempts to quantify the optimum embedment. Two approaches exist to achieve this. The first is to seek 50% embedment from compaction after construction and thus allow the traffic to cause further embedment.

This tactic aims to avoid bleeding in the wheel track by allowing space for additional embedment once the road has been opened to traffic. This approach however causes the aggregates that are not in the wheel tracks to be vulnerable to being removed by traffic (NCHRP, 2005).

The second approach involves catering for 70% embedment during construction across the entire width of road. This second tactic adjusts the binder application rate according to the measured or estimated surface hardness and includes hardness as a design parameter (NCHRP, 2005).

The disadvantages of this approach is that there is a risk of aggregate loss across the entire road width together with a vulnerability to bleeding if design calculations do not align with the existing road surface.

Aggregate Spread Rate

Figure 2-52: Aggregate spread on road surface

Aggregate spread rate is deduced from charts founded on the ALD and flakiness index of the aggregate as can be seen in Figure 2-53.

65
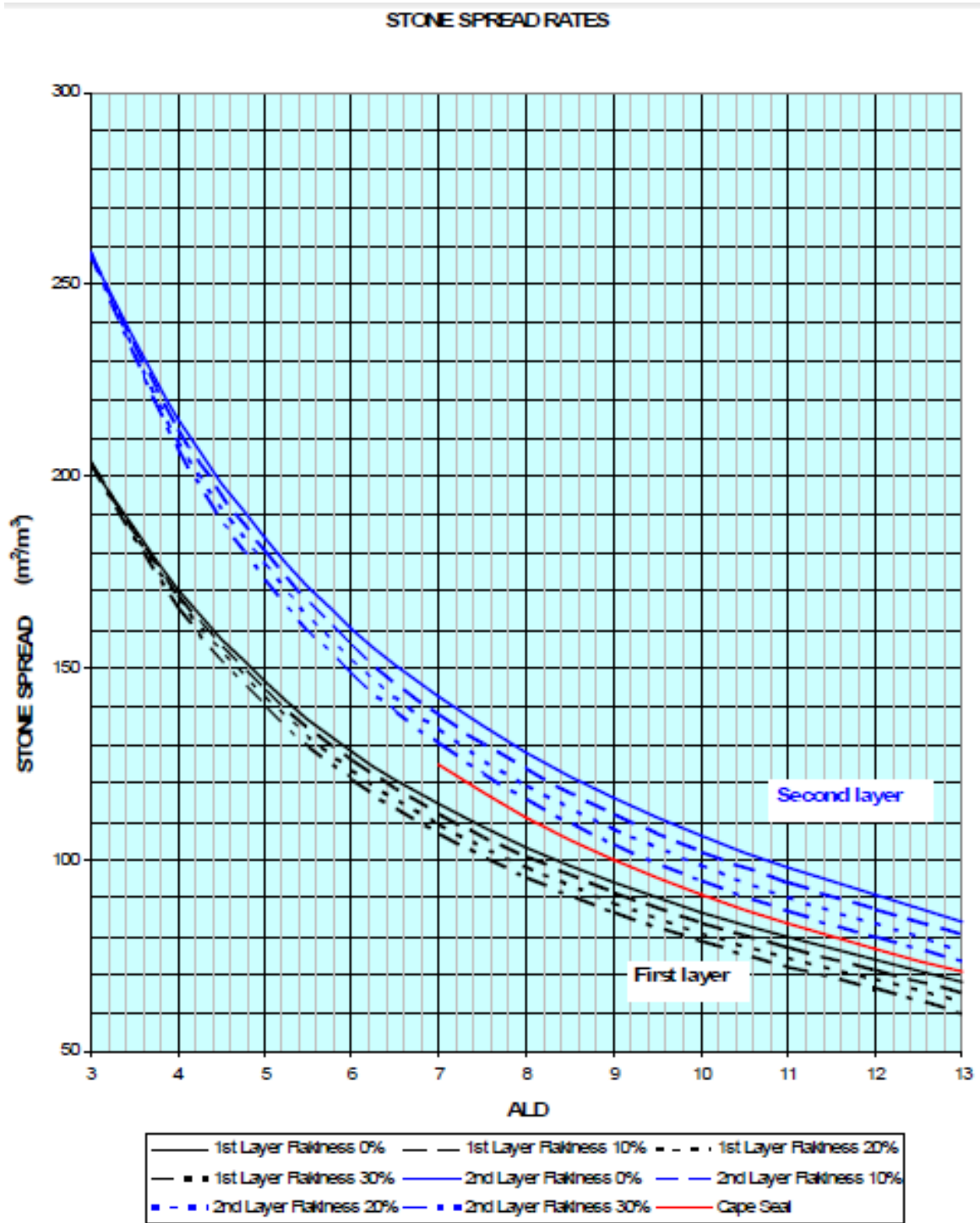
Figure 2-53: Determination of aggregate spread rate using ALD of aggregate (TRH 3, 2007)

2.5.4.7.   Illustration of Sprayed Seal Design Procedure

Table 2-17: Design Procedure of a 13.2mm Single Sprayed Seal placed on an existing 19mm Cape Seal

Description	Unit	Reference	Quantity	Comments
Design Parameters				
Stone	mm	Reseal design	13.2	
ALD	mm	Quarry Report	8.64	
Existing Texture Depth	mm	TMH 6 Method ST1	0.3	
Ball Penetration	mm	Ball Penetration TMH 6 Method ST4	1.5	
Climate	Weinert N	TRH 3	05-Feb	Moderate Climatic Region
Terrain		Visual Inspection, TMH9		Relatively flat with no significant gradients
Slow Moving and Chanelised Traffic		Visual Inspection, TMH9		Single lanes with no slow moving traffic except for stop-controlled intersections
Traffic	Light vehicles	Road Database	4390	Both directions
	Heavy vehicles	Road Database	448	Both directions
	ELV / day / lane	LV+40xHV	11155	Directional split of 50-50 assumed
Existing Seal	mm	Visual Inspection	19	Cape Seal
Specifications	l/m^2	COLTO Table 4403/1	1.4	Tack Coat (net cold bitumen)
	m^2/m^3		100	Spread Rate
	m^2/m^3	TRH 3 Figure F2	95	Spread Rate using ALD and Flakiness Index
Fogspray			N/A	Usually applied on newly constructed single and double seals. Useful to prevent aggregate loss due to excessive delay in application of aggregate (especially when modified binders are used)

Table 2-18: Continuation of Design Procedure of a 13.2mm Single Sprayed Seal placed on an existing 19mm Cape Seal

Description	Unit	Reference	Quantity	Comments
Design Parameters				
Target Texture	mm	TRH 3, Page 35	0.7	Based on design speed of 80km/hr
Min Binder			0.7	
Design	l/m^2	TRH 3, Appendix E	0.7	ALD 8mm Single
Max Binder			1.62	
Min Binder			0.7	
Design	l/m^2	TRH 3, Appendix E	0.94	ALD 9mm Single
Max Binder			1.77	
Min Binder			0.7	
Design	l/m^2	TRH 3, Appendix E	0.85	ALD 8.64mm Single (Interpolated)
Max Binder			1.67	
Adjustments				
Climate		TRH 3, Page 86	0	No adjustment for modified binder. Also adjustment only for Weinert values less than 2(wet climate) and greater than 5 (dry climate)
Gradient			0	No adjustment
Existing Texture		TRH 3 Fig 7.2	0	No adjustments as it is used to determine the quantity of extra binder required to prevent whip-off on course textures
Aggregate Packing		TRH 3, Page 85, 87 & Figure F-3, F-4	0	Dense shoulder to shoulder aggregate matrix is preferred for the reseal, therefore no adjustment is required

2.6.   Overview of Fatigue Performance for Bituminous Mixtures

When evaluating failure of pavement structures, fatigue is considered the main mode, causing a decline in the quality of the pavement materials and ultimately the entire pavement structure. The initiation and propagation of fatigue cracks are caused by the repetitive submission to tensile forces that are at intensities well below that required to induce immediate fracture (Twagira, 2006). Airey, 1995, defined fatigue as the "phenomenon of fracture under repeated or fluctuating stress having a maximum value generally less than the tensile strength of the materials".

Another definition is that of ASTM (1964), which describes fatigue as "the process of progressive localized permanent structural change occurring in materials subjected to conditions that produce fluctuating stresses and strains at some point or points and which may culminate in cracks or complete fracture after a sufficient number of fluctuations".

Fatigue starts when a material is continuously subjected to loading that will induce a tensile strain within the material. In-situ materials that form part of a pavement structure, behave as loaded beams, in the beginning of their life. At the bottom of these respective pavement layers, tensile strains start to build up, that will eventually be of a high magnitude that in turn will dissolve the bonds that were developed in the bituminous layers. Liebenberg, (2003) describes this stage as the formation of cracks, which can be very small, and in some cases, even microscopic.

In bituminous layers, fatigue cracking is a dominant load-related distress that takes place when traffic induced loads are continuously applied to the surface of the pavement. The resistance to cracking and fracture is provided by the layer's mix to fatigue resistance. Other distresses are permanent deformation and failure of bound materials due to reflective and thermal cracking. Within the sprayed seal context, only crack initiation is considered important, since the seal thickness is almost negligible for crack propagation to be of significance.

2.7.   Basic Asphalt Fatigue Fundamentals and how these Relate to Fatigue of Seals

Asphalt properties that influence fatigue performance are binder type and condition (ageing), film thickness, temperature, traffic load/stress/displacement and can be summarized as follows in Table 2-19.

Table 2-19: Factors affecting the Stiffness and Fatigue Response of Asphalt Paving Mixtures (American Society of Testing Materials, 1982)

Factor	Change in Factor	Effect of Change in Factor		
		On Stiffness	On Fatigue Life in Controlled-Stress (Load Constant) Testing Mode	On Fatigue Life in Controlled-Strain (Displacement Constant) Testing Mode
Asphalt Content	Increase	Increase	Increase	Increase
Air Void Content	Decrease	Increase	Increase	Increase
Aggregate Gradation	Open to Dense	Increase	Increase	Decrease
Temperature	Decrease	Increase	Increase	Decrease
Asphalt Viscosity (Stiffness)	Increase	Increase	Increase	Decrease

These factors are explored below in terms of the performance of thin asphalt layers and related to that of seals.

2.7.1. Effect of Air Voids and Asphalt Content on Fatigue Damage

Pell and Cooper (1975) demonstrated that there is a need to carefully control the air voids and asphalt content of bituminous mixes. The asphalt mix system is comprised of asphalt (binder and filler material), aggregate and air and the relative quantities of these three components significantly affect the pavement's performance. Each component's proportion is selected during the mix design stage.

Harvey et al. (1995) indicated that the asphalt proportion should be adequately large to resist fatigue, provide durability as well as workability. It should however be selected small enough to reduce the potential and/or effect of rutting, bleeding and structural instability of the asphalt mix.

Subsequently, for the air-void content (relative porosity/compaction), they considered both mix design as well as construction specifications. It was shown that the air-void content should be selected adequately small to prevent break down of the mix during load resistance, but not so small as to promote structural instability and bleeding (Harvey et al., 1995).

Decreasing the air-void content (porosity) of asphalt mixes results in increased mix stiffness, which is possibly from an increase in the volumetric proportions of asphalt and aggregate. These are the mix components that are capable of bearing applied stresses. A smaller air-void content has at least two effects that likely contribute to longer fatigue life. First, because air transmits little or no stress, replacing some of its volume with asphalt and aggregate reduces the stress level in these components. Second, a smaller air-void content creates a more homogenous asphalt-aggregate structure-one with fewer, smaller, and more uniformly

distributed voids-which results in less stress concentration at critical solid-air interfaces (Harvey et al., 1995).

Increased bitumen content and decreased air-void content result in increased pavement fatigue life Increased asphalt content means increased thickness of the binder film between aggregate particles and an increased proportion of bitumen over a cross-section normal to the direction of tensile stress. Because bending strains are concentrated in the binder (the binder is much more compliant than the stiffer aggregate particles), thicker films result in smaller binder strain if the overall mixture strain is not altered by the added bitumen (Harvey et al., 1995).

Moreover, because tensile stresses must ultimately be transferred through the binder, more asphalt means more asphalt area in cross-section and, hence, less stress in the asphalt. The effects are complicated, however, by the related effects of bitumen content on mix stiffness and, as a result, on the stresses and strains that must be resisted in situ.

Similarly as for a porous asphalt mix, the performance of seals is also affected by the binder and air-void content. Higher binder content increases the binder film thickness covering the aggregate, as illustrated in Figure 2-54. An increased binder film thickness has a greater bearing capacity to sustain traffic loading, since it correlates to smaller binder strain. For this reason, the pre-coating of aggregate is preferred. However, excessive bitumen will result in fattiness/ bleeding of the sprayed seal (TRH 3, 2007).
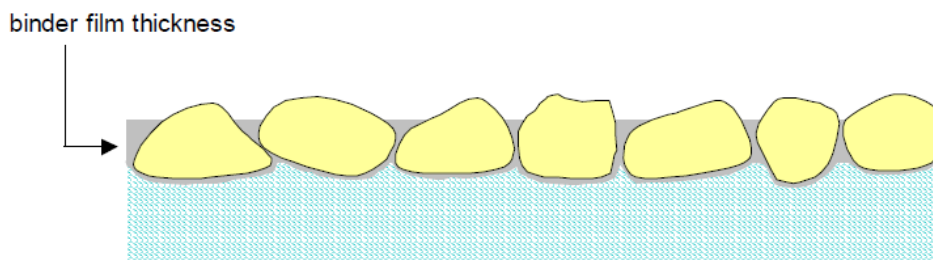
Figure 2-54: Binder Film Thickness Covering the Aggregate (Oliver, 2004)

Reduced air-void content decreases the available spaces that can be filled with bitumen, resulting in a weaker, unstable sprayed seal. Increased air-void content results in a high porous sprayed seal, which cannot achieve the desired tight packing of aggregates (mosaic cover).

2.7.2. Effect of Aggregate Gradation on Fatigue Damage

Kim et al. (1992) conducted a laboratory study to investigate the effects of aggregate type and gradation on the fatigue and permanent deformation of HMA mixtures. Diametral fatigue and uniaxial incremental static creep tests were performed on HMA specimens. The results of these tests indicated that the aggregate type (shape) had a significant effect on fatigue resistance and permanent deformation properties. The aggregates with angular shape and rough texture produced better performance. The variations in the coarse aggregate gradations did not affect the permanent deformation properties significantly.

Maupin (1970) conducted a laboratory study to evaluate the effect of particle shape and surface texture on the fatigue behaviour of asphalt. The study used three different particle shapes, round, sub-angular, and angular. Asphalt concrete mixtures were produced with uncrushed gravel (round), limestone (sub-angular), and slabby slate (angular). Beam specimens were prepared and tested with constant strain fatigue. The laboratory study concluded that rounded gravel mixture had a longer fatigue life than the other mixtures.

TRH 3 (2007) indicates that a larger aggregate size yields a greater life expectancy for the sprayed seal. This can be ascribed to the fact that a larger aggregate will require more binder to cover the aggregate, hence a thicker bitumen film thickness, than for smaller aggregate sizes. Bitumen film thickness is important since it influences the rate at which the bitumen hardens and ultimately reaches the end of its service life.

A larger aggregate size can also carry heavier traffic volume, since a larger stone has better stress distribution at the aggregate contact points, since it has an increased surface area.

The following sprayed seal life expectancies are documented in Appendix B of TRH 3 (2007):

Table 2-20: Life Expectancy of Seals (TRH 3, 2007)

Seal Type	Life Expectancy of Seals (Years)			
	Traffic (elv/lane)	New Construction	Reseal on Sound Underlying Structure	Reseal on Fatigued Underlying Structure/ Active Cracks
6.7mm and Sand	<2000	6	6	4
	2000-10 000	3	3	2
	>10 000	-	-	-
9.5mm and Sand	<2000	8	8	5
	2000-10 000	6	6	3
	>10 000	3	3	-
13.2mm and Sand	<2000	12	12	7
	2000-10 000	9	9	4
	>10 000	6	6	2
13.2mm and 6.7mm	<2000	14	-	-
	2000-10 000	10	-	-
	>10 000	8	-	-
Cape Seal (19mm)	<2000	14	-	-
	2000-10 000	10	-	-
	>10 000	8	-	-
Cape Seal (13.2mm)	<2000	12	-	-
	2000-10 000	8	-	-
	>10 000	5	-	-

Table 2-21: Continuation of Life Expectancy of Seals (TRH 3, 2007)

Seal Type	Life Expectancy of Seals (Years)			
	Traffic (elv/lane)	New Construction	Reseal on Sound Underlying Structure	Reseal on Fatigued Underlying Structure/ Active Cracks
Sand Seal	<2000	4	7	3
	2000-10 000	2	3	2
	>10 000	-	-	-
Fine Slurry	<2000	4	4	2
	2000-10 000	2	2	1
	>10 000	-	-	-
Coarse Slurry	<2000	7	7	4
	2000-10 000	4	4	2
	>10 000	2	2	-
6.7mm	<2000	-	6	4
	2000-10 000	-	4	2
	>10 000	-	-	-
9.5mm	<2000	-	10	6
	2000-10 000	-	6	3
	>10 000	-	-	-
13.2mm	<2000	-	12	7
	2000-10 000	-	9	4
	>10 000	-	6	2
13.2mm and Polymer Modified Binder (Homogenous)	<2000	-	14	8
	2000-10 000	-	10	6
	>10 000	-	8	3
13.2mm and Polymer Modified Binder (Non-Homogenous)	<2000	-	16	10
	2000-10 000	-	13	7
	>10 000		10	5

2.7.3. Effect of Temperature on Fatigue Damage

As discussed in *Section Behaviour of Bitumen,* bitumen is a viscous-elastic material whose properties are dependent on temperature and rate of loading. Bitumen becomes stiff and brittle at low temperatures, which together with the effect of traffic loads, encourage crack growth. The fatigue damage/ cracking of an asphalt mix are influenced by traffic loads, the stiffness properties of the mix and the distribution of stresses and strains within the layer. The amount of strain experienced is dependent on the temperature, which can be linked to the stiffness of the asphalt mix (Koole, Valkering and Staple, 1989).

In 1994, Deacon et al. set out to investigate the effect temperature exerts on the stiffness of asphalt mixes and the development of temperature equivalency factors for fatigue. They carried out flexural fatigue testing in a strain-controlled mode, at four temperatures, ranging from 5°C to 25°C. They found that temperature influenced the initial flexural stiffness and the gradient/slope of the initial fatigue-life curve, as could be expected. The fatigue-life curve that includes the influence of temperature and strain can be described as:

$$N_f = 10^{(20.0341-0.2261T)} * \varepsilon^{(-5.9138+0.1056T)}$$ Equation (6)

Where:

N_f = Laboratory fatigue life

ε = Maximum tensile strain

T = Temperature (°C)

Furthermore, the effects of varying temperature influences crack reflection, since the movement of the crack/ joint may be brought on by the bending and shearing mechanism that result from temperature changes and are further influenced by daily and seasonal variations in temperature (TRB, 2010).

The main influence on bitumen hardening in seals is reaction with atmospheric oxygen, which is a slow process whose rate is greatly influenced on site by the temperature of the binder, the reactivity of the binder and the binder film thickness (Oliver, 2004).

To understand the temperature of the binder, it is important to consider the effects of the temperature of the geographic location, albedo (solar radiation reflection) and the aggregate thermal conductivity. Oliver's empirical seal life model in 1987, however, did not describe the effect of the bitumen film thickness on the hardening process. This is however paramount in the hardening process, since an increase in binder film thickness, the medium through which oxygen moves, will cause a slower rate of hardening.

In previous years, Dickinson (2000) also found that the temperature of the site location and bitumen reactivity to be important influences on the rate of bitumen hardening.

2.7.4. Effect of Binder Film on Resisting Crack Reflection

Crack reflection is described as the cracking of a surface above underlying cracks or joints, with movement of some form in the underlying layers as its possible source, as illustrated in Figure 2-55.
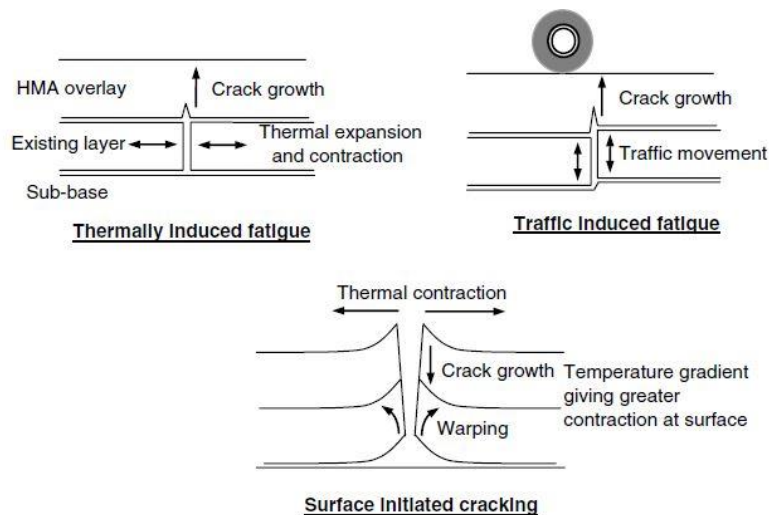
Figure 2-55: Mechanisms of Crack Reflection (Nunn, 1989)

Two crack growth types exist, namely (TRB, 2010):

- Existing joints/ cracks cause stress concentrations at the bottom of the asphalt layer, which will result in continual crack growth into the asphalt surface.
- If the stress-concentrating influence of the current joints/ cracks is removed by some process, a secondary effect will occur, in that a maximum deflection of the surface will occur under a wheel load at the crack. Maximum stresses will occur at this point, causing crack growth to start, at this particular point, as can be seen in Figure 2-56 below.
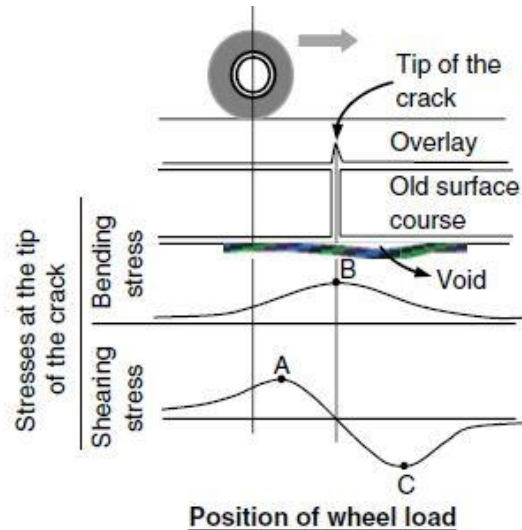
Figure 2-56: Shear and Bending Mechanism of Crack Reflection (Lytton, 1989)

The performance of seals is often influenced by age-related conditions, such as the durability of the exposed bitumen film, i.e. the resistance to heat and air over time. The integrity of the sprayed seal and its ability to protect the underlying layers is however influenced much sooner by the reflection of cracks from the underlying layers through the sprayed seal (Wilson et al., 2010). For both seals and asphalt, the ability of the binder to

75

resist crack reflection is critical for fatigue performance and the same binder tests can generally be used for seals as well as for asphalt mixtures.

In order to better assess the binder's capacity to resist crack reflection in seals, the ARRB Group Ltd ranked different binders by using their relative fatigue lives in a single asphalt mixture. This exercise produced results faster and cheaper than performing road trials, although it is still a lengthy process to prepare asphalt beams and conduct fatigue testing on each beam. An alternative was considered, which subjected a number of binders to toughness tests at 4°C and 10°C, using different extension speeds (Wilson et al., 2010).

Force-extension curves were reproduced during the test and the speed of the Toughness test was set to ensure that the binders investigated in this study would not break during the test. A good correlation was found between the fatigue lives of a wide variety of binders and Force Ratio values at either 10°C or 4°C. Based on the data obtained in their investigation, measurement of the Force Ratio was concluded as a method to rank a binder's fatigue life and hence its relative ability to resist reflective cracking in a sprayed seal (Wilson et al., 2010).

The condition (ageing) tests of binder, as discussed in *Section 2.4.2.6. Performance of Binder*, is however preferred for asphalt fatigue testing.

2.7.5. Effect of Loading Considerations on Fatigue Damage

In a controlled displacement loading, the displacement is retained at constant level, while the force is required to decrease gradually to maintain the initial strain. The applied force will gradually decrease after crack initiation, as the flexural stiffness of the mixture reduces to generally half of its initial stiffness, which is defined as the failure or termination condition (ARRB, 1999). The point of failure is selected randomly selected as a particular reduction in initial flexural stiffness, generally 50%. This selection is because there is no properly-defined fracture of the test specimen.

Constant strain loading tests are representative of relatively thin pavements that are less than 100mm thick. The mixture stiffness controls the stress levels, which in directly influence the rate of crack propagation. The measured fatigue lives includes the loading repetitions till crack propagation (Pell, 1973). Asphalt mixtures that are more flexible (lower flexural stiffness) perform better under constant strain loading than compared to constant stress loading (controlled force), at the same strain levels.

In this type of loading the fatigue lives are relatively longer because the crack propagation is included in the measured "fatigue life", but more due to dependency that exists between the specimen geometry and the development of damage. Thinner 4PB specimens would have slower damage development. Sprayed seals are relatively thin, which would imply that during fatigue testing, damage will develop much more slowly. Furthermore, the initial dissipated energy for each loading repetition is insignificant and the rate of energy absorbance (dissipation) is relatively slow until the stage at which the crack propagation is dominant, which is one of the last stages in the loading series (test).

In a controlled force loading, the force level is kept constant. When this constant force is applied repetitively it causes the displacement to increase to twice its initial amplitude. This occurs when the flexural stiffness is reduced to 50% of its initial stiffness value, which is defined as the failure condition. The loading termination is set as the point at which fracture of the test specimen occurs (AARB, 1999).

Button et al. (1987), found that this type of loading does not explain crack initiation and propagation effectively, since they found that the number of cycles to crack propagation is relatively small compared to the number of cycles to failure. In this case, the termination condition is defined as the point at which the test sample fractures (breaks). It has been noted further that the rate of crack propagation in the laboratory is more rapid, than that which occur under prevalent in-situ conditions, as observed by Pell (1973).

Rao Tangella et al. (1990) found that controlled stress (force) loading tests are more sensitive to asphalt mixture variables than controlled strain (displacement) loading tests. Pell (1973) found that during controlled stress (force), the stiffness of the mixture will determine the strain level and subsequently the fatigue life. Asphalt mixtures with higher initial flexural stiffness have been observed to have a longer fatigue life and are representative of loading responses in thicker pavement layers that exceed 100mm.

Asphalt mixes with stiffer bituminous binders have shown to have increased fatigue lives and measured flatter gradients for the stress-fatigue graphs, regardless of whether the repeated flexure testing was performed with the two-point bending or four-point bending apparatus (Bazin and Saunier 1967; Epps and Monismith 1972; Pell and Cooper 1975).

Constant stress loading tests are more severe than constant strain loading, as the energy is absorbed by the test specimen at a higher rate in constant stress loading, as can be observed by the fracturing of the specimen. Furthermore the initial dissipated energy per loading repetition is relatively high and the subsequent rate of energy dissipation is more rapid than compared to that of the constant strain loading (ARRB, 1999). Below is an illustration of the controlled displacement and controlled force loading configurations.
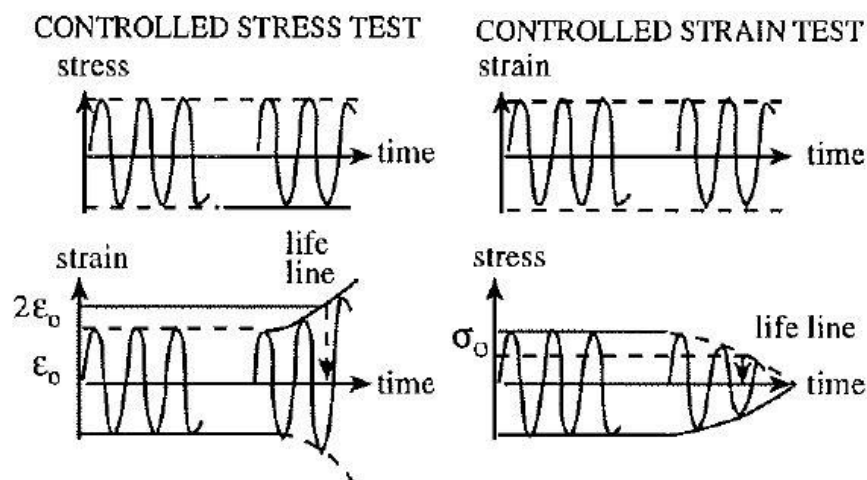
Figure 2-57: Description of principles of controlled displacement and controlled force loading configurations (Bonaure, Gravois and Udron, 1980).

See below *Section 2.8 Principles of Fatigue Testing* for further discussion.

2.8.   Principles of Fatigue Testing

There exist numerous possible fatigue testing techniques, both in the laboratory as well as in the field that can be useful to describe the fatigue responses of bituminous mixtures. According to Tangella, et al. (1990), these techniques contain an assortment of test methods, types of equipment, types of specimens, type and modes of loading, test conditions (e.g. , temperature, frequency of loading, etc) and analysis methods.

The available test methods were categorized into the following groups simple flexure, supported flexure, directs axial, diametrical, fracture mechanics (propagation of cracks) and wheel-traffic testing (heavy vehicle simulation). The group used the following criteria to determine the suitability of each method for its possible use as a laboratory standard:

- Sensitivity to mixture variables,

- Ability to simulate real-life (field) circumstances,

- Ability to estimate fundamental characteristics that can be used as input in suitable design performance models,

- Easy and simplicity of operation of test,

- Time required to carry out test,

- Cost of test equipment

- Reliability, accuracy and precision of results.

In laboratory tests, fatigue response has been shown to be a function of mode of loading, that is, the method by which stress and strain are permitted to vary during repetitive loading (Tangella et al., 1990). Limits to the loading conditions range from the controlled-stress (load controlled) mode, where the load or stress amplitude remains constant during testing, to the controlled-strain (displacement load) mode, where the deformation or strain amplitude is maintained constant, as illustrated in Figure 2-58 below.

Figure 2-58: Load (stress constant) controlled versus displacement (strain constant) controlled (Broek, 1989)

Load controlled tests are preferred when evaluating the fatigue response of thick hot mix asphalt pavements (HMA), as they favour bituminous mixtures that are relatively stiffer. Displacement controlled tests are preferred for the fatigue evaluation of relatively flexible mixtures. In the South African context, displacement controlled tests are thus preferred as they provide results that are more comparative to field observations. Monismith et al. (1977) provided the following comparison (Table 2-22) between the two loading types.
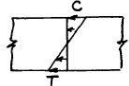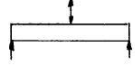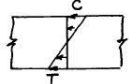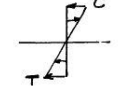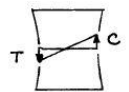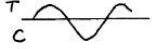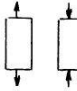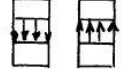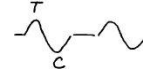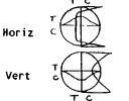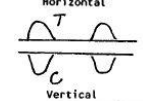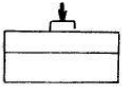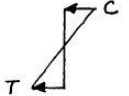
Table 2-22: Differences between Load Controlled and Load Controlled Loading (Monismith et al., 1977)

Variables	Load (Stress) Controlled	Strain (Displacement) Controlled
Thickness of bituminous mixture	Relatively thick	Relatively thin (3 inches or 76.2mm)
Definition of failure or cycles till test completion	Well defined test termination; specimen will fracture visibly	Random test termination
Scatter in fatigue test data	Less	More
Required number of specimens	Smaller	Larger
Simulation of long term effects	Long term influences such as age lead to increased stiffness over time, which leads to increased fatigue life	Long term influences such as age lead to increased stiffness over time, but with reduced fatigue life
Magnitude of fatigue life, N	Normally shorter	Normally longer
Effect of bituminous mixture variables	More susceptible	Less susceptible
Rate of energy dissipation	Increased	Reduced
Rate of crack propagation	Faster than real life (in-situ conditions)	Slower than real life (in-situ conditions)
Beneficial effects of rest periods	More beneficial	Less beneficial

The group furthermore found that the three most favourable tests were those based on simple flexure, diametral fatigue and fracture mechanics. Airey, (1995) advocated that the simple flexural test is the favoured test method used to define fatigue properties, when considering the various advantages and disadvantages of the different fatigue testing techniques mentioned above. Simple flexural tests have the advantage of being well known, (widely applied and readily interpreted). Furthermore the results that are obtained can be applied directly in pavement design analysis, with the added benefit that the basic method can be used for different concepts such as the dissipated energy and fracture mechanics.

Airey (1995) further showed that, within the different types of simple flexure tests, the third-point loading or four-point loading researched by Tangella (1989), Monismith (1981;1973), Monismith and Deacon (1969) or IPC (1998) respectively, are favoured to cantilever and centre-point load researched by Gerritsen and Jongeneel (1988), Van Dijk (1977), Bonnot (1972) and Bonnaur et al. (1982), Kingham and Kallas (1972) because fatigue failure is started in a region of uniform stress. The following summary was provided by Tangella, (1990) to illustrate the basic properties of the fatigue test methods (adapted from Porter and Kennedy, 1975).

Table 2-23: Basic Principles of Various Fatigue Testing (Tangella, 1990)

Test	Loading Configuration	Stress Distribution	Loading Waveform	Loading Frequency, cps	Performance Deformation Allowed?	State of Stress	Failure Zone
Third Point Flexure			Haversine load rest-1.9	1-1.67	No	Uniaxial	Uniform Bending Moment
Center Point Flexure			Sine, Triangular Rectangular load rest, 1:100 max	1:100	No	Uniaxial	Tensile Stress
Cantilever			Sine (Bonnot), Sine, Triangular load rest, 1:100 max (Van Dijk) max	25 (Bonnot), 1:100 (Van Dijk)	No	Uniaxial	Tensile Stress
Rotating Cantilever				16.67	No	Uniaxial	Uniform Bending Moment
Axial				8.33-25	No	Uniaxial	Uniform Bending Moment
Diametral				1	Yes	Biaxial	Tensile Stress
Supported Flexure			Haversine	0.75	Yes	Uniaxial	Tensile Stress

80

From the summary it is apparent that repeated load diametrical tests differ significantly from other methods, since it has a biaxial stress state while flexural, rotating cantilever and axial tests have a uniaxial state of stress. Flexural tests use pulsating load of triangular or square shape, while a continuous sinusoidal loading is found for rotating cantilever tests. The axial test makes used of a sinusoidal or haversine pulse with or without a rest period. A continuous loading design, such as that used in rotating cantilever test, generally yields a smaller fatigue life.

Pronk (1999) commented that due to difference in tests set-ups i.e. four point beam (4PB), two point trapezoidal (2PB), semi-circular bending (SCB) and circular bending (NAT) and clarifications of these tests methods, synchronization of the different tests methods to derive similar fatigue lives are not probable. He however suggested that in the estimation of fatigue lives using dissipated energy technique, it is likely to statistically account for the observed differences with Weibull volume effect.

In the field it has been observed that three continuous loading pulses will be applied by a rotating wheel over a pavement layer, instead of the single pulse applied in the laboratory. These pulses are; compressive stress as wheel approach the layer, then tensile stress as the wheel moves over the point, and finally a compressive stress again as the wheel moves away, (Raithby and Sterling, 1972). For this reason, the size of the initial compressive strain is estimated as one seventh that of the tensile strain pulse at the bottom of the pavement layer. A comment was made by Barksdale and Miller (1977) that without this small initial compressive stress pulse, the reduction in fatigue life should have been at most in the order of only 10 to 15 percent.

2.9.   Approaches used to Characterize Fatigue

2.9.1. Classic Approach

In the classical tactic, basic failure using Wöhler-type fatigue relationship is employed. In essence this relationship empirically links the amount of load repetitions to failure, N_f , to the maximum tensile strain, ε_t , that is found in the bottom of the asphalt layer, as follows;

$$N_f = k_1 (\varepsilon_t)^{-k_2} \qquad \qquad \text{Equation (7)}$$

Where:

N_f = amount of load repetitions to fatigue life

ε_t = maximum tensile strain found in the bottom of the asphalt layer, also the applied tensile strain in the 4PB test

k_1, k_2 = material coefficients

The material coefficients $k_1 \ and \ k_2$ are obtained experimentally and they vary depending on mixture properties, temperatures and the methods of testing. This correlation is therefore only valid for the specific type of bituminous mix tested (Twagira, 2006). Monismith et al. (1985) and Medani and Molenaar (2003) advocated a correlation that takes the initial mixture stiffness, S_i into account and that includes varying testing temperatures and frequencies, as follows:

81

$$N_f = k_1 (\varepsilon_t)^{-k_2} (S_0)^{-c} \qquad\qquad \text{Equation (8)}$$

Where:

N_f = amount of load repetitions to fatigue life

ε_t = maximum tensile strain found in the bottom of the asphalt layer, also the applied tensile

S_0 = initial mixture stiffness

k_1, k_2, c = material coefficients

Different fatigue lives have been observed for different variations in the test parameters.

Different fatigue lives have been observed for different variations in the test parameters. Pell and Cooper (1975) found that the line for the fatigue life (see Figure 2-59) for certain materials at different testing temperatures is almost parallel with longer fatigue lives at a higher testing temperature. This trend was also found when tests were conducted at different speeds (different rate of loadings). When the results were plotted in terms of tensile strain, ε_t, it was found that the results from various stiffness coincide, showing that strain is indeed the criterion of failure. The strain criterion in fatigue performance therefore takes the temperature and rate of loading (speed) into account.
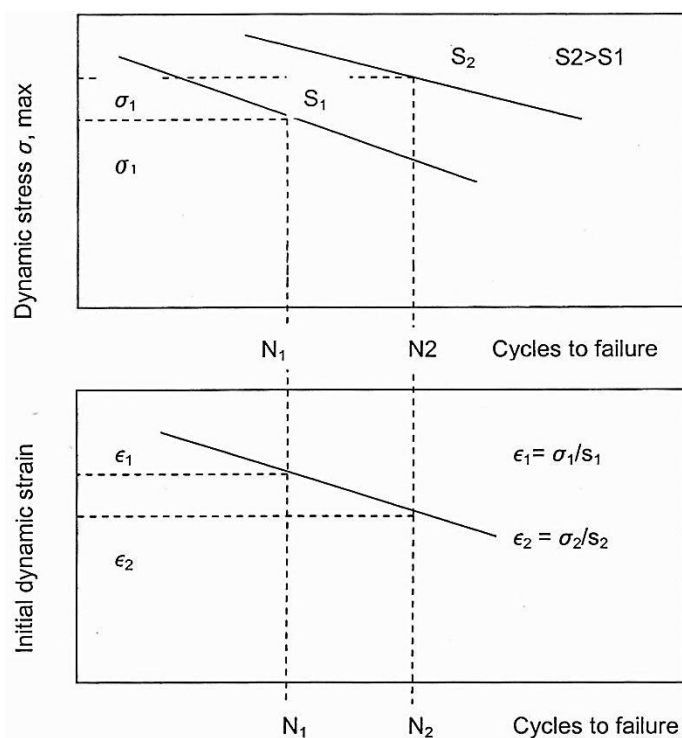
Figure 2-59: The Strain Criteria (Pell and Cooper, 1975)

Medani and Molenaar (2003) showed that at low temperature and short loading time the bituminous material is brittle, whereas with an increase in temperature and loading time the

material is flexible. Brittle fatigue behaviour is indicative of a higher fatigue life, N_f, and flexible behaviour of a lower N_f value.

2.9.2. Dissipated Energy Approach

It has also been shown that a correlation exists between the amount of load repetitions and the cumulative energy that is dissipated during these load repetitions (Van Dijk et al., 1977; Tangelli, 1990; Tayebali et al., 1992 and Pronk, 1999). To characterize fatigue they employed an energy tactic that showed that the "cumulative" dissipated energy to failure is linked to fatigue life as follows:

$$N_f = k_1 W_N^{-z}$$
Equation (9)

Where,

N_f = amount of load repetitions to fatigue life

W_N = cumulative dissipated energy to failure

k_1, z = material coefficients

It has further been shown that the cumulative dissipated energy to failure, W_N is linked to that of the ith cycle, w_i, (Van Dijk and Visser, 1977) as follows:

$$W_N = \sum w_i$$
Equation (10)

For sinusoidal loading the ith cycle, w_i, is developed as:

$$w_i = \pi \varepsilon_i^2 S_i \sin \varphi_i$$
Equation (11)

Where:

w_i = dissipated energy at i^{th} cycle

ε_i = strain at i^{th} cycle

S_i = stiffness of mixture at i^{th} cycle

φ_i = phase shift between stress and strain at i^{th} cycle

During controlled-energy loading the amount of dissipated energy per cycle remains constant and the cumulative dissipated energy is found by multiplying the initial dissipated energy with the amount of load repetitions to failure, as follows:

$$W_N = w_0 \, N_f \qquad \qquad \text{Equation (12)}$$

or rearranged as:

$$N_f = \frac{W_N}{\pi \varepsilon_0^2 S_0 \sin \varphi_0} \qquad \qquad \text{Equation (13)}$$

Where:

ε_0 = initial strain

S_0 = initial stiffness of mixture

φ_0 = initial phase shift between stress and strain

Besides the controlled-energy loading mode, the loading dependent energy relation factor is also useful (Van Dijk, 1975). The energy relation factor is defined as follows:

$$\psi = \frac{N_f w_0}{W_N} \qquad \qquad \text{Equation (14)}$$

This factor is mainly linked to the test and the mixture stiffness as can be seen in Figure 3345. For stress-controlled tests, ψ will be ≤ 1 and for strain-controlled tests, ψ will be ≥ 1. In the case where materials are fully elastic ($S_{mix} \approx 26 \, GPa$) controlled stress and controlled strain tests would have no difference.

Considering the energy relation factor, the dissipated energy equation then becomes:

$$N_f = \frac{W_N \psi}{\pi \varepsilon_0^2 S_0 \sin \varphi_0} \qquad \qquad \text{Equation (15)}$$

And for regression analyses, it becomes:

84

$$N_f = A(W_N)^a (\psi)^b (\varepsilon_0)^{-c} (S_0)^{-d} (\sin \varphi_0)^{-e}$$

Equation (16)

From above equation, it can be seen that for both controlled-stress and controlled-strain loading, both the cumulative dissipated energy and the initial energy contribute to the fatigue life, as follows:

$$N_f \propto W_N, w_0$$

Equation (17)

Or alternatively:

$$N_f \propto W_N, \varepsilon_0, S_0, \varphi_0$$

Equation (18)

In laboratory testing stress, strain and the phase angle between the two can be determined. Also, it is possible to obtain the cumulative dissipated energy at any number of loading cycle.

The classic and dissipated energy tactics are both empirical in nature because neither tackles the challenge of exactly how damage develops from the start to the end of the loading period. They relate the fatigue behaviour of bituminous materials to test conditions, in the case of the classic tactic it is to the initial tensile strain and the initial stiffness. Whereas, in the case of the dissipated energy tactic it is to the terminal test condition, the cumulative dissipated energy to failure.

 As was detailed previously the dissipated energy method indicates a certain mixtures' resistance and furthermore relates the fatigue behaviour of visco-elastic materials to the build-up of distortion energy as a result of repeated load applications. However for it to be used in the mechanistic design method, ψ, φ and W_N have to be determined.

2.9.3. Simplified Approach

Other than the classical and dissipated energy approaches a number of simplified techniques have also been accepted to predict fatigue performance for pavement designs (AASHTO, 1972; Brown et al., 1982; Asphalt Institutes, 1982 and Shell, 1990). This tactic is considered for cases in which data obtained from above mentioned tactics (phase angle, energy relation factor, total dissipated energy and fatigue life) are not available, for the bituminous mixture in question. Relationships for this mixture can then be simplified if a reduction in accuracy is not critical.

In such cases the following may be employed:

- If there are similar mixtures, their data may be used.
- For increased accuracy, a number of fatigue tests can be conducted.

The Nottingham University formulated a general correlation between the ring-and ball softening point of asphalt mixtures, binder content(volume basis), tensile strain and amount of load repetitions till failure, as follows,

85

$$\log \varepsilon_t = \frac{14.39 \log V_B + 24.2 \log \text{T}_{RB} - 46.06 - \log N_f}{5.13 \log V_B + 8.63 \log \text{T}_{RB} - 15.8}$$

Equation (19)

Where:

ε_t = allowable tensile strain

N_f = amount of load repetitions to fatigue life

V_B = binder content (% volume)

T_{RB} = initial binder ring and ball softening point (°C)

From the Shell the fatigue strain is approximated as:

$$\varepsilon_t = (0.856 V_B + 1.08) S_{mix}^{-0.36} N_f^{-0.2}$$

Equation (20)

Where:

ε_t = allowable tensile strain

N_f = amount of load repetitions to fatigue life

V_B = binder content (% volume)

S_{mix} = stiffness of the mixture

Shell's model for the fatigue strain differs from the actual one by not more than 30 to 40 percent.

The Asphalt Institute proposed the following relationship:

$$N_f = 18.4C(4.325 * 10^{-3} \varepsilon_t^{-32.91} S_{mix}^{-0.854}$$

Equation (21)

Shell and the Asphalt Institute both have the same variable, C is a correction factor found from:

$$C = 10^M$$

Equation (22)

Where:

$$M = 4.84(\frac{V_B}{V_A + V_B} - 0.69)$$

Equation (23)

Where:

V_A = aggregate content (% volume)

V_B = binder content (% volume)

Furthermore Finn et al. (1977) also developed an expression based on field data from the AASHTO and laboratory data, as follows:

$$\log N_f = 15.947 - 3.219 \log \varepsilon_t - 0.854 \log \frac{E^*}{10^3}$$

Equation (24)

Where:

N_f = amount of load repetitions to fatigue life

ε_t = allowable tensile strain

E^* = complex modulus of asphalt (psi), can be estimated from the resilient modulus (M_R)

The expressions detailed above are only estimations and shouldn't be used for evaluation of mixture, but only for pavement designs. Although they are only approximations these relationships are quite useful as they reflect the property of the bituminous mixtures in the ring-and-ball softening point temperatures or in the stiffness of the asphalt.

One always finds differences between results from laboratory tests and field data. In general it is found that a pavement's fatigue life as calculated from laboratory fatigue tests is usually lower than the fatigue life as observed in the field (Jenkins, 2000).

Various factors can be used to explain this difference. These may be traffic wander, crack propagation and even the partial "healing" that the pavement may undergo between periods of rest from loading (SHELL, 1978). In highway pavements fatigue can be 10 to 100 times higher than that found with laboratory testing that is subjected to critical distress settings.

There remains then a challenge to develop meaning relationships between laboratory and field data. A way to solve this problem is to use shift factors to relate characteristics from laboratory simulated environments to that of the real environment.

3. Research Approach

3.1. Background

The use of bituminous road surfacing on pavement bases has a limited life, because bitumen reacts with oxygen in the air, leading to atmospheric oxidation, loss of volatiles and permanent physical hardening of the bitumen. These mechanisms of hardening are the ultimate result of ageing that cannot be reversed. When a particular critical viscosity level is reached, this is determined by the local climatic condition, the bituminous surfacing cracks or loses its structural integrity. It is at this stage that a particular type of repair would be prescribed to continue the level of service for road users.

The revision of the SAPDM for thin surfacing bituminous materials as detailed in the 2010 inception report called for improved damage models for thin bituminous surfacing, including hot mix asphalt wearing courses and base courses, ultra-thin surfacing layers and seals using conventional and modified binders. This research study formed part of the thin surfacing subdivision that focused on seals. The project team sampled aged seals from different locations across South Africa and subsequently recovered binder analysis, permeability tests, Indirect Tensile Tests (ITT) tests and fatigue tests were performed. The author of this study specifically focused on laboratory fatigue testing and relating trends in flexural stiffness reduction to crack patterns observed on the road itself.

Various test variables were taken into account, these were; seal types, age of seals, climatic regions, position in road, previous traffic and type of binders were considered. Figure 3-1 below shows the geographical locations from the five (5) provinces across South Africa from which the sprayed seal samples were extracted; namely Western Cape, Eastern Cape, Northern Cape, KwaZulu-Natal and Limpopo Province.
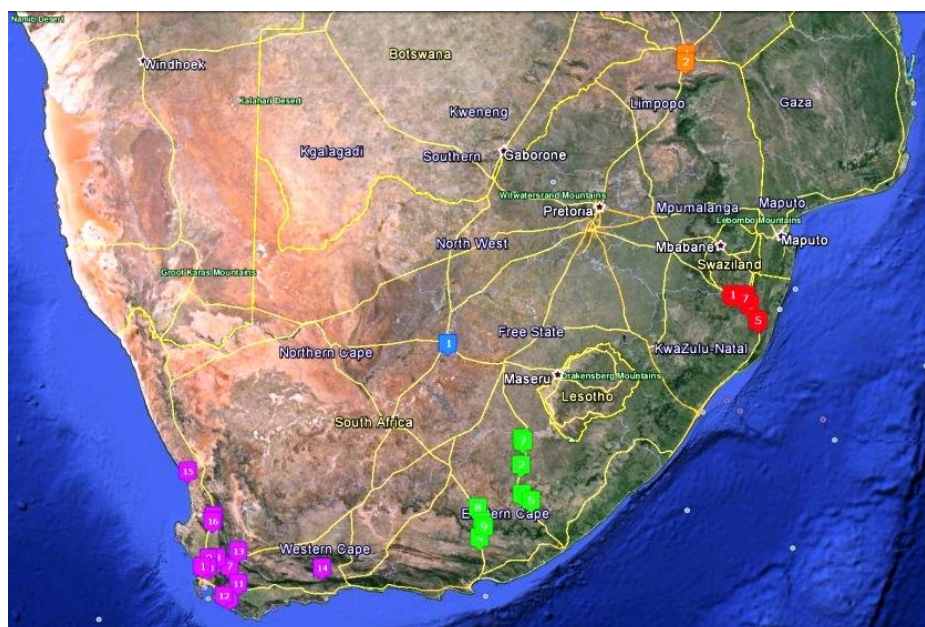
Figure 3-1: Geographical locations from which samples were taken (Google Earth)

88

Sprayed seal slabs were sampled from 35 different sites across South Africa and transported to the University of Stellenbosch in the Western Cape Province. At each geographical location samples were taken considering the following wheel track positions:

- Outside Wheel Track (either shoulder, outer wheel track or between wheel track)
- Inner Wheel Track (either outer wheel track, between wheel track or inner wheel track)

Detailed information of the various samples can be seen in Appendix 7B.

3.2. Sample Distribution

From these sprayed seal slabs the researcher prepared three (3) batches. The first batch (approximately one third) was sent to the Council of Scientific and Industrial Research (CSIR) in Pretoria for recovered binder analysis.

Another third were cut for Marvil Permeability tests and Indirect Tensile Tests (ITT) for final year undergraduate students and the last third used to manufacture seal beams that were subjected to flexural testing in the 4PB beam apparatus, which is the main focus of this study.

Figure 3-2 A and B below depict the arrival of the sampled seal slabs after extraction from existing road networks across South Africa.

Figure 3-2 A and B: Arrival of Sampled Sprayed Seal Slabs at the University of Stellenbosch

3.2.1. Recovered Binder Analysis and Marvil Permeability Tests

As discussed in *Section Bituminous Binders* the bitumen content and bitumen properties form an integral part in the performance of the sprayed seal. A third of the Sprayed Seal slabs were sent to the CSIR in Pretoria and a binder recovery analysis was performed.

Subsequently, the penetration index which is a measure of the bitumen temperature susceptibility was deduced from the Shell Nomogrpah for SP/Pen. The bitumen properties of the sampled seals can be seen in Appendix 7D. A third of the sprayed seal samples were used for Marvil Permeability Tests (Annandale, 2012). As seals age, they become prone to

cracking, which increases permeability. Marvil permeability test results can be seen in Appendix 7E.

3.2.2. Developing of Fatigue Testing of Sprayed Seal Beams using the Four Point Bending Beam Apparatus

3.2.2.1.   Four Point Bending (4PB) Beam Testing Approach

A third of the sprayed seal slabs were used in developing fatigue testing using the 4PB Beam Apparatus. It was decided to use the Four Point Bending Beam Apparatus, because compared to the Multi Modal Loading Simulator (MMLS) machine, which is ideal for empirical performance testing, it could determine the actual stiffness modulus of the sprayed seal, from which fatigue characteristics could be derived from the Classical Approach by Wohler, as defined below as:

$$N_f = k_1(\varepsilon_t)^{-k_2}$$
<div align="right">Equation (25)</div>

Where:

N_f = amount of load repetitions to fatigue life

ε_t = maximum tensile strain found in the bottom of the asphalt layer, also the applied tensile   strain in the 4PB test

k_1, k_2 = material coefficients

Similarly to the MMLS that can measure the actual rutting deformation, with the 4PB Beam Apparatus the research approach could use frequency sweep testing to see the effect of rutting at low temperatures, as well as the effect of fatigue at higher temperatures.

The MMLS machine is however more representative of the seal sprayed seal environment, in terms of the wheel load and the resultant deflection of the surfacing layer, but it requires a far greater set-up than the 4PB apparatus and far more test considering all the different variables for the research approach.

Furthermore, the MMLS normally tests seals that were constructed in the laboratory, whereas the aim or purpose of this research study was to assess specimens extracted from various existing roads in South Africa. With new seals, the set-up for testing can be done relatively without challenges, whereas with sampled seals from existing roads, the conventional set-up requires careful modification. Especially important would be to ensure adequate support below the sprayed seal, to prevent the wheel pulling the seal layer in the direction of the wheel path.

Testing with the 4PB apparatus was not previously attempted and also had various challenges, which will be discussed further in this section. The initial approach was however motivated by the fatigue characterisation guideline for Hot Mix Asphalt (HMA), which was adopted for South Africa and defined by CSIR in 2000 as follows:

Table 3-1: Guideline for the Interpretation of Fatigue Test Data at Constant Strain (CSIR, 2000)

Relative Fatigue Performance	Number of Load Repetitions at Strain Regime at 5°C and 10Hz		
	Low Strain (180 - 230με)	Medium Strain (230 - 380με)	Low Strain (380 - 430με)
Good	>2 400 000	>130 000	>60 000
Medium	1 000 000 - 2 400 000	30 000 – 130 000	20 000 – 60 000
Poor	<1 000 000	<30 000	<20 000

The guideline is not strictly applicable for seals, but the guideline was used for comparative purposes. The guideline states that there are unavoidable differences in support conditions, traffic axle configurations and wander, traffic speeds, type pressure and axle loads that can lead to a significant variation in actual tensile strains for a uniform section of road, which is true for HMA as well as for seals.

Since, the HMA Guideline advises that it is not appropriate to represent the strain condition in a road by a single strain value and suggests that it is more appropriate to calculate a range of expected strains using a probabilistic response model, and then characterizing the working strain range of pavement as low, medium or high, the same approach was adopted for the fatigue characterisation of seals.

The HMA guideline further recommends that beams should be tested at the strain level that falls within the appropriate strain regime and a minimum of 3 beams should be tested at the strain regime. The graphical presentation of the strain regimes are presented in Figure 3-3 below.

Figure 3-3: Strain Regimes for the Four Point Beam Fatigue Performance of HMA (CSIR, 2000)

From the figure above it can be seen that good fatigue performance in the bituminous mixture is illustrated by the upper limit line, in between it is either medium-poor or good-medium and below lower limit line indicates poor performance of the mixture.

3.2.2.2.   Applicable Strain Levels

In order to use the fatigue testing apparatus however a standard beam with dimensions listed in ASTM D7460-10 "Standard Test Method for Determining Fatigue of Compacted Asphalt Concrete Subjected to Repeated Flexural Bonding" was required. The required length of 380mm and width of 63mm could easily be achieved, but the same could not be easily obtained for the required 50mm height for the specimen. This proofed to be the greatest challenge during the start-up of the research approach.

A decision was made to add a material to the bottom of the seal beam that would provide the additional height needed for the specimen to be of acceptable standard. This material had to provide a type of support that could simulate a G1, granular base in a typical pavement system, with modulus in the order of 1000MPa, but that would also not show any fatigue characteristics, for simplicity sake. A two part fast-cast polyurethane, referred to F16, was procured from AMT Composites in Cape Town and showed reasonable promise, as can be seen in Table 3-2.

Table 3-2: Properties of F16 - Polyurethane as Obtained from Supplier

Properties	Standards	Units	Values
Hardness	ISO 868-85	Shore D1	72
Flexural Modulus of Elasticity (Ef)	ISO 178-93	MPa	1000
Flexural Strength	ISO 178-93	MPa	37
Compressive Yield	ISO 604-97	MPa	33
Charpy Shock Resistance	ISO 1791/D	kJ/m^2	13

Standard beams were manufactured from only this material (Figure 3.4 A and B) and subjected to flexural bending testing trials in the laboratory.

Figure 3-4 A and B: Two Part Fast-Cast Polyurethane Beam

The first point of departure was to determine the applicable strain level. This was done by testing the upper limit of the High Strain Regime, which was recommended to be 430µε. The

possibility of extending this upper limit was considered and the first trial test was performed at 480με.

From the flexural bending testing at 480με, 10°C and loading frequency of 10Hz it could be seen that the material did not lose any significant amount of flexural stiffness after 3.5 million load repetitions and an average of 1433 MPa was recorded as its modulus, as can be seen in Figure 3-5, comparable to that of a pre-cracked cemented sub-base or base layer, with FWD back calculated stiffness ranging between 1000 and 1500MPa (De Beer, 1985 and Freeme et al., 1982). Failure mode for cemented layers is fatigue cracking, with reduction in flexural stiffness.
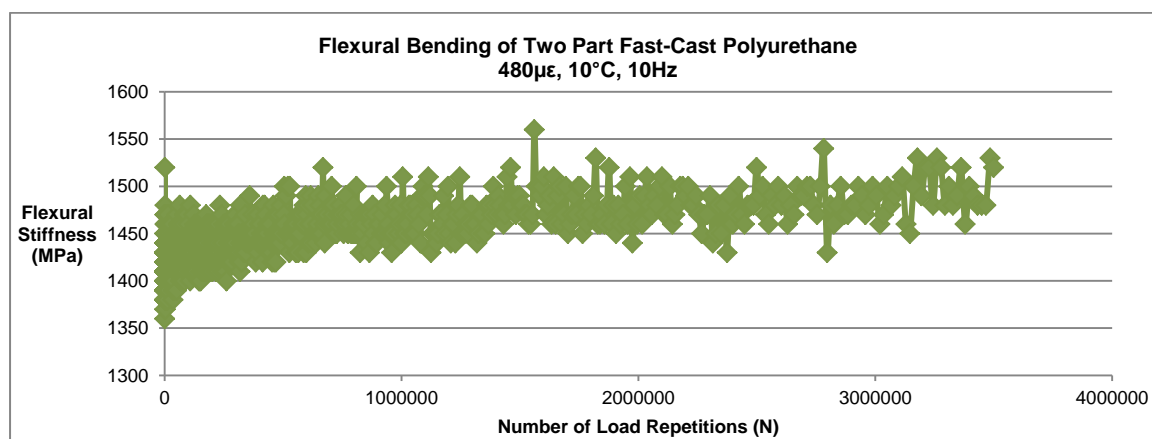
Figure 3-5: Flexural Bending of F16 - Polyurethane Beam, 480με, 10°C, 10Hz

From the first trial it appeared that the F16-Polyurethane did not fit the strain criteria as defined for HMA mixtures, but more importantly it suggested the possibility of a higher strain regime. A second flexural bending testing was performed at 520με, 10°C and at a loading frequency of 10Hz which also indicated that the material did not lose any significant amount of flexural stiffness after 3.5 million load repetitions and an average of 1419 MPa was recorded as its modulus, as can be seen in Figure 3-6.
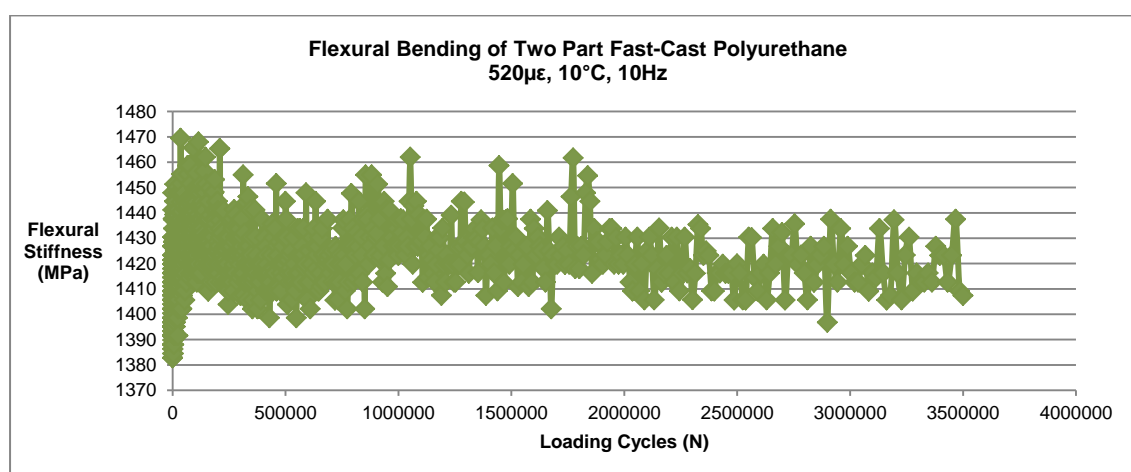
Figure 3-6: Flexural Bending of F16 - Polyurethane Beam, 520με, 10°C, 10Hz

A third flexural bending testing was performed at a higher strain, at 680με, 10°C and a loading frequency of 10Hz and also indicated that the material did not lose any significant

amount of flexural stiffness after 3.5 million load repetitions and an average of 1358 MPa was recorded as its modulus, as can be seen in Figure 3-7.
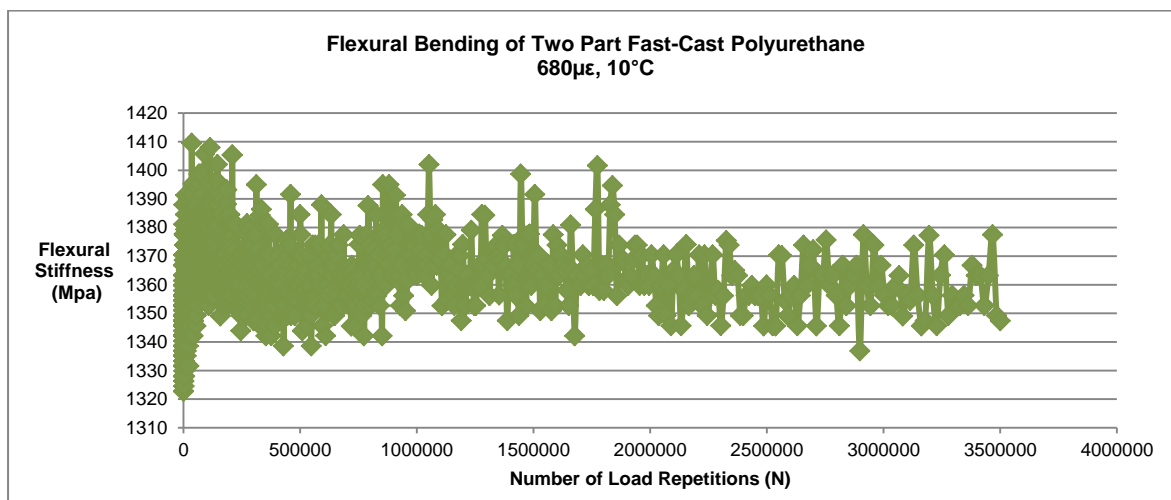
Figure 3-7: Flexural Bending of F16 - Polyurethane Beam, 680µε, 10°C, 10Hz

The trial testing of the F16-Polyurethane beams paved the way for the development of the fatigue testing of composite beams, comprising of sampled sprayed seal and F16-Polyurethane material. The following summary from the trial testing:

Table 3-3: Summary of Trial Testing of F16-Polyurethane Beams

	Low Strain (480µε)	Medium Strain (+40µε) (520µε)	High Strain (+160µε) (680µε)
Average Flexural Stiffness (MPa)	1433	1419	1358

Since the High Strain was set at 680µε, which is four (4) times the initial strain, it made more sense to have equal increments of strain increase (480µε, 520µε, 600µε); therefore it was decided to set the high strain limit at 600µε. The following average flexural stiffness for the adjusted high strain limit was interpolated from the trial test as follows:

Table 3-4: Adjusted High Strain Limit

	High Strain Limit, 680µε (Trial Test)	Adjusted High Strain Limit, 600µε (Interpolated)
Average Flexural Stiffness (MPa)	1358	1398

94

Figure 3-8 below illustrates the relationship between the test strain levels and resultant flexural stiffness from the trial testing of the polyurethane beams.
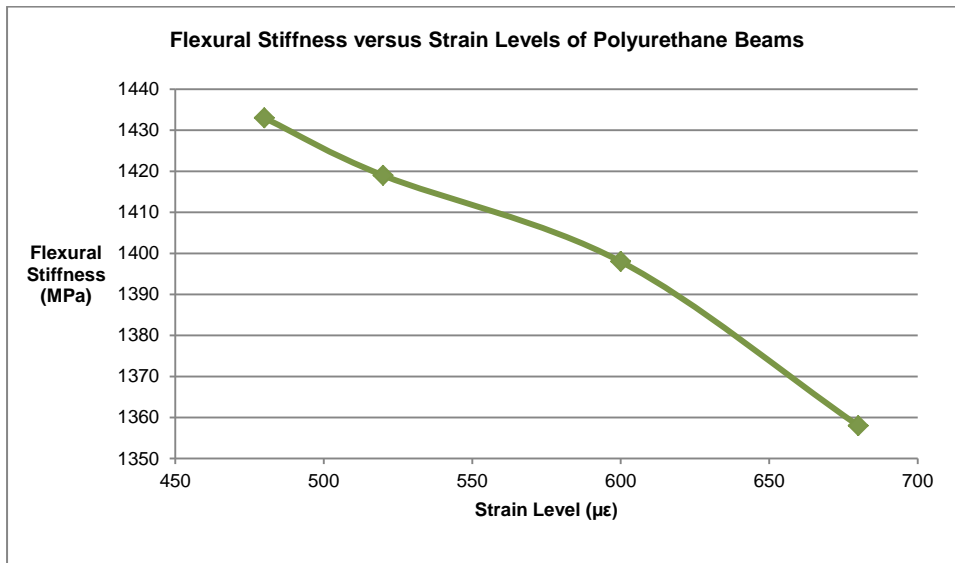
Figure 3-8: Flexural Stiffness versus Strain Levels of Polyurethane Beams

Low strain level 480µε, medium strain level 520µε and high strain level 600µε were set as the applicable strain levels at which the composite sprayed seal / F16-Polyurethane beams would be tested at. Sprayed seal slabs for the seal beams to be tested were thoroughly inspected for any defects and cleaned as can be seen in Figure 3-9 A and B. Samples with defects were excluded.

Figure 3-9 A and B: Inspection and Cleaning of Sprayed Seal Slabs before Cutting into Beams

Thereafter, three beams were cut from the sampled sprayed seal slabs and inserted into a wooden mould, as can be seen in Figure 3-10 A-D.

95

Figure 3-10 A-D: Cutting of Sprayed Seal Beams and Placing into Wooden Mould

Subsequently, the F16 - Polyurethane was added to the sprayed seal beam (See Figure 3-11 A and B) and after 2min the polyurethane set and completely bonded to the seal.

Figure 3-11 A and B: Sprayed Seal Beam Casted With Two Part Fast-Cast Polyurethane

Lastly the composite beam was refined (See Figure 3-12 A and B) to fit within the tolerances of the ASTM standards and then tested (See Figure 3-13 A and B).

Figure 3-12 A and B: Refined Sprayed Seal-Polyurethane Beam

Figure 3-13 A and B: Testing of Composite Beam in 4PB Beam Apparatus

Seals are relatively thin and after being in service for many years, they tend to become brittle and break quickly. During the inspection of the slabs some were found to be disintegrated or cracked and these were excluded from this study.

The characterisation of fatigue properties in this study was established by carrying out two (2) groups of testing:

- Group 1:

One fatigue test at two strain levels (480 and 600με) and associating the respective number of load repetition to failure (fatigue life). The numbers of load repetitions to failure are the numbers of repetition to the point of crack initiation in the pavement layer, or beam specimen.

The Wöhler parameters were determined from a regression analysis plotted on log-log scale using strain levels and loads repetitions to failure. One frequency sweep test at 520με from which Master Curves were produced.

The following tables indicate the seal/polyurethane beams tested in the first group of testing.

Table 3-5: Sprayed Seal Beams Tested in Group 1_Western Cape Province

No.	Province	Type of Seal	Seal Name	Age (Years)	Frequency Sweep (µε)	Fatigue Testing (µε)
1	Western Cape	Single	DR 2216_ BWT _1km_13mm	10	520	480, 600
2			DR 2216_ IWT _1km_13mm			
3			MR 536_ BWT _4.3km_ 19mm	19		
4			MR 536_ IWT _4.3km_19mm			
5		Double	DR1123_IWT _23.4km_13+7mm	17		
6		Cape	MR174_OWT_9km_19mm	10		
7			MR23_OWT_17km_19mm	10		

Table 3-6: Sprayed Seal Beams Tested in Group 1_Eastern Cape Province

No.	Province	Type of Seal	Seal Name	Age (Years)	Frequency Sweep (µε)	Fatigue Testing (µε)
1	Eastern Cape	Cape	N6_5_OWT _46km_19mm	4	520	480, 600

Table 3-7: Sprayed Seal Beam Tested in Group 1_Northern Cape Province

No.	Province	Type of Seal	Seal Name	Age (Years)	Frequency Sweep (µε)	Fatigue Testing (µε)
1	Northern Cape	Double	N8_8_SHDR _5.6km_19+9mm	6	520	480, 600

Table 3-8: Sprayed Seal Beams Tested in Group 1_KwaZulu-Natal Province

No.	Province	Type of Seal	Seal Name	Age (Years)	Frequency Sweep (µε)	Fatigue Testing (µε)
1	KwaZulu-Natal	Double	N2_31_OWT_N_Bound_3.6km_ 13+7mm	11	520	480, 600
2			N2_31_OWT_S_Bound_3.6km_ 13+7mm	11		

- Group 2:

One frequency sweep test at 480με from which Master Curves were produced. The following table indicates from which sites and positions in the road, seal/polyurethane beams could be produced.

Table 3-9: Sprayed Seal Beams Tested in Group 2_Western Cape Province

		Sprayed Seal Information			Beam Testing	
No.	Province	Type of Seal	Seal Name	Age (Years)	Frequency Sweep (με)	Fatigue Testing (με)
1	Western Cape	Single	DR1681_BWT _5km_13mm	11	480	-
2			DR1452_BWT _14.1km_13mm	12		
3		Double	DR2175_IWT _3km_13+7mm	6		
4			DR2175_BWT _3km_13+7mm	6		
5			MR269_OWT _3km_13+7mm	13		
6		Cape	TR2701_OWT_5km_19mm	23		
7			DR1398_OWT_1km_19mm	23		
8			DR1398_SHDR_ 1km_19mm	23		

Table 3-10: Sprayed Seal Beams Tested in Group 2_Eastern Cape Province

		Sprayed Seal Information			Beam Testing	
No.	Province	Type of Seal	Seal Name	Age (Years)	Frequency Sweep (με)	Fatigue Testing (με)
1	Eastern Cape	Cape	N6_5_SHDR_53.4km_19mm	12	480	-
2		Multiple	N6_4_SHDR_ 8km_19+6+6	9		

Table 3-11: Sprayed Seal Beam Tested in Group 2_Northern Cape Province

		Sprayed Seal Information			Beam Testing	
No.	Province	Type of Seal	Seal Name	Age (Years)	Frequency Sweep (με)	Fatigue Testing (με)
1	Northern Cape	Double	N8_8_OWT _5.6km_19+9mm	6	480	-

Table 3-12: Sprayed Seal Beam Tested in Group 2_KwaZulu-Natal Province

	Sprayed Seal Information				Beam Testing	
No.	Province	Type of Seal	Seal Name	Age (Years)	Frequency Sweep (µε)	Fatigue Testing (µε)
1	KwaZulu-Natal	Double	N2_31_OWT _41.2km_13+7mm	6	480	-
2			R63_ OWT _6km_13+7mm	7		

Table 3-13: Sprayed Seal Beam Tested in Group 2_Limpopo Province

	Sprayed Seal Information				Beam Testing	
No.	Province	Type of Seal	Seal Name	Age (Years)	Frequency Sweep (µε)	Fatigue Testing (µε)
1	Limpopo	Multiple	N1_29_OWT_ 79.8km_19+6+6	9	480	-

3.2.2.3. *Structural Mechanics Solution*

The flexural stiffness values measured with the 4PB beam apparatus was for the entire composite Sprayed Seal - F16 Polyurethane beam. However the focus of the study was on the performance of the sprayed seal only. Therefore it was required that the data be split into the two respective layers that made up each composite beam.

From the Direct Beam Theory the following solution for a composite cross section as illustrated in Figure 3-15 was obtained:
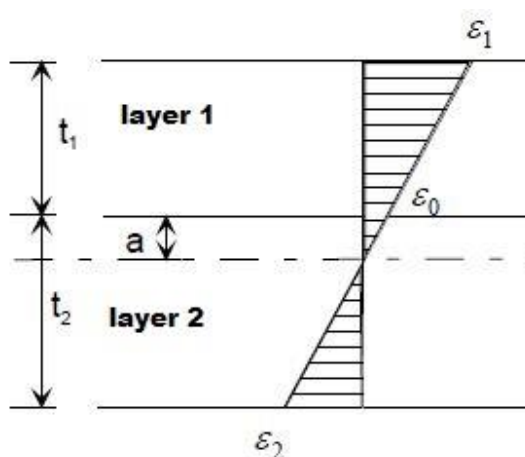
Figure 3-14: Illustration of Composite Beam Cross Section

$$a = \frac{(-E_1 A_1 t_1 + E_2 A_2 t_2)}{2(E_1 A_1 + E_2 A_2}$$

Equation (26)

100

Where:

a = Distance between layer 1 and the neutral axis of the composite cross section

E_1 = Stiffness of Layer 1 (Seal Layer)

A_1 = Area of Cross Section of Layer 1

t_1 = Thickness (Height) of Layer 1

E_2 = Stiffness of Layer 2 (F16 Polyurethane Layer)

A_2 = Area of Cross Section of Layer 2

t_2 = Thickness (Height) of Layer 2

$$EI = E_1 I_1 + E_2 I_2 + \left(a + \frac{t_1}{2}\right)^2 E_1 A_1 + \left(\frac{t_2}{2} - a\right)^2 E_2 A_2$$

Equation (27)

Where:

E = Stiffness of Composite Cross Section

I = Moment of Inertia of the Cross Section

E_1 = Stiffness of Layer 1 (Sprayed Seal Layer)

I_1 = Moment of Inertia of Layer 1 (Sprayed Seal Layer)

E_2 = Stiffness of Layer 2 (F16 - Polyurethane Layer)

I_2 = Moment of Inertia of Layer 2 (F16 Polyurethane l Layer)

a = Distance between layer 1 and the neutral axis of the composite cross section

t_1 = Thickness (Height) of Layer 1

t_2 = Thickness (Height) of Layer 2

A_1 = Area of Cross Section of Layer 1

A_2 = Area of Cross Section of Layer 2

With the aid of MATLAB and the Direct Beam Theory, the following implicit solution was obtained for the Sprayed Seal Layer:

$E_1 = 1/8/I_1 /A_1 *(-4*E_2 *I_2 *A_1 -E_2 *A_2 *A_1 *t_1 ^2 -2*E_2 *A_2 *A_1 *t_1 *t_2 -E_2 *A_2 *A_1 *t_2 ^2 +4*$
$4*I_1 *E_2 *A_2 + (16*E_2 ^2*I_2 ^2*A_1 ^2 +16*E ^2*I ^2*A_1 ^2 +16*I_1 ^2*E_2 ^2*A_2 ^2 +E_2 ^2$
$*A_2 ^2*A_1 ^2*t_1 ^4 +E_2 ^2*A_2 ^2*A_1 ^2*t_2 ^4 +16*I_1 *E_2 ^2*A_2 ^2*A_1 *t_1 *t_2 32*I_1 *E_2 ^2$
$*A_2 *I_2 *A_1 +32*I_1 *E_2 *A_2 *E *I *A_1 +8*I_1 *E_2 ^2*A_2 ^2*A_1 *t_2 ^2 +8*I_1 *E_2 ^2*A_2 ^2$
$-32*E_2 *I_2 *A_1 ^2*E *I +8*E_2 ^2*I_2 *A_1 ^2*A_2 *t_1 ^2 +16*E_2 ^2*I_2 *A_1 ^2*A_2 *t_1 *t_2$
$+8E_2 ^2*I_2 *A_1 ^2*A_2 *t_2 ^2 -8*E *I *A_1 ^2*E_2 *A_2 *t_1 ^2 +16*E *I *A_1 ^2*E_2 *A_2 *t_1 *t_2$
$-8*E *I *A_1 ^2*E_2 *A_2 *t_2 ^2 +4*E_2 ^2*A_2 ^2*A_1 ^2*t_1 ^3*t_2 +6*E_2 ^2*A_2 ^2*A_1 ^2*t_1 ^2$
$*t_2 ^2 +4*E_2 ^2*A_2 ^2*A_1 ^2*t_1 *t_2 ^3) ^ (1/2))$

Equation (28)

3.2.2.4.   Sinusoidal versus Haversine Loading

This study also set out to investigate whether or not it is possible to do haversine fatigue testing in controlled deflection mode on a composite beam, as illustrated in Figure 3-15 below.
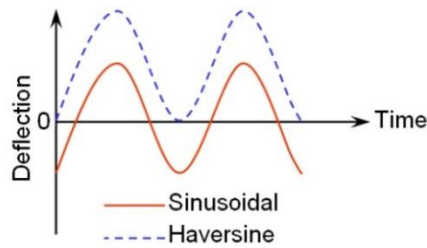
Figure 3-15: Sinusoidal and Haversine Loading Waveform

Figure 3-16 illustrates the deflection input and the stress and strain outputs that occur in the HMA beam during the test. Since the neutral position of the beam does not change in the sinusoidal test, both strain and stress developed are sinusoidal causing alternating tension and compression in the beam.
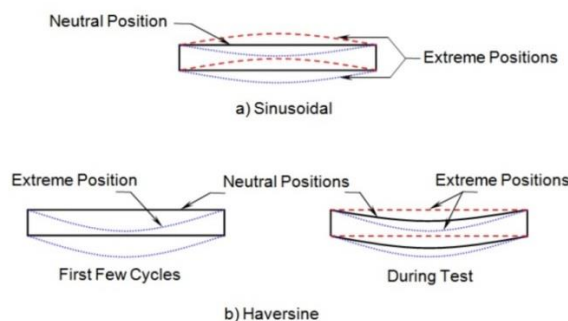
Figure 3-16: Extreme positions and neutral positions for Sinusoidal and Haversine Loading Waveforms

102

3.3. IPC 4PB Fatigue Testing System

The IPC fatigue testing system used in this study functions as a closed–loop response servo system powered with pneumatic strength (see Figure 3-17 and Figure 3-18). This system consists of the following three parts:

1. Interface Software

2. Control and Data Acquisition System (CDAS)

3. Test Device
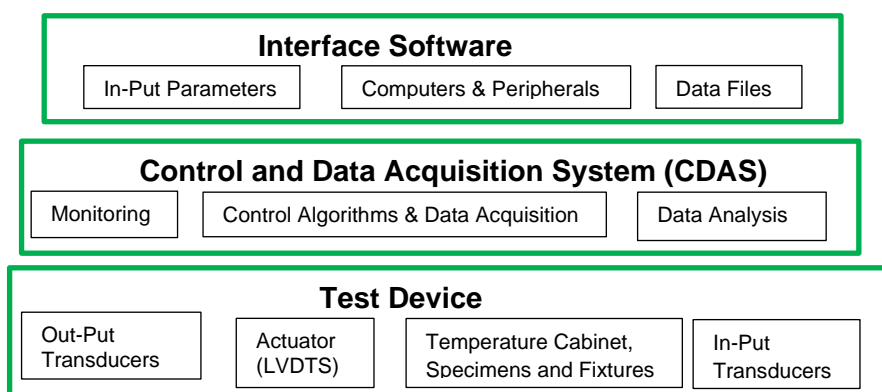
Figure 3-17: Fatigue Testing System (IPC, 1998)
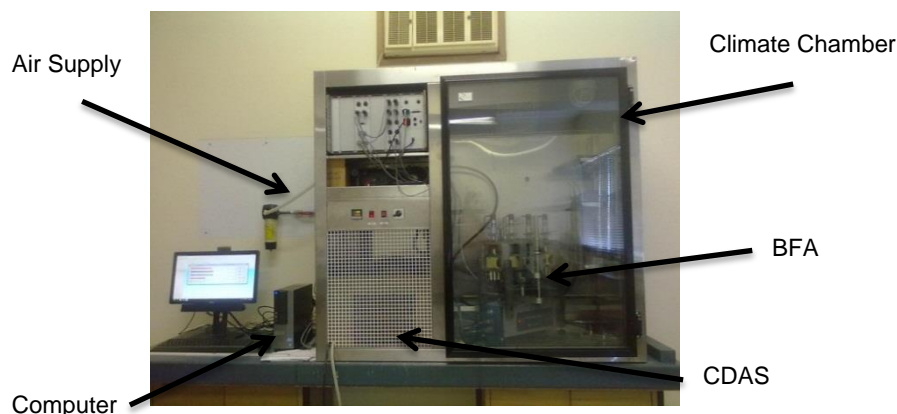
Figure 3-18: Pictorial Components of Fatigue Testing System

3.3.1. IPC Beam Fatigue Apparatus (BFA)

Four point fatigue life testing is done by means of the Beam Fatigue Apparatus (BFA), which is a stand-alone system that subject beam specimens to flexural bending until failure occurs as can be seen in Figure 3-19.

103
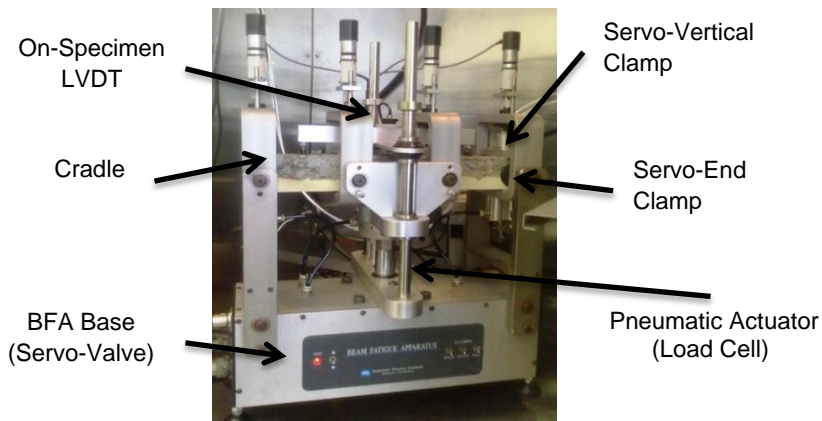
Figure 3-19: Beam fatigue apparatus (BFA)

ASTM D7460-10 "Standard Test Method for Determining Fatigue of Compacted Asphalt Concrete Subjected to Repeated Flexural Bonding" defines this failure as the number of load repetitions till 50% of the initial flexural stiffness is reached. The beam specimen is centered laterally and clamped by pneumatic clamps at the side of the frame. This frame mechanism permits rotation and free translation of the clamps, allowing the BFA to apply loads at the third points of the beam.

Furthermore, the servo-motor powered vertical clamps focus the beam at four points by means of a self-adjusted pre-determined clamp force. This force remains constant throughout the duration of the test. The servo motors are functioning uninterrupted throughout the test in order to absorb the slack resulting from creeping (permanent deformation) of the surface at the clamping surfaces.

The climate chamber as illustrated in Figure 3-18 is part of the testing apparatus but not of the closed loop feedback system, which means that the testing temperature can be adjusted manually. The BFA and the specimen to be tested are both placed inside the climate chamber (thermostat refrigerator control). The climate chamber is spacious enough to house the BFA and at least 6 beam specimens. It furthermore allows the loading frame to be adjusted when the test is set-up.

In order to determine the specimen's core and skin temperature a dummy HMA beam is used. This is also used to monitor the test temperature for the duration of the test. The dummy is only an indication of the actual core temperature of the specimen being tested and caution should be given to it as it may even be not be an accurate indication. This is due to the dummy being very susceptible to its environment.

3.3.2. Loading cradle, testing model and pneumatic system

A servo-controlled pneumatic actuator is built into the base of the BFA that allows the loading frame to be adjusted. An actuator span of 9kN is applied beneath the specimen. This is conflicting with the real pavement environment where traffic loads are applied at the top of the surfacing (Twagira, 2006). Though that may be the case, cracks originate from the bottom of both the layer/test specimen.

During the test the two central supports of the specimen is triggered to deflect in a sinusoidal (both directions) wave form (See Figure 3-20). This occurs with help of the CDAS which produce cyclic loading by manoeuvring the servo-controlled pneumatic actuator that is mechanically fixed to the frame loaded with the beam specimen.
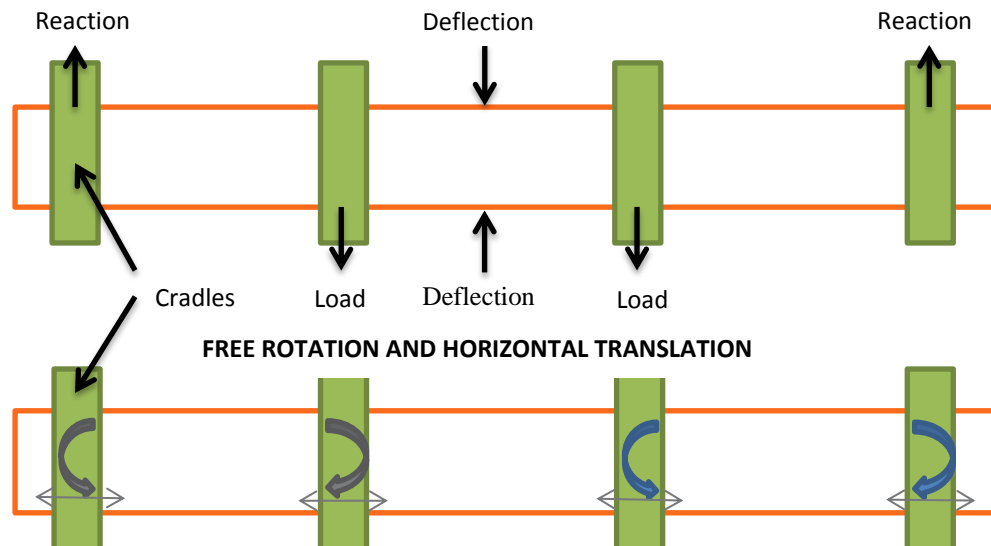
Figure 3-20: Loading Characteristics of Four Point Bending (IPC, 1998)

The frame mechanism consists of four points, the two central supports separated at a distance of 118.5mm and the two outer supports at a distance of 355.5mm. The outer two supports are fixed vertically during the test set-up, allowing only horizontal translation. The two central supports are free to move vertically. Fatigue failure is initiated in a section of uniform stress because the beam is stressed at the two inner supports (Twagira, 2006). The clamps at all four supports are servo-electronically maneuvered.

The performance of the transducers and pneumatic servo actuator depend on:

- Clean air supply at minimum pressure of 600kPa.

Low pressure will not permit the system to reach maximum force. After the air supply has been regulated at 600kPa it is passed through a 5micron filter constructed onto the regulator. Next the 5 liter collector is used to buffer the air supply before it enters the 0.5micron filter and the micro-mist separator.

- Dry air supply.

Regular draining of the filters is important to remove the build-up of water in the supply. The presence of water can block the air supply due to freezing of the condensation water in the cooling system at low test temperatures like 5°C and/or damage the servo-valve. When testing with untreated compressed air and at low temperatures it was previously found that the number of filters was not sufficient to prevent the block up of water and in this case various changes were made to improve the situation (Twagira, 2006).

Control data acquisition (CDAS), fatigue testing software (FTS) and microcomputer:

For a fatigue test a microcomputer (personal), software and CDAS is required for monitoring and controlling purposes (Teyabali et al., 1992, IPC, 1998). The computer initiates the CDAS to control the loading function of the specimen also the obtaining of data from the transducers that are attached to the test specimen.

Linear variable displacement transducers (LVDT) are placed above the specimen and measure deflections of the top of the inner third of the beam. All the important timing, control

105

and data gaining functions are provided for transducers and the frame by means of the closed loop response system. This data is then obtained from the CDAs and presented on the computer's screen in real time.

The CDAS is fitted with different input channels for correct functioning. For fatigue testing the following four, amongst others, are most important. They are:

1. Temperature control component indicating specimen's core and skin temperature.

2. Input from load cell.

3. External LVDT measuring the on-specimen displacement.

4. Internal LVDT measuring the ram/actuator displacement.

The test parameters used in the CDAS can be set by means of the fatigue testing software. The FTS records the applied load and deflection at every 10th cycle of the test. Each one of these cycles are conveyed to the computer, stored and displayed and then only updated from time to time on a logarithmic basis.

As the test proceeds the following parameters are recorded:

- Number of load repetitions (load cycles)
- Minimum and maximum applied load
- Minimum and maximum beam deflection
- Maximum tensile stress
- Maximum tensile strain
- Phase angle
- Flexural stiffness
- Modulus of elasticity
- Dissipated energy
- Cumulative dissipated energy

These test results can then be reviewed, printed or imported into a spreadsheet program for further analysis because the FTS creates a data file to store the test results.

3.3.3. Operation of the Fatigue Testing System (FTS)

Figure 3-21 schematically shows the operation of the fatigue testing system. Here it can be seen how the servo-controlled pneumatic actuator applies a load to the test specimen and how the two input transducers (load cell and external LVDT) convert deflection movements into standard electronic signal and the resulting display of test output on the computer provided by the CDAS.
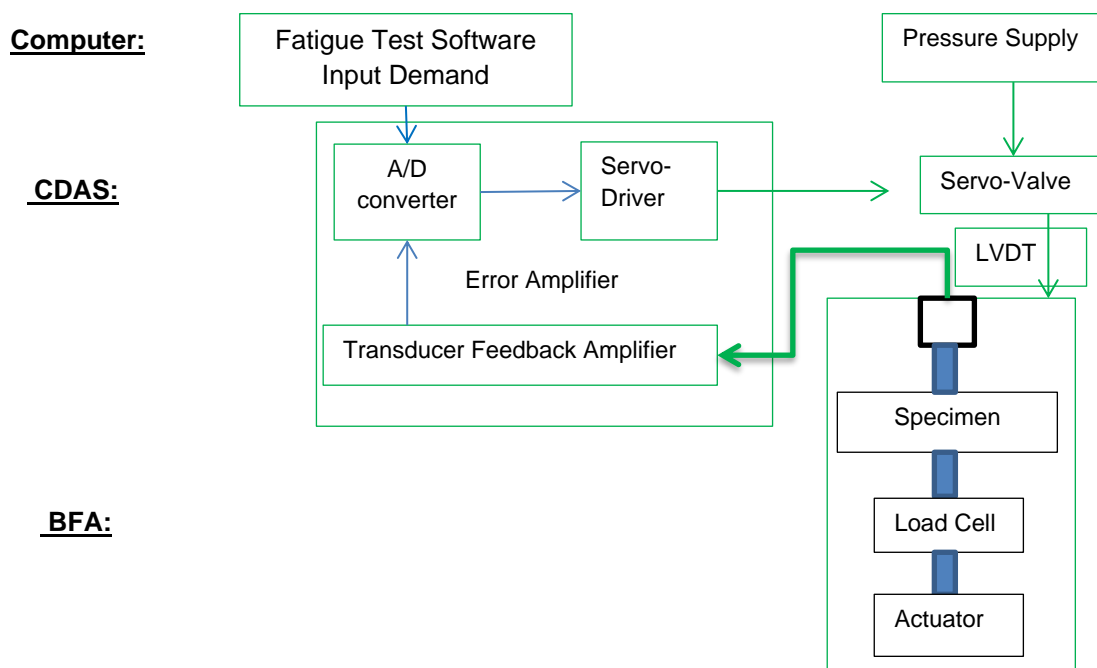
Figure 3-21: Operation of Fatigue Testing system (closed loop feedback servo-controlled) (IPC, 1998)

From the feedback of the input transducer, the CDAS is able to control and monitor the test parameters according to the requirements of the computer for the flexural test. For instance, if a constant level of strain is required, the CDAS is able to adjust the applied load so that the beam specimen is subjected to the same amount of strain at every cycle.

These changes are then sent by means of an error amplifier to the pneumatic actuator, servo valve and driver to normalize the air pressure and loading force to eradicate the error, as follow:

$$Drive\ ERROR = Input\ DEMAND - Position\ FEEDBACK \qquad \text{Equation (29)}$$

Following the removing of the error, the control loop is electronically closed and the test continues for each cycle until the termination conditions are reached.

3.4.   4PB Fatigue Testing Method

3.4.1. Testing Flexural Stiffness

The general procedure for determining flexural stiffness is based on ASTM D7460-10 "Standard Test Method for Determining Fatigue of Compacted Asphalt Concrete Subjected to Repeated Flexural Bonding". In this study the test method was modified by introducing a composite specimen, calculating the flexural stiffness of the composite and then calculating

the flexural stiffness of the seal only using direct beam theory (Mechanics of Materials, Roy R. Craig, 2011) in MATLAB.

For fatigue testing of asphalt mixes, the American Standard, ASTM D7460-10, 321 specifies a fatigue test temperature of 25°C, whereas the European Standard, EN 12697-26, specifies a mean fatigue test temperature of 20°C. Mullins (2006), however found that these high fatigue test temperatures were not practical within the laboratory setup as shear failure occurred at the clamps of the loading cradle.

In a sprayed seal context these high temperatures also introduce a great amount of healing within the specimen, whereas at low temperatures seals are most sensitive. As a result the beam specimens were conditioned at a test temperature of 10°C in the climate chamber before the test was started. This temperature was seen as a fair intermediate temperature between 5°C at which the surfacing layer is stiffened and cracks may occur and 25°C at which the surfacing layer is softened and rutting occurs, within the laboratory controlled environment.

HMA guideline considered 5°C for a 50mm height specimen. For seals however the layer thickness ranged between 15-35mm and the researcher was concerned that the specimens would accumulate damage during conditioning in the climate chamber that would influence the actual test results.

Specimens are generally conditioned for at least four hours before the test is started or until the dummy specimen in the climate chamber is +- 0.5°C of the test temperature. Conditioning of the specimen is important because it allows the specimen to stabilize at the testing temperature. The dummy specimen is quite sensitive to changes in the cabinet's temperature when the door is opened and closed. Care should therefore be given to keep the temperature constant, since the temperature of the dummy is fed back to the temperature control system.

Following conditioning, the specimen is placed in the BFA cradle and the test is setup as can be seen in Appendix A. The beam specimens were tested in strain-controlled mode, since maximum strain is considered a good indication of crack initiation, compared to stress controlled (Airey, 1995), with sinusoidal loading waveform at a loading frequency of 10Hz.

The suitability of Haversine loading was also investigated (See Section Sinusoidal versus Haversine Waveform Loading) and was found that the loading changed into sinusoidal loading.

3.4.2. Testing Parameters

Several test input parameters were entered so that the CDAS could control and monitor the loading function of the specimen and gather data from the test. These parameters were as follow:

- Operator identification
- Specimen identification and dimensions using Vernier calliper)
- Loading wave (sinusoidal)
- Loading frequency (10 Hz)
- Termination criteria, either the termination stiffness (50% of initial stiffness) or the maximum load repetitions (load cycles)

3.4.3. Termination Conditions

The flexural stiffness is ended as soon as one of the following occurs:

- The flexural stiffness is below the initial stiffness calculated at the first 50th loading cycle, or
- The amount of load repetitions reaches the amount specified by the operator before the test was started.

It is useful to set the termination stiffness artificially low and the amount of load repetitions artificially high in order to accurately assess the termination criteria. These values can be changed during the test period. Input parameters should be consistently entered and it should be ensured that every file agrees with the intended test.

3.4.4. Calculation of Flexural Stiffness

Maximum Tensile Stress:

$$\sigma_t = \frac{C_o\, P\, 10^6}{bh^2}$$

Equation (30)

Where:

σ_t = Maximum tensile stress (kPa)

C_o = Space between outside clamps (≈ 355.5mm)

P = Peak force (kN)

b = Average width of specimen (mm)

h = Average height of specimen (mm)

Maximum Tensile Strain:

$$\varepsilon_t = \frac{12\delta h 10^6}{3{C_o}^2 - 4{C_i}^2}$$

Equation (31)

Where:

ε_t = Maximum tensile strain (mm/mm)

δ = Peak deflection between two inner supports (mm)

h = Average height of specimen (mm)

C_o = Space between outside clamps (≈ 355.5mm)

C_i = Space between inside clamps (≈ 118.5mm)

Maximum Flexural Stiffness:

$$S = \frac{\sigma_t}{\varepsilon_t}$$

Equation (32)

Where:

S = Stiffness (MPa)

σ_t = Maximum tensile stress (kPa)

ε_t = Maximum tensile strain (mm/mm)

Phase Angle;

$$\varphi_t = 360fs$$

Equation (33)

Where:

φ_t = Phase angle (°)

f = Load frequency (Hz)

s = Time lag between maximum load and deflection (s)

Dissipated Energy per Cycle;

$$D = \pi\,\varphi_t \varepsilon_t \sin \varphi_t$$

Equation (34)

Where:

D = Dissipated energy per cycle (J/m^3)

φ_t = Phase angle (°)

ε_t = Maximum tensile strain (mm/mm)

Cumulative Dissipated energy:

$$\sum_i^n D_i$$

Equation (35)

Where:

D_i = Dissipated energy for each load cycle

3.5. Developing Master Curves

3.5.1. Overview

Bitumen behaves differently at different temperatures and with different loading rates. It has been observed as being neither purely elastic nor purely viscous. Bitumen when loaded at low temperature (or very quickly) has an elastic response, whereas when loaded at high temperatures (or very slowly) has a viscous response. Francken (1977) showed that for intermediate loading rate the two combines and a visco-elastic response is observed as can be seen in the Figure 3-22.
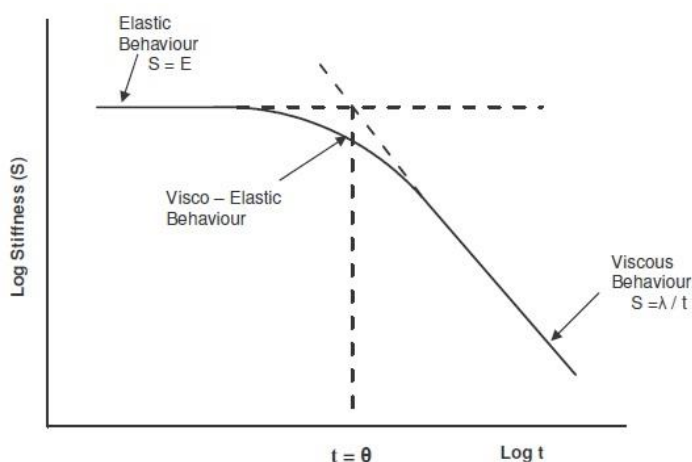
Figure 3-22: Stiffness of rheological materials as a function of loading time (Francken, 1977)

The fatigue performance of the bituminous materials is therefore strongly influenced by the stiffness characteristics. Medani et al. (2003) determined that due to the visco-elastic characteristics, the stiffness properties of the material must be established if the behaviour of the mix in both load induced and thermal stress and strain distribution in pavement layers.

Medani however said this for asphalt mixes, but the same concept applies to seals as they too can be seen as bituminous mixes, although non-homogenous. Initially seals are individual entities of bitumen and aggregate, but with time the two combine into an almost "carpet-like" sprayed seal layer.

Stiffness has been used as a measurement to quantity mixture quality for mixture design and pavements in order to assess deterioration and age-hardening patterns of bituminous mixtures, in the laboratory as well as in the field, (Epps et al., 2000). The stiffness of the mixture is predicted from the master curve i.e. the correlation between the mix stiffness, temperature and frequency (loading time). In recent times the 4PB-beam testing or the indirect tensile test is employed to define this relationship, (Medani et al., 2003 and Fritz et al., 1999).

The stiffness modulus of bituminous mixtures increases with increasing frequencies and decreasing temperature. Airey, (1995) explored the influence of deflection and loading frequency (primary variables) and temperature together with loading waveform (secondary variables) on the resultant stiffness and fatigue life of beam specimens subjected to fatigue testing in the four point beam bending apparatus. He showed that, as maximum strain is an acceptable gauge for outlining crack initiation, stiffness is detrimental in defining the fatigue performance of bituminous mixtures.

Many research projects have also shown that laboratory practices cannot define a complete set of stiffness values for a certain test temperature and over the full range of loading time. Laboratory procedures however have restrictions in determining a broad set of stiffness values over the complete range of loading time at a certain temperature. For this reason, laboratory measurements are done over a smaller loading frequency (time range) but at various temperatures, (Francken, 1977). He recommended the frequency sweep test, which tests at various temperatures over a short loading time.

3.5.2. Principle of Time-Temperature Superposition

The time-temperature relationship of a bituminous binder requires the setting up of a mathematical model that would describe said dependency, as well as material properties for an extensive range of temperatures and loading frequency from insufficient measurements made in a laboratory. Three dimensional non-linear constitutive correlations for time-temperature reliant material models are many times mathematically complex. For this reason conventional approaches lessen the three dimensional classification, i.e. modulus, time and temperature to two dimensional difficulties by making use of time-temperature superposition, (Mihai et al., 1996).

The development of a master curve is founded on the principle of thermo-rheological simplicity or time-temperature superposition, which expresses the stiffness or other visco-elastic moduli as a function of reduced time. This infers that the stiffness values of the mixtures can be obtained at different conditions; either at non-equilibrium behaviour (low temperatures) or at Newtonian behaviour (high temperature) or at linear visco-elastic behaviour (intermediate region).

Chehab et al. (2002) have shown that this property based on the work of Schapery et al. (1997) may be applicable even if the linear visco-elastic conditions are violated with respect to the principle of time-temperature superposition.

Stiffness moduli data measured at various temperatures are expressed as logarithm of the modulus against the logarithm of loading time and the subsequent data are "repositioned" in relation to the frequency (time of loading), until the various experimental data curves combine into only one function called the "Master Curve". This curve is created by means of a randomly designated reference temperature, (T) to which all experimental data are shifted. The shift factor at the selected reference temperature is equal to one.

This shift factor may be detailed in tabular, graphical format or regressed to fit some pre-set function such as Arrhenius or Williams-Landel-Ferry models (See below). Researchers have shown that the master curve can be mathematically expressed by means of the following relation:

112

$$\log f_{eq} - \log f = \log a_t$$

Equation (36)

Where:

f_{eq} = Frequency at which master curve should be read

f = Frequency at which test was performed (measured in Hz)

a_t = Shift factor to be applied

Literature (among other methods) indicated the following three techniques as most frequently used for calculation of shift factor (a_t) for the creation of the master curve. These are:

- Graphical shifting of experimental results,

- Making use of the Arrhenius type equation,

- Making use of the Williams-Landel-Ferry (WLF) equation.

These techniques are described below.

3.5.2.1. Graphical Shifting of Experimental Results

The measured stiffness values are plotted against log loading time or log frequency. After selection of a reference temperature, the values of the other temperatures are repositioned horizontally until they merge with the curve for the reference temperature. The shift factor can be attained by inter-or extrapolation).

The data attained at other temperatures are then repositioned until the extended reference curve is fixed. This technique was explained by Germann and Lytton (1977) as shown in Figure 3-23.
Measured results are repositioned as follows:

$$T_{master} = e^{\{\ln(t_{old}) - \ln(\overline{\alpha_i})\}}$$

Equation (37)

Where:

$$\ln(\bar{\alpha}) = \frac{\sum_{i=1}^{m} \ln(\alpha_i)}{m}$$

Equation (38)

$$\ln(\alpha_i) = \ln(T_{old,i}) - \ln(T_{new,i})$$

Equation (39)

$$T_{new,i} = 10^{(\log T_2 - \Delta x_i)}$$

Equation (40)

113

Where:

$$\Delta x_i \quad = \frac{\Delta y}{\tan \beta} = \frac{\delta x}{\delta y} \cdot \Delta y \qquad\qquad \text{Equation (41)}$$

$$\delta x \quad = \{\log(T_1) - \log(T_2)\} \qquad\qquad \text{Equation (42)}$$

$$\delta y \quad = \{\log(E_1) - \log(E_2)\} \qquad\qquad \text{Equation (43)}$$

$$\text{Equation (44)}$$
$$\Delta y \quad = \{\log(E_i) - \log(E_2)\}$$
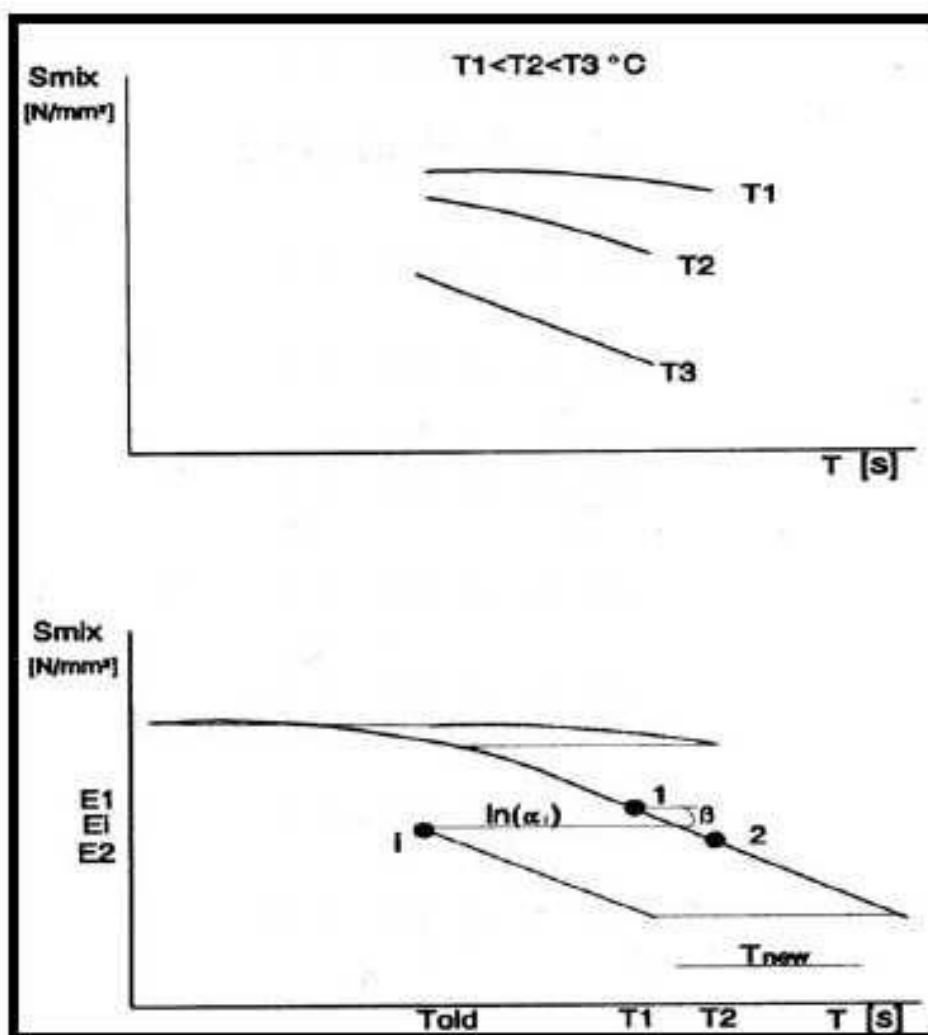
Figure 3-23: Setting up of master curve using fitting of experimental curve methods after Germann and Lytton, (1997)

$T_{new,i}$ is the repositioned time-value of data value i, repositioned over $\ln(\alpha_t)$, such that it exactly fits the reference curve. T_{master} is the repositioned time-value of value i, shifted over the mean shift factor for that specific temperature $\ln(\alpha_t)$.

Arrhenius type equation

One general formula for the shift factor is an Arrhenius type model (Francken et al., 1988, Jacobs 1995, Lytton et al., 1993), which can be seen below;

$$log\, f_{eq} - \log f = log\alpha_t$$
<div align="right">Equation (45)</div>

$$\log(\alpha_t) = \left(\frac{1}{T} - \frac{1}{T_{ref}}\right).C = \log(e)\left(\frac{1}{T} - \frac{1}{T_{ref}}\right).\frac{\Delta H}{R}$$
<div align="right">Equation (46)</div>

Where:

T = experimental or test temperature (K)
T_{ref} = the reference temperature selected (K)
C = constant (K)
ΔH = activation energy (J/mol)
R = ideal gas constant, 8.314(J/(mol.K))

Other variables are as previously defined.

In literature, different values were reported for the constant C, depending on the defining temperature:

- C = 10920, K, Francken et al. (1988)

- C = 13060, K, Lytton et al. (1993)

- C = 7680, K, Jacobs, (1995)

Williams-Landel-Ferry (WLF) equation

A second preferred formula for the determination of the shift factor is the Williams-Landel-Ferry (WLF) model (Williams et al., 1955), which can be seen as;

$$log\, f_{eq} - \log f = log\alpha_t$$
<div align="right">Equation (47)</div>

$$log\alpha_t = \frac{-C_1 \cdot (T - T_{ref})}{C_2 + (T - T_{ref})}$$
<div align="right">Equation (48)</div>

Where:

<div align="right">115</div>

T　　= Experimental or test temperature (K)
T_{ref}　= Reference temperature selected (K)
C_1, C_2　= Empirical constants

Other variables are as previously defined.

In literature, different values were reported for the constants C1 and C2.

- C1 = 9.5 and C2 = 95, Sayegh, (1967)

- C1 = 19 and C2 = 92, Lytton et al. (1993)

3.5.3. Construction of Master Curves

Medani et al. (2003) indicated that when the difference between the reference temperature and the temperature to be shifted is less than 20°C, then the Arrhenius type model is applicable for the study. In this study that was the case and the Arrhenius type model was applied.

A typical example of shifting the experimental stiffness can be seen below in Figure 3-24.
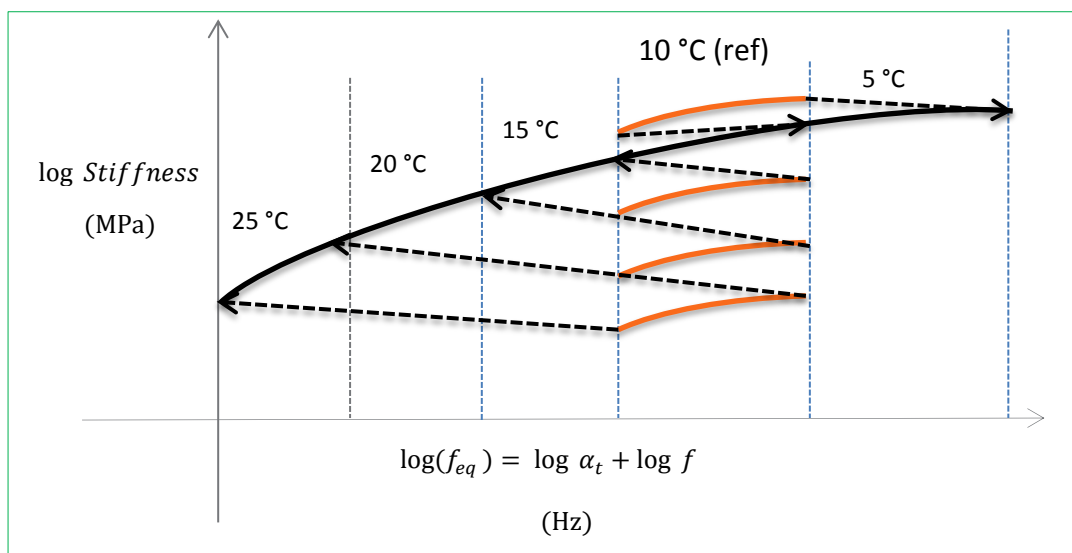
Figure 3-24: Example of typical Arrhenius type model

3.5.4. Frequency Sweep Tests

In order to determine the stiffness at different temperatures and frequencies the frequency sweep test method was used. In this method, the temperatures and frequencies are alternated and the resulting stiffness recorded. Frequency sweep tests and fatigue tests share the same specimen preparation and as a result time spent on specimen preparation was reduced. The following table shows the conditions used for testing.

Table 3-14: Test Parameters for Frequency Sweep Test

Type of Test	Displacement
Loading Waveform	Sinusoidal
Peak to Peak Strain (µε)	520, 480
Applied Tensile Strain (µε)	260, 240
Stiffness Measurement (cycles)	50
Termination Condition (cycles)	300
Test Temperatures (°C)	5; 10; 15; 20; 25
Test Frequencies (Hz)	0.5; 1; 2; 5; 10

During Test Group 1 the tests were conducted at peak to peak 520 µε (applied tensile of 260 µε) to provide information on the middle range between 480 and 600 µε which were used to carry out the fatigue tests. During Test Group 2 the tests were conducted at 480µε, to minimize damage caused by a higher applied strain.

For a systematic approach the tests were started at the lowest temperature and frequency. Figure 3-25 shows a typical example of a frequency sweep test. From these stiffness values, isotherms are obtained, which aid in constructing the master curve.
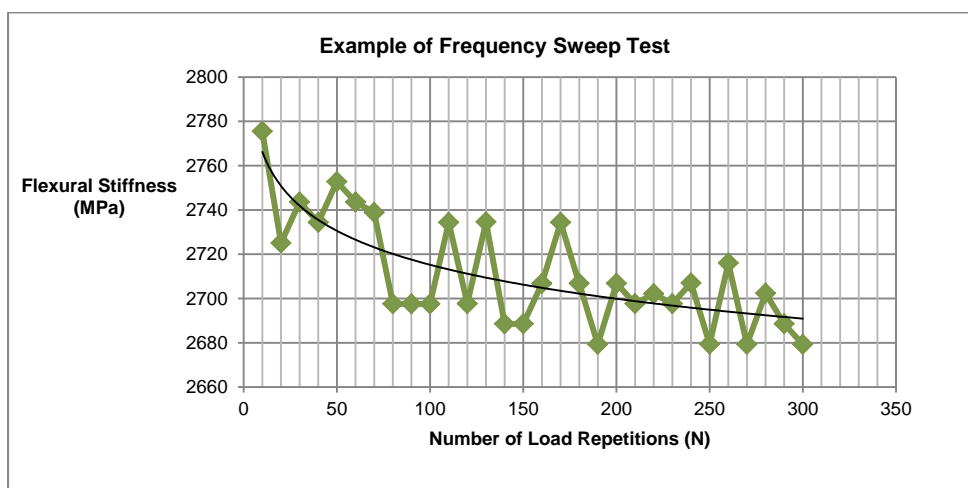
Figure 3-25: Typical Example of a Frequency Sweep Test

Once the isotherms were obtained from the frequency sweep test, they were shifted onto the Arrhenius type model. This was done by selecting a reference temperature of 10 °C. The

117

Arrhenius type model was most suitable to determine the shift factor, because the difference between the shifted temperature and the reference temperature was less or equal to 20 °C, as supported by Cheung (1995). If this difference exceeded 20°C, the William-Landel-Ferry (WLF) equation would be an appropriate selection.

The Arrhenius shift factor is:

$$\log(\alpha_t) = \left(\frac{1}{T} - \frac{1}{T_{ref}}\right) \cdot C = \log(e) \left(\frac{1}{T} - \frac{1}{T_{ref}}\right) \cdot \frac{\Delta H}{R}$$

Equation (49)

The master curve is then read off at the following frequency, f_{eq}:

$$\log(f_{eq}) = \log \alpha_t + \log f$$

Equation (50)

C =10 920 (Francken, 1988) was used in the Arrhenius type model. Jenkins (2000) showed that using other constants do not significantly enhance the correlation coefficient. A good fit was found using this constant for Half-Warm Foamed bituminous mixes and since this study uses Warm Mix Asphalt as a reference, Francken's constant is applicable.

The expected variation is to be found in the regression line. This is not only from the influence of random errors, but it is also from assuming that C and H are not dependent on temperature. Saygeh (1967), however found this assumption to not always hold weight as the activation energy can be reduced by 60%, by only increasing the temperature by 60°K from 253 °K.

3.6. Experimental Design

The figure below illustrates the experimental design that was followed in this research study, with the two (2) test groups. Firstly, a frequency sweep test was performed at the low strain level of 480µε.

Secondly, the conventional fatigue testing was followed with one low (480µε) and one high strain level (600µε), with the frequency sweep tests performed at an intermediate strain (520µε).

Variables within Research Study

1. Types of Seals:
   - Single
   - Double
   - Cape
   - Multiple

2. Climate (Revised Thornthwaite's Moisture Index):
   - Humid
   - Moist subhumid
   - Dry subhumid
   - Semiarid
   - Arid

3. Seal Age:
   - Youngest: 4 Years
   - Oldest: 23 Years

4. Position in Road:
   - In Wheel Track (IWT)
   - Outer Wheel Track (OWT)
   - Between Wheel Track (BWT)
   - Shoulder

5. Previous Traffic:
   - Average Annual Daily Traffic (AADT)
   - Percentage (%) Heavies

Group 1 →

Frequency Sweep Master Curve:

1 Beam (400x65x50mm)

- Test Temperatures: 5;10;15;20;25°C
- Test Frequency: 0.5; 1; 2; 5 10Hz

Group 2 →

Fatigue Testing:

2 Beams (400x65x50mm)

- Test Temperature: 10°C
- Test Frequency: 10Hz
- Strain Level: 520με

Frequency Sweep Master Curve:

1 Beam (400x65x50mm)

- Test Temperatures:

Figure 3-26: Experimental Design

3.7.   Statistical Analysis

This section details the statistical analysis that was followed once all the results for different seal types were extracted from those of the different composite sprayed seal beams. This analysis was performed to evaluate the significance of the test variables on the resultant fatigue values. The test variables were age of specimens, effective thickness, climate and the strains applied during the various tests.

From the fatigue testing results values were obtained for flexural stiffness and these were used to calculate fatigue. Flexural stiffness was listed as a test variable and not as a dependent variable in the analysis; because it is understood that flexural stiffness is used as a direct input to obtain fatigue values and therefore contributed to the test variables.

Fatigue was defined as the dependent variables since it relies on the combination of the test variables; age, effective thickness, climate, strain and flexural stiffness. It was therefore decided that the use of a multivariate analysis would be most suitable in this research study. Hair et al. (2010) described a multivariate analysis as the simultaneous investigation of two or more independent (predictor) variables that have an impact on the outcome of the dependent variable under examination. The independent variables were listed as age, effective thickness, climate, strain and flexural stiffness and the dependent variable was listed as fatigue.

There are often times confusion between Multivariate Analysis and Multivariate Analysis Of Variance (MANOVA). The latter is described as 'a statistical analysis used to assess the significance of the effect of one or more independent variables on two or more dependent variables. It is usually used when the dependent variables are thought to be inter-correlated' (Richarme 2001). In this study fatigue was the only dependent variable and the use of a MANOVA would not have been appropriate. This allowed for a univariate analysis of variance to be performed, using a multiple regression. Multiple regression forms part of multivariate analysis as it is a statistical method that estimates a dependent variable based on numerous independent variables (Richarme 2001; and Princeton University 2012).

The multiple regression analysis done in this study was performed using SPSS, which is one of the largest statistical packages that is reliable and relatively easy to use to carry out nearly every type of statistical analysis (Howell, 2004). The following analyses were performed using SPSS:
- Individual influence of independent variables on the dependent variable
- Combined influence of independent variables on the dependent variable
- Influence of interaction between independent variables

These analyses were used to investigate whether or not there existed significant relationships between the dependent variable; fatigue and the different predictors; age, effective thickness, climate, strain and flexural stiffness. It was furthermore investigated whether or not test variables were inter-correlated and whether or not these correlations were significant.

3.7.1. Understanding Linear Regression

This study comprised of one dependent variable (fatigue) and three independent variables (age, effective thickness, climate, strain and flexural stiffness). The theory of regression analysis is explained in terms of only one independent variable, because it would be burdensome to do it for multiple variables.

The theory starts off with a curve-fitting explanation. In order to best-fit a particular curve to a known set of points, the concept of least squares is used. Least square is the minimum sum of the squares of the residuals (the offsets) of the points from the curve. "The sum of the squares of the offsets is used instead of the offset absolute values because this allows the residuals to be treated as a continuous differentiable quantity" (Wolfram Research, Inc. 2013).

Vertical offsets are normally minimised instead of perpendicular offsets as can be seen in Figure 3-27 because this is associated with the creation of the fitted function (x estimates y). The use of vertical residuals furthermore allows a variation from best fit line to best fit polynomial as illustrated by Wolfram Research, Inc. (2013).

vertical offsets   *perpendicular offsets*
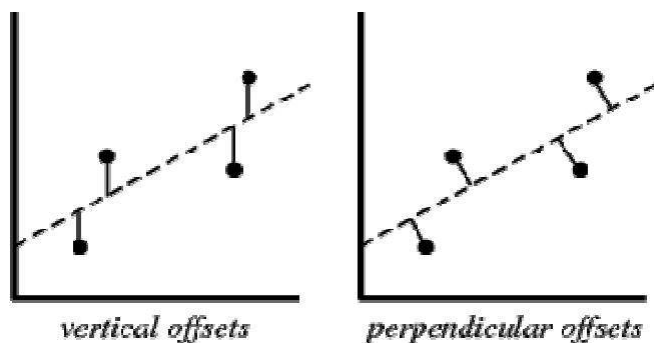
Figure 3-27: Curve Fitting to a Number of Points (Wolfram University, Inc. 2013)

The fitting procedure for vertical least squares continues by obtaining the sum of the squares of the vertical deviations, also known as R^2, of a set containing n data points from a particular function. The fitted function is termed as $(\hat{x}_i, \hat{y}_i)$, and the data points that were used to fit the curve are labelled as (x_i, y_i).

The resulting offset (residual) is defined as:

$$R^2 = \sum_1^n (y_i - \hat{y}_i)^2$$ Equation (51)

The term, R^2, is minimised to obtain the best fit line using the following expressions (for the linear relationship of $\hat{y} = m\hat{x} + b$):

$$\frac{d(R^2)}{dm} = 0$$ Equation (52)

$$\frac{d(R^2)}{db} = 0$$ Equation (53)

Each set of residuals are denoted by:

$$y_i = mx_i + b + R$$ Equation (54)

 Where:

m = slope of the fitted relationship
b = $\hat{y}$-intercept

Substituting for R^2 yields:

$$\frac{d(R^2)}{dm} = -2\sum_{i=1}^n (y_i - mx_i - b)x_i = 0$$ Equation (55)

121

$$\frac{d(R^2)}{db} = -2\sum_{i=1}^{n}(y_i - mx_i - b) = 0$$

Equation (56)

Solving for m and b yields (Wolfram Research, Inc. 2013:

$$m = \frac{n\sum_{i=1}^{n}x_iy_i - \sum_{i=1}^{n}x_i\sum_{i=1}^{n}y_i}{n\sum_{i=1}^{n}x_i^2 - (\sum_{i=1}^{n}x_i)^2}$$

Equation (57)

$$b = \frac{n\sum_{i=1}^{n}y_i - \sum_{i=1}^{n}x_i^2 - \sum_{i=1}^{n}x_i\sum_{i=1}^{n}x_iy_i}{n\sum_{i=1}^{n}x_i^2 - (\sum_{i=1}^{n}x_i)^2}$$

Equation (58)

The goodness of fit, r^2, is found from (Wolfram Research, Inc. 2013):

$$r^2 = \frac{(n\sum_{i=1}^{n}x_iy_i - \sum_{i=1}^{n}x_i\sum_{i=1}^{n}y_i)^2}{[n\sum_{i=1}^{n}x_i^2 - (\sum_{i=1}^{n}x_i)^2][n\sum_{i=1}^{n}y_i^2 - (\sum_{i=1}^{n}y_i)^2]}$$

Equation (59)

$$r^2 = R^2$$

Equation (60)

The goodness of fit coefficient r^2 ranges from +1 to -1, with +1 showing a perfect positive fit, -1 showing a perfect negative fit and no fit depicted by 0. The error existing between the fitted point and the actual vertical point y_i is given by:

$$e_i = y_i - \hat{y_i}$$

Equation (61)

The predictor of variance in the error e_i is given by:

$$S^2 = \sum_{i=1}^{n}\frac{e_i^2}{n-2}$$

Equation (62)

From this follows the standard errors for m and b (Wolfram Research, Inc. 2013):

$$SE(m) = \frac{s}{\sqrt{\sum_{i=1}^{n}(x_i - \bar{x})^2}}$$

Equation (63)

$$SE(b) = s\sqrt{\frac{1}{n} + \frac{(\bar{x})^2}{\sum_{i=1}^{n}(x_{i-}\bar{x})^2}}$$

Equation (64)

Where:

$\bar{x}$ = mean of x values

3.7.2. Analysis of Variance

Eckel, (2008) described ANOVA as a statistical tool to compare averages of three or more independent variables. This tool can also be used to evaluate whether or not a significant correlation exists between the different variables as detailed by Princeton University, (2012). To perform an ANOVA, with multiple regressions, the following sums of squares are employed (Wolfram Research, Inc. 2013):

- Total Sum of Squares (SST):

SST is the total deviations in the dependent variable as described by Gupta, (2000). Eckel, (2008) explained that it is calculated by obtaining the sum of squared deviations that exist between each observation and also the overall average (i.e. the mean of means).

$$SST = \sum_{i=1}^{k} \sum_{j=1}^{n} y_{ij}^2 - \frac{\left(\sum_{i}^{k} \sum_{j=1}^{n} y_{ij}\right)^2}{Kn}$$ Equation (65)

Where:

n   = Number of replicates (pairs of identical observations)
K   = Number of factor levels (number of treatment groups or independent variables)
y_{ij} = j^{th} observation in factor level i

- Regression Sum of Squares (SSR):

SSR is described as the amount of SST that can explained using (Gupta 2000 and Wolfram Research, Inc. 2013):

$$SSR = \sum_{i=1}^{k} \sum_{j=1}^{n} (y_{ij} - \bar{y_i})^2 = \frac{1}{Kn} (\sum_{i}^{k} \sum_{j=1}^{n} y_{ij})^2$$

Equation (66)

- Error Sum of Squares (SSE):

The error sum of squares or residual sum of squares is the amount of SST that can't be described using any model (Gupta 2000 and Wolfram Research, Inc. 2013):

$$SSE = \sum_{i=1}^{k} \sum_{j=1}^{n} (y_{ij} - \bar{y_i})^2 = SST - SSR$$

Equation (67)

Where:

$\bar{y_i}$ = Average (mean) of observations within the factor level, i.

The sum of squares computes the F-value, which evaluates the overall (global) significance of the model (Davis n.d.). If the value for F increases, the model becomes more significant according to CSDN, (2010). F is calculated as follows:

$$F = \frac{MSR}{MSE}$$

Equation (68)

Where:

MSR = mean square of regression
MSE = mean square of residuals

It is important to draw distinctions between the different types of variables used as input in SPSS:

- Nominal Variables:

These types of variables are used for qualitative classification, which cannot be ordered into a certain hierarchy. Colours and gender are examples of nominal variables (UNESCO n.d.).

- Ordinal Variables:

The numerical codes of these types of variables indicate a particular order or meaningful sequence. Assistant professor, associate professor and full professor are examples of ordinal variables. Further examples are low, medium and high (UNESCO n.d.).

- Scale Variables:

These types of variables are used for quantitative classification and it would make sense to calculate an "average" for these types of variables. They can be measured on both a linear and nonlinear scale (UNESCO n.d.). Following variable input, the following tables would appear as typical output tables for an analysis of variance (ANOVA).

Table 3-15: Example of Model Summary from SPSS Output

Model	R	R Square	Adjusted R Square	Std. Error of the estimate
1	0.923[a]	0.853[a]	0.839	147.846

a.Predictors: (Constant), Variables listed

Table 3-16: Example of ANOVA from SPSS Output

Category		Degrees of Freedom (df)	Mean Square	F-ratio
Model	SSR	K-1	$MSR = \dfrac{SSR}{K-1}$	$\dfrac{MSR}{MSE}$
Error	SSE	K(n-1)	$MSE = \dfrac{SSE}{K(n-1)}$	
Total	SST	Kn-1	$MST = \dfrac{SST}{Kn-1}$	

a.Predictors: (Constant), Variables listed
b.Dependent Variable: Variable listed

Table 3-17: Example of Coefficients from SPSS Output

Model		Unstandardized Coefficients		Standardized Coefficients	t	Sig.
		B	Std. Error	Beta		
1	(Constant)	771.56	165.21		2.35	0.000
	Variable1	265.23	62.35	.568	13.26	0.000
	Variable2	256.31	35.56	.356	21.26	0.000
	Variable3	265.31	25.35	.265	23.21	0.000

a.Dependent Variable: Variable listed

4. Results and Synthesis

Four point bending (4PB) fatigue testing is a well-known method used by researchers to determine progression in reduction of flexural stiffness that is further used to characterize fatigue life, using the methods discussed in Chapter 2 of this thesis. Although this is preferred by many, it is not always practically possible to carry out in site laboratories, as flexural bending tests can be very time consuming.

Currently 4PB fatigue tests are only carried out on asphalt mixes and their results used in determining fatigue lives. In this research study, the author modified the conventional use of the 4PB beam apparatus, by testing flexural bending of thin surfacing bituminous materials, i.e. Seals. Many similarities exist between asphalt and seals (see Chapter 2) which justify the subjection of seals to flexural bending tests.

4.1.   Effective Thickness of Seal Layer

The layer thickness of a single layer of sprayed seal is closely related to the average least dimension (ALD) of the stone aggregate used. The seal thickness is approximately equal to the ALD of the stone aggregate. Figure 4-1 illustrates the variation in thickness of the seal beams produced.

Due to the great variation in seal thickness, effective thickness was selected as a more suitable thickness reference or the seals and was measured by calculating the average of ten thickness measurements taken with a Vernier Caliper in the front middle third and also the back middle third of the beam.
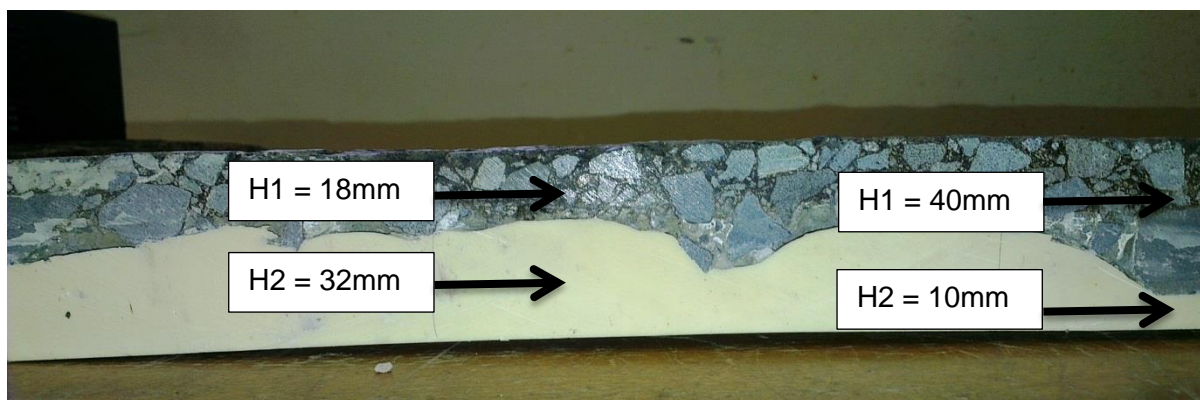
Figure 4-1: Variation in thickness in sprayed seal beam

Tables 4-1 to 4-4 indicate the effective layer thickness of the seals that were subjected to flexural bending. These values, measured in the laboratory, were added to the MATLAB analysis to extract the flexural stiffness values of only the sprayed seal (see Chapter 3).

Table 4-1: Effective Layer Thickness of Single Seals

Type of Seal	Seal Name	Age	Effective thickness of seal layer (mm)		
			B1	B2	B3
Single	DR 2216_ BWT_1km_13mm	10	16.17	16.46	16.75
	DR 2216_ IWT _1km_13mm	10	16.56	16.09	16.63
	DR1681_BWT _5km_13mm	11	22.26	22.02	22.71
	DR1452_BWT _14.1km_13mm	12	21.99	21.71	21.6
	MR 536_ BWT _4.3km_ 9mm	19	21.65	21.54	21.23
	MR 536_ IWT _4.3km_9mm	19	21.71	21.02	21.08

Table 4-2: Effective Layer Thickness of Double Seals

Type of Seal	Seal Name	Age	Effective thickness of seal layer (mm)		
			B1	B2	B3
Double	N8_8_OWT _5.6km_19+9mm	6	27.14	27.33	27.35
	N8_8_SHDR _5.6km_19+9mm	6	27.43	27.83	27.37
	N2_31_OWT _41.2km_13+7mm	6	33.40	33.47	33.38
	DR2175_IWT _3km_13+7mm	6	30.02	30.01	30.12
	DR2175_BWT _3km_13+7mm	6	30.04	30.08	30.13
	R63_ OWT _6km_13+7mm	7	23.83	23.68	23.16
	N2_31_OWT_N_Bound_3.6km_13+7mm	11	27.55	27.60	27.70
	N2_31_OWT_S_Bound_3.6km_13+7mm	11	27.19	27.50	27.24
	MR269_OWT _3km_13+7mm	13	12.46	12.52	12.34
	DR1123_IWT _23.4km_13+7mm	7	17.31	17.16	17.04

Table 4-3: Effective Layer Thickness of Cape Seals

Type of Seal	Seal Name	Age	Effective thickness of seal layer (mm)		
			B1	B2	B3
Cape	N6_5_OWT _46km_19mm	4	36.33	36.19	36.43
	MR174_OWT_9km_19mm	10	30.47	30.39	30.07
	MR23_OWT_17km_19mm	10	26.26	26.45	26.23
	N6_5_SHDR_53.4km_19mm	12	35.96	36.11	35.58
	TR2701_OWT_5km_19mm	23	19.09	19.01	19.33
	DR1398_OWT_1km_19mm	23	27.19	27.33	27.14
	DR1398_SHDR_ 1km_19mm	23	27.30	27.31	27.33

Table 4-4: Effective Layer Thickness of Multiple Seals

Type of Seal	Seal Name	Age	Effective thickness of seal layer (mm)		
			B1	B2	B3
Multiple	N6_4_SHDR_ 8km_19+6+6	9	33.175	32.845	32.87
	N1_29_OWT_ 79.8km_19+6+6	9	27.45	27.63	27.745

Measurements from above tables indicate that effective layer thicknesses of the seals exceeded the average least dimensions of the stone aggregate used in the construction of the sprayed seal. For instance, a 13.2mm single seal would have an ALD of 8.64, which is much thinner than the measured 16, 21 and 22mm. Sprayed seal slabs were however sampled with pieces of the underlying base still bonded to their underside.

This was done because it was practically impossible to remove only the sprayed seal layer from the base, especially since these layers were bonded to a film of prime that was applied to the underlying base to promote adhesion. As a result, seals were removed from the road with prime and parts of the underlying base, resulting in an effective layer thickness that exceeds the ALD of the stone aggregate.

The following sensitivity analysis was performed to see the effect of the effective thickness on the flexural stiffness values resulting from the MATLAB analysis.
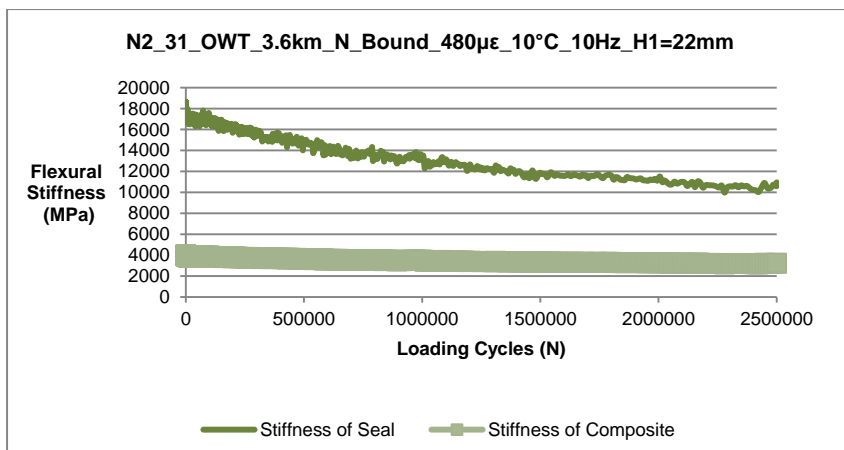
Figure 4-2: Flexural stiffness reduction of double seal with 22mm effective thickness
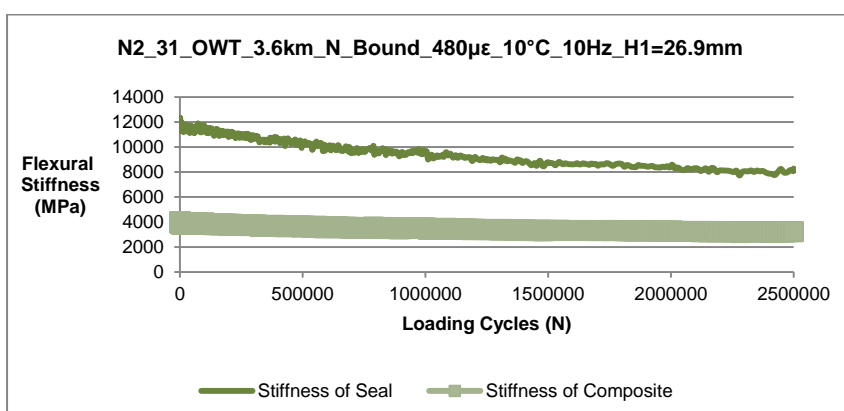
Figure 4-3: Flexural stiffness reduction of double seal with 26.9mm effective thickness
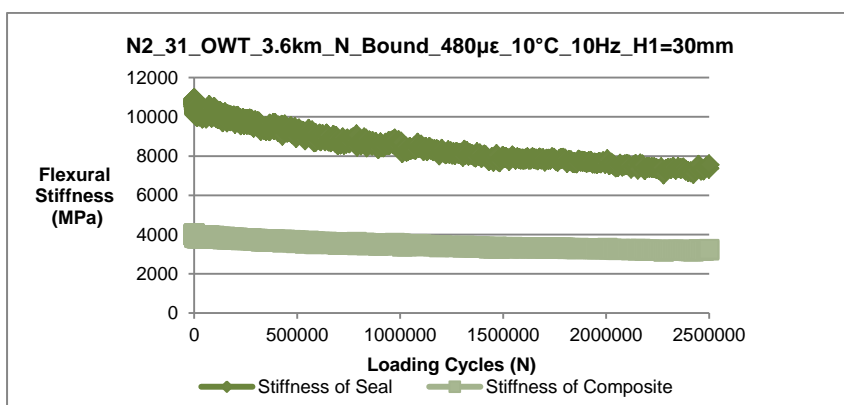
Figure 4-4: Flexural stiffness reduction of double seal with 30mm effective thickness

Figure 4-5 provides a summary of the influence of effective thickness on flexural stiffness.
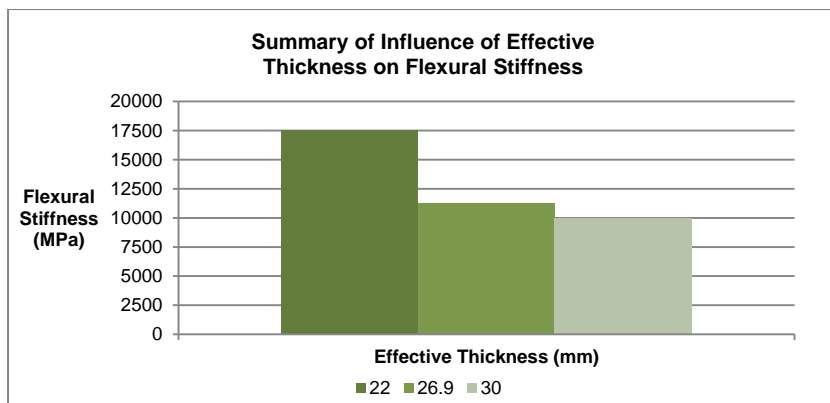
Figure 4-5: Summary of Influence of Effective Thickness on Flexural Stiffness

From above figures it can be seen that the flexural stiffness analysis using MATLAB is highly sensitive to the effective thickness of seal layer used as input and its significance in predicting the outcome of fatigue for the different seals will be presented further in this chapter. The direct beam theory, used in the analysis, involved the separation of the seal-polyurethane composite beam into the two respective individual layers (See Chapter 3).

4.2. Response of Seals to Frequency Sweep measured at 480με

4.2.1. Single Seals

Table 4-5 below summarizes the results of the frequency sweep tests at 480με, performed on the first group of single seals with test reference temperature ranges, 5°C, 10°C and 25°C and test reference frequency of 10Hz.

Table 4-5: Master Curve Results of Single Seals from Group 1

Type of Seal	Age	Seal Location	$T_{ref}\_5°C\_10Hz$	$T_{ref}\_10°C\_10Hz$	$T_{ref}\_25°C\_10Hz$
			(MPa)	(MPa)	(MPa)
Single	11	DR1681_BWT _5km_13mm	5536	4170	1886
	12	DR1452_BWT _14.1km_13mm	8093	5958	2529

It was expected that the younger seal, DR1681_BWT_5km, would yield higher flexural stiffness values, but this was not the case. When comparing the master curve stiffness values for $T_{ref}\_10°C\_10Hz$ with that of the traffic, it was found that the younger seal, DR1681, in this case, had less traffic and a lower flexural stiffness. Possibly ageing rather than damage dominated the behaviour.

For the older seal, DR1452, a higher flexural stiffness together with an increased traffic volume was reported. The comparison is illustrated in Figure 4-6.
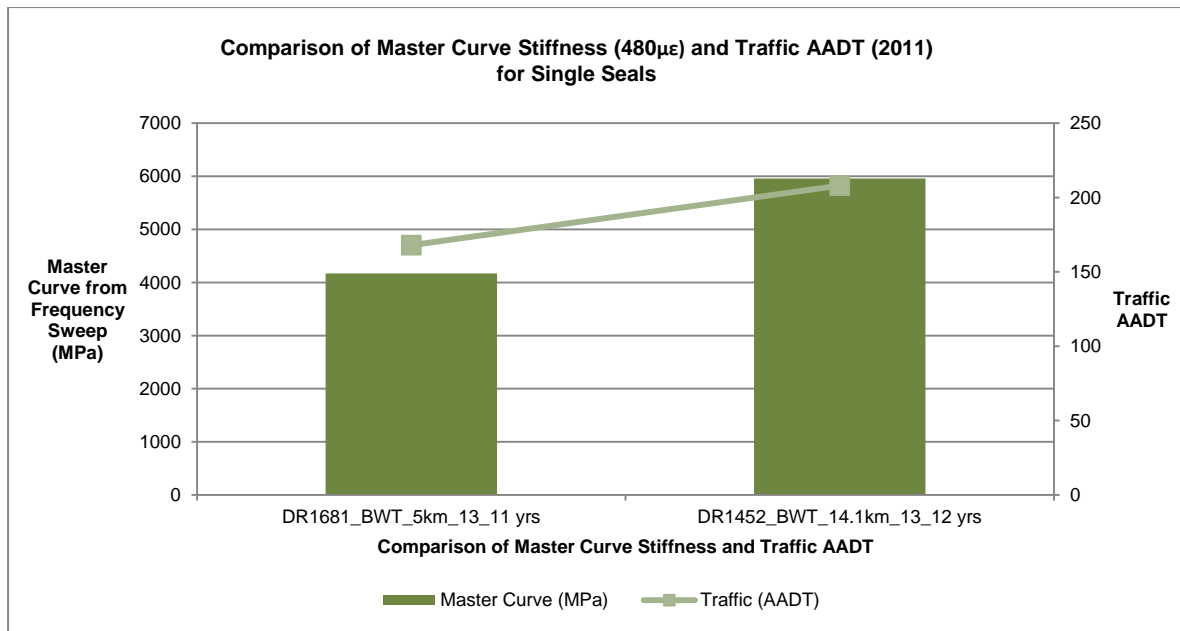
Figure 4-6: Comparison of Master Curve Stiffness (480µε) and Traffic AADT (2011) for Single Seals

4.2.2. Double Seals

Table 4-6 below summarizes the results of the frequency sweep tests at 480µε, performed on the first group of double seals with test reference temperature ranges, 5°C, 10°C and 25°C and test reference frequency of 10Hz.

Table 4-6: Master Curve Results of Double Seals from Group 1

Type of Seal	Age	Seal Location	Tref_5°C_10Hz (MPa)	Tref_10°C_10Hz (MPa)	Tref_25°C_10Hz (MPa)
Double	6	N8_8_OWT _5.6km_19+9mm	6556	4397	1438
	6	N2_31_OWT _41.2km_13+7mm	13757	9921	3974
	6	DR2175_IWT _3km_13+7mm	7451	4994	1630
	6	DR2175_BWT _3km_13+7mm	7202	5045	1863
	7	R63_OWT _6km_13+7mm	19956	15362	7388
	13	MR269_OWT _3km_13+7mm	17477	12173	4425

131

The *lowest stiffness comparison* was found for N8_8_OWT_5.6km_19+9_6yrs and DR2175_3km_13+7_6yrs for both sampled from the inner wheel track as well as between the wheel tracks. These two (2) locations have the same ages for the double seals, both being six (6) years into their lifespans, but are within different climatic zones.

N8_8 is located in the Northern Cape Province, which is well known for its dry climate, whereas DR2175 is situated in the Western Cape Province, which has moderate climatic conditions. The stiffness values were however not influenced greatly by the climatic zone difference. This finding illustrates the challenge that exists in separating the influence of traffic from that of climatic (ageing). These two effects usually work in conjunction with each other.

Stiffness values were not influenced by the traffic volumes for this particular comparison either, since it was found that both locations measured relatively low flexural stiffness values, especially considering that DR2175 received significantly lower traffic volumes than N8_8, approximately ten percent of its traffic volume.

The effect of the aggregate stone size also didn't show markedly differences in the measured stiffness values, the larger of the two being 19+9mm aggregate packing for N8_8 compared to the smaller 13+7mm aggregate packing for DR2175.

The *middle highest stiffness comparison* was found between N2_31_OWT_41.2km_13+7_6yrs in KwaZulu-Natal Province and MR269_OWT_3km_13+7_13yrs in the Western Cape Province. The former of these two samples have about half of the age of the latter and they are furthermore marked by different climatic zones from which they were sampled from.

N2_31 is located in the KwaZulu-Natal Province, which is well known for its wet climate, while MR269 is situated in the Western Cape Province, which has moderate climatic conditions. The stiffness values about 18.5% lower in the wetter region. Furthermore this double sprayed seal received 1617 higher average annual daily traffic than MR269, but measured lower stiffness values. Thus a younger double sprayed seal, subjected to higher traffic volumes, in a wet climatic region, measured lower stiffness values.

The *highest stiffness value* was measured for R63_OWT_6km_13+7_7yrs, located in the KwaZulu-Natal Province that is within a wet climatic region, but with the lowest traffic volume of all the double seals compared. This sprayed seal was also relatively similar in age than most of the double seals compared in this section. Thus a relatively young double sprayed seal, subjected to low traffic volumes, in a wet climatic region, measured the highest stiffness values.

Figure 4-7 summarizes the comparisons within the double sprayed seal group that was subjected to frequency sweep testing at 480με, with test reference temperature of 10°C and test reference frequency of 10Hz.

Figure 4-7: Comparison of Master Curve Stiffness (480με) and Traffic AADT (2011) for Double Seals

4.2.3. Cape Seals

Table 4-7 below summarizes the results of the frequency sweep tests at 480με, performed on the first group of cape seals with test reference temperature ranges, 5°C, 10°C and 25°C and test reference frequency of 10Hz.

Table 4-7: Master Curve Results of Cape Seals from Group 1

Type of Seal	Age	Seal Location	$T_{ref}\_5°C\_10Hz$ (MPa)		$T_{ref}\_10°C\_10Hz$ (MPa)		$T_{ref}\_25°C\_10Hz$ (MPa)	
Cape	12	N6_5_SHDR_ 53.4km_19mm	12265	10315	9221	8783	4150	4495
	23	TR2701_OWT_5km_19mm	6738	5634	4829	4696	1901	2072
	23	DR1398_OWT_ 1km_19mm	11434	9636	8742	8281	4124	4490
	23	DR1398_SHDR_1km_19mm	15947	13058	11808	11110	5093	5656

From the tabulated results two distinctive trends can be observed. A comparison between TR2701_OWT_5km_19_23yrs and DR1398_OWT_1km_19_23yrs indicate that as traffic volumes increase yield a reduced flexural stiffness.

The second trend is observed when comparing N6_5_SHDR_53.4km_19_12yrs and DR1398_SHDR_1km_19_23yrs. It can be seen that as the cape seals age together with an increase in traffic volumes, the flexural stiffness values increase as well.

DR1398_1km_19_23yrs were sampled from the outer wheel track position as well as from the shoulder position. It was found that the shoulder sample measured a higher stiffness. This could be due to the shoulder generally receives very low traffic volumes, since its main purpose is to provide a safe environment for vehicles to make an emergency stop, if the need should occur. There is therefore less traffic to keep the binder soft and active, resulting in a stiffer seal.

Figure 4-8 summarizes the comparisons within the cape sprayed seal group that was subjected to frequency sweep testing at 480με, with test reference temperature of 10°C and test reference frequency of 10Hz.
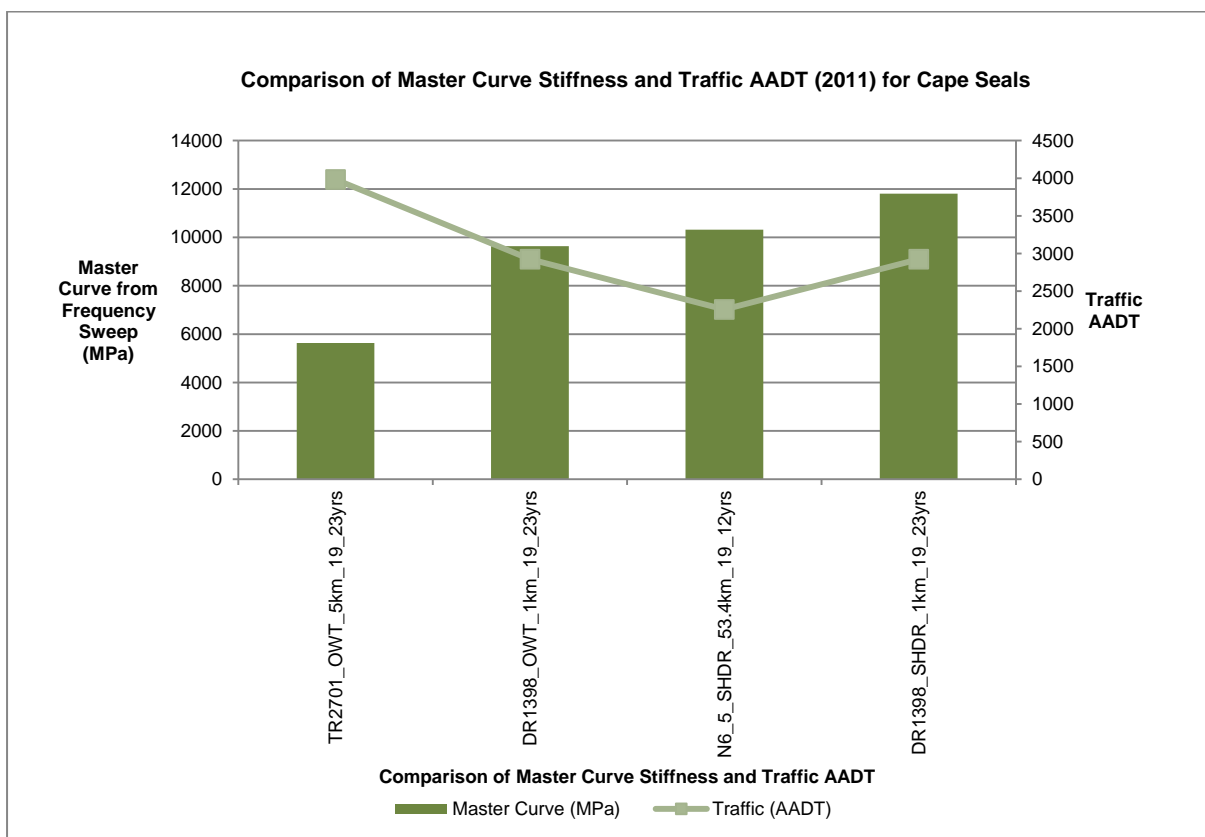
Figure 4-8: Comparison of Master Curve Stiffness (480με) and Traffic AADT (2011) for Cape Seals

4.2.4. Multiple Seals

Table 4-8 summarizes the results of the frequency sweep tests at 480με, performed on the multiple seals with test reference temperature ranges, 5°C, 10°C and 25°C and test reference frequency of 10Hz.

Table 4-8: Master Curve Results of Multiple Seals from Group 1

Type of Seal	Age	Seal Location	Tref_5°C_10Hz (MPa)	Tref_10°C_10Hz (MPa)	Tref_25°C_10Hz (MPa)
Multiple	9	N6_4_SHDR_ 8km_19+6+6	8329	6084	2527
	9	N1_29_OWT_ 79.8km_19+6+6	6612	5404	3072

Results of same aged multiple seals indicated differences in flexural stiffness values. The difference between the two however is that N6_4_SHDR_8km, was sampled from the shoulder position of the road, that generally receives less traffic than in the outer wheel track, which is where N1_29_OWT_79.8km was sampled.

Figure 4-9 below summarizes the comparisons within the cape sprayed seal group that was subjected to frequency sweep testing at 480με, with test reference temperature of 10°C and test reference frequency of 10Hz.
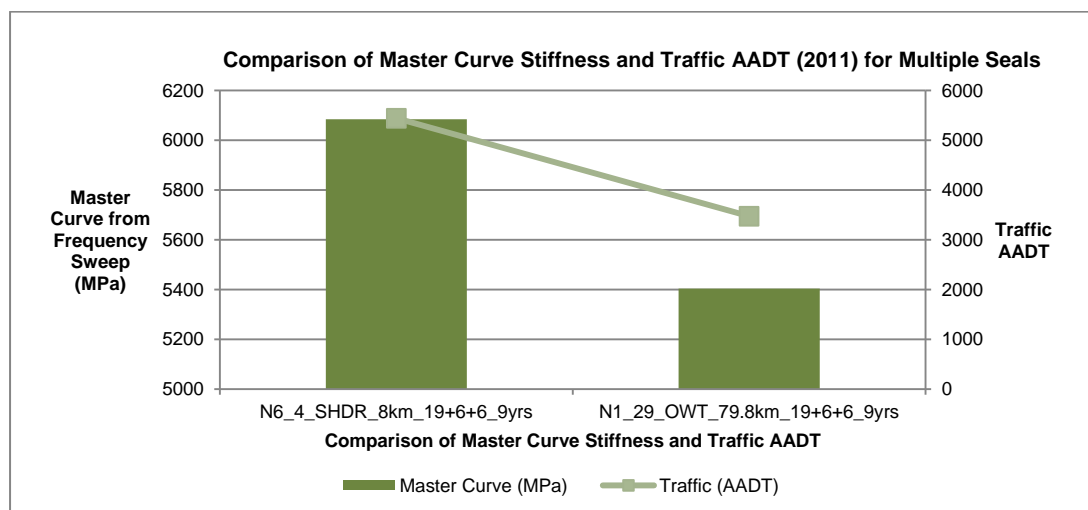
Figure 4-9: Comparison of Master Curve Stiffness (480με) and Traffic AADT (2011) for Multiple Seals

4.3.   Response of Seals to Frequency Sweep measured at 520με

4.3.1. Single Seals

Table 4-9 below summarizes the results of the frequency sweep tests at 520με, performed on the first group of single seals with test reference temperature ranges, 5°C, 10°C and 25°C and test reference frequency of 10Hz.

Table 4-9: Master Curve Results of Single Seals from Group 2

Seal Location	T$_{ref}$_5°C_10Hz	T$_{ref}$_10°C_10Hz	T$_{ref}$_25°C_10Hz
	(MPa)	(MPa)	(MPa)
DR 2216_ IWT _1km_13mm	7008	4445	1243
DR 216_BWT _1km_13mm	6833	4638	1568
MR536_IWT _4.3km_9mm	18613	12475	4072
MR536_BWT _4.3km_9mm	5395	4212	2107

In wheel track results of DR2216 didn't show significant differences in flexural stiffness values when compared to the results of between the wheel tracks. Results for MR536 however showed a noteworthy difference in flexural stiffness values for the two sampled positions.

Higher values were measured in the wheel tracks than between the wheel tracks. The combined effect of ageing and traffic could be possible causes for this difference.

Figure 4-10 summarizes the comparisons within the single sprayed seal group that was subjected to frequency sweep testing at 520µε, with test reference temperature of 10°C and test reference frequency of 10Hz.
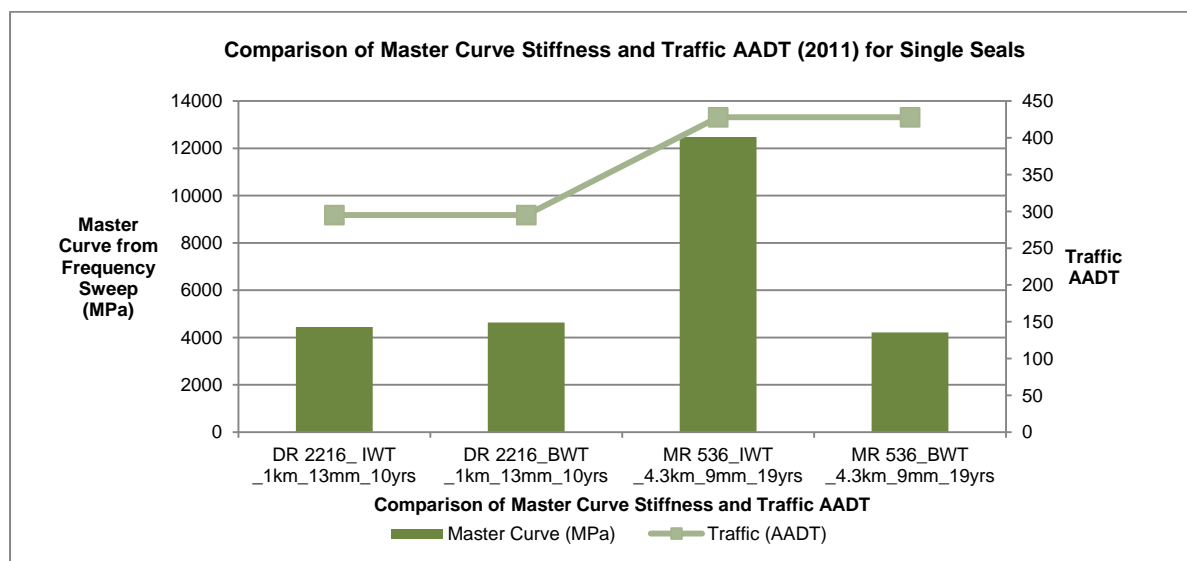
Figure 4-10: Comparison of Master Curve Stiffness (520µε) and Traffic AADT (2011) for Single Seals for Group 2

4.3.2. Double Seals

Table 4-10 below summarizes the results of the frequency sweep tests at 480µε, performed on the first group of single seals with test reference temperature ranges, 5°C, 10°C and 25°C and test reference frequency of 10Hz.

Table 4-10: Master Curve Results of Double Seals from Group 2

Seal Location	T_{ref}_5°C_10Hz	T_{ref}_10°C_10Hz	T_{ref}_25°C_10Hz
	(MPa)	(MPa)	(MPa)
N8_8_SHDR _5.6km_19+9mm	8263	5655	1957
N2_31_OWT_N_ Bound_3.6km_ 13+7mm	13644	10810	5633
N2_31_OWT_S_ Bound_3.6km_ 13+7mm	7822	5991	2839
DR1123_IWT _23.4km_13+7mm	3831	3230	2002

Results for N8_8_SHDR were relatively close to flexural stiffness values of N2_31_South Bound, but slightly higher. This could be possibly due to the former comprising of larger aggregate. TRH 3 (2007) indicates prolonged lifetimes for larger sized aggregates, which agrees with the higher flexural stiffness values.

Results within N2_31_OWT_3.6km showed significant differences, with the North Bound direction indicating higher stiffness values. It is possible that traffic isn't equally split between the two directions of travel; a high concentration of traffic was possibly present in one direction that kept the binder "fresh" and active, yielding lower stiffness results.

Overall results, with the exception of the N2_31_OWT_North Bound, showed a reduction of flexural stiffness with an increase in time, due to the degradation effects of ageing.

Figure 4-11 summarizes the comparisons within the double sprayed seal group that was subjected to frequency sweep testing at 480µε, with test reference temperature of 10°C and test reference frequency of 10Hz.
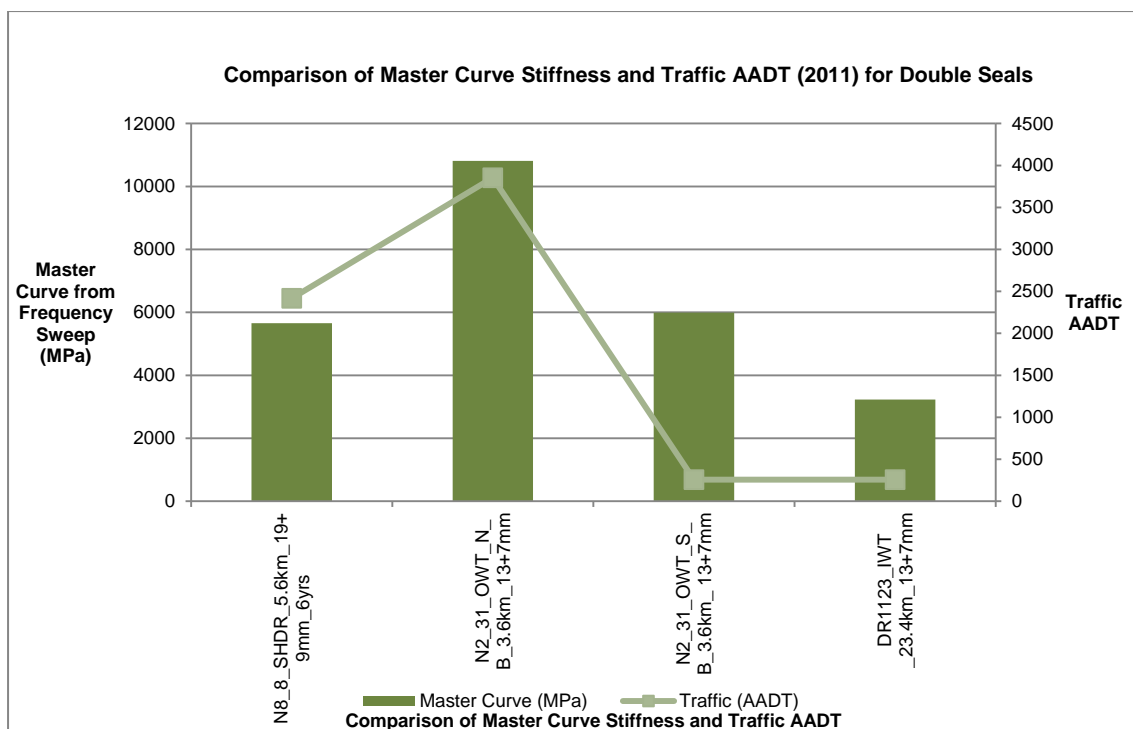
Figure 4-11: Comparison of Master Curve Stiffness (520µε) and Traffic AADT (2011) for Double Seals for Group 2

4.3.3. Cape Seals

Table 4-11 below summarizes the results of the frequency sweep tests at 480µε, performed on the first group of single seals with test reference temperature ranges, 5°C, 10°C and 25°C and test reference frequency of 10Hz.

Table 4-11: Master Curve Results of Cape Seals from Group 2

Seal Location	T_{ref}_5°C_10Hz	T_{ref}_10°C_10Hz	T_{ref}_25°C_10Hz
	(MPa)	(MPa)	(MPa)
N6_5_OWT_ 46km _19mm	17052	12371	5039
MR174_OWT_ 9km _19mm	15520	10657	3722
MR23_OWT_ 17km_19mm	15278	9910	2950

Seals with the same age (MR174_OWT_9km compared with MR23_OWT_17km), measured relatively similar flexural stiffness values, regardless of the difference in effective thickness of between the seal layers. A decrease in flexural stiffness is related to an increase in seal age.

138

The magnitude of flexural stiffness for the multiple seals and the variation is significantly lower than that of Cape Seals (and others).

Figure 4-12 summarizes the comparisons within the Cape Seal group that was subjected to frequency sweep testing at 480µε, with test reference temperature of 10°C and test reference frequency of 10Hz.

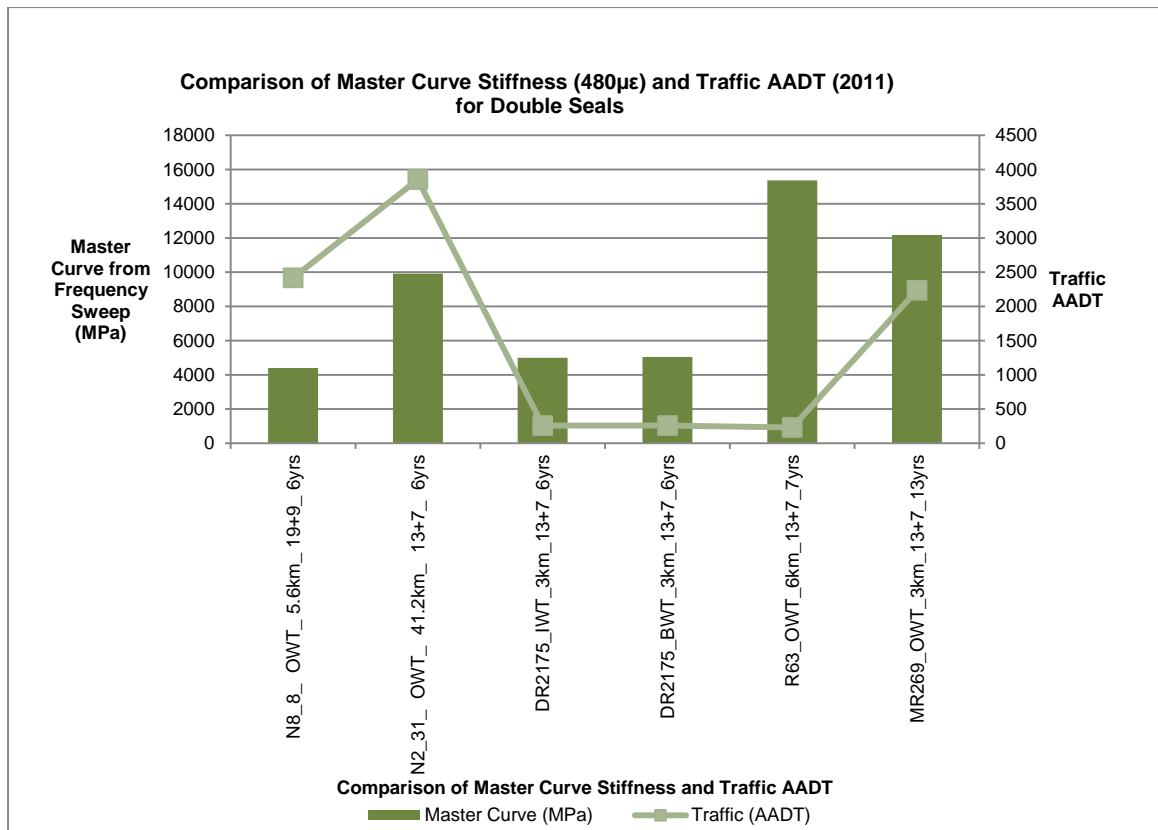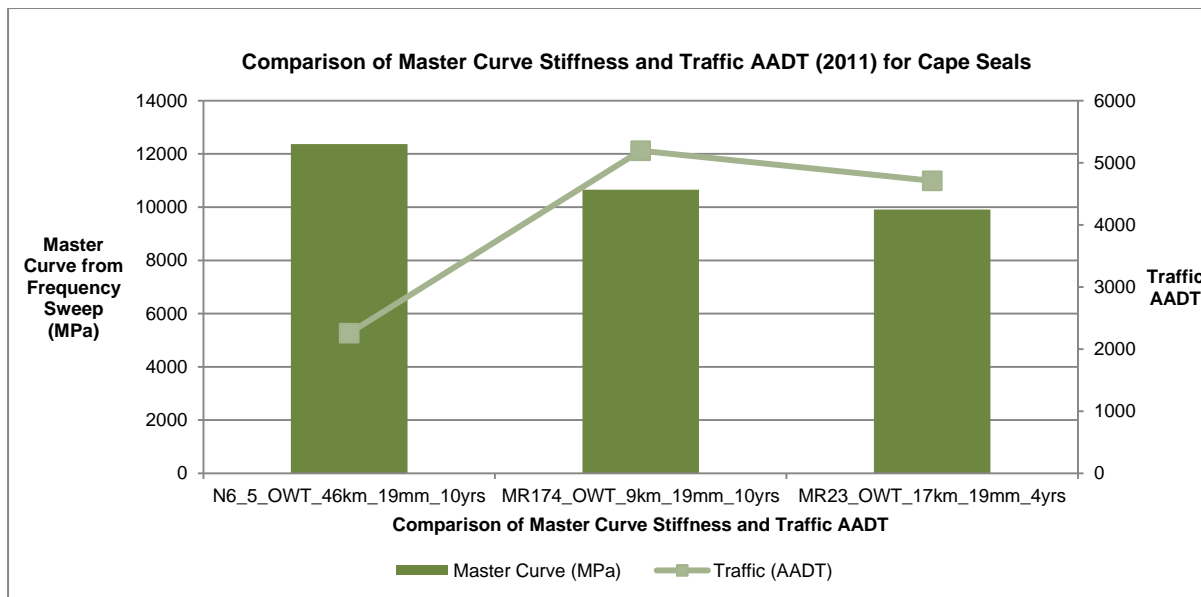**Figure 4-12: Comparison of Master Curve Stiffness (520µε) and Traffic AADT (2011) for Cape Seals for Group 2**

4.4. Fatigue Results measured at 480με and 600με

4.4.1. Single Seals

Table 4-12: Results of Fatigue Testing for Single Seals

Seal Location	Strain Level (με)	Initial Stiffness (MPa)	20% Reduction in Flexural Stiffness (MPa)	$N_{20\%}$	30% Reduction in Flexural Stiffness (MPa)	$N_{30\%}$	40% Reduction in Flexural Stiffness (MPa)	$N_{40\%}$	50% Reduction in Flexural Stiffness (MPa)	$N_{50\%}$
DR 2216_ IWT _1km_13mm	480	4132	3305	5.59E+04	2892	1.57E+06	2479	7.43E+07	2066	7.09E+09
	600	4990	3992	1.20E+05	3493	1.36E+06	2994	2.24E+07	2495	5.37E+07
DR 2216_ BWT _1km_13mm	480	8051	6441	1.55E+06	5636	4.03E+07	4831	1.73E+09	4026	1.48E+11
	600	7213	5771	2.58E+04	5049	1.18E+05	4328	6.79E+05	3607	5.39E+06
MR 536_ IWT _4.3km_9mm	480	6505	5204	2.30E+16	4553	4.08E+23	3903	9.53E+31	3252	7.53E+41
	600	11525	9220	1.41E+05	8067	2.93E+06	6915	9.73E+07	5762	6.13E+09
MR 536_ BWT _4.3km_ 9mm	480	4309	3448	4.44E+06	3017	6.24E+08	2586	5.37E+07	2155	1.61E+14
	600	3957	3166	2.67E+05	2770	4.87E+06	2374	1.39E+08	1978	7.32E+09

4.4.2. Double Seals

Table 4-13: Results of Fatigue Testing for Double Seals

Seal Location	Strain Level (µε)	Initial Stiffness (MPa)	20% Reduction in Flexural Stiffness (MPa)	$N_{20\%}$	30% Reduction in Flexural Stiffness (MPa)	$N_{30\%}$	40% Reduction in Flexural Stiffness (MPa)	$N_{40\%}$	50% Reduction in Flexural Stiffness (MPa)	$N_{50\%}$
N8_8_SHDR _5.6km_19+9mm	480	4510	3608	1.35E+04	3157	6.27E+04	2706	3.69E+05	2255	3.00E+06
	600	5745	4596	1.03E+03	4021	2.81E+03	3447	8.96E+03	2872	3.53E+04
N2_31_OWT_N_ Bound_3.6km_ 13+7mm	480	12161	9729	1.32E+06	8513	7.57E+07	7297	8.09E+09	6080	2.03E+12
	600	7542	6034	3.32E+08	5280	1.92E+11	4525	2.96E+14	3771	1.74E+18
N2_31_OWT_S_ Bound_3.6km_ 13+7mm	480	10874	8699	2.16E+05	7612	2.81E+06	6524	5.45E+07	5437	1.82E+09
	600	4562	3650	1.32E+05	3194	1.03E+06	2737	1.11E+07	2281	1.83E+08
DR1123_IWT _23.4km_13+7mm	480	16072	12858	1.33E+04	11250	5.58E+04	9643	2.93E+05	8036	2.08E+06
	600	6466	5173	6.99E+03	4526	2.46E+04	3880	1.05E+05	3233	5.89E+05

4.4.3. Cape Seals

Table 4-14: Results of Fatigue Testing for Cape Seals

Seal Location	Strain Level (με)	Initial Stiffness (MPa)	20% Reduction in Flexural Stiffness (MPa)	$N_{20\%}$	30% Reduction in Flexural Stiffness (MPa)	$N_{30\%}$	40% Reduction in Flexural Stiffness (MPa)	$N_{40\%}$	50% Reduction in Flexural Stiffness (MPa)	$N_{50\%}$
N6_5_OWT_46km _19mm	480	12056	9645	1.11E+04	8439	30977	7.23E+03	101394	6028	4.12E+05
	600	10970	8776	1.19E+04	7679	35188	6.58E+03	123220	5485	5.43E+05
MR174_OWT_9km _19mm	480	9961	7969	8.70E+03	6973	24495	5.98E+03	80920	4981	3.33E+05
	600	7045	5636	1.43E+04	4932	30332	4.23E+03	72110	3523	2.01E+05
MR23_OWT_17km _19mm	480	16830	13464	9.22E+03	11781	22466	1.01E+04	62783	8415	2.12E+05
	600	7751	6200	1.10E+04	5425	23119	4.65E+03	54697	3875	1.51E+05

142

Single Seals:

Results of DR2216_BWT_1km and MR536_BWT_4.3km indicated strain dependency when comparing initial stiffness values, with a higher strain level yielding lower flexural stiffness values.

The results for the remainder of the seals however showed an opposing trend, higher flexural stiffness values were found for higher strain levels. This doesn't agree with the theory that greater test intensity (applied strain) will measure a lower flexural bending response from the subjected specimen beam.

Too little data exists to determine whether specimens were strain dependent or not. Fatigue results however showed strain dependency, with the exception of MR536_IWT_4.3km when using $N_{20\%}$ as the failure criteria.

Double Seals:

Three out of four results indicate strain dependency when comparing initial stiffness. When considering fatiguing (the reduction of flexural rigidity with time) only half of the results for double seals indicated this trend.

Furthermore, the possibility of investigating suitable failure criteria presented itself. Results showed that a 20% reduction in initial flexural stiffness were comparable with fatigue lives of asphalt.

Cape Seals:

Comparison of initial stiffness values showed that results followed the strain dependency trend, whereas varied results were found when considering fatiguing. N6_5_OWT_46km all possible failure criteria indicated to be not strain dependent.

For MR174_OWT_9km and MR23_OWT_17km there was also no strain dependency for $N_{20\%}$ and $N_{30\%}$, but when 40% and 50% reduction of initial stiffness was the defined failure criteria, results showed strain dependency.

In general, the fatigue results indicated high variability and a statistical analysis was performed to investigate the significance of the different variables on the outcome of fatigue, as discussed in the following section.

4.5.   Statistical Analysis

4.5.1.   Statistical Significance of Individual Variables on Fatigue

4.5.1.1.   Influence on Fatigue ($N_{20\%}$) – Single Seals

Table 4-15: Model Summary of $N_{20\%}$_Single Seals

No.	Constant, a	R	R Squared	Adjusted R Squared	Std. Error of the Estimate
1	Age	0.444[a]	0.197	0.063	3.82
2	Climate	0.158[a]	0.025	-0.138	4.21
3	Effective Thickness	0.477[a]	0.227	0.099	3.75
4	Moment of Inertia	0.482[a]	0.233	0.105	3.74
5	Log (Strain)	0.469[a]	0.220	0.090	3.77
6	Log (Flexural Stiffness)	0.074[a]	0.005	-0.160	4.26

Table 4-16: ANOVA Summary of $N_{20\%}$_Single Seals

No.	Constant, a	Regression			Residual			Total		Significance of Regression	
		SSR	df	Mean Square	SSE	df	Mean Square	SST	df	F	Sig.
1	Age	21.5	1	21.5	87.8	6	14.6	109.3	7	1.47	0.271[b]
2	Climate	2.7	1	2.7	106.6	6	17.8	109.3	7	0.154	0.709[b]
3	Effective Thickness	24.8	1	24.8	84.4	6	14.1	109.3	7	1.77	0.232[b]
4	Moment of Inertia	25.4	1	25.4	83.9	6	14.0	109.3	7	1.82	0.226[b]
5	Log (Strain)	24.1	1	24.1	85.2	6	14.2	109.3	7	1.70	0.241[b]
6	Log(Flexural Stiffness)	0.598	1	0.598	108.7	6	18.1	109.3	7	0.033	0.862[b]

Table 4-17: Coefficient Summary of N$_{20\%}$_Single Seals

No.	Model	Unstandardized Coefficients		Standardized Coefficient	t	Sig.
		B	Std. Error	Beta		
1	Age	0.364	0.301	0.444	1.213	0.271
	Constant	1.462	4.567	-	0.320	0.760
2	Climate	255.00	650.28	0.158	0.392	0.709
	Constant	-1014.15	2603.39	-	-0.390	0.710
3	Effective Thickness	0.681	0.512	0.477	1.329	0.232
	Constant	-6.119	9.777	-	-0.626	0.554
4	Moment of Inertia	$117.7*10^6$	$87.284*10^6$	0.482	1.348	0.226
	Constant	2.204	3.623	-	0.608	0.565
5	Log (Strain)	-35.805	27.498	-0.469	-1.302	0.241
	Constant	104.490	75.075	-	1.392	0.213
6	Log (Flexural Stiffness)	1.773	9.762	0.074	0.182	0.862
	Constant	0.235	35.917	-	0.007	0.995

- Significance of Age on Fatigue ($N_{20\%}$) in Single Seals:

Coefficient, R = 0.444, suggests that there is a weak relationship between the ages of single seals and fatigue ($N_{20\%}$), while the coefficient of determination, R = 0.197, suggests that only 20% of the variance in the fatigue values of the single seals can be explained by the respective ages of the single seals that were tested.

Significance, p = 0.271, means there is only 72.9% probability that the ages of the single seals can influence the outcome of fatigue ($N_{20\%}$). The regression model is therefore not statistically significant.

- Significance of Climate on Fatigue ($N_{20\%}$) in Single Seals:

Coefficient, R = 0.158, suggests that there is an even weaker relationship between the climate from which the single seals were sampled and the fatigue values, than compared with the ages of the single seals. Furthermore the coefficient of determination, $R^2 = 0.025$, suggests that only 3% of the variance in the fatigue values can be explained by the effect of climate.

Significance, p = 0.709, means there is only 29% probability that the climate of the single seals can influence the outcome of fatigue ($N_{20\%}$). The regression model is therefore not statistically significant.

- Significance of Effective Thickness on Fatigue ($N_{20\%}$) in Single Seals:

Coefficient, R = 0.477, suggests that there exists also a weak relationship between the effective thickness of the single seals and the fatigue values. The coefficient of determination, $R^2 = 0.227$, suggests that only 23% of the variance in the fatigue values can be explained by the effective thickness of the single seals.

Significance, p = 0.232, meaning there is only 76.8% probability that the effective thickness of the single seals can influence the outcome of fatigue ($N_{20\%}$). The regression model is therefore not statistically significant.

- Significance of Moment of Inertia on Fatigue ($N_{20\%}$) in Single Seals:

Coefficient, R = 0.482, suggests that a weak relationship exists between the moment of inertia (non-linearity of the thickness of the sampled single seal) and the fatigue values. The coefficient of determination, $R^2 = 0.233$, furthermore suggests that only 23% of the variance in fatigue results for the single seals can attributed to the effect of the non-linearity of the thickness of the single seals.

Significance, p = 0 .226, meaning there is only 77.4% probability that the moment of inertia of the cross section of the single seal beams can influence the outcome of fatigue ($N_{20\%}$). The regression model is therefore not statistically significant.

- Significance of Log (Strain) on Fatigue ($N_{20\%}$) in Single Seals:

Coefficient, R = 0.469, suggests that a weak relationship exists between the logarithmic value of the applied test strain and the fatigue of single seals. The coefficient of determination, R^2 = 0.220, furthermore suggests that only 22% of the variance in the fatigue values can be attributed to the effect of the logarithmic value of the applied test strain.

Significance, p = 0.241, means there is only 75.9% probability that the logarithmic strain at which the single seals were tested can influence the outcome of fatigue ($N_{20\%}$). The regression model is therefore not statistically significant.

- Significance of Log (Flexural Stiffness) on Fatigue ($N_{20\%}$) in Single Seals:

Coefficient, R = 0.074, suggests that a very weak relationship exists between the logarithmic value of the flexural stiffness that was used as a direct input in the Classical Fatigue Characterisation Approach, as detailed in *Chapter 2 Literature Study.* Furthermore only 0.5% of the variance in the fatigue values can be explained by the logarithmic value of the flexural stiffness, described by the coefficient of determination, R^2 = 0.005.

Significance, p = 0.862, means there is only 13.8% probability that the logarithmic flexural stiffness from the flexural testing of the single seals can influence the outcome of fatigue ($N_{20\%}$). The regression model is therefore not statistically significant.

In general, there exist weak relationship plots between the six (6) independent variables in the regression models from the output of the SPSS analysis and the dependent outcome from the fatigue values obtained from the flexural bending tests carried out in the laboratory.

None of the regression models were found to be statistically significant. However, the independent individual variable for single seals that best influenced the fatigue values ($N_{20\%}$), in descending order, are Moment of Inertia, Effective Thickness, Log (Strain), Age, Climate and Log (Flexural Stiffness).

The complete statistical analysis for the individual seal variables is detailed in Appendix 7J.

4.5.1.2. Summary of Results

Single Seals

The influence of single variables on the outcome of the fatigue results were assessed and summarized. From the statistical analysis very low significance was found for the single seals when the influence of single variables was assessed.

It was nevertheless found that the fatigue criteria that yielded the highest relative significance were when fifty percent reduction in the initial flexural stiffness was considered as the "failure point".

For this termination criterion it was found that the Moment of Inertia, Log (Strain), Effective Thickness and Ages of the seals had the greatest influence on the fatigue results obtained, as illustrated in Figure 4-13.
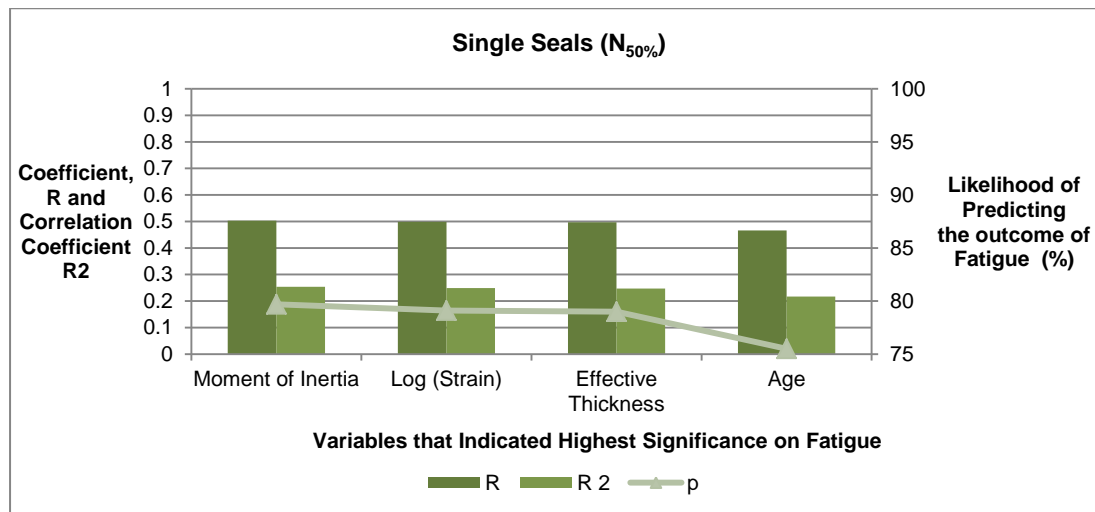
Figure 4-13: Significance of Single Seals on Fatigue (N$_{50\%}$)

From the results for single seals it is clear that the effective thickness plays an important role in the fatigue results and the subsequent statistical significance. A sensitivity analysis was therefore carried out on the above four variables to assess the influence of the effective thickness on the statistical analysis. This was done by reducing the measured effective thickness by 4.9mm and also by increasing the measured effective thickness by 3.1mm.

Tables 4-18 to 4-21 detail the effect of varying the effective thickness.

Table 4-18: Influence of Effective Thickness on the Significance of Moment of Inertia on Fatigue

Failure Criteria	Moment of Inertia		
	Sig, p (-4.9mm)	Sig, p (measured)	Sig, p (+3.1mm)
N$_{20\%}$	22.8	77.4	56.4
N$_{30\%}$	63.2	78.2	68.1
N$_{40\%}$	69.4	70.9	74.1
N$_{50\%}$	94.9	79.7	79.00

Table 4-19: Influence of Effective Thickness on the Significance of Effective Thickness on Fatigue

Failure Criteria	Effective Thickness		
	Sig, p (-4.9mm)	Sig, p (measured)	Sig, p (+3.1mm)
N$_{20\%}$	21.1	76.8	56
N$_{30\%}$	62.5	77.5	67.7
N$_{40\%}$	68.7	70.3	73.6
N$_{50\%}$	94.5	79	79.00

From the two tables above it can be seen that significance greatly increased for a thinner single seal, indicating that it will have a reduced fatigue life, compared to a thicker single seal. The variable, moment of inertia is 94.9 significant, whereas the effective thickness indicates 94.5% significance on the outcome of fatigue. Aggregate size is therefore the most important seal design factor to ensure the lifetime of the Single Seal. In general the thicker single seals indicted reduced significance.

Table 4-20: Influence of Effective Thickness on the Significance of Age on Fatigue

Failure Criteria	Age		
	Sig, p (-4.9mm)	Sig, p (measured)	Sig, p (+3.1mm)
$N_{20\%}$	28.8	72.9	49
$N_{30\%}$	56.7	73.8	62.2
$N_{40\%}$	63.4	66.7	68.9
$N_{50\%}$	93.3	75.5	75.30

From the table above the ages of the thinner single seals indicated high significance for the outcome of fatigue, compared to that of the thicker single seals. Ages of thinner single seals will influence fatigue life significantly.

Table 4-21: Influence of Effective Thickness on the Significance of Log (Strain) on Fatigue

Failure Criteria	Log (Strain)		
	Thinner	Measured	Thicker
$N_{20\%}$	80.9	75.9	75.5
$N_{30\%}$	86.5	77.2	73.8
$N_{40\%}$	87.3	70.8	74.1
$N_{50\%}$	88	79.1	79.10

From the table above it can be seen that the significance improved slightly for the thinner single seals and reduced for the thicker single seals. Thinner single seals will therefore fail sooner under the same applied load (traffic) than thicker single seals.

For the complete sensitivity analyses refer to Appendix J1.

Double Seals

The influence of double seals on fatigue furthermore indicated low significance, except for the variable, Climate, which indicated a strong positive relationship for all four termination conditions that was analysed. The greatest significance was found when twenty percent reduction was considered as the failure criterion.

For this termination criterion it was found that the Climate, Log (Flexural Stiffness), Effective Thickness and Moment of Inertia of the seals had the greatest influence on the fatigue results obtained, as illustrated in Figure 4-14.
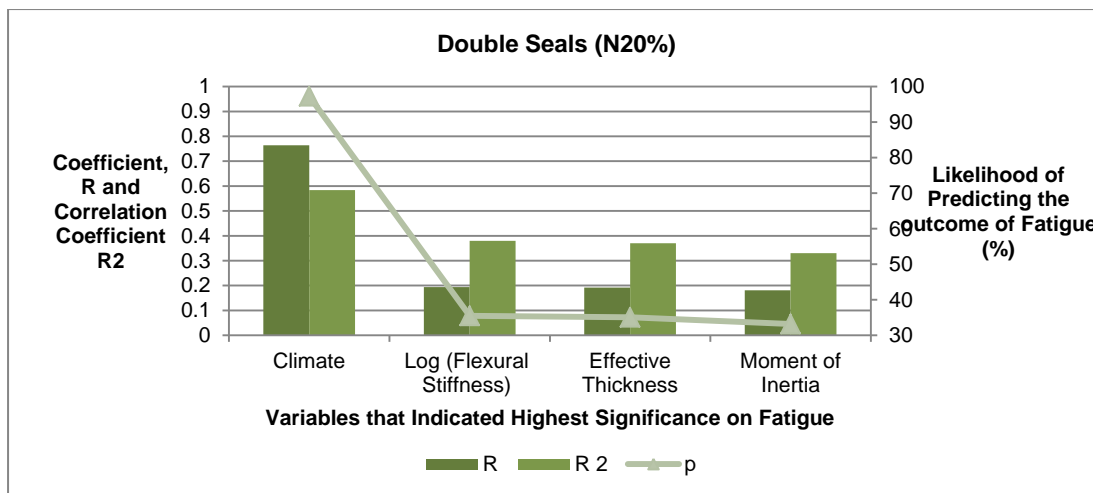
Figure 4-14: Significance of Double Seals on Fatigue (N$_{20\%}$)

Cape Seals

For the influence of the cape seal variables, strong positive relationships existed between the individual variables and the outcome of fatigue. The greatest significance was found when fourty percent reduction was considered as the failure criterion.

For this termination criterion it was found that the Effective Thickness, Moment of Inertia, Climate and age of the seals had the greatest influence on the fatigue results obtained, as illustrated in Figure 4-15 below.
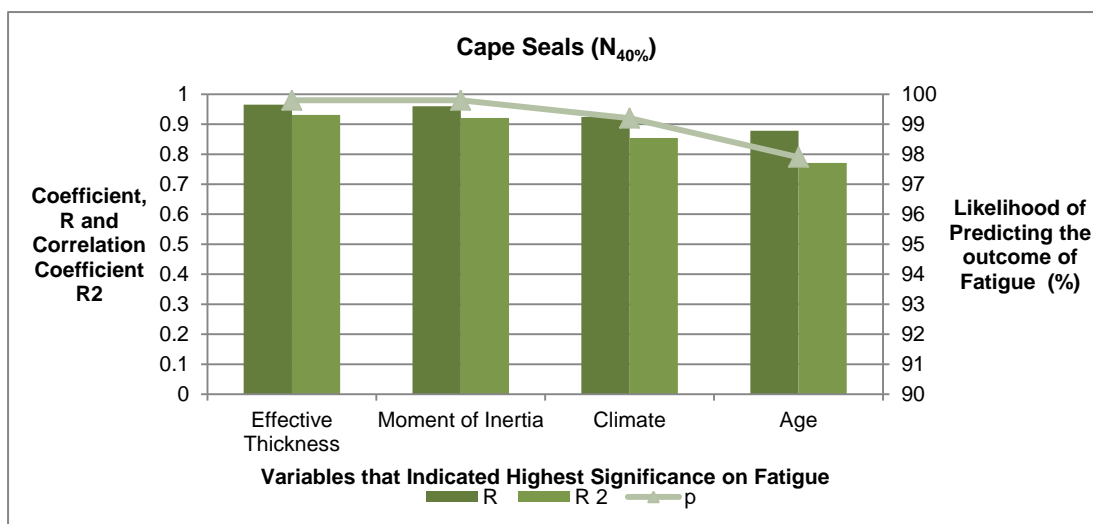
Figure 4-15: Significance of Cape Seals on Fatigue (N$_{40\%}$)

From the assessment of the significance of the single variables on the fatigue results it could be seen that the single seals and cape seals yielded high significance at a higher fatigue level. For single seals the trend could be explained when one considers that a single seal layer is relatively thin and its structural support is from the underlying base layer.

It could mean that a single seal layer can be absorbed as part of the base layer, i.e as an additional prime layer, thus creating uniformity. The idea of a supporting base was added in this study as the fast-cast polyurethane that made up the composite beam that was subjected to flexural bending.

For cape seals it is possible that the slurry mixture applied on top of the single sized aggregate in turn provides uniformity in the seal layer, similar to HMA mixtures that indicate significant failure at a greater reduction in initial flexural stiffness. This "cushioning" effect thus adds to the structural capacity of the cape seal and enables it to withstand an extended loading period, before failure occurs.

Assessment of the influence of the variables on the fatigue results indicate that for double seals the highest significance was found at the lowest failure condition possible. Considering the reduced uniformity in double seals, since that a double seal is not thin enough to be part of the base layer and considering that there is no slurry mixture as with the cape seal, it becomes clear that the double seals experiences the effects of fatigue relatively early in its life.

The structural capacity of the double seal is then primarily governed by the interlock between the two differently sized aggregates that make up the seal structure. Left without the structural support of the system (base in the case of single seals and slurry in the case of cape seals), the interlock is ultimately at the mercy of the climatic environment in which the seal functions, a variable which yielded the highest significance on the fatigue results.

4.5.2. Statistical Significance of Combination of Variables on Fatigue

The influence of the combination of variables on the outcome of the fatigue results were assessed and summarized above. From the statistical analysis very low significance was found for the single seals when the influence of combinations of single seal variables was assessed, similar to the influence of individual single seal variables on the outcome of fatigue.

Figure 4-16 illustrates the combination of variables that indicated the highest significance on fatigue.
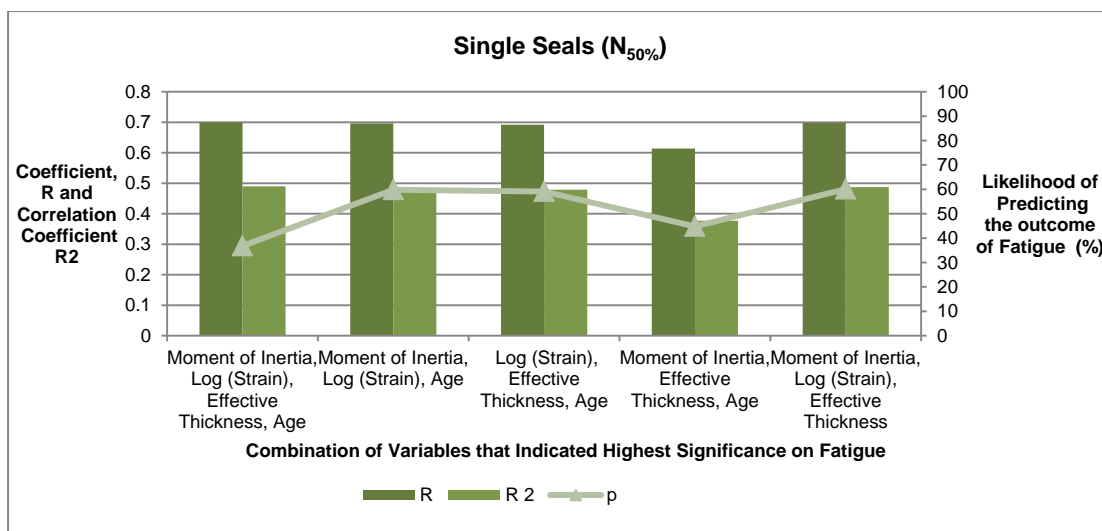
Figure 4-16: Significance of Combination of Single Seal Variables on Fatigue (N$_{50\%}$)

The influence of the combination of double seal variables on the outcome was also investigated and it was found that three of the five different combination groups yielded the same probability, at 73.2%. These are illustrated in Figure 4-17 below.
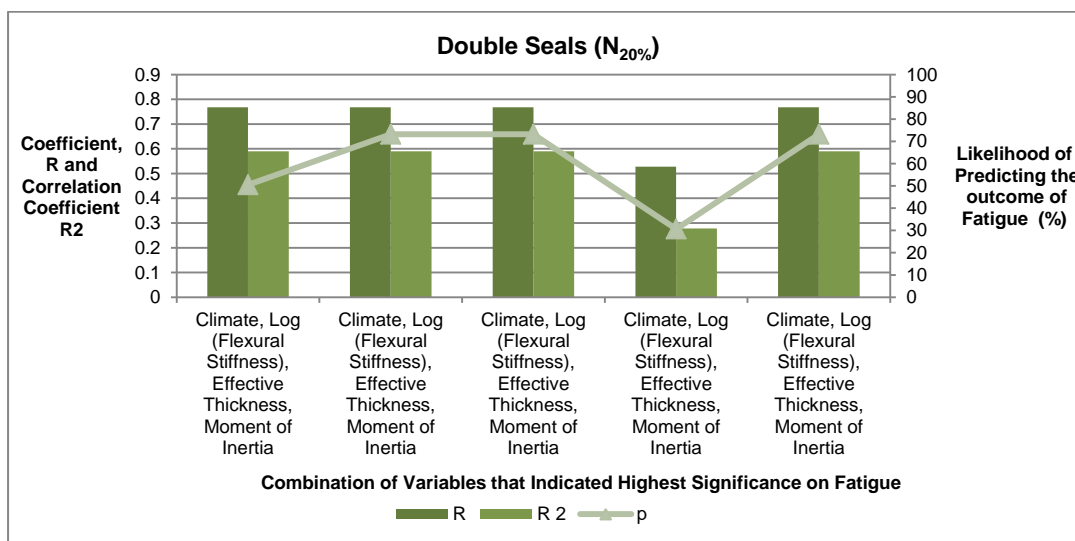
Figure 4-17: Significance of Combination of Double Seal Variables on Fatigue (N$_{20\%}$)

The influence of the combination of cape seal variables on the outcome was also investigated and it was found that the combination with the highest relative probability of 98.8% was for the combination of Effective Thickness, Moment of Inertia an Ages. These are illustrated in Figure 4-18.

152
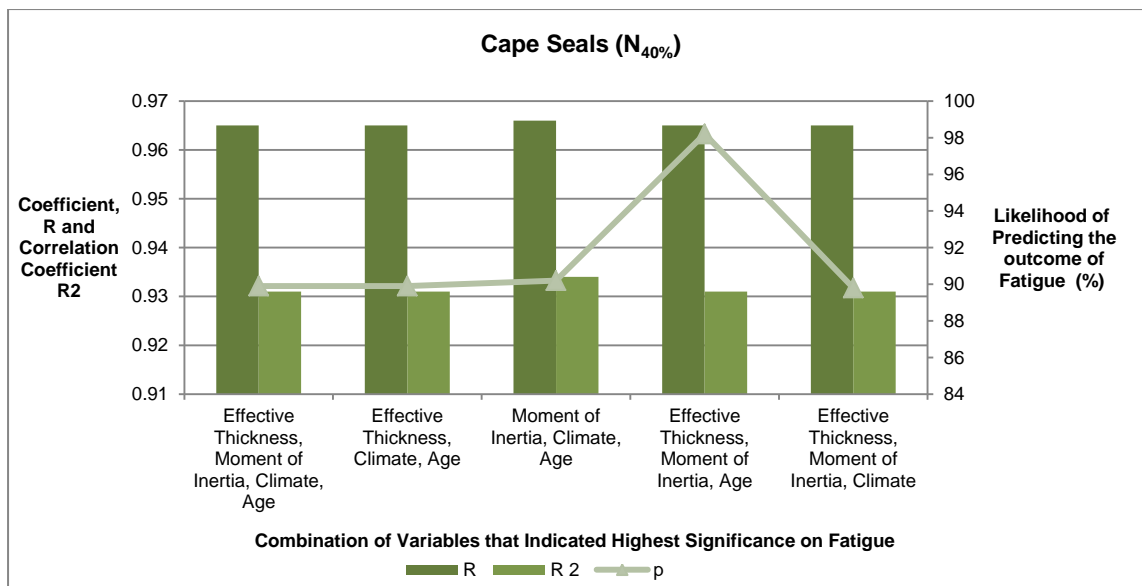
Figure 4-18: Significance of Combination of Cape Seal Variables on Fatigue (N$_{40\%}$)

4.5.3. Statistical Significance of the Interaction of Variables on Fatigue

The influence of the interaction between variables on the outcome of the fatigue results were assessed and summarized above. From the statistical analysis low significance was found for the single seals when the influence of the interaction between single seal variables was assessed, similar to the influence of individual and combination of single seal variables on the outcome of fatigue. Figure 4-19 below illustrates the interaction between variables that indicated the highest significance on fatigue.
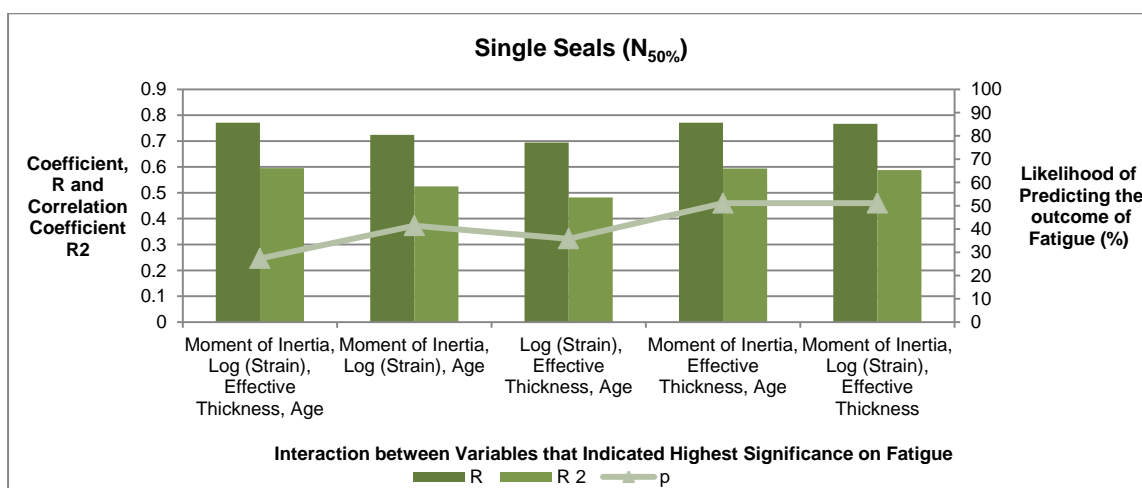
Figure 4-19: Significance of the Interaction between Single Seal Variables on Fatigue (N$_{50\%}$)

The influence of the interaction between the double seal variables on the outcome was also investigated and it was found that the highest probability was for the interaction between

Climate, Log (Flexural Stiffness) and Moment of Inertia. These are illustrated in Figure 4-20 below.
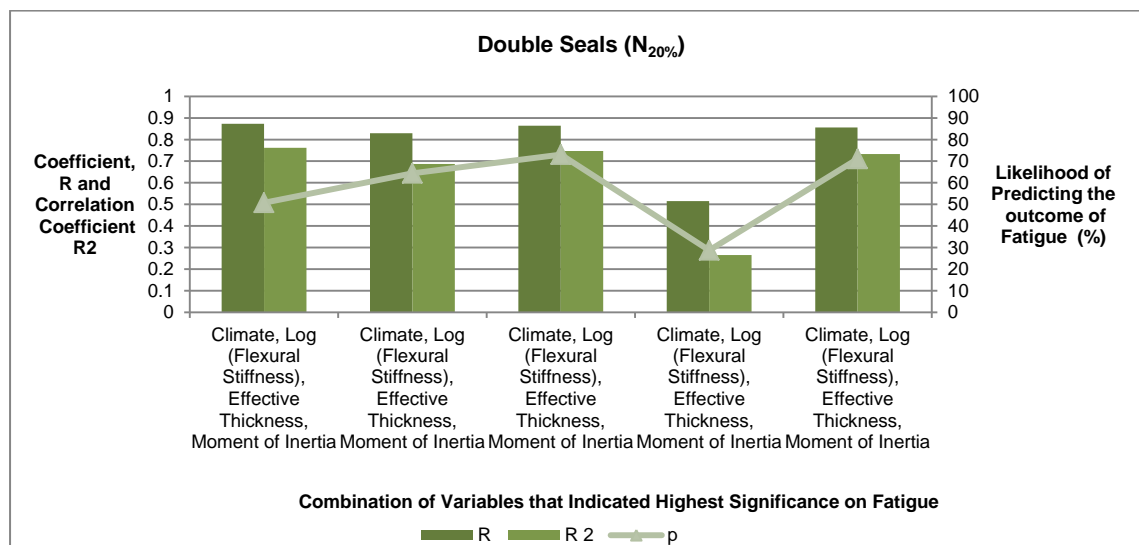
Figure 4-20: Significance of the Interaction between Double Seal Variables on Fatigue ($N_{20\%}$)

The influence of the interaction between cape seal variables on the outcome was also investigated and it was found that the combination with the highest relative probability of 98.2% was for the interaction between Effective Thickness, Moment of Inertia an Ages. These are illustrated in Figure 4-21 below.
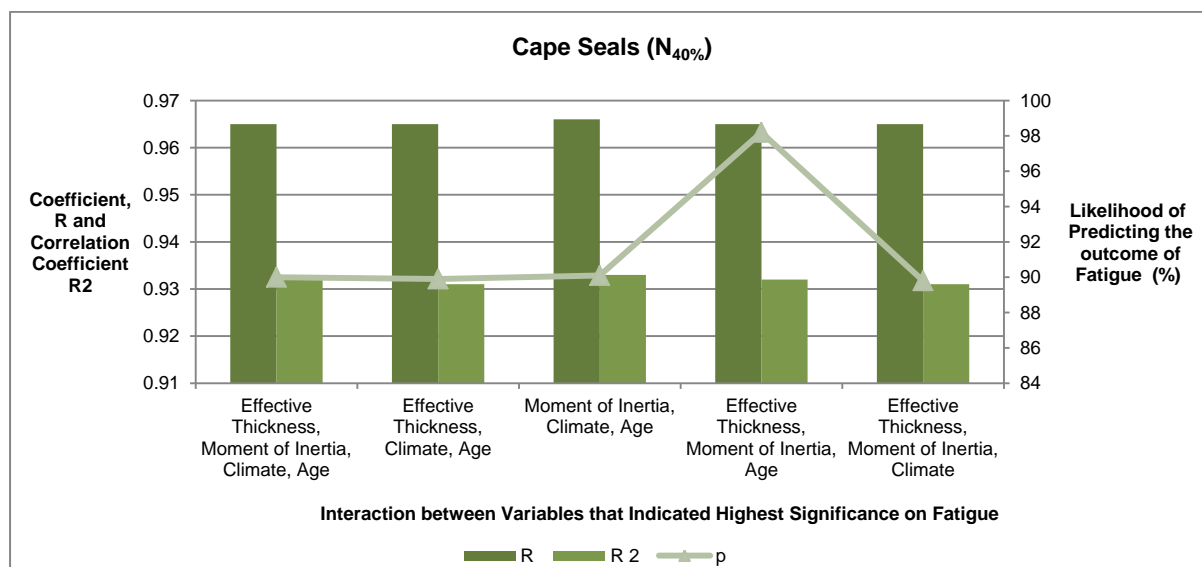
Figure 4-21: Significance of the Interaction between Cape Seal Variables on Fatigue ($N_{50\%}$)

4.6.   Summary and Discussion of Findings

Response of seals to frequency sweep testing at 480με indicated that as the age of single seals increase, so do their stiffness value, particularly when traffic volumes increase. This trend was also observed during the single seal response to frequency sweep testing performed at the higher strain of 520με. As the seal binder ages it essentially becomes stiffer, due to the loss of volatiles during the hardening process. Aged single seals reported lower bitumen contents and reduced penetration depths, indicative of "harder" seals. Samples from the inner wheel track reported higher stiffness values, which implies that this position in the road received less traffic to keep the binder soft.

This trend was however not observed in the single seal with the smallest aggregate size (MR536_9mm_19years). Results varied when compared to larger aggregate sizes as well as when comparing the results between the two sampled positions; inner wheel track and outer wheel track. For the inner wheel track, higher stiffness values were reported, which agrees with above mentioned trend, since this seal was in service for 19 years and underwent extensive ageing of its binder, which could also be seen in its reduced binder content and penetration depth. A smaller aggregate size has a reduced surface area that can be covered with bitumen, which would imply lower performance in crack resistance, but since this seal was in service for almost double that of the other single seals, it can explain the higher stiffness values that were measured in the frequency sweep test.

For the outer wheel track however, this trend was not observed, but instead a much lower stiffness was measured for the seal beam extracted from between the wheel track, which gives the impression that the binder was softer with less traffic. This is however not the case, since this position reported lower binder content and penetration depth, indicating that it was indeed stiffer than the sample from the inner wheel track. Permeability results indicated that both samples were impermeable and from the visual assessments it could be seen that the seals were still relatively intact. In attempting to answer this vast difference in stiffness between the two positions, one has to consider not only that the seal was in service for 19 years, but also the possibility of construction imperfections for highly variable single seals.

A single seal relies heavily on only one layer of single sized aggregate and one binder application to provide its structural stability and is therefore the most unforgiving of all the sprayed seals. Any small variation in application rates during construction will only be highlighted further by the effects of traffic. An aggregate spread rate that is too high creates a non-uniform surface with a poor aggregate interlock pattern. This interlock can further be broken down by the effects of traffic in the form of aggregate whip-off, which results in a weaker section in the road width. Alternatively, a high binder application rate can result in bleeding of the surface where the aggregate interlock is insufficient, causing a reduction in structural integrity. Since between the wheel track reported lower binder content than the inner wheel track, it is possible that this section in the road width experienced more damage due to aggregate and binder loss and therefore reported lower stiffness values.

The single seals were all from the Western Cape Province that has a moderate climate; the influence of climate could therefore not be investigated. Considering however that the single seal is so easily influenced, it can only be speculated that its environment will also play a major role on its performance.

Response for double seals was largely influenced by the climatic regions from which the seals were extracted. When comparing the responses between moderate and wet climatic zones, it could be seen that the wetter region provided a double seal with reduced flexural stiffness, especially when subjected with high traffic volumes. The effect of climate and traffic can be seen in the stress and strains imposed on the seal. Horizontal stresses develop from the braking, turning and acceleration of traffic wheels, together with the wheel loading, tyre

type, pressure and coefficient of friction between the road and the wheel. Subsequently, a colder climate can cause build-up of strain in the binder, which causes it to eventually crack.

The ages of the double seals did not considerably influence this particular observation, although aged seals did indicate higher stiffness values, which could be attributed to the ageing of the binder.

Response for cape seals, to frequency sweep testing at 480µε indicated that with increased traffic volumes, the stiffness of the seals was likewise reduced. This comparison within the cape seal group also highlighted the differences between various sampled positions. Samples extracted from the shoulder of the road section measured higher stiffness values, possibly due to the reduced traffic volumes that were imposed on these sections of the road width. This section therefore has less traffic to keep the binder active and soft, resulting in a stiffer sprayed seal.

Multiple seals were only measured during group 1 of the frequency sweep testing, which was performed at 480µε. Comparison with higher strain at 520µε was thus not possible, but comparison within the group indicated that the seal sample extracted from the shoulder position also yielded higher stiffness values, compared to the seals extracted from the inner wheel track. A comparison could however not be made between the two sampled positions for the same location, to fully assess the effect of traffic. The author thus drew from the previous observation made from the cape seals.

Furthermore multiple seals indicated that the sample from the wetter climate measured lower stiffness values, but with a reduced traffic volume. This is similar to the trend in double seals and can be explained by considering that multiple seals are essentially double seals with an added single layer of aggregate, in this case the multiple seals were 19mm + 6mm + 6mm.

The fatigue characterizing presented the opportunity to investigate the applicable fatigue failure point/limit for the various tested seals. The loading consideration affects the fatigue damage development. The fatigue testing carried out in this study considered displacement loading, which is preferred for more flexible, thinner pavement layers. This type of loading has a longer damage development since the crack propagation is included in the measured "fatigue life" and the termination point is selected arbitrarily, for asphalt it is selected at fifty percent reduction in initial flexural stiffness. For sprayed seals this would therefore imply an even longer damage development. Whether this damage development was in line with that of asphalt was investigated and it was found that it was not the case for all the sprayed seals.

For single seals it was found that the highest relative significance was yielded when the conventional HMA guideline for failure criterion was considered, that being fifty percent reduction in flexural stiffness, similar to the termination condition for asphalt. Single seals however yielded very low significance, possibly due to the relatively low contribution this type of seal, makes to the pavement system. For single seals the results were "dominated" by the effect of the added polyurethane dimension, which in-situ relates to the underlying base layer. In essence the base layer can be seen as "absorbing" the single seal.

For double seals a twenty percent reduction was considered as the failure point, while for cape seals this was defined as fourty percent reduction in initial flexural stiffness had the highest significance on the outcome of fatigue. For the double seals, the seal had no cushioning effect from above (slurry mixtures), not did it was it thin enough to be absorbed by the underlying base layer (as in case with single seal). Here the effect of the aggregate interlock became crucial in determining the failure point/level.

For the Cape Seals a fourty percent reduction in initial flexural stiffness yielded the highest significance, which could possibly be explained by the effect of the slurry mixtures provided

a "cushioning "effect, which caused the seal to withstand longer loading periods, which was the opposite for the double seals.

It was evident that the volumetric of the sprayed seals played a major role in the fatigue performance. The more three dimensional (3D) the seal, the more it simulated asphalt behaviours.

Likelihood of predicting fatigue was investigated for the individual variables, combination of variables as well as the interaction between variables. For single seals fatigue ($N_{50\%}$) was most influenced by Moment of Inertia, Log (Strain), Effective Thickness, Age. For double seals fatigue ($N_{20\%}$) was most influenced by Climate, Log (Flexural Stiffness), Effective Thickness, Moment of Inertia. For cape seals fatigue ($N_{40\%}$) was most influenced by are Climate, Effective Thickness, Moment of Inertia, Age.

Combination of variables from highest significance individual variables, were investigated and found that highest significance was for the combination of Moment of Inertia, Log (Strain) and Effective Thickness for single seals. For double seals the similar significance were found for combinations of variables that included the variable climate. For cape seals the combination of effective thickness, moment of inertia and ages had the highest likelihood of predicting the outcome of fatigue.

The interaction between variables from the various combination groups were also investigated and it was found that the single seals, the interaction between Moment of Inertia, Effective Thickness and Age and also the interaction between Moment of Inertia, Log (Strain) and Effective Thickness had the highest significance.

For double seals the interaction between Climate, Log (Flexural Stiffness) and Moment of Inertia, while for cape seals the interaction between effective thickness, moment of inertia and ages had the highest significance on the outcome of fatigue.

5. Conclusions and Recommendations

5.1. Conclusions

The research objectives were defined in the introduction of this report as:

- Develop fatigue relations for seals.
- Give indication of timing for maintenance.

Setting up of fatigue relations was quite challenging, considering the challenges as discussed in the previous section. Fatigue characterisation was however developed in terms of the influence of the variables on the outcome of fatigue.

Furthermore, this characterisation process could not completely follow the HMA guidelines for fatigue testing, as it was found that different type of seals failed at different loading conditions, which is related to their expected lifetimes.

Seal Type

- For Single Seals, very low significance was yielded, but the relative highest significance was for $N_{50\%}$.
- For Double Seals, mostly low significance was yielded, except for climate, the relative highest significance was for $N_{20\%}$.
- For Cape Seals, the highest significance was yielded, with $N_{40\%}$ being the applicable termination criteria.

For the indication of maintenance it can thus be possible to recommend that once fifty percent reduction in flexural stiffness is reached for single seal, maintenance is due. Similarly once twenty and fourty percent reduction occurs for double and cape seals respectively.

Ageing and Climate

- For Single Seals, the effects of ageing and climate did not significantly influence the fatigue performance.
- For Double Seals, the climatic regions had the highest significance on the fatigue performance of the seal, while the effects of ageing indicated very low influence.
- For Cape Seals, ageing and climate showed high significance on the fatigue.

Effective Thickness

- For Single Seals, the effective thickness formed part of the top three variables that affected fatigue.
- For Double Seals, the effective thickness influenced fatigue similarly to that of the Single Seals.
- For Cape Seals, the effective thickness was the second highest contributing factor to fatigue, after the effect of the climate and even before that of ageing.

Traffic, Permeability and Aggregate Size

- For Single Seals, the effect of traffic combined with the resultant increase in permeability indicated the highest contributing factor to fatigue, regardless of aggregate size.
- For Double Seals, the effect of traffic and increased permeability caused more fatigue damage for smaller sized seals, than for the larger seals.
- For Cape Seals, the effect of aggregate size was not assessed, since all were 19mm. The effect of traffic with increased permeability caused fatigue damage, similar to Single and Double Seals.
- For Multiple Seals, the effects were similar to that of Double Seals.

Strain Levels

- For Single Seals, the effect of applied strain, combined with effective thickness was the second highest influence on fatigue. At higher strain levels, performance of the seals was reduced.
- For Double Seals, the effect of strain was relatively low, compared to other variables.
- For Cape Seals, the effect on fatigue was similar to that of Double Seals.

Other Variables influencing fatigue

The position from which samples were extracted and beams produced furthermore influenced fatigue. The majority of the results indicated improved fatigue performance for samples from the wheel track itself, compared to the samples from the shoulder and between the wheel tracks.

    5.2.   Discussion of Challenges

Seals are relatively thin surfacing layers and even though care was given during the extraction from the road and the transportation to the laboratory, some samples were still damaged in the process. For this unfortunate reason, beams could not be produced from both the locations (SHDR/OWT) and (IWT/BWT) to better draw comparisons.

In order to test the seals in the 4PB apparatus an additional dimension had to be added to the height of the specimen in order to fit in the test apparatus. For this reason, a fast-cast polyurethane material was casted against the sprayed seal, which fortunately did not indicate fatigue characteristics of its own, but however added an element of "reinforcement" to the sprayed seal. This led to extremely long testing times in the laboratory, after which the results still had to be interpolated to reach "failure".

Results from the fatigue testing were highly scattered with conflicting patterns/ trends in fatigue characteristics, which could have been due to low amount of beams that were tested. In this research approach only two beams were tested, one at 480με and the other at 600με. These two represented the upper and lower strain levels, from which the fatigue relations were drawn up. The HMA guideline however recommends that 3 beams be tested at low strain, medium as well as high strain levels. This was however not possible due to the low amount of beams available for testing.

Variables to consider for four different types of seals were quite high and required relatively more tests as well as repeat tests to truelly give justice to variables that influence the performance of the seals.

5.3. Future Research

Recommendation for future research should consider testing only one type of sprayed seal and do an exhaustive investigation on the variables that influence the fatigue characteristics of that particular type of sprayed seal.

A study should be done primarily on cape seals, since this type of seals yielded the highest significance on the outcome of fatigue. The investigation should consider various types of slurry mixtures and aggregate size, as it became evident that the more "uniform" the cape seal the better it performed.

Furthermore double seals should also be investigation, since this type of sprayed seal relies solely on the effect of the aggregate packing for its performance. This seal is therefore also the most "exposed" to its climate and the effect of traffic loads.

A Finite Element Modelling (FEM) of the 2 layer system and the 4PB beam set up can also provide more detailed insight on the fatigue response of the bi-layer system.

The Master Curves can also be further analysed in terms of the analysis done by Geoff Rowe and Charles Glover, which links "s", ""m" parameters, R-Value (Reological Index), Cross-over Frequency to fatigue.

6. References

1. AASHTO. 1972. *AASHTO Interim Guide for Design of Pavements Structures*, American Association of State Highway and Transportation Officials, Washington, DC.

2. Accelerated Polishing Machine, n.d. Online Catalogue. Available at: http://www.capco.co.uk/acatalog/Online_Catalogue_Accelerated_Polishing_Machine_20.html. [02/08/2015].

3. Airey, G.D., 1995. *Fatigue testing of asphalt mixtures using the laboratory third-point loading fatigue testing system*. Masters Dissertation, University of Pretoria, Pretoria, South Africa.

4. Alderson A. & Oliver J., 2008. *Seal Disress Mechanisms: An Initial Study into Flushing.* Australia, Austroads Inc.

5. American Society of Testing Materials. (1982). *Resistance to Plastic Flow of Bituminous Mixtures Using Marshall Apparatus*, ASTM-D 1559-82. Philadelphia.

6. Anderson A., 2006. *Update of the Austroads Sprayed Seal Design Method.* Australia, Austroads Inc.

7. Annandale, W. 2012. *Permeability of Surfacing Seals*. University of Stellenbosch (Final Year Skripsie).

8. Arnold, G., Steven, B., Alabaster, D., Fussell, A. 2005. *Effect on pavement wear of increased mass limits for heavy vehicles* – Stage 4. *Land Transport New Zealand Research Report 280.* 30 pp.

9. ASTM, 2008. *Standard Test Method for Determining Fatigue Failure of Compacted Asphalt Concrete Subjected to Repeated Flexural Bending*, ASTM Designation: D 7460 – 08, ASTM International, 100 Barr Harbor Drive, PO Box C700, West Conshohocken, PA.

10. Asphalt-Institute. 1982. *Reseach and Development of the Asphalt Institute's Thickness Design Manual (MS-1), 9th ed. Research Report 82-2ts*, Asphalt Institute, Lexington, KY.

11. Assimwe, A. K. 2013. *Surface run-off behaviour of bitumen emulsions used for the construction of seals.* University of Stellenbosch (Master's Thesis).

12. ASTM E 961. 2001. Standard Test Method for Measuring Pavement Macro-texture Depth Using a Volumetric Technique.

13. ASTM. 1964. *STP 91A: Tentative guide for fatigue testing and the structural analysis of fatigue data.* American Standard Test Methods, 2nd Edition, West Conshohocken, PA, United States.

14. Bahia, H, Jenkins, K & Hanz, A. 2008. *Performance grading of bitumen emulsions for sprayed seals.* 1st International sprayed sealing conference. Adelaide, South Australia: Australian Road Research Board (ARRB).

15. Ball, G. F. A. and Patrick, J. E. 1998. *Flushing Processes in Chipseals: Effects of Trafficking.* Transfund New Zealand Research Report *122.*

16. Ball, G. F. A., Logan, T. C. & Patrick, J. E. 1999. *Flushing Processes in Chipseals: Effects of Water.* Transfund New Zealand Research Report 156*.*

17. Ball, G.F.A., Owen, M.T. 1998. *Chipseal lifetimes in New Zealand.* Proceedings of 9th Road Engineering Association of Asia and Australasia Conference (REAAA), Vol.1: 453-458, Wellington, New Zealand, 3-8 May, 1998.

18. Barksdale, R.D. and Miller, J. H., III. 1977. *Development of Equipment and Techniques for Evaluating Fatigue and Rutting Characteristics of Asphalt Concrete Mixes.* Report SCEGIT-77-147. School of Civil Engineering, Georgia Institute of Technology, Atlanta.

19. Barksdale, R.D. and Miller, J.H., 1977. *Development of equipment and techniques for valuating fatigue and rutting characteristics of asphalt concrete mixes.* Report SCEGIT-77-147. School of Civil Engineering, Georgia Institute of Technology, Atlanta.

20. Bazin, P., and Saunier, J. 1967. *Deformability, Fatigue and Healing Properties of Asphalt Mixes.* Proceedings, Second International Conference on the Structural Design of Asphalt Pavements, University of Michigan.

21. Blatt, H.,Tracy, R.J. and Owens, B.E. 2006. *Petrology, Igneous, Sedimentary, and Metamorphic.* 3rd Edition.W.H. Freeman & Company, New York.

22. Bonnaure, F., Gravois, A., and Udron, J. 1980*. A New Method of Predicting the Fatigue Life of Bituminous Mixes.* Proceedings of Association of Asphalt Paving Technologists, Vol.49, pp. 499-529.

23. Bonnaure, F., Huibbers, A.H.J.J. and Booders, A., 1982. *A laboratory investigation of the influence of rest periods on fatigue characteristics of bituminous mixes.* Proceedings, the Association of Asphalt Paving Technologists, Vol. 51, pp 104.

24. Bonnot, J., 1972. *Assessing the properties of materials for the structural design of pavements.* Proceedings, Third International Conference on the Structural Design of Asphalt Pavements, London, pp 200-213.

25. Broek, D. 1989. *The Practical use of Fracture Mechanics.* Kluwer Academic Publishers.

26. Brown, S.F., Brunton, J.M., and Pell, P.S. 1982. *The Development and Implementation of Analytical Pavement Design for British Conditions.* Proceedings, Fifth International Conference on the Structural Design of Asphalt Pavements, University of Michigan, Ann Arbor, Michigan, 3-16.

27. Button, J.W. & Lytton, R.L. 1987. *Evaluation of Fabrics, Fibers, and Grids in Overlays.* Proceedings of the Sixth International Conference on Structural Design of Asphalt Pavements, The University of Michigan, 1: 925-934.

28. CEN European Committee for Standardisation, 2001. Bituminous mixtures-Test methods hot mix asphalt-Part 26: Stiffness. European Standard, Draft prEN 12697-26.

29. Charles J. Glover, Richard R. Davison, Chris H. Domke, Yonghong Ruan, Pramitha Juristyarini, Daniel B. Knorr, Sung H. Jung. 2005. *Development of a New Method for assessing asphalt binder durability with field validation.* Texas Transport Institute Report.

30. COLTO. 1998. *Standard Specifications for Road and Bridge Works for State Road Authorities.* Published by the South African Institute of Civil Engineering (SAICE), Pretoria.

31. Craig, R.R. 2011. *Mechanics of Materials.*3rd Edition. John Wiley & Sons Inc, USA.

32. CSIR, 2000*. Interim guideline for the design of hot-mix asphalt in South Africa,* prepared as part of the Hot-Mix Asphalt Design Project, Transportek, CSIR, Pretoria, South Africa.

33. De Beer, M. 1985. *Behaviour of cementitious subbase layers in bitumen base road structures.* M.Eng Thesis, University of Pretoria, Pretoria.

34. Deacon, J., Tayebali, A., Coplantz, J., Finn, F., and Monismith, C.L. 1994. *Fatigue Response of Asphalt-Aggregate Mixes, Part III – Mix Design and Analysis.* Strategic Highway Research Program Report: No. SHRP-A-404, National Research Council, Washington, DC, USA.

35. Deacon, J.A. Coplantz, J.S. Tayebali, A. A. and Monismith, C. L., "Temperature considerations in asphalt-aggregate mixture analysis and design," *Transportation Reseach Record No. 1454, Asphalt Concrete Mixture Design Performance*, ed Washington, DC, USA: Transportation Reseach Board, 1994, pp. 97-112.

36. Dickinson, E.J. 2000. *Prediction of the hardening of bitumen in pavement surfacings by reaction with atmospheric oxygen.* Road Materials and Pavement Design: an International Journal, Vol.1, no.3, pp 255-79.

37. Distin, T. 2008a. *Development of performance requirements for binder distributors in South Africa.* 1st sprayed sealing conference – cost effective high performance surfacings. Adelaide, Australia: ARRB Group Ltd. [Online]. Available: http://www.arrb.com.au/sealing/PDF/Distin-2.pdf [2/05/2012].

38. Distin, T. 2008b. *Development of performance requirements for binder distributors in South Africa.* [Online]. Available http://www.sabita.co.za/documents/Binder%20distributors.pdf [08/07/2012].

39. Eckel, S. 2008. Lecture 7: ANOVA. [Online]. Available: http://wwwhsc.usc.edu/~eckel/biostat2/notes/notes7.pdf [21/02/2013].

40. Epps, J. A. 1969. *Influence of Mixture Variables on the Flexural Fatigue and Tensile Properties of Asphalt Concrete.* Doctor of Engineering Thesis, University of California, Berkeley.

41. Epps, J.A., and Monismith, C.L.1972. *Fatigue of Asphalt Concrete Mixtures - Summary of Existing Information*, in STP 508, ASTM, 19-45.

42. Flintsch, G. W., Le, E. D., McGhee, K. K., All-Qadii, I. L. 2003. *Pavement surface macrotexture measurement and application.* Paper presented at the Annual Meeting of Transportation Research Board. Washington, D.C. January 13-18.

43. Freeme, C.R., Maree, J.H. and Viljoen, A.W. 1982. *Mechanistic design of asphalt pavements and verification using the Heavy Vehicle Simulator.* In: International Conference on the structural design of asphalt pavements, 5th, Delft, Holland: pp 156 - 173.

44. Friction Test Machine, n.d. Online Catalogue. Available at: http://www.jetmaterials.com/product/other-aggregates-rocks/skid-resistance-and-friction-tester/ [02/08/2015]

45. Gerritsen, A. H., & Jongeneel, D. J.1988. Fatigue Properties of Asphalt Mixes Under Conditions of Very Low Loading Frequencies.

46. Gransberg, D & James, D. 2005. NCHRP Synthesis 342: *Chip seal best practices.* [Online]. Available: http://onlinepubs.trb.org/onlinepubs/nchrp/nchrp_syn_342.pdf [05/11/2011].

47. Gransberg, D & James, D. 2005. NCHRP Synthesis 342: *Chip seal best practices.* [Online]. Available: http://onlinepubs.trb.org/onlinepubs/nchrp/nchrp_syn_342.pdf 05/11/2011].

48. Hair, J.F., Black, W.C., Babin, B.J., & Anderson, R E. 2010. *Multivaraite data analysis.* 7th edition. United States of America: Pearson Education Inc.

49. Hanson, F.M. 1935. 'The bituminous surface treatment of rural highways', Conference of NZ Society of Civil Engineers 1934-35, Vol 21, pp 89-178.

50. Hanz, A., Arega, Z. and Bahia, H. 2008b. *Advanced methods for quantifying emulsion setting and adhesion to aggregates.* [Online]. Available: http://uwmarc.wisc.edu/files/2008_ISAET_Hanz_Quantification_of_Emulsion_Setting_and_Adhesion_paper.pdf [09/10/2012].

51. Harvey, J. Deacon, J. Tsai, B. W. Monismith, C. 1995*. Fatigue Performance of Asphalt Concrete Mixes and its Relationship to Asphalt Concrete Pavement Performance in California.* Berkeley: Institute of Transportation Studies, University of California at Berkeley.

52. Herrington P.R, Ball G.F.A, Patrick J.E, Towler J.I, 2012. *Aggregate breakdown as a cause of chip seal flushing. 25th ARRB Conference-Shaping the future: Linking policy, research and outcomes.* Perth, Australia, 2012.

53. HMA. 2001. *Interim Guidelines for Design of Hot Mix Asphalt in South Africa.*South Africa.

54. Holtrop, W. 2008. *Sprayed Sealing Practice in Australia.* 1st Sprayed Sealing Conference-Cost Effective High Performance Surfacings. Adelaide, Australia.

55. Hooiberg, A.J. (Editor), Volumes 2 and 3, 1965, *Bituminous Materials: Asphalts, Tars, Pitches* (Volume 1, 1964), Interscience Publishers.

56. IPC (Industrial Process Control Ltd), 1998. *Beam fatigue apparatus.* Reference Manual. Boronia, Australia.

57. Jenkins, KJ. 2000. *Mix design considerations for cold and half-cold bituminous mixes with emphasis on foamed bitumen*. PhD Thesis, University of Stellenbosch, South Africa.

58. Judd D. et al., 2008. *The use and Performance of Bitumen Rubber in Spray Seals in RSA.*1st Sprayed Sealing Conference-Cost Effective High Performance Surfacings, Adelaide, Australia.

59. Kearby, J. P., 1953. "Tests and Theories on Penetration Surfaces", *Proceedings, Highway Research Board*, Vol 32.

60. Kim Y.R., Yim N. and Khosla N.P, 1992. *Effect of aggregate type and gradation on fatigue and permanent deformation of asphalt concrete .ASTM STP 1147, Philadelphia*, pp 310-328.

61. Kingham, R. Ian, and Kallas, B. F., 1972. *Laboratory Fatigue and its Relationship to Pavement Performance.* Third International Conference on the Structural Design of Asphalt Pavements, Volume I Proceedings.

62. Koddipily, S., Henning, T., Ingham, J. 2012. Cenek, P. *Detecting Flushing of Thin-Sprayed Seal Pavements Using Pavement Management Data.* 1st Sprayed Sealing Conference-Sustaining Sprayed Seal Practise. Melbourne, Australia.

63. Kummer, H.W. 1966. *Unified Theory of Rubber and Tire Friction.* Pennsylvania State University College of Engineering, University Park, Pennsylvania, USA.

64. Lawson, W. D. and Senagheera, S. 2009. *Chip Seal Maintenance - Solutions for Bleeding and Flushed Pavement Surfaces. Transportation Research Record:* Journal of the Transportation Research Board, 2108, 61-68.

65. Leyland, R., Paige-Green, P. 2010. *Climatic Zones: Identification and Characterisation of Climatic Zones.* Version: 1st Draft. CSIR, South Africa.

66. Little, D. and Bashin, A. 2006. *Using surface energy measurements to select materials for asphalt pavement*; final report for NCHRP project 9-37; Web-only document 104; Texas Transportation Institute; Texas A&M University System, College Station, Texas, USA.

67. Little, D.N. and Jones, J.R. 2003*. Chemical and Mechanical Mechanisms of Moisture Damage in Hot Mix Asphalt Pavements*. National Seminar in Moisture Sensitivity, San Diego, California.

68. Lombard, L. 2014. *Influence of Surface Seal Variables on Bitumen Bond Strength Properties.* University of Stellenbosch (Master's Thesis).

69. Lytton, R.L. 1989. *Use of Geotextiles for Reinforcement and Strain Relief in Asphaltic Concrete.* Geotextiles and Geomembranes, 8: 217-237.

70. Majidzadeh, K., and F. N. Brovold. 1968. *Special Report 98: State of the Art: Effect of Water on Bitumen–Aggregate Mixtures*. HRB, National Research Council, Washington, D.C.

71. Manual 10. 2012. *Bituminuous surfacings for low volume roads and temporary deviations*. 2nd edition. South Africa: SABITA.

72. Manual 11. 1993. *Labour enhanced construction for bituminous surfacings* South Africa: SABITA.

73. Manual 2. 2007. *Bituminous Binders for Road Construction and Maintenance.* 4th Edition. South Africa: SABITA.

74. Marais, C.P. 1979. *Advances in the Design and Application of Bituminous Materials in Road construction.* PhD Thesis, University of Natal, Durban.

75. Maupin, G.W. *Effect of Particle Shape and Surface Texture on the Fatigue Behaviour of Asphaltic Concrete.* Highway Research Record, No.313, 1970.

76. McMurry, J. 2000. Organic chemistry (5th edition). Pacific Grove, California: Brooks/Cole.

77. Medani, T.O. and Molenaar, A.A.A., 2003. *Estimation of fatigue characteristics of asphalt mixes using simple tests.* Wegbouwkundige werksdagen, The Netherlands.

78. Milne, T.I., 2004. *Towards a Performance Related Seal Design Method for Bitumen and Modified Road Seal Binders,* PhD Thesis, Stellenbosch University, Stellenbosch.

79. Mo, L.T., Huurman, M. Wu, S. and Molenaar, A.A.A. 2009. Ravelling investigation of porous asphalt concrete based on fatigue characteristics of bitumen-stone adhesion and mortar. J. Mater. Des., 30: 170-179.

80. Molenaar, A.A.A. 2013. *Rheology and the Stiffness of Bituminous Binders and Asphalt Mixtures and Effects of Ageing.* Delft University of Technology, Netherlands.

81. Monismith, C. L., Inkabi, K., McLean, D. B., and Freeme, C. R. 1977. *Design Considerations forAsphalt Pavements*, Report No. TE 77-1, University of California,Berkeley.

82. Monismith, C.L. and Deacon, J.A.1969. Fatigue of Asphalt Paving Mixtures, *Proceedings of the American Society of Civil Engineers Vol.95*, Ann Arbor, Michigan, USA, pp. 317-346.

83. Montgomery, D. C. & Runger, G. C, 2007. *Applied statistics and probaaility for engineers.*4th edition. United States of America:John Wiley & Sons Inc.

84. Morgan, P & Mulder, A. 1995. *The Shell Bitumen Industrial handbook*. UK.

85. Muller, J, Sadler, D & Van Zyl, G D. n.d. *Bitumen emulsions in sprayed seals: experience and current best practice in South Africa*. ISAET (International Symposium on Asphalt Emulsion Technology).

86. Mullins L..S, 2006. *Fatigue properties of emulsion treated materials,* Master Thesis, Stellenbosch University, South Africa.

87. Muthen, K.M. and Bergh, A.O. 1997. Highly Flexible Surfacings, CSIR, Transportek.

88. National B1 Road in Namibia, n.d. [Online]. Available: http://commonwealthy.tumblr.com/post/123885132996/a-scene-of-the-b1-road-just-outside-of [01/08/2015].

89. National Cooperative Highway Research Program (NCHRP). 2010. *Asphalt Fatigue Life Prediction Models- A Literature Review.* Available online at: https://www.arrb.com.au/admin/file/content13/c6/ARR%20334%20Asphalt%20fatigue.pdf ARRB Transport Research Ltd, Victoria [06/11/2012]

90. National Cooperative Highway Research Program (NCHRP). 2010. *Mixing and Compaction Temperatures of Asphalt Binders in Hot-Mix Asphalt.* Available online at: http://onlinepubs.trb.org/onlinepubs/nchrp/nchrp_rpt_648.pdf   Transportation Research Board, Washington, D.C. [06/11/2012]

91. National Roads Board (NRB) 1968, *Manual of sealing and paving practice,* Prepared for Road Research Unit, National Roads Board, Wellington, New Zealand. NCHRP. (2004). *Mechanistic-Empirical Design of New and Rehabilitated Pavement Structures*, National Cooperative Highway Research Program, NCHRP Project 1-37A, National Research Council, Washington, DC.

92. NDT (Non-destructive Testing) Resource Centre. n.d. *Surface Energy (Surface Wetting Capability).* [Online]. Available: http://www.ndtedorg/EducationResources/CommunityCollege/PenetrantTest/PTMaterials/surfaceenergy.htm [10/12/2011].

93. Neaylon K. and Urquhart R. 2013. *The 1st Sprayed Sealing Alliance Workshop: International Best Practice (Perth).* Australia, ARRB Group Ltd.

94. Nunn, M. E. 1989. *An investigation into reflection cracking in composite pavements.* RILEM International Conference on Reflection Cracking. Liege, Belgium.

95. Oliver J. W. H., 2004. *Prediction of the Life of Sprayed Seals and the Effect of Climate, Durability and Seal Size.* 6th International Conference on Managing Pavements.

96. Oliver, JWH 1999. *The performance of sprayed seals*, research report No. 326, ARRB Transport Research Ltd., Vermont South, Vic.

97. Oliver, JWH 2004, 'Prediction of the life of sprayed seals and the effect of climate, durability and seal size', *International conference on managing pavements, 6th, 2004, Brisbane, Queensland*, Department of Main Roads, Brisbane.

98. Pearl, R.M. 1955. *The minerals and rocks*; fifth printing; MC Graw-Hill Book Company inc., New York, NY, USA.

99. Pell, P. S. 1973. Characterisation of Fatigue Behaviour," in *Structural Design of Asphalt Concrete Pavements to Prevent Fatigue Cracking*. Special Report 140, Highway Research Board, 49-64.

100. Pell, P.S. and Cooper, K.E., 1975. *The effect of testing and mix variables on the fatigue performance of bituminous materials.* Proceedings, Association of Asphalt Paving Technologists, Vol 44, pp 1-37.

101. Petersen, J. C. Quantitative Functional Group Analysis of Asphalts Using Differential Infrared Spectrometry and Selective Chemical Reactions: theory and Application. In *Transportation Research Record 1096*, TRB, National Research Council, Washington, D.C., 1986, pp. 1–11.

102. Petersen, J. C., H. Plancher, E. K. Ensley, G. Miyake, and R. L. Venable. Chemistry of the Asphalt–Aggregate Interaction: Relationships with Pavement Moisture Damage Predication Tests. In *Transportation Research Record 483*, TRB, National Research Council, Washington, D.C., 1982, pp. 95–104.

103. Peterson, C.J., Plancher, H., Ensley, E. K., Miyake, G., and Venable, R. L.1982. Chemistry of Asphalt-Aggregate Interaction: Relationship with Moisture Damage Predication Test. Transportation Research Record, 843, 95.

104. Porter, B. P. and Kennedy, T. W. (1975). *Comparison of Fatigue Test Methods for Asphaltic Materials.* Research Report 183-4. Center for Highway Research. The University of Texas at Austin.

105. Princeton University. 2007. *Interpreting regression output.* [Online]. Available: http://dss.princeton.edu/online_help/analysis/interpreting_regression.htm [15/02/2013].

106. Pronk, A.C. 1999. Fatigue lives of asphalt beams in 2 and 4point dynamic bending tests based on a new fatigue life definition using the dissipated energy concepts. *Road and Hydraulic Engineering Division*, Rijkswaterstaat, The Netherlands.

107. Koole, R. C. Valkering, C. P. and Stapel, F. D. R. Development of pavement design program for use on personal computer, in Proc. The 5the Conference on Asphalt Pavements for Southern Africa (CAPSA 5), Manzini, Swaziland, 1989, pp. 33-43.

108. Raithby, K.D and Sterling, A.B., 1972. *Some Effects of Loading History on the Fatigue Performance of Rolled Asphalt.* Great Britain Transport and Road Research Laboratory Report LR 496, Crowthome, Berkshire.

109. Read, J. and Whiteoak, D. 2003. *Shell bitumen handbook.* 5th edition. UK: Thomas Tz

110. Rebbechi J & Sharp K, 2009. *Guide to Pavement Technology, Part 3: Pavement Surfacings.* Australia. Austroads Inc.

111. Rebbechi J. & Anderson A., 2009. *Guide to Pavement Technology, Part 4K: Seals.* Australia. Austroads Inc.

112. Rebbechi J., 2008. *Guide to Pavement Technology, Part 4F: Bituminous Binders.* Australia. Austroads Inc.

113. Road Network Information System n.d. Western Cape Government. https://rnis.pgwc.gov.za/rnis/rnis_web_reports.main [10/12/2013].

114. Roberts, F.L., Kandhal, P.S., Brown, E.R., Lee, D-Y and Kennedy, T.W.*Hot Mix Asphalt Materials, Mixture Design and Construction* 2nd edition, 1966. NAPA Education Foundation, Lanham, Maryland.

115. Roberts, J. and Rope, R. 1998. *The AARB Integrated Project Level Pavement and Life Cycle Costing Model for Sealed Granular Pavements*, ARR 324, ARRB Transport Research.

116. Robertson, R. E. 2000.*Chemical Properties of Asphalts and Their Effects on Pavement Performance.* Transportation Research Circular No. 499, Washington, D.C.: Transportation Research Board.

117. Roque R, Thompson M, Anderson D, c1989, *Bituminous Seal Coats: Design, Performance, Measurements, and Performance Prediction.* Transportation Research Record 1300.

118. Rust, F.C and Hugo, F. c1988. Towards Performance Related Design Criteria and Specifications for Modified Binders.

119. SABITA, 2011. *Manual 30: A Guide to the Selection of Bituminous Binders for Road.*

120. SABITA, 2013. *SABITA Information Sheet #1 - Bitumen,* Pretoria: SABITA.

121. SANRAL, 2011. *Traffic Count Information Mega Yearbook.* Pretoria. South Africa.

122. SANS 3001 Series. Current. *Test Methods to Replace Those in TMH1.*

123. SANS 3001-BT11:2012. *South African National Standard. Civil engineering test methods. Part BT11: Texture depth measurement for the design of surfacing seals.* South Africa: SABS Standards Division.

124. SAPEM (South African Pavement Engineering Manual). 2013. South Africa: South African National Roads Agency Ltd.

125. Shell International Petroleum Company, Ltd.1978. *Shell Pavement Design Manual*, London.

126. Tangella Rao, S.C.S., Craus, J., Deacon, J.A and Monismoth, C.L., 1990. *Summary report on fatigue response of asphalt mixtures: Prepared for Strategic Highway Research Project A-003-A.* Report TM-UCB-A-003A-89-3, University of California, Berkeley.

127. Teyabali, A., Rowe, G. and Sousa, J., 1992. *Fatigue response of asphalt-aggregate mixtures.* Paper presented at the annual meeting of the Association of Asphalt Paving Technologists, Charleston, South Carolina.

128. TG 1. 2007. *Technical guideline: the use of modified binders in road construction.* 2nd edition. Pretoria: Asphalt Academy.

129. The South African Pavement Design Method Inception Design Report, 2010. Sanral, South Africa.

130. TMH1. 1986. Technical Methods for Highways. *Standard Methods of Testing Road Construction Materials,* Committee of State Road Authorities, Pretoria.

131. TMH9. 1986. Technical Methods for Highways. *Pavement Management Systems,* Committee of State Road Authorities, Pretoria.

132. Transit New Zealand, Road Controlling Authorities and Roading New Zealand 2005, *Chipsealing in New Zealand*, Transit New Zealand. Road Controlling Authorities and Roading New Zealand, Wellington, New Zealand.

133. TRH12. 1997. *Flexible Pavement Rehabilitation Investigation and Design.* Technical Recommendations for Highways. DRAFT.

134. TRH14. 1985 (reprinted 1989) *Guidelines for Road Construction Materials.* Technical Recommendations for Highways, ISBN 0 7988 3311 4. CSRA. Pretoria.

135. TRH3 (Technical Recommendations for Highways). 2007. *Design and construction of surfacing seals.* Pretoria, South Africa: South African National Roads Agency Ltd.

136. TRH3 (Technical Recommendations for Highways). 2007. *Guidelines for Road Construction Materials* Pretoria, South Africa: South African National Roads Agency Ltd.

137. Twagira, E.M. 2006. *Characterisation of Fatigue Performance of Selected Cold Bituminous Mixes.* University of Stellenbosch (Master's Thesis).

138. Twagirimana, E. 2014. *Evaulation of Adhesion Properties in Bitumen-Aggregate Systems for Winter Surfacing Seals by Using Bitumen Bond Strength Test.* University of Stellenbosch (Master's Thesis).

139. U.S. Geological Survey. 1993. *What is Ground Water?* Open-File Report 93-643. Online. Available at: http://pubs.usgs.gov/of/1993/ofr93-643/pdf/ofr93-643.pdf [02/08/2015]

140. Van Dijk, W. and Visser, W. 1977*. The Energy Approach to Fatigue for Pavement Design.* Proceedings at the Association of Asphalt Paving Technologists, Vol. 46, 1.

141. Van Lent, D. 2008. *Aggregate characterisation in relation to bitumen-aggregate adhesion.* Master's Thesis. Delft University of Technology. Netherlands.

142. Van Zyl, G. 2008. *Selection of the Most Appropriate Seal Type.* 1st Sprayed Sealing Conference-Cost Effective High Performance Surfacings. Adelaide, Australia.

143. Van Zyl, G.D. 2007. Measurement and interpretation of seal design parameters used in the South African seal design method. *International Conference on Asphalt Pavements in Southern Africa.* Gaborone, Botswana.

144. Van Zyl, G.D. n.d. '*Seal and thin surfacing technology'*. TRB workshop 153. South African highway technology and practice. [Online]. Available: http://www.nra.co.za/content/TRB3.pdf [19/09/2012].

145. Vuong B., Jameson G., Fielding B., 2008. *Guide to Pavement Technology, Part 4J: Aggregate and Source Rock.* Australia. Austroads Inc.

146. Weinert, H.H., 1980. *The Natural Road Construction Materials of Southern Africa.* H & R Academia. Cape Town.

147. Wilson,G. Fernando, T., Budija M. and Urquhart, R. *Crack Reflection in Sprayed Seals-The Search for a Binder Test.* BP Australia Pty. Ltd., Australia.

7. Appendices

Appendix 7 A: IPC Four Point Bending (4PB) Beam Test Set-Up

Specification:

The operating method for the Beam Fatigue Apparatus (BFA) is detailed in the Manufacturer's Operations Manual. Each beam specimen will be tested in agreement with this method.

Preparation of the Test:

The next steps need to be followed before the test can be carried out:

1. Measure the width and depth of the beam specimen at five positions:
    - Within 20mm of every end.
    - Within 10mm at the centre of the beam.
    - Within 10mm of points positioned 90mm in either direction from the centre of the beam.

    The average five values for the width and depth of the beam specimen shall be reported to the nearest 0.1mm. If any of the five values for each of the dimensions vary with greater than 1.5mm from the respective average value, the beam shall be not be used.

2. Position the beam in the controlled temperature cabinet and set the apparatus to the desired test temperature. Permit at least four hours for the beam to adjust to the test temperature.
3. Begin the operation by switching the computer ON, followed by the main air supply valve, CDAS and air valve to BFA. End the operation in the reverse sequence.

4. Use the computer software (UTM 21) to record the following test control limits:
    - Description of the operator and the test.
    - Identification (beam label), dimensions and properties (beam condition) of the beam.
    - Mode of loading (sine).
    - Frequency of loading (pulse).
    - Peak tensile strain.
    - Termination criteria (highest allowable amount of loading cycles and termination stiffness).
5. Place the loading frame cradle in the centre of its stroke using jog up/down control. This is reached when the level on Channel B is nearly zero.
6. Insert the provided location draw-bars to fix the pivot points to the right spacing.
7. Place the beam in the loading frame cradle so that the overhang is equal at either end of the frame. Be careful not to push against the on-specimen LVDT during insertion of the beam. Check/adjust the levels of the transducer. Close the side clamps (end plastic clamps) that will keep the specimen in position at the end.
8. Lower the inner and outer clamps at the four points to keep the specimen in position. Leave these clamps in lower position throughout the test.
9. Withdraw the location draw-bars.
10. Regulate the on-specimen displacement transducer to the centre of its stroke.

11. Permit at least 30 to 40 minutes to assist the relieving of the clamping stresses of the specimen before the start of the test and also for the gaining of temperature equilibrium (outer/skin). Once again make sure that the transducer level is near zero and alter it, if necessary.
12. Fasten the lock nut of the on-specimen transducer.
13. Confirm that the temperature of the core of the dummy specimen is at the desired temperature within the required tolerance before the test can be started.

Operation of the Test:

1. Start (RUN) the test.
2. Verify the termination conditions at the 50th loading cycle, whilst the test is running. The data acquisition software (CDAS) calculates the flexural stiffness at this loading cycle and records this value as the *Initial Flexural Stiffness*. Also confirm that the selected peak tensile strain level is obtained at this loading cycle.
3. After the first 50 loading cycles, record the required termination conditions. To ensure the achievement of the failure conditions approximately 40% of the stiffness of the initial stiffness of CDAS should be recorded. The quantity of loading cycles should be overly high, say 5million depending on the desired strain level. The test will run until the termination stiffness is reached or the quantity of loading cycles has been applied.
4. At the end of the application of loading cycles, remove the beam from the frame cradle.
5. Convert the test file to an ASCII file and store both files in the hard drive of the computer or on an external hard drive.

Appendix 7 B: Sample Information

Table 7-1: Samples Extracted from Western Cape Province

No.	Road No.	Material Description	Age	Nearest Location	km Position	GPS X	GPS Y
Western Cape Province							
1	DR1123	13mm + 7mm Double Seal	17	Klipheuwel	23.4	S33°41' 8.7"	E18°32'32.3"
2	DR1398	13mm + 7mm Double Seal	22	Rawsonville	2	S33°40'52.3"	E19°17'32.9"
3	DR1398	13mm + 7mm Double Seal	5	Rawsonville	22.25	S33°32'41.3"	E19°12'21,5"
4	DR2175	13mm + 7mm Double Seal	6	Kardoesie – Piekenierskloof	3	S32°36'12.2"	E18°56'04.2"
5	DR2175	13mm + 7mm Double Seal	3	Kardoesie – Piekenierskloof	6	S32°34'46.2"	E18°55'17.8"
6	MR269	13mm + 7mm Double Seal	13	Hemel en Aarde-Hermanus	3	S34°23'12.5"	E19°15'11.0"
7	DR1398	19mm Cape Seal	23	Slanghoek	1	S33°41'04.3"	E19°18'06.6"
8	MR23	19mm Cape Seal	4	Wellington -Gouda	17	S33°29'49.5"	E18°57'49.2"
9	MR174	19mm Cape Seal	10	Malmesbury	9	S33°30'35.7"	E18°44'04.8"
10	MR188	19mm Cape Seal	15	Durbanville	23.5	S33°43'26.8"	E18°41'47.7"
11	DR1298	13,2mm Cape Seal	4	Genadendal	22	S34°03'00.2"	E19°31'09.9"
12	TR2701	19mm Cape Seal	23	Arabella	5	S34°19'27.7	E19°06'04.1"
13	DR1452	13mm Single Seal	12	Kersieplaas Lakenvlei	14.1	S33°20'14.6"	E19°33'02.5"
14	DR1681	13mm Single Seal	11	Calitsdorp	5	S33°39'10.8"	E21°46'01.3"
15	DR2216	13mm Single Seal	10	Vredendal-Strandfontein	1	S31°36'56.8"	E18°15'31.4"
16	MR536	9mm Single Seal	19	Eendekuilpad-Kruiwepad	4.3	S32°41'45.6"	E18°52'54.6"

Table 7-2: Samples Extracted from Eastern Cape Province

No.	Road No.	Material Description	Age	Nearest Location	km Position	GPS X	GPS Y
				Eastern Cape Province			
1	N6/4	19mm+6mm+6mm Multiple Seal	9	Queenstown	8	S31°53'01.1"	E26°47'42.8"
2	N6/4	19mm+6mm Double Seal	5	Sterkstroom - Aliwal Noord	87.4	S31°16'13.6"	E26°44'02.7"
3	N10/3	19mm+6mm+6mm Multiple Seal	23	DaggaBoer	32.6	S32°31'32.2"	E25°50'10.0"
4	N10/2	19mm+6mm+6mm Multiple Seal	6	Golden Valley	11	S32°51'41.0"	E25°47'31.8"
5	R61/5	19mm Cape Seal	4	Queenstown	3	S32°00'20.3"	E27°01'50.3"
6	N6/5	19mm Cape Seal	12	Aliwal Noord	53.4	S30°43'03.9"	E26°42'29.3"
7	N6/5	19mm Cape Seal	10	Aliwal Noord 2	46	S30°46'11.9"	E26°44'54.8"
8	N10/3	19mm Cape Seal	4	Cradock	69.2	S32°13'29.7"	E25°43'06.4"
9	N10/3	19mm Cape Seal	8	Cradock-Cookhouse	18.2	S32°37'13.6"	E25°53'33.9"

Table 7-3: Samples Extracted from Northern Cape Province

No.	Road No.	Material Description	Age	Nearest Location	km Position	GPS X	GPS Y
				Northern Cape Province			
1	N8/8	19mm+9mm Double Seal	6	Kimberley	5.6	S28°48'34.0"	E24°48'38.4"

Table 7-4: Samples Extracted from Limpopo Province

No.	Road No.	Material Description	Age	Nearest Location	km Position	GPS X	GPS Y
				Limpopo Province			
1	N1/29	19mm+6mm+6mm Multiple Seal	5	Beitbridge	102.6	S22°16'8.64"	E29°59'46.13"
2	N1/29	19mm+6mm+6mm Multiple Seal	9	Musina	79.8	S22°26'38.4"	E30°00'00.8"

175

Table 7-5: Samples Extracted from KwaZulu-Natal Province

No.	Road No.	Material Description	Age	Nearest Location	km Position	GPS X	GPS Y
KwaZulu-Natal Province							
1	N2/32	13mm + 7mm Double Seal	1	Mbekakanye	37	S27°21'44.6"	E31°31'11.6"
2	N2/32	13mm + 7mm Double Seal	5	Pongola	21	S27°21'20.7"	E31°40'22.4"
3	R63	13mm + 7mm Double Seal	7	Pongola Nature Reserve	6	S27°20'03.5"	E31°51'21.7"
4	N2/31	13mm + 7mm Double Seal	6	Pongola Dam 2	41.2	S27°31'45.0"	E31°58'09.6"
5	N2/31	13mm + 7mm Double Seal	11	St Lucia	3.6 North Bound	S27°50'32.38"	E32°12'26.68"
6	N2/31	13mm + 7mm Double Seal	11	St Lucia	3.6 South Bound	S27°50'32.38"	E32°12'26.68"
7	N2/31	19mm+6mm+6mm Multiple Seal	6	Pongola dam 1	59.6	S27°24'31.8"	E31°51'03.6"

Appendix 7 C: Traffic History of Sampled Locations

The South African Road Network is administered by various entities.

Western Cape Province

The road infrastructure in the Western Cape, excluding the urban areas and the national roads, is owned and managed by the Roads Infrastructure Branch of the Provincial Administration of the Western Cape. The road network is categorized into:

- Trunk roads
- Main roads
- Divisional roads
- Minor roads.

The road network currently consists of approximately 33 000 kilometres of Trunk, Main, Divisional and Minor roads of which 6 700 km are surfaced. Approximately 10 300 km of the unsurfaced road network are proclaimed as Trunk, Main and Divisional roads and are commonly referred to as gravel roads. The remaining 16 000 km of unsurfaced roads could be described as earth roads and tracks.

The following traffic history was obtained from the Road Network Information System (RNIS) that is administered by the Western Cape Provincial Administration:

Table 7-6: Traffic History for Sampled Locations in the Western Cape Province (RNIS)

No.	Road Name & Stakevalue	Type of Seal	Nearest Location	Traffic History (Construction Till 2011)						
				Age	Light Vehicles	Taxis	Buses	Heavy Vehicles	Total Heavies	AADT
Western Cape Province										
1	DR1123_km 23.400	13mm + 7mm Double Seal	Klipheuwel	17	354	2	5	129	134	490
2	DR1398_ km 2.000	13mm + 7mm Double Seal	Rawsonville	22	1563	37	19	160	179	1779
3	DR1398_km 22.300	13mm + 7mm Double Seal	Worcester	5	505	9	8	49	57	571
4	DR2175_km 3.000	13mm + 7mm Double Seal	Citrusdal Area	6	195	2	5	56	61	258
5	DR2175_km 6.000	13mm + 7mm Double Seal	Citrusdal Area	3	195	2	5	56	61	258
6	MR269_km 3.000	13mm + 7mm Double Seal	Hermanus	13	2056	20	10	150	160	2236
7	DR1398_km 1.000	19mm Cape Seal	Rawsonville	23	2557	57	30	281	311	2925
8	MR23_km 17.000	19mm Cape Seal	Wellington	4	3596	37	24	1052	1076	4709

Table 7-7: Continuation of Traffic History for Sampled Locations in the Western Cape Province (RNIS)

No.	Road Name & Stakevalue	Type of Seal	Nearest Location	Traffic History (Construction Till 2011)						
				Age	Light Vehicles	Taxis	Buses	Heavy Vehicles	Total Heavies	AADT
			Western Cape Province							
9	MR174_ km 9.000	19mm Cape Seal	Malmesbury	10	4338	67	21	768	789	5194
10	MR188_ km 23.500	19mm Cape Seal	Klipheuwel	15	2910	68	24	822	846	3824
11	DR1298_ km 22.000	13,2mm Cape Seal	Genadendal	4	250	3	18	32	50	303
12	TR2701_ km 5.000	19mm Cape Seal	Kleinmond	23	3623	43	21	297	318	3984
13	DR1452_ km 14.100	13mm Single Seal	Ceres	12	173	1	1	33	34	208
14	DR1681_ km 5.000	13mm Single Seal	Calitsdorp	11	156	3	0	9	9	168
15	DR2216_ km 1.000	13mm Single Seal	Lutzville	10	264	14	8	9	17	295
16	MR536_ km 4.300	9mm Single Seal	Eendekuil	19	311	6	7	104	111	428

Eastern Cape Province

The road infrastructure in the Eastern Cape Province is owned and managed by the South African National Roads Agency (SANRAL). The following traffic history was obtained from SANRAL's 2011 yearbook:

Table 7-8: Traffic History for Sampled Locations in the Eastern Cape Province (Source: SANRAL):

No.	Road Name & Stakevalue	Type of Seal	Nearest Location	Traffic History (Construction Till 2011)			
				Age	Light Vehicles	Heavy Vehicles	AADT
	Eastern Cape Province						
1	N6/4_km 8.000	19mm+6mm+6mm Multiple Seal	Queenstown	9	1836	420	2256
2	N6/4_km 87.400	19mm+6mm Double Seal	Jamestown	5	1836	420	2256
3	N10/3_km 32.600	19mm+6mm+6mm Multiple Seal	Cradock	23	995	579	1574
4	N10/2_km 11.000	19mm+6mm+6mm Multiple Seal	Cookhouse	6	1709	583	2292
5	R61/5_km 3.000	19mm Cape Seal	Queenstown	4	2313	252	2565
6	N6/5_km 53.400	19mm Cape Seal	Aliwal Noord	12	1836	420	2256
7	N6/5_km 46.000	19mm Cape Seal	Aliwal Noord 2	10	1836	420	2256
8	N10/3_km 69.200	19mm Cape Seal	Cradock	4	995	579	1574
9	N10/3_km 18.200	19mm Cape Seal	Cookhouse	8	995	579	1574

Northern Cape Province

The road infrastructure in the Northern Cape Province is owned and managed by the South African National Roads Agency (SANRAL). The following traffic history was obtained from SANRAL's 2011 yearbook:

Table 7-9: Traffic History for Sampled Locations in the Northern Cape Province (Source: SANRAL):

No.	Road Name & Stakevalue	Type of Seal	Nearest Location	Traffic History (Construction Till 2011)			
				Age	Light Vehicles	Heavy Vehicles	AADT
			Northern Cape Province				
1	N8/8_ km 5.600	19mm+9mm Double Seal	Kimberley	6	1951	467	2418

Limpopo Province

The road infrastructure in the Limpopo Province is owned and managed by the South African National Roads Agency (SANRAL). The following traffic history was obtained from SANRAL's 2011 yearbook:

Table 7-10: Traffic History for Sampled Locations in the Limpopo Province (Source: SANRAL):

No.	Road Name & Stakevalue	Type of Seal	Nearest Location	Traffic History (Construction Till 2011)			
				Age	Light Vehicles	Heavy Vehicles	AADT
			Limpopo Province				
1	N1/29_km 102.600	19mm+6mm+6mm Multiple Seal	Beitbridge	5	4225	1216	5441
2	N1/29_km 79.800	19mm+6mm+6mm Multiple Seal	Musina	9	2372	1103	3475

KwaZulu-Natal Province

The road infrastructure in the KwaZulu-Natal Province is owned and managed by the South African National Roads Agency (SANRAL). The following traffic history was obtained from SANRAL's 2011 yearbook:

Table 7-11: Traffic History for Sampled Locations in the Northern Cape Province (Source: SANRAL):

No.	Road Name & Stakevalue	Type of Seal	Nearest Location	Traffic History (Construction Till 2011)			
				Age	Light Vehicles	Heavy Vehicles	AADT
			KwaZulu-Natal Province				
1	N2/32_km 37.000	13mm + 7mm Double Seal	Pongola/ Mkuze	1	2741	1112	3853
2	N2/32_km 21.000	13mm + 7mm Double Seal	Pongola/ Mkuze	5	2741	1112	3853
3	R63_km 6.000	13mm + 7mm Double Seal	Pongola/ Mkuze	7	200	30	230
4	N2/31_km 41.200	13mm + 7mm Double Seal	Pongola/ Mkuze	6	2741	1112	3853
5	N2/31_km 3.600 N/B*	13mm + 7mm Double Seal	Pongola/ Mkuze	11	2741	1112	3853
6	N2/31_km 3.600 S/B*	13mm + 7mm Double Seal	Pongola/ Mkuze	11	2741	1112	3853
7	N2/31_km 59.600	19mm+6mm+6mm Multiple Seal	Pongola/ Mkuze	6	2741	1112	3853

Appendix 7 D: Binder Recovery Analysis

Table 7-12: Binder Properties of Sampled Seals from Western Cape Province

No.	Road Name & Stakevalue	Type of Seal	Age	Sampled Transverse Position	CSIR Reference	Binder Content (%)	Penetration (dmm)	Softening Point	Ash Content* (%)	Penetration Index (Shell Nomograph SP/Pen)
1	DR1123_ km 23.400	13mm + 7mm Double Seal	17	IWT	IWT	7.3	14	68.2	0.7	-0.25
2	DR1398_ km 2.000	13mm + 7mm Double Seal	22	OWT	SHDR	5	12	71	0.5	0
				IWT	OWT	5.1	14	68.8	0.9	-0.24
3	DR1398_ km 22.300	13mm + 7mm Double Seal	5	OWT	BWT	4.8	23	60.8	0.6	-0.55
				IWT	IWT	5.1	25	59.8	0.8	-0.5
4	DR2175_km 3.000	13mm + 7mm Double Seal	6	OWT	BWT	5.5	21	62.6	1	-0.6
				IWT	IWT	5.2	20	62.8	1.3	-0.65
5	DR2175_km 6.000	13mm + 7mm Double Seal	3	OWT	BWT	2	24*	65.8	1	0.2
				IWT	OWT	2.9	23*	61.2	0.6	-0.2
6	MR269_km 3.000	13mm + 7mm Double Seal	13	OWT	SHDR	7.3	19	64	0.3	-0.4
				IWT	OWT	6.1	20	64.8	0.3	-0.2
7	DR1398_km 1.000	19mm Cape Seal	23	OWT	OWT	4.4	13	69	1.8	-0.2
				IWT	SHDR	4.4	11	73.4	1.4	0
8	MR23_km 17.000	19mm Cape Seal	4	OWT	SHDR	3.6	14	66.8	0.9	-0.4
				IWT	OWT	4.2	20	61.6	0.9	-0.6

Note: *Assumed value from penetration pattern/trend of similar aged seals

Table 7-13: Continuation of Binder Properties of Sampled Seals from Western Cape Province

No.	Road Name & Stakevalue	Type of Seal	Age	Sampled Transverse Position	CSIR Reference	Binder Content (%)	Penetration (dmm)	Softening Point	Ash Content* (%)	Penetration Index (Shell Nomograph SP/Pen)
9	MR174_km 9.000	19mm Cape Seal	10	OWT	SHDR	4.8	22	62.4	1.1	-0.5
				IWT	OWT	5.1	24	61.2	0.9	-0.5
10	MR188_km 23.500	19mm Cape Seal	15	OWT	SHDR	5.9	10	71.8	0.9	-0.1
				IWT	OWT	6.5	16	67.4	0.9	-0.1
11	DR1298_km 22.000	13,2mm Cape Seal	4	OWT	SHDR	6.7	25	59.2	0.8	-0.7
				IWT	OWT	6.9	26	58.4	0.8	-0.8
12	TR2701_km 5.000	19mm Cape Seal	23	OWT	SHDR	6.1	28	57.6	0.9	-0.8
				IWT	OWT	6	26	58.2	1.1	-1
13	DR1452_km 14.100	13mm Single Seal	12	OWT	BWT	6.7	13	72.2	0.6	0.3
				IWT	OWT	6.4	12	72.6	0.5	0.2
14	DR1681_km 5.000	13mm Single Seal	11	OWT	BWT	8.55	16*	73.8	0.6	0.5
				IWT	OWT	4.8	14*	76.4	0.9	0.8
15	DR2216_km 1.000	13mm Single Seal	10	OWT	BWT	7	20	69.8	0.6	0.5
				IWT	IWT	7.2	19	71.2	0.5	0.8
16	MR536_km 4.300	9mm Single Seal	19	OWT	BWT	5.1	13	73.8	0.6	0.4
				IWT	IWT	5.7	14	72.4	0.4	0.4

Note: *Assumed value from penetration pattern/trend of similar aged seals

184

Table 7-14: Binder Properties of Sampled Seals from Eastern Cape Province

No.	Road Name & Stakevalue	Type of Seal	Age	Sampled Transverse Position	CSIR Reference	Binder Content (%)	Penetration (dmm)	Softening Point	Ash Content* (%)	Penetration Index (Shell Nomograph SP/Pen)
1	N6/4_km 8.000	19mm+6mm+6mm Multiple Seal	9	OWT	SHDR	3.8	18*	62.2	0.3	-0.8
				IWT	OWT	2.5	15*	68.4	0.7	-0.2
2	N6/4_km 87.400	19mm+6mm Double Seal	5	OWT	SHDR	10.8	16*	65.6	0.7	-0.4
				IWT	OWT	8.7	15*	66.8	0.8	-0.5
3	N10/3_km 32.600	19mm+6mm+6mm Multiple Seal	23	OWT	Shoulder	4.4	10	73	0.8	0
				IWT	OWT	4	8	75.6	1.2	0.1
4	N10/2_km 11.000	19mm+6mm+6mm Multiple Seal	6	OWT	SHDR	3.8	17*	64.4	0.4	-0.5
				IWT	OWT	4	16*	64.6	0.5	-0.4
5	R61/5_km 3.000	19mm Cape Seal	4	OWT	SHDR	4.5	21	60.8	0.3	-0.6
				IWT	OWT	4.5	21	60.4	0.6	-0.6
6	N6/5_km 53.400	19mm Cape Seal	12	OWT	SHDR	3.9	16	65.4	1.1	-0.4
				IWT	OWT	4.1	18	64	2.6	-0.5
7	N6/5_km 46.000	19mm Cape Seal	10	OWT	SHDR	4.4	17	65.4	0.8	-0.5
				IWT	OWT	4.3	22	61.8	1.4	-0.5
8	N10/3_km 69.200	19mm Cape Seal	4	OWT	SHDR	4.4	16	68	1.4	0
				IWT	OWT	5.2	14	69.2	1.2	-0.3
9	N10/3_km 18.200	19mm Cape Seal	8	OWT	BWT	4	20	63.4	1.3	-0.5
				IWT	OWT	3.7	20	63.2	2	-0.6

Note: *Assumed value from penetration pattern/trend of similar aged seals

Table 7-15: Binder Properties of Sampled Seals from Northern Cape Province

No.	Road Name & Stakevalue	Type of Seal	Age	Sampled Transverse Position	CSIR Reference	Binder Content (%)	Penetration (dmm)	Softening Point	Ash Content* (%)	Penetration Index (Shell Nomograph SP/Pen)	Bitumen Stiffness
				Northern Cape Province							
1	N8/8_km 5.6	19mm+9mm Double Seal	6	OWT	SHDR	4.6	16*	65	1.6	-0.5	107
				IWT	OWT	5.3	18*	64.4	0.6	-0.4	120

Note: *Assumed value from penetration pattern/trend of similar aged seals

Table 7-16: Binder Properties of Sampled Seals from Limpopo Province

No.	Road Name & Stakevalue	Type of Seal	Age	Sampled Transverse Position	CSIR Reference	Binder Content (%)	Penetration (dmm)	Softening Point	Ash Content* (%)	Penetration Index (Shell Nomograph SP/Pen)
1	N1/29_km 102.6	19mm+6mm+6mm Multiple Seal	5	OWT	SHDR	4.2	8*	86	0.8	1.9
				IWT	OWT	3.2	9*	79.8	0.4	0.6
2	N1/29_km 79.8	19mm+6mm+6mm Multiple Seal	9	OWT	SHDR	6.15	16*	64.2	0.3	-0.6
				IWT	OWT	4.6	14*	68.5	0.4	-0.4

Note: *Assumed value from penetration pattern/trend of similar aged seals

Table 7-17: Binder Properties of Sampled Seals from KwaZulu-Natal Province

No.	Road Name & Stakevalue	Type of Seal	Age	Sampled Transverse Position	CSIR Reference	Binder Content (%)	Penetration (dmm)	Softening Point	Ash Content* (%)	Penetration Index (Shell Nomograph SP/Pen)
1	N2/32_km 37	13mm + 7mm Double Seal	1	OWT	SHDR	5.7	28*	56.4	0.6	-1.3
				IWT	OWT	6.9	30*	55.4	0.6	-1.1
2	N2/32_km 21	13mm + 7mm Double Seal	5	OWT	SHDR	6.5	16*	66.8	0.6	-0.3
				IWT	OWT	6.6	18*	63.4	0.6	-0.7
3	R63_km 6	13mm + 7mm Double Seal	7	OWT	BWT	4.8	8	78.4	1.1	0.5
				IWT	OWT	4.7	9	78.8	1.6	0.4
4	N2/31_km 41.2	13mm + 7mm Double Seal	6	OWT	SHDR	3.7	10*	74	1.7	0.2
				IWT	OWT	5.05	14*	68.6	1	-0.3
5	N2/31_km 3.6 North Bound	13mm + 7mm Double Seal	11	OWT	SHDR	4.6	12*	70.2	1.4	-0.1
				IWT	OWT	3.7	11*	73	1.96	0.1
6	N2/31_km 3.6 South Bound	13mm + 7mm Double Seal	11	OWT	SHDR	5.4	14*	68.4	1.4	-0.2
				IWT	OWT	4.4	14*	68.6	1.3	-0.1
7	N2/31_km 59.6	19mm+6mm+6mm Multiple Seal	6	OWT	BWT	4.3	18*	63.8	0.8	0.6
				IWT	OWT	3.8	17*	69.4	1.1	0.2

Note: *Assumed value from penetration pattern/trend of similar aged seals

Appendix 7 E: Marvil Permeability Test Results

Table 7-18: Marvil Permeability of Single Seals (Annandale, 2012)

Seal Information	Position in Road	Age	Impermeable	Permeable	
				Horizontal	Vertical
DR2216_13mm _km 1	IWT	10	√		
	OWT		√		
DR1681_13mm _km 5	BWT	11		√	
	OWT				√
DR1452_13mm _km 14.1	BWT	12			√
MR536_13mm _ km 4.3	IWT	19	√		
	BWT		√		

Table 7-19: Marvil Permeability of Double Seals (Annandale, 2012)

Seal Information	Position in Road	Age	Impermeable	Permeable	
				Horizontal	Vertical
N2_32_13+7mm _km 37	SHDR	1			√
DR2175_13+7mm _km 6	BWT	3		√	
	OWT			√	
N2_32_13+7mm _km 21	OWT	5			√
	SHDR				√
N8_8_19+9mm _km 5.6	OWT	6			√
N2_31_13+7mm _km 41.2	OWT	6			√
	SHDR				√

Table 7-20: Marvil Permeability of Cape Seals (Annandale, 2012)

Seal Information	Position in Road	Age	Impermeable	Permeable	
				Horizontal	Vertical
MR23_19mm _km 17	OWT	4		√	
	SHDR			√	√
DR1298_13mm _km 22	OWT	4	√		
	SHDR		√		
MR174_19mm _km 9	OWT	10	√		
	SHDR		√		
DR1398_19mm _km 1	OWT	23			√
	SHDR		√		
TR2701_19mm _km 5	OWT	23			√
	SHDR		√		

Table 7-21: Marvil Permeability of Multiple Seals (Annandale, 2012)

Seal Information	Position in Road	Age	Impermeable	Permeable	
				Horizontal	Vertical
N1_29_19+6+6mm _km 102.6	OWT	5		√	
	SHDR		√		
N6_4_19+6+6mm_ km 87.4	OWT	5			√
	SHDR				√
N2_31_19+6+6mm_ km 59.6	OWT	6		√	
	BWT			√	
N10_2_19+6+6mm_ km 11	OWT	6			√
N1_29_19+6+6mm_ km 79.8	OWT	9		√	
	SHDR			√	
N6_4_19+6+6mm_ km 8	OWT	9			√

Appendix 7 F: Additional Testing During Set-Up

Appendix 7 F1: Warm Mix Asphalt (WMA)

TYPE D_10% Reclaimed Aspahlt_ Control_60-70_Slab 2_480µε
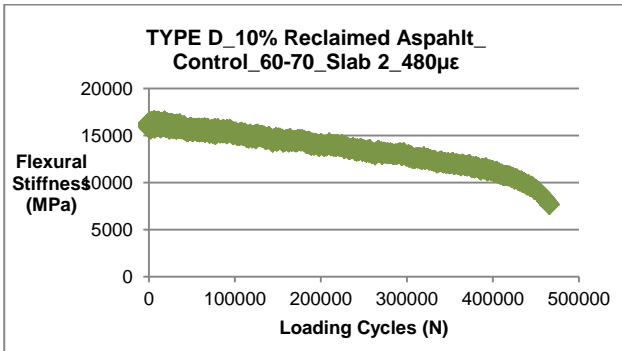
Figure 7-1: Fatigue Testing_50cm_480µε_10°C_10Hz

TYPE D_10% Reclaimed Asphalt_ Control_60-70_Slab 2_600µε
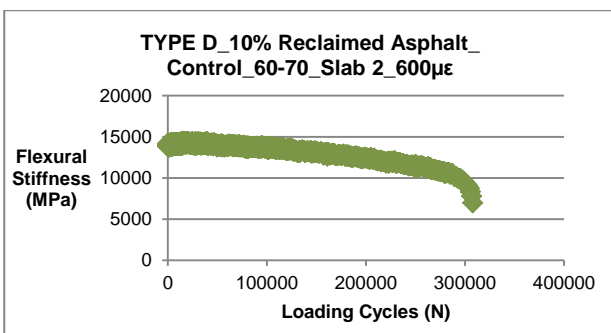
Figure 7-2: Fatigue Testing_50cm_600µε_10°C_10Hz

20cm WMA and 30cm Polyurethane

20cm WMA + 30cm F16_480µε_10°C_10Hz
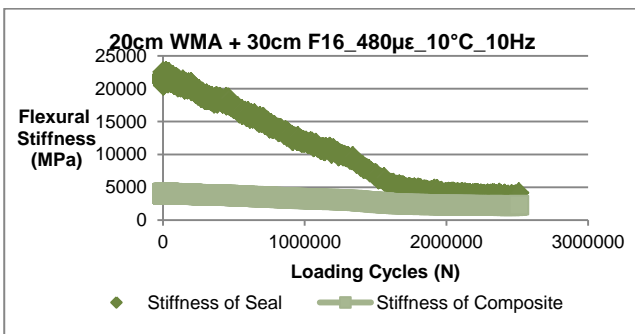
Figure 7-3: Fatigue Testing_20cm WMA + 30cm F16 Polyurethane_480µε_10°C_10Hz

20cm WMA + 30cm F16_600µε_10°C_10Hz
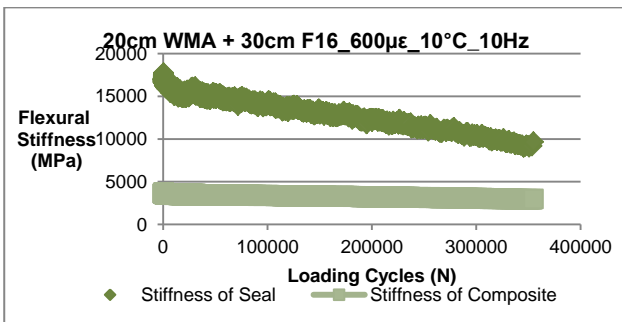
Figure 7-4: Fatigue Testing_20cm WMA + 30cm F16 Polyurethane_600µε_10°C_10Hz

190
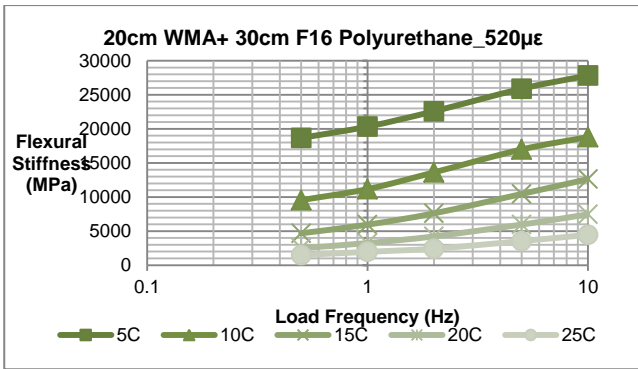
**Figure 7-5: Frequency Sweep Testing_20cm WMA + 30cm F16 Polyurethane_520µε**
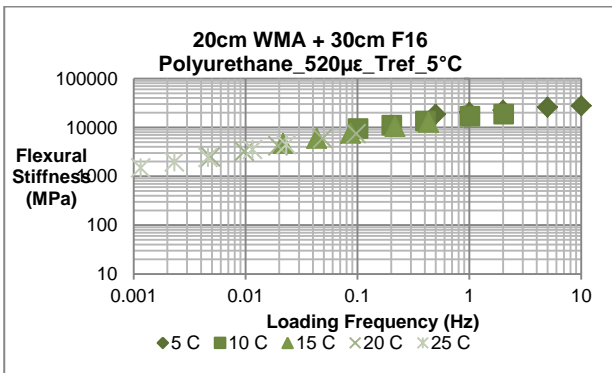
Figure 7-6: Master Curve_20cm WMA + 30cm F16 Polyurethane_520µε_Tref_5°C
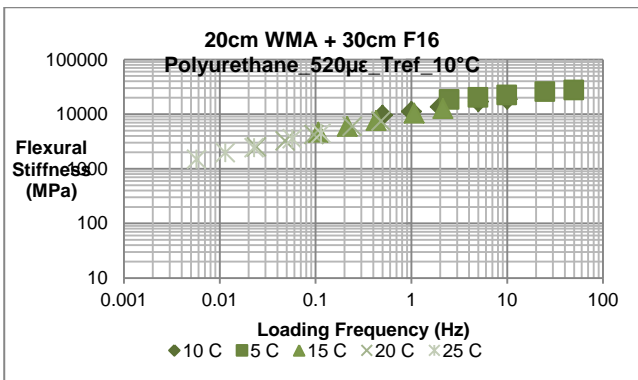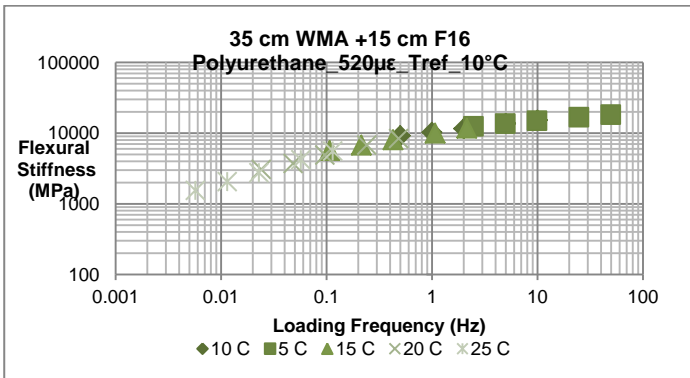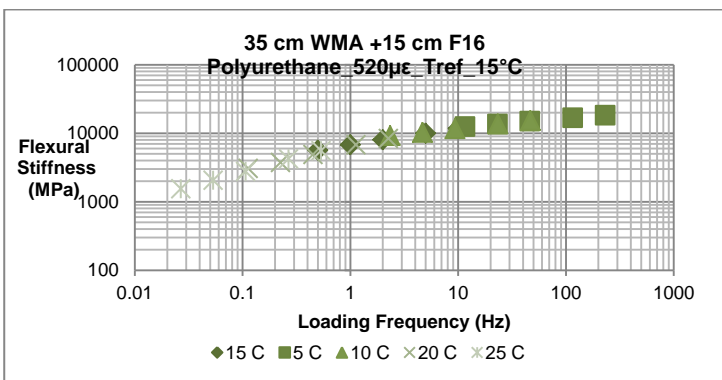

Figure 7-7: Master Curve_20cm WMA + 30cm F16 Polyurethane_520µε_Tref_10°C
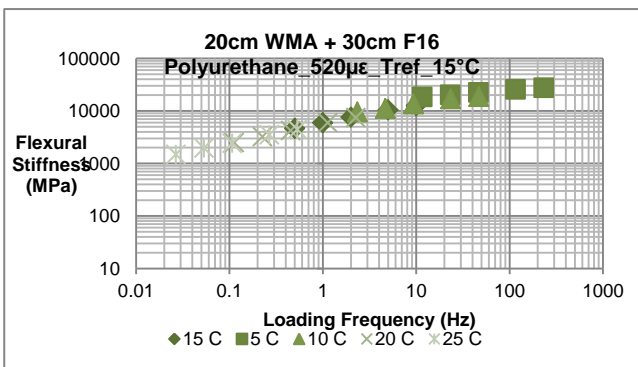
Figure 7-8: Master Curve_20cm WMA + 30cm F16 Polyurethane_520µε_Tref_15°C
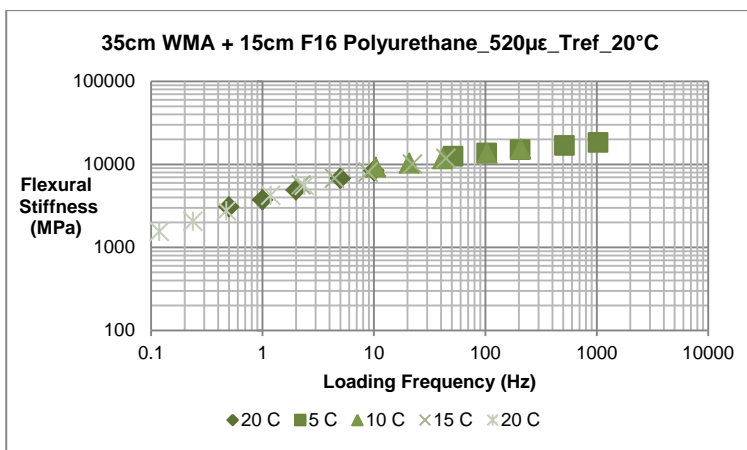
191
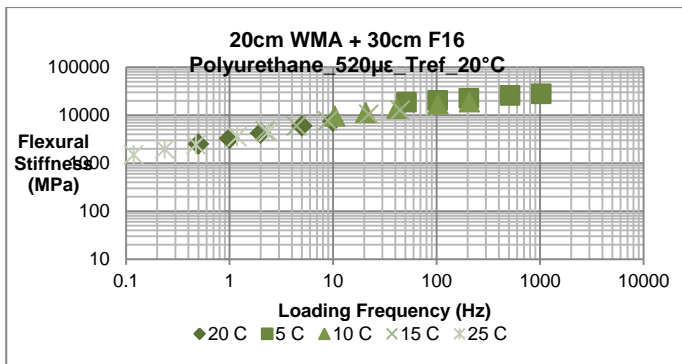
Figure 7-9: Master Curve_20cm WMA + 30cm F16 Polyurethane_520µε_Tref_20°C
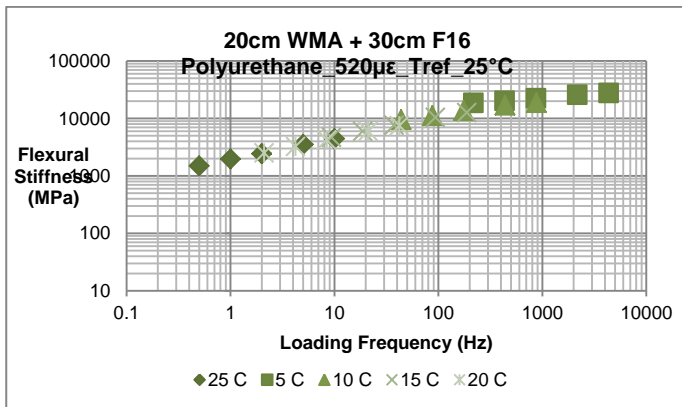
Figure 7-10: Master Curve_20cm WMA + 30cm F16 Polyurethane_520µε_Tref_25°C

35cm WMA + 15cm F16 Polyurethane:
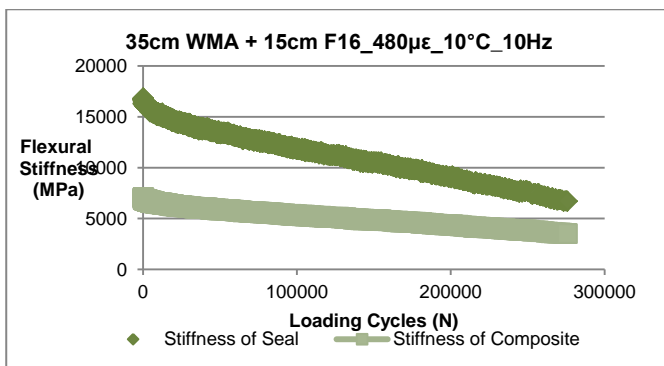
Figure 7-11: Fatigue Testing_20cm WMA + 30cm F16 Polyurethane_480µε_10°C_10Hz
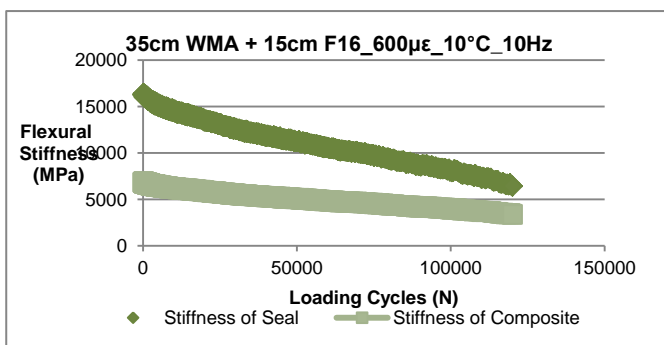
Figure 7-12: Fatigue Testing_20cm WMA + 30cm F16 Polyurethane_600µε_10°C_10Hz

192
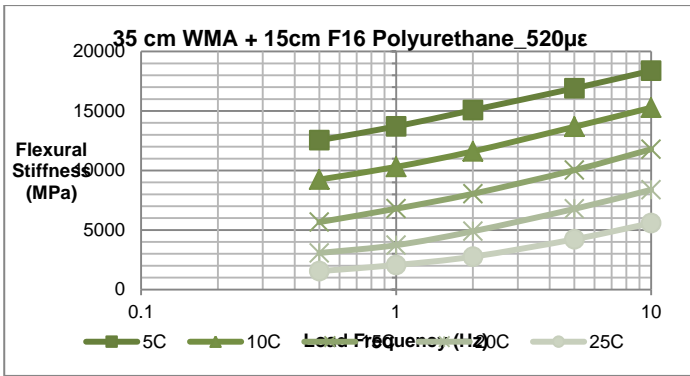
Figure 7-13: Frequency Sweep Testing_35cm WMA + 15cm F16 Polyurethane_520με
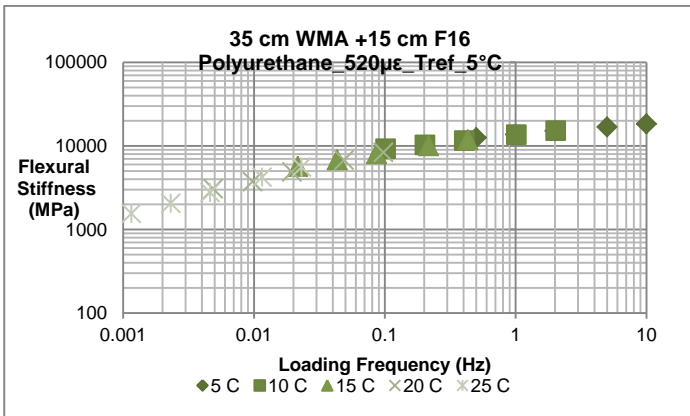
Figure 7-14: Master Curve_35cm WMA + 15cm F16 Polyurethane_520με_Tref_5°C

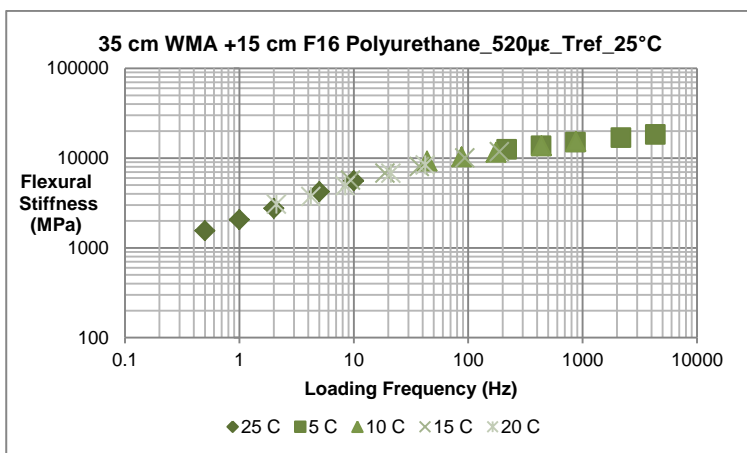**Figure 7-15: Master Curve_35cm WMA + 15cm F16 Polyurethane_520με_Tref_10°C**

Figure 7-16: Master Curve_35cm WMA + 15cm F16 Polyurethane_520με_Tref_15°C

193

Figure 7-17: Master Curve_35cm WMA + 15cm F16 Polyurethane_520µε_Tref_20°C

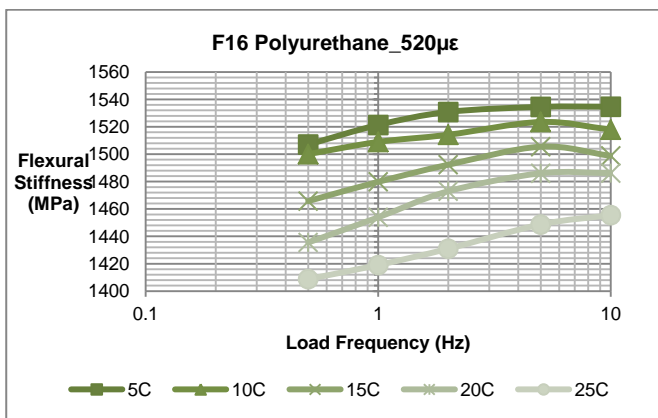**Figure 7-18: Master Curve_35cm WMA + 15cm F16 Polyurethane_520µε_T$_{ref}$_25°C**

Figure 7-19: F16 Polyurethane Isotherms Average 3 Frequency Sweep Tests_520µε
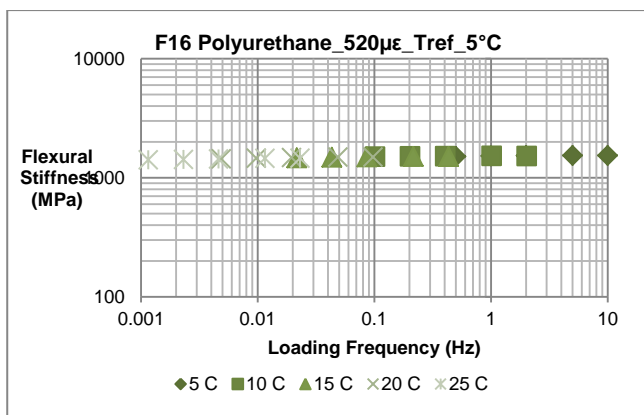
Figure 7-20: F16 Polyurethane Master Curve_520µε_Tref_5°C
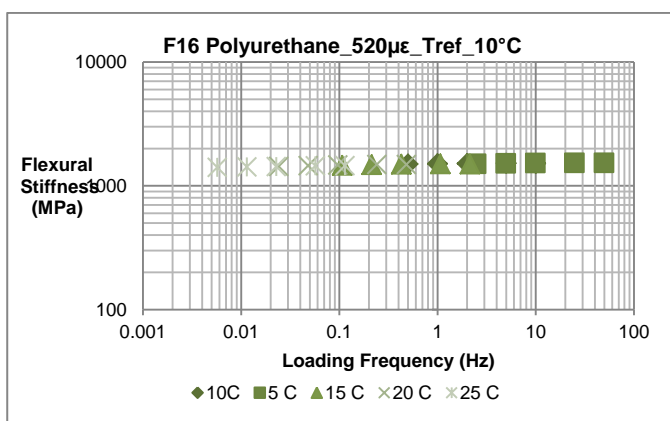

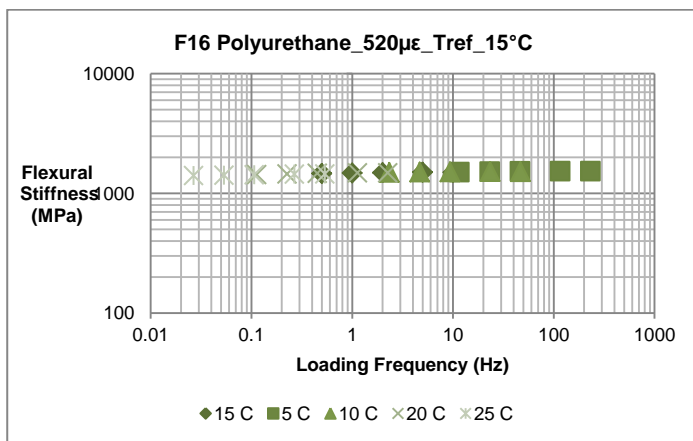**Figure 7-21: F16 Polyurethane Master Curve_520µε_Tref_10°C**

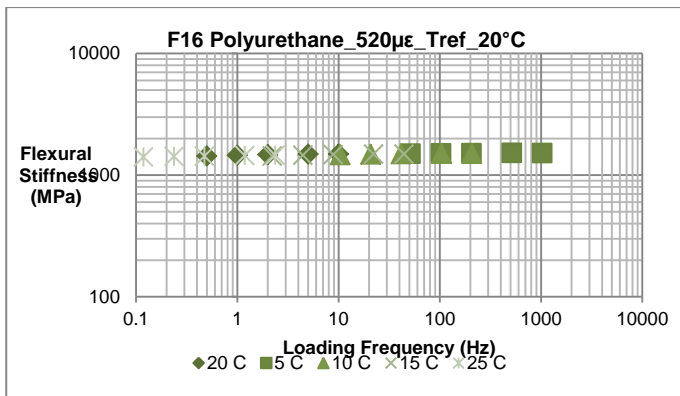**Figure 7-22: F16 Polyurethane Master Curve_520µε_Tref_15°C**

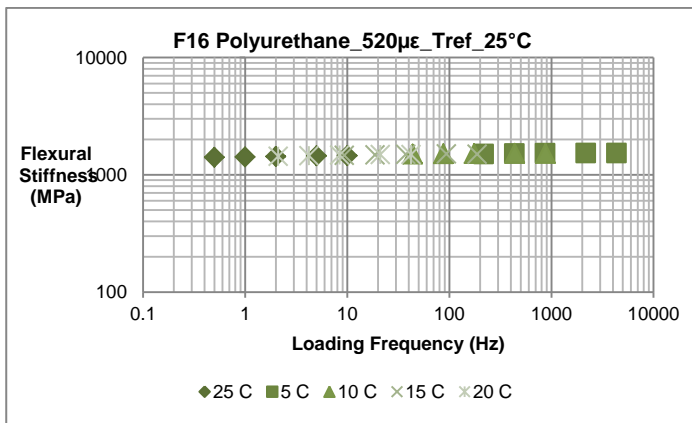**Figure 7-23: F16 Polyurethane Master Curve_520µε_Tref_20°C**

Figure 7-24: F16 Polyurethane Master Curve_520µε_Tref_25°C

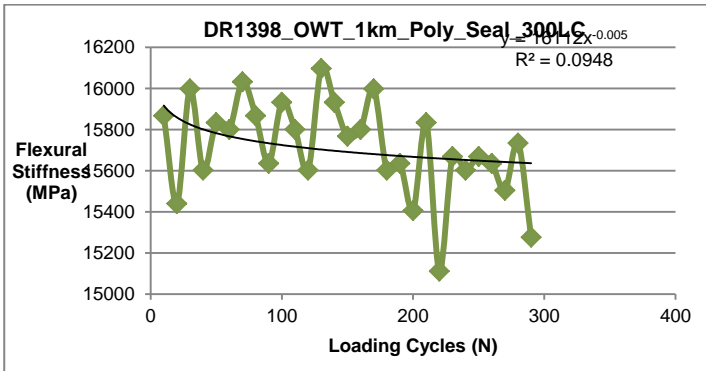## Appendix 7 F2: Upside Down Testing of Beams

Figure 7-25: Initial Stiffness_DR1398_OWT_1km_Poly_Seal_300LC
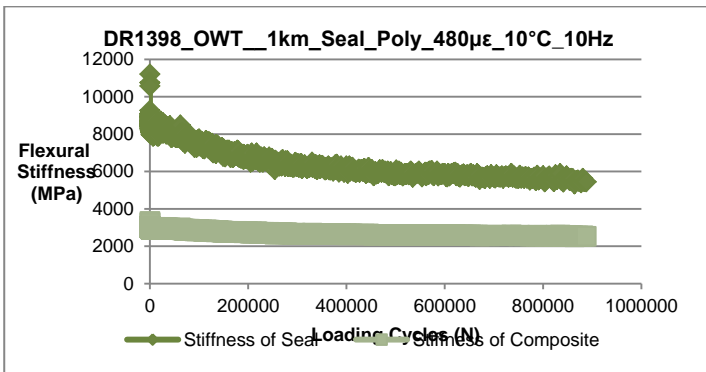
Figure 7-26: Fatigue Testing_DR1398_OWT_1km_Seal_Poly_480με_10°C_10Hz
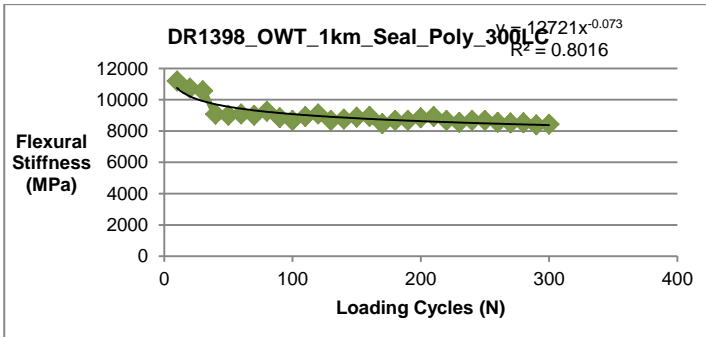
Figure 7-27: Initial Stiffness_DR1398_OWT_1km_Seal_Poly_300LC
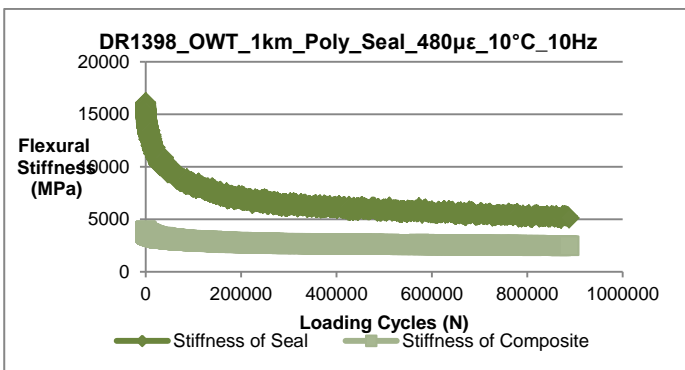
Figure 7-28: Fatigue Testing_DR1398_OWT_1km_Poly_Seal_480με_10°C_10Hz

Appendix G: Graphs of Isotherms and Master Curves from Group 1
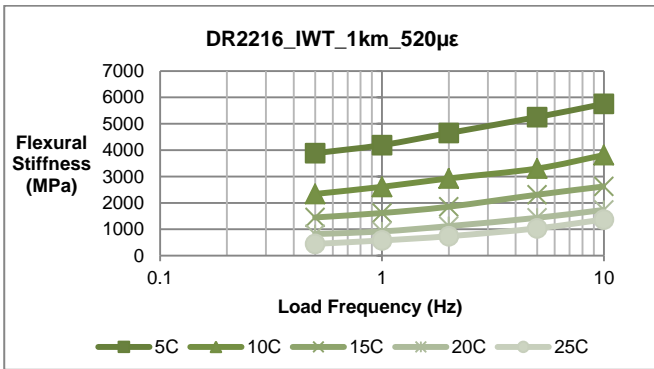
Figure 7-29: Frequency Sweep Testing_DR2216_IWT_1km_520µε
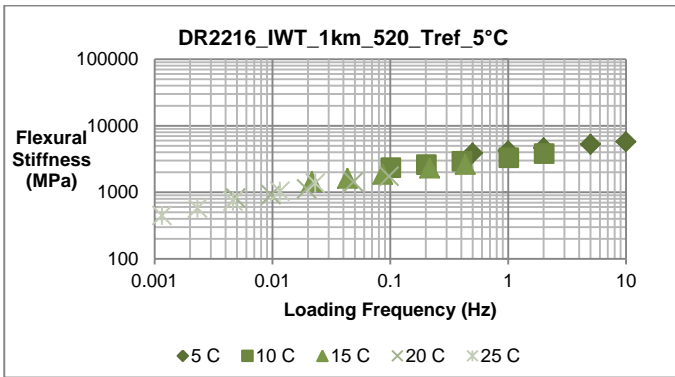
Figure 7-30: Master Curve_DR2216_IWT_1km_520µε_Tref5°C
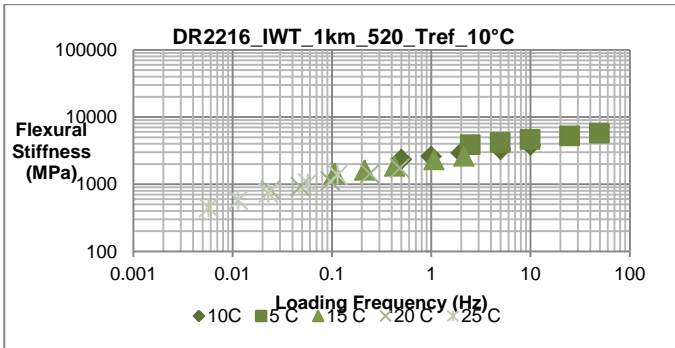
Figure 7-31: Master Curve_DR2216_IWT_1km_520µε_Tref10°C
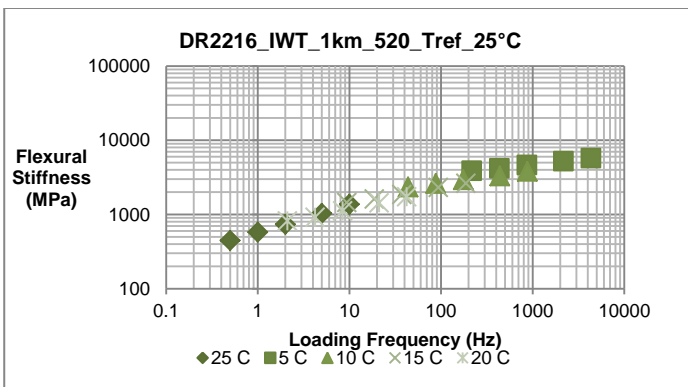
Figure 7-32: Master Curve_DR2216_IWT_1km_520µε_Tref25°C

198
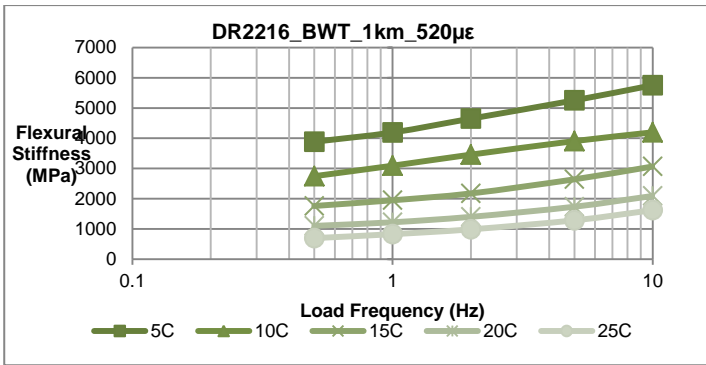
Figure 7-33: Frequency Sweep Testing_DR2216_BWT_1km_520με
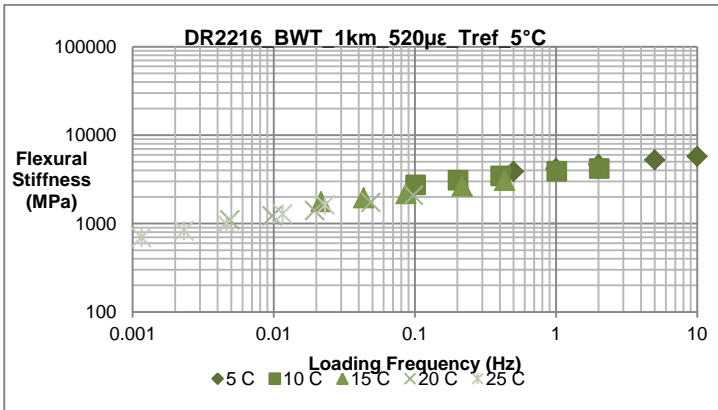
Figure 7-34: Master Curve_DR2216_BWT_1km_520με_Tref5°C
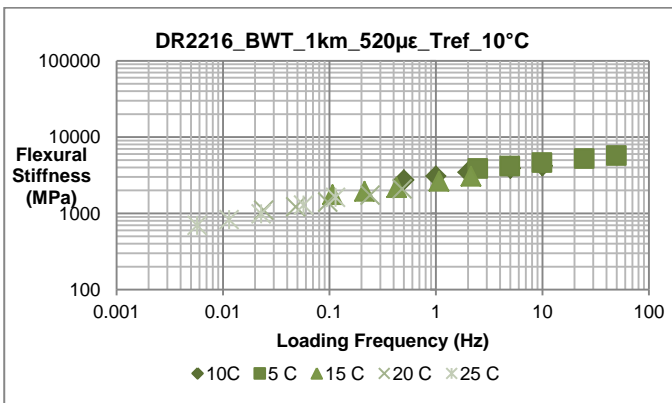
Figure 7-35: Master Curve_DR2216_BWT_1km_520με_Tref10°C
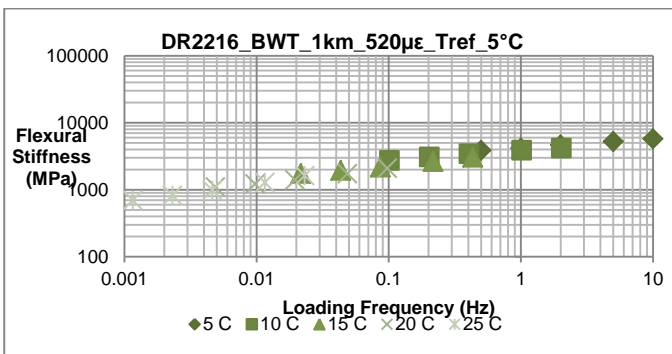
Figure 7-36: Master Curve_DR2216_BWT_1km_520με_Tref5°C

199
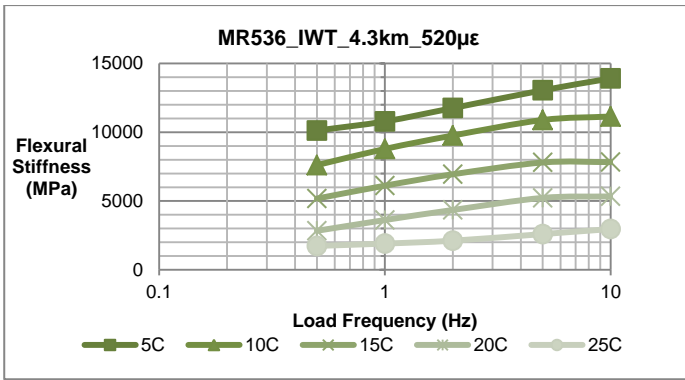
Figure 7-37: Frequency Sweep Testing_MR536_IWT_5.3km_520µε
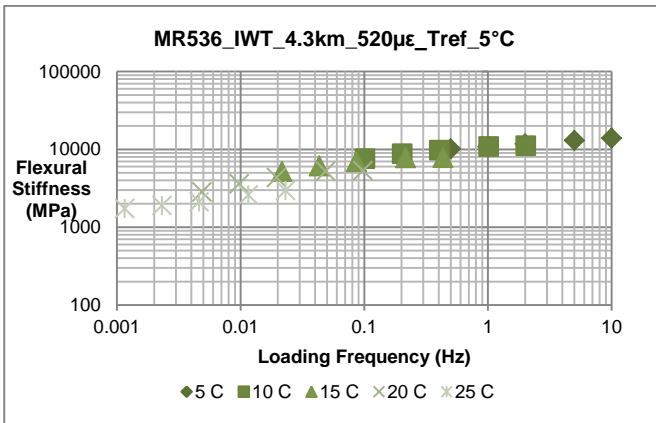
Figure 7-38: Master Curve_MR536_IWT_5.3km_520µε_Tref5°C
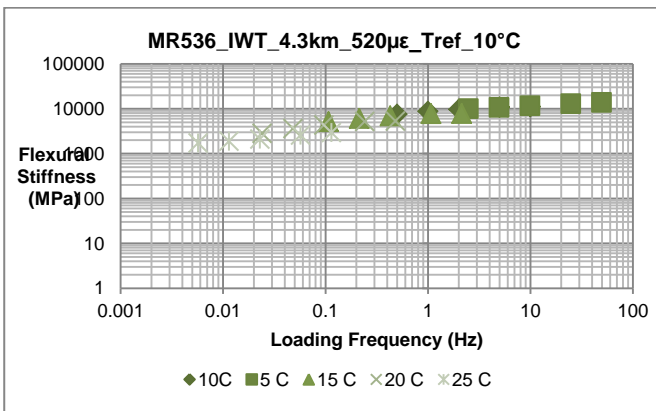
Figure 7-39: Master Curve_MR536_IWT_5.3km_520µε_Tref10°C
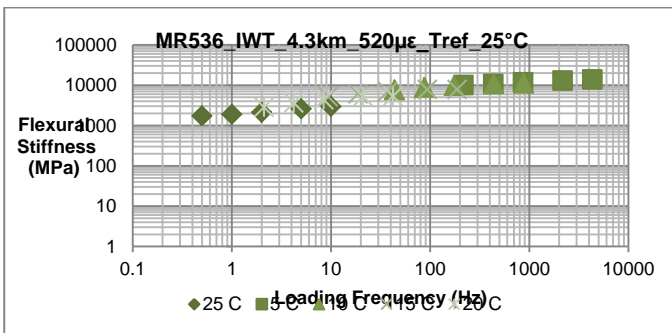
Figure 7-40: Master Curve_MR536_IWT_5.3km_520µε_Tref25°C
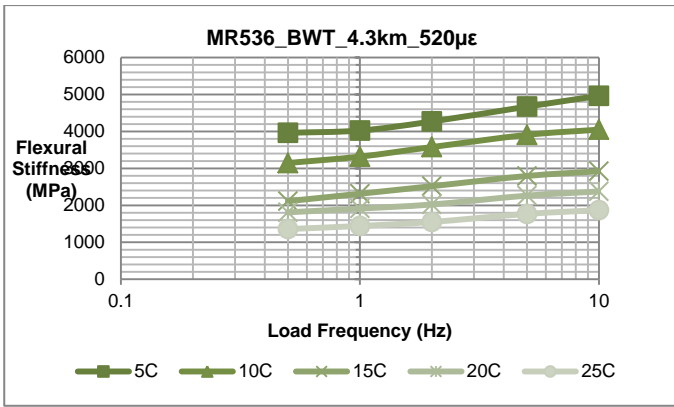
Figure 7-41: Frequency Sweep Testing_MR536_BWT_5.3km_520µε
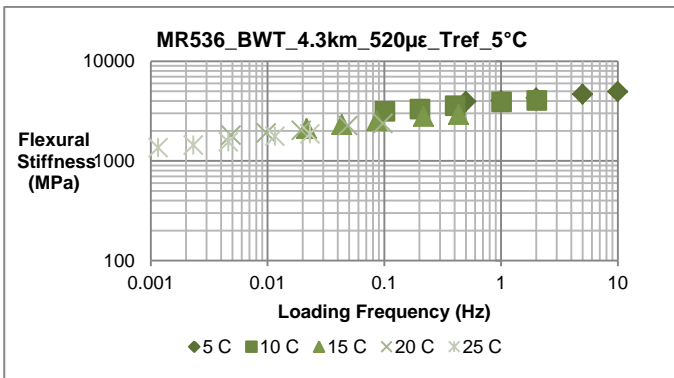
Figure 7-42: Master Curve_MR536_BWT_5.3km_520µε_Tref5°C
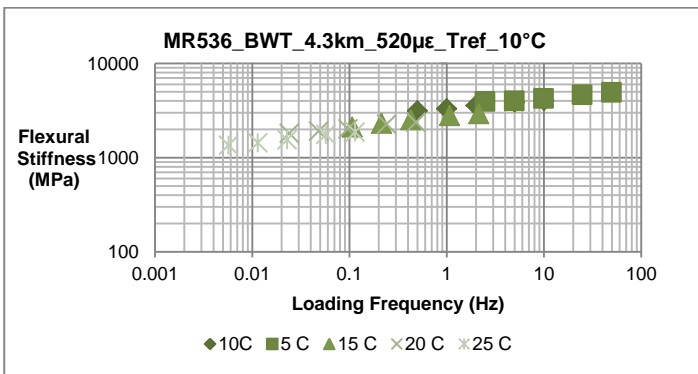
Figure 7-43: Master Curve_MR536_BWT_5.3km_520µε_Tref10°C
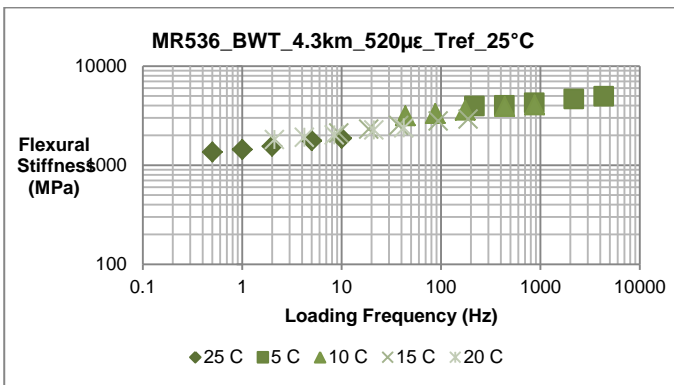
Figure 7-44: Master Curve_MR536_BWT_5.3km_520µε_Tref25°C

Appendix H: Graphs of Isotherms and Master Curves of Group 2
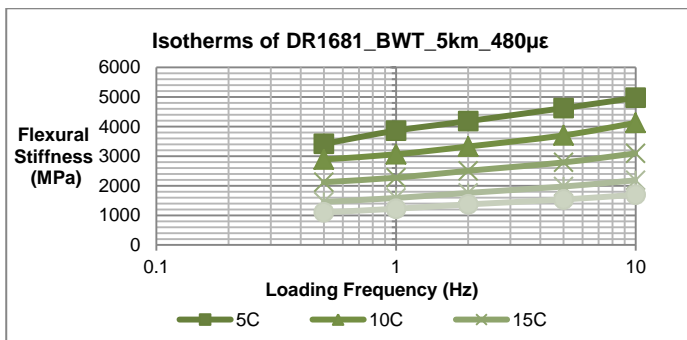
Figure 7-45: Frequency Sweep_DR1681_BWT_5km_480µε
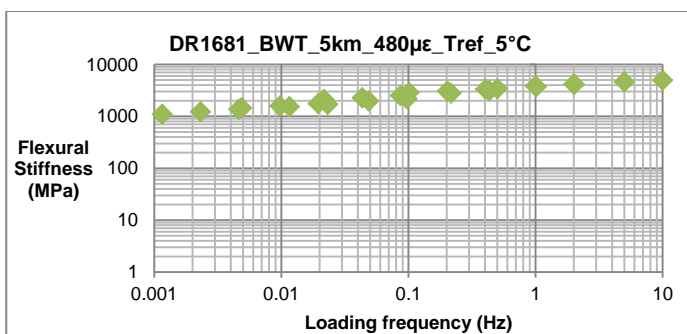
Figure 7-46: Master Curve of DR1681_BWT_5km_480µε_T_{ref}_5°C
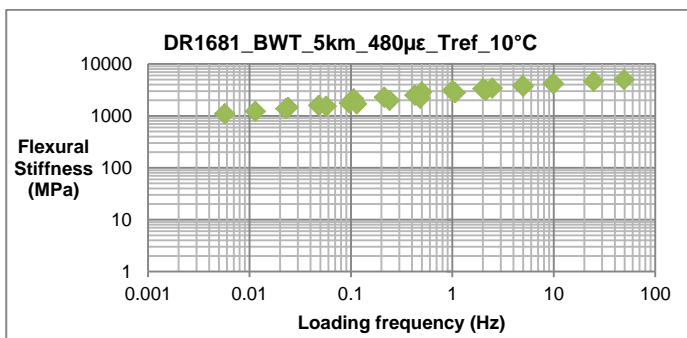
Figure 7-47: Master Curve of DR1681_BWT_5km_480µε_Tref_10°C
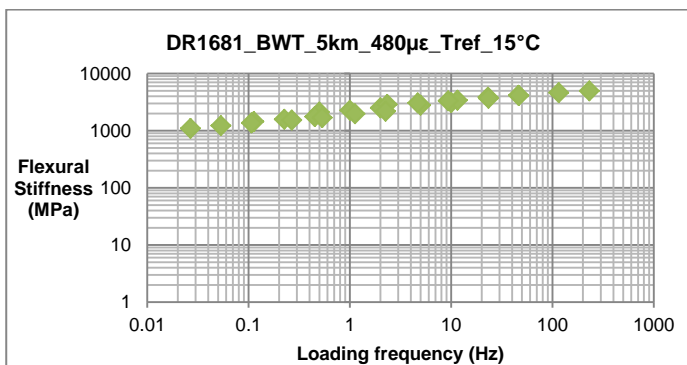
Figure 7-48: Master Curve of DR1681_BWT_5km_480µε_T_{ref}_15°C
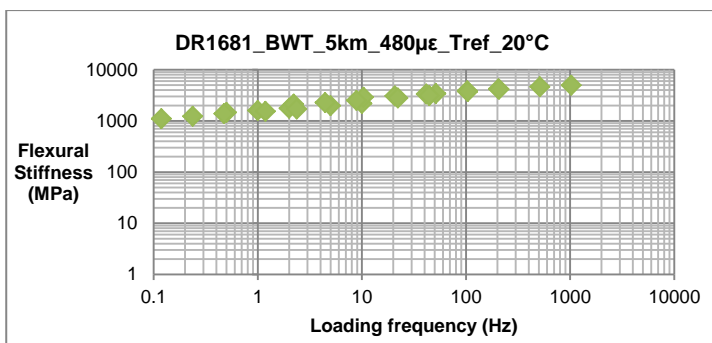
Figure 7-49: Master Curve of DR1681_BWT_5km_480με_T$_{ref}$_20°C
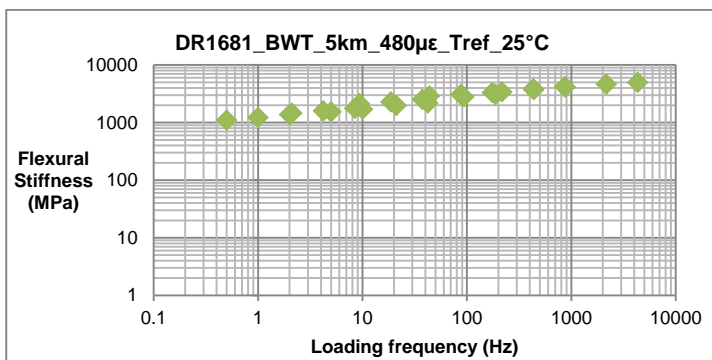
Figure 7-50: Master Curve of DR1681_BWT_5km_480με_T$_{ref}$_25°C
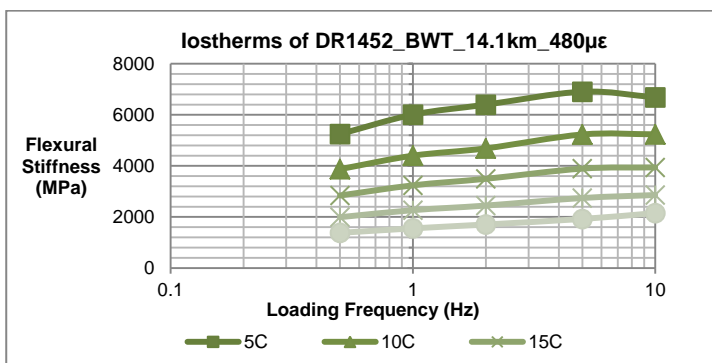
Figure 7-51: Isotherms of DR1452_BWT_14.1km_480με
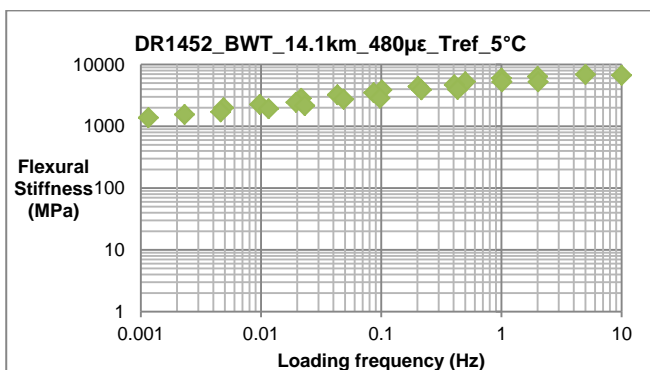
Figure 7-52: Master Curve of DR1452_BWT_14.1km_480με_T$_{ref}$_5°C
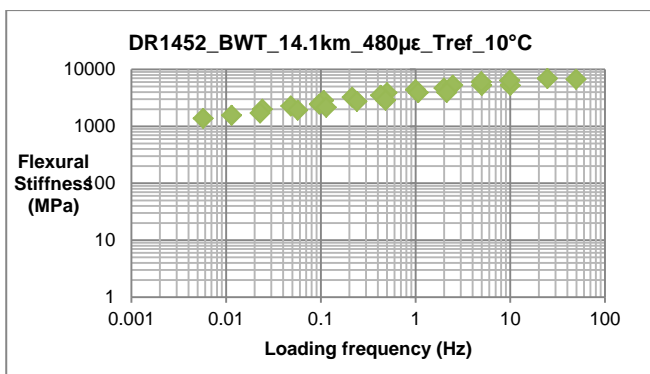
Figure 7-53: Master Curve of DR1452_BWT_14.1km_480µε_T$_{ref}$_10°C
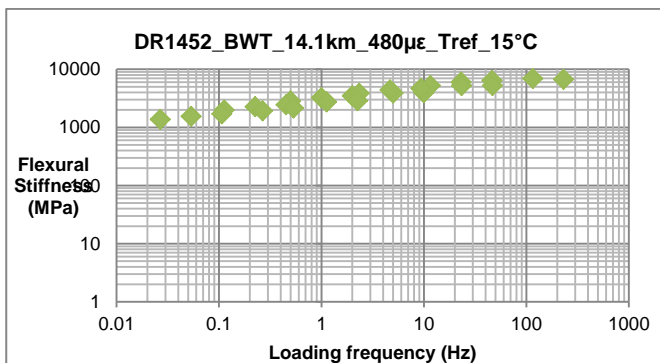
Figure 7-54: Master Curve of DR1452_BWT_14.1km_480µε_T$_{ref}$_15°C
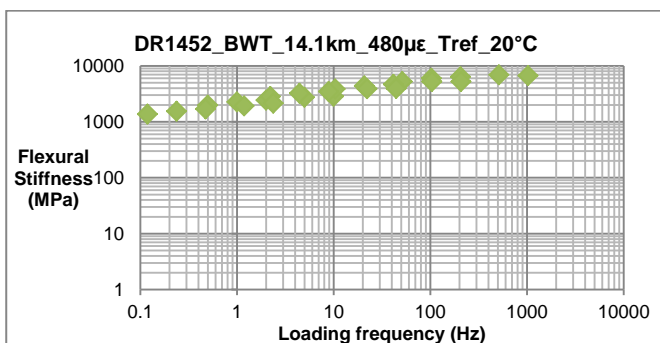
Figure 7-55: Master Curve of DR1452_BWT_14.1km_480µε_T$_{ref}$_20°C
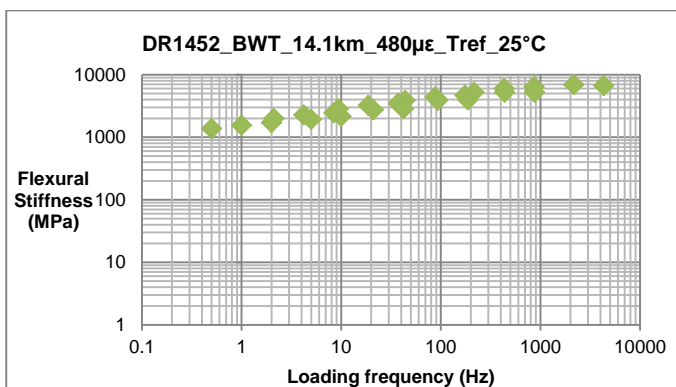
Figure 7-56: Master Curve of DR1452_BWT_14.1km_480µε_T$_{ref}$_25°C
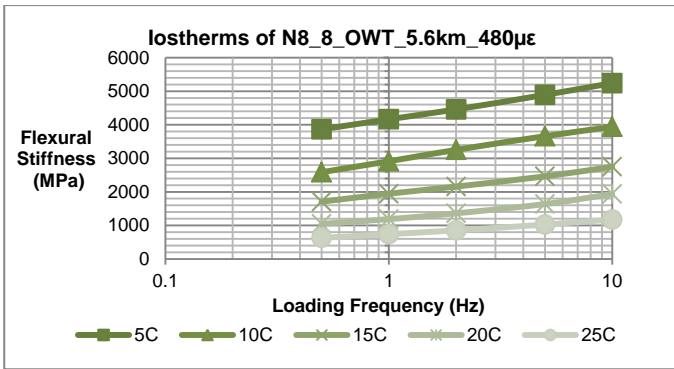
Figure 7-57: Isotherms of N8_8_OWT_5.6km_480µε
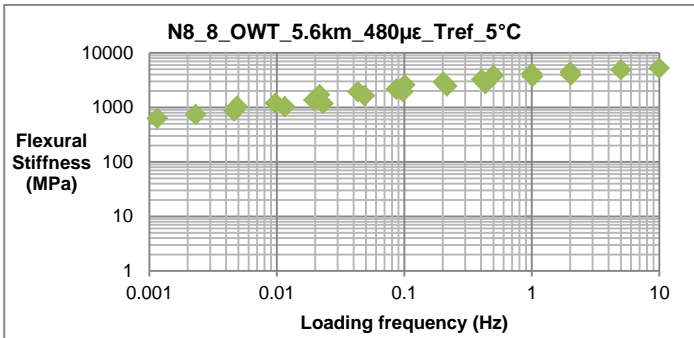
Figure 7-58: Master Curve of N8_8_OWT_5.6km_480µε_T$_{ref}$_5°C
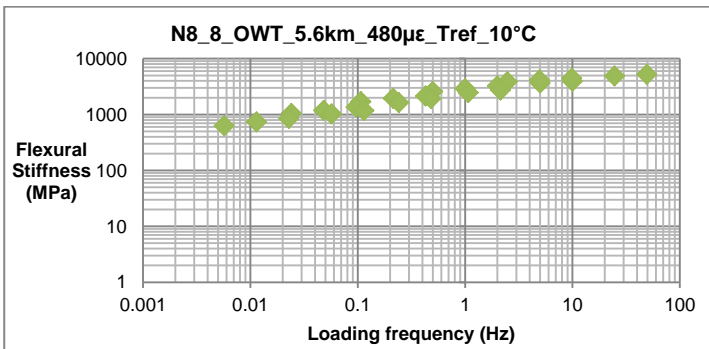
Figure 7-59: Master Curve of N8_8_OWT_5.6km_480µε_T$_{ref}$_10°C
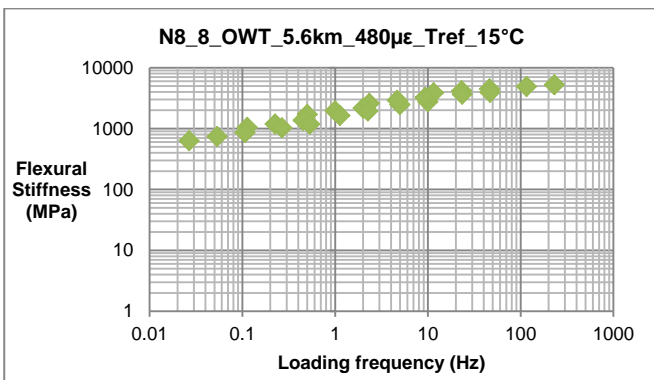
Figure 7-60: Master Curve of N8_8_OWT_5.6km_480µε_T$_{ref}$_15°C
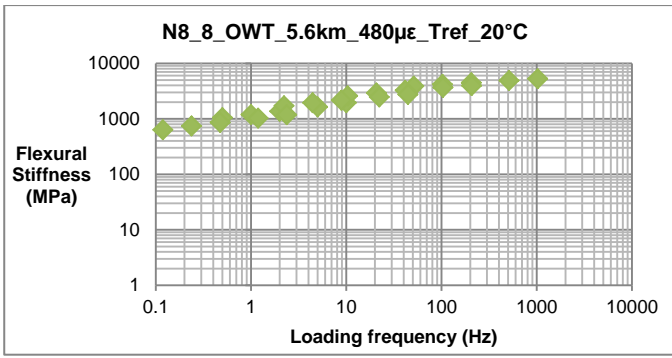
Figure 7-61: Master Curve of N8_8_OWT_5.6km_480µε_T$_{ref}$_20°C
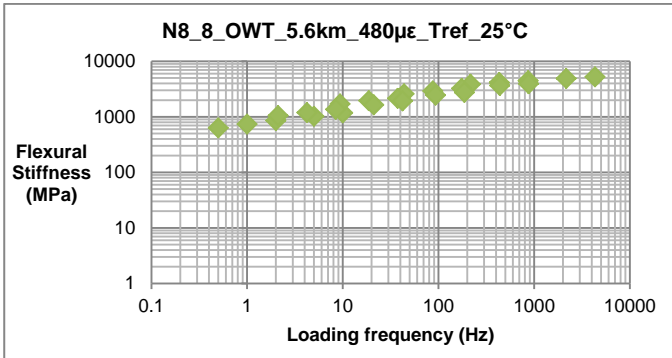
Figure 7-62: Master Curve of N8_8_OWT_5.6km_480µε_T$_{ref}$_25°C
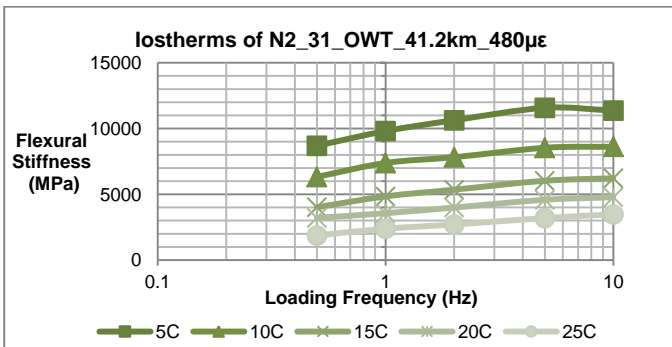
Figure 7-63: Isotherms of N2_31_OWT_41.2km_480µε
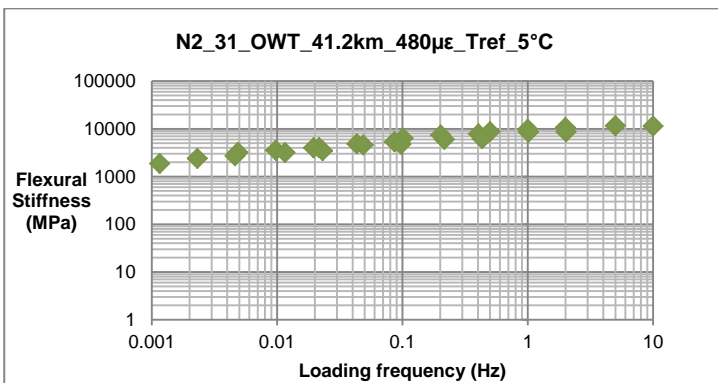
Figure 7-64: Master Curve of N2_31_OWT_41.2km_480µε_T$_{ref}$_5°C
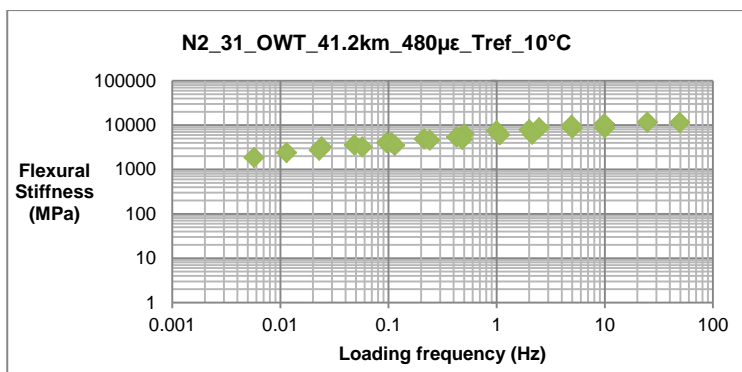
Figure 7-65: Master Curve of N2_31_OWT_480με_T$_{ref}$_10°C
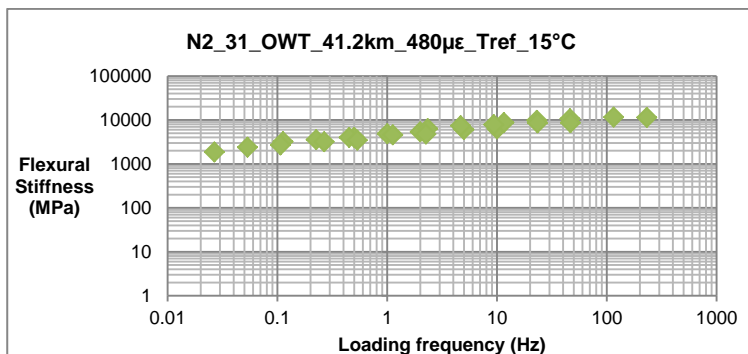
Figure 7-66: Master Curve of N2_31_OWT_480με_T$_{ref}$_15°C
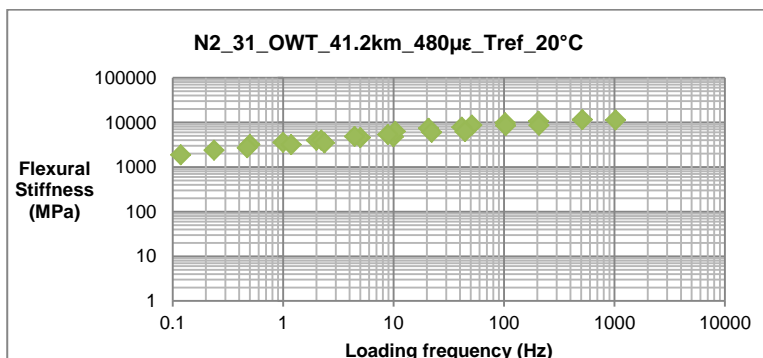
Figure 7-67: Master Curve of N2_31_OWT_480με_T$_{ref}$_20°C
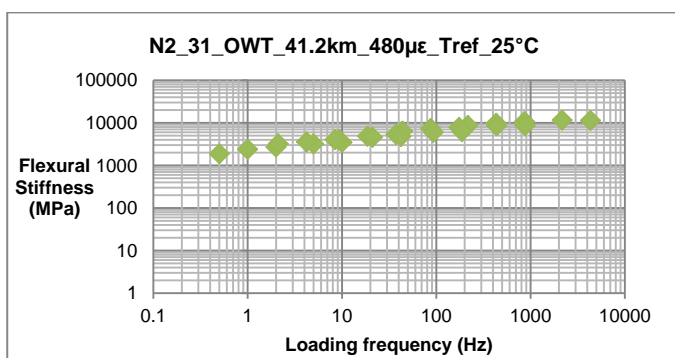
Figure 7-68: Master Curve of N2_31_OWT_41.2km_480με_T$_{ref}$_25°C
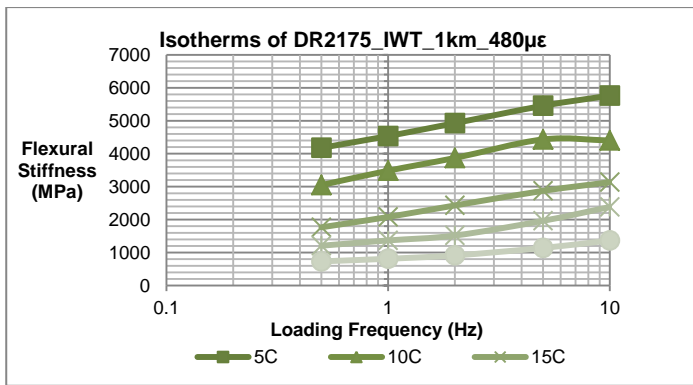
Figure 7-69: Isotherms of DR2175_IWT_1km_480με
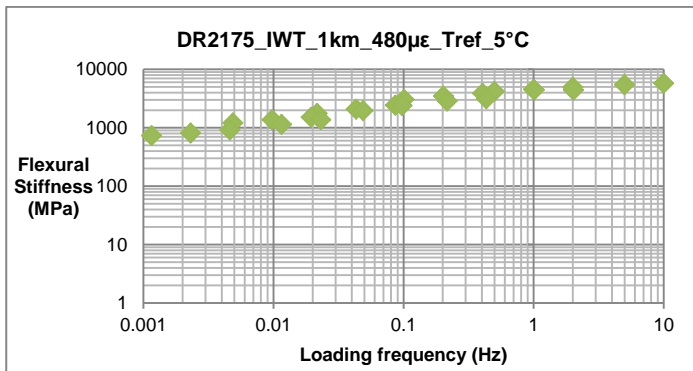
Figure 7-70: Master Curve of DR2175_IWT_1km_480με_T$_{ref}$_5°C
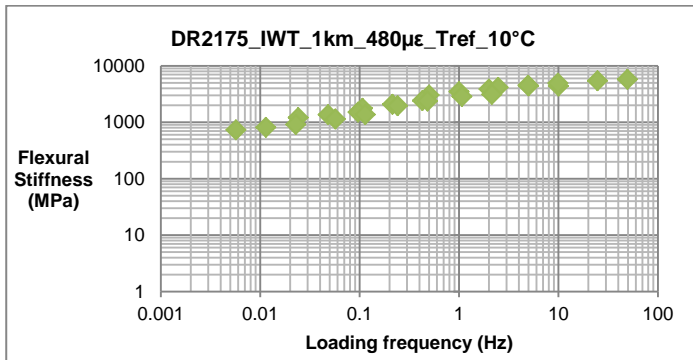
Figure 7-71: Master Curve of DR2175_IWT_1km_480με_T$_{ref}$_10°C
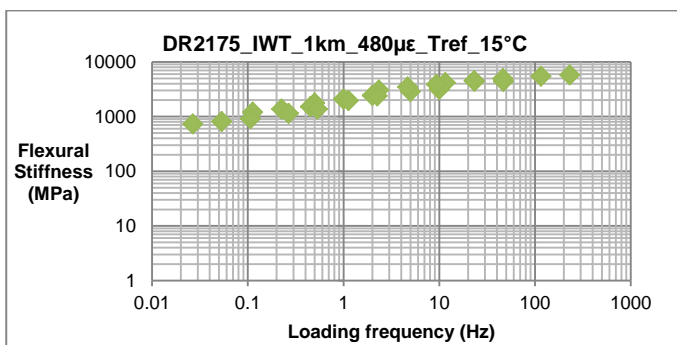
Figure 7-72: Master Curve of DR2175_IWT_1km_480με_T$_{ref}$_15°C
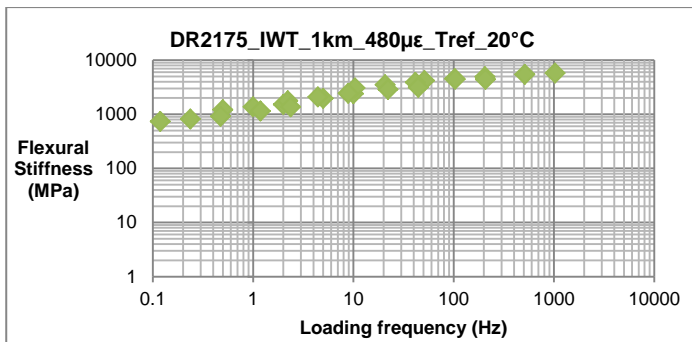
Figure 7-73: Master Curve of DR2175_IWT_1km_480µε_T$_{ref}$_20°C
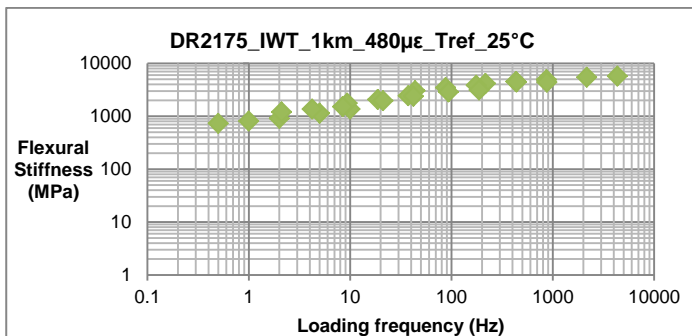
Figure 7-74: Master Curve of DR2175_IWT_1km_480µε_T$_{ref}$_25°C
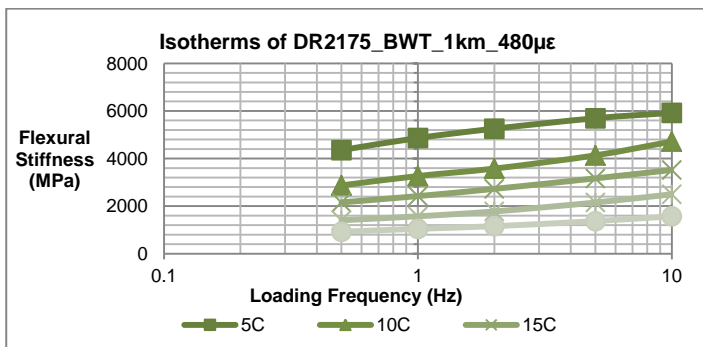
Figure 7-75: Isotherms of DR2175_BWT_1km_480µε
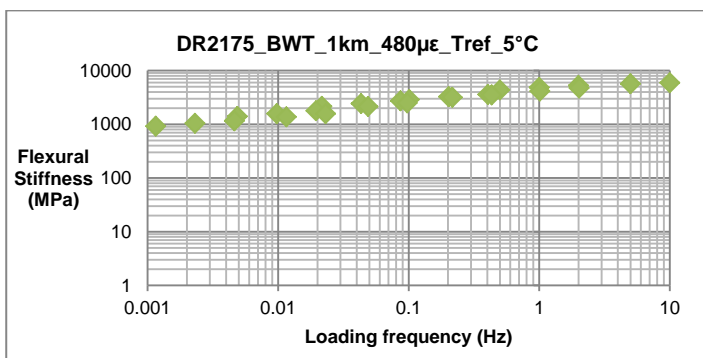
Figure 7-76: Master Curve of DR2175_BWT_1km_480µε_T$_{ref}$_5°C

209
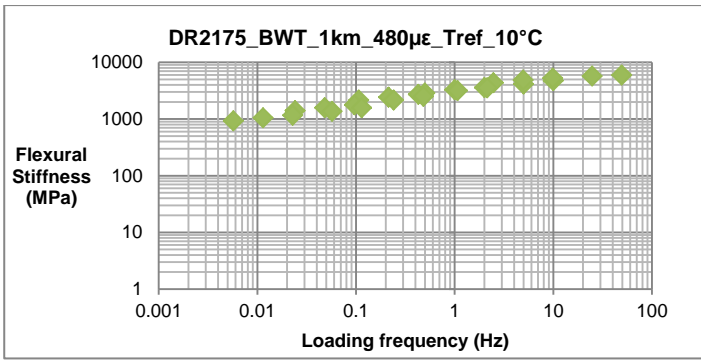
Figure 7-77: Master Curve of DR2175_BWT_1km_480µε_T$_{ref}$_10°C
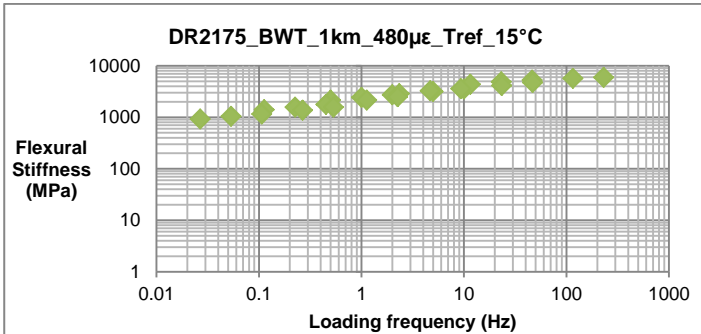
Figure 7-78: Master Curve of DR2175_BWT_1km_480µε_T$_{ref}$_15°C
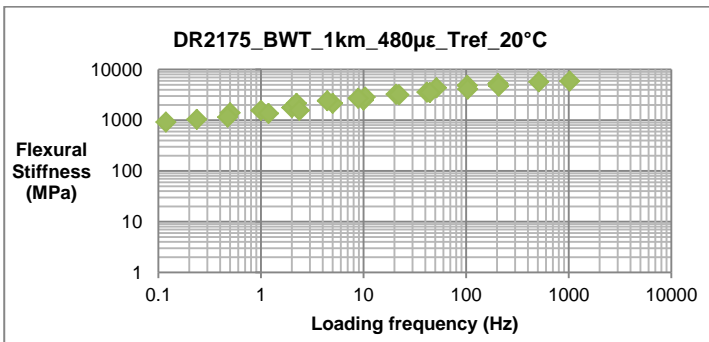
Figure 7-79: Master Curve of DR2175_BWT_1km_480µε_T$_{ref}$_20°C
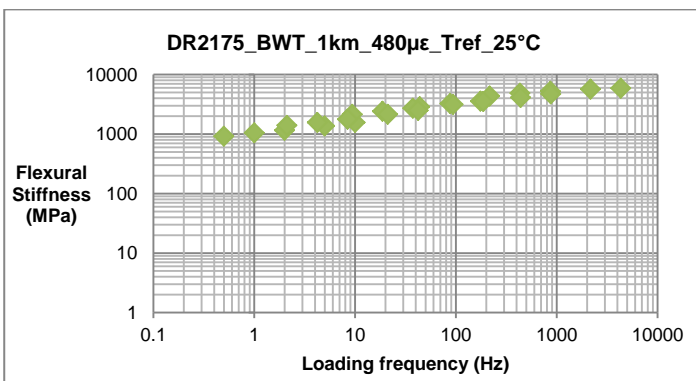
Figure 7-80: Master Curve of DR2175_BWT_1km_480µε_T$_{ref}$_25°C

210
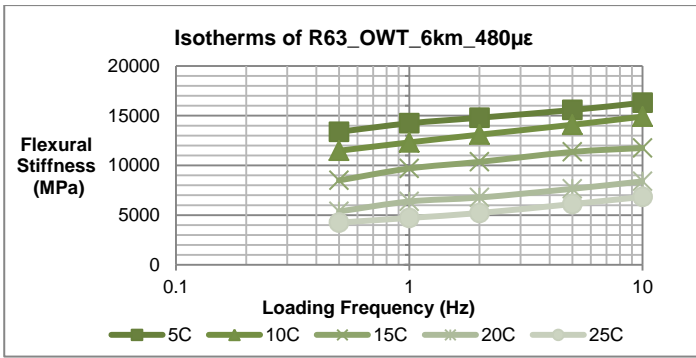
Figure 7-81: Isotherms of R63_OWT_6km_480με
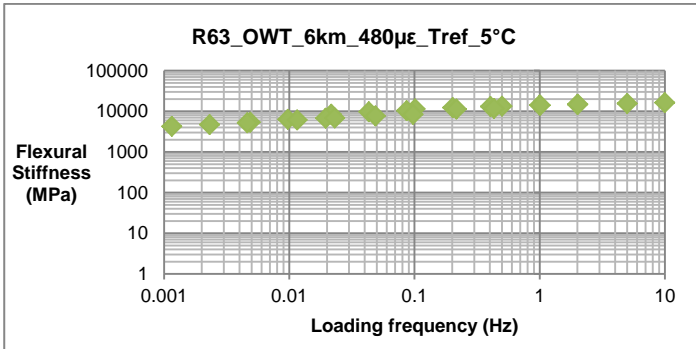
Figure 7-82: Master Curve of R63_OWT_480με_T$_{ref}$_5°C
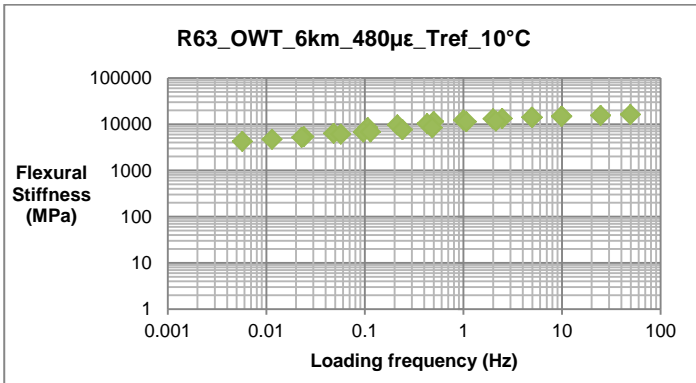
Figure 7-83: Master Curve of R63_OWT_480με_T$_{ref}$_10°C
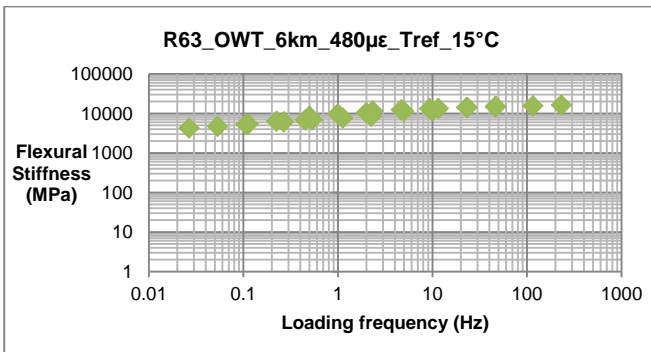
Figure 7-84: Master Curve of R63_OWT_480με_T$_{ref}$_15°C
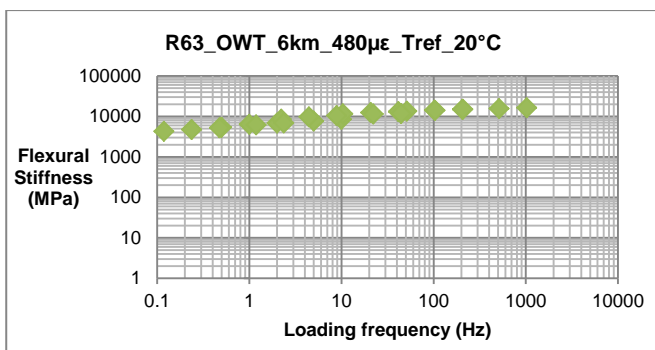
Figure 7-85: Master Curve of R63_OWT_480µε_T$_{ref}$_20°C
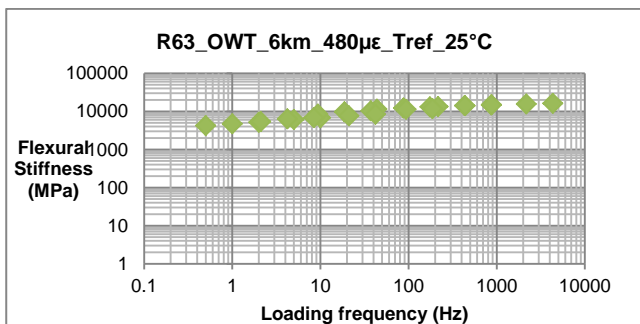
Figure 7-86: Master Curve of R63_OWT_480µε_T$_{ref}$_25°C
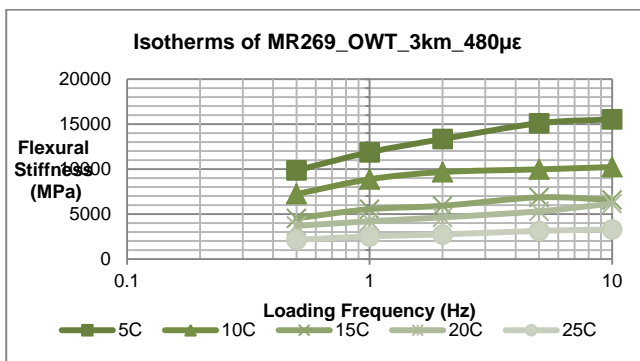
Figure 7-87: Isotherms of MR269_OWT_480µε
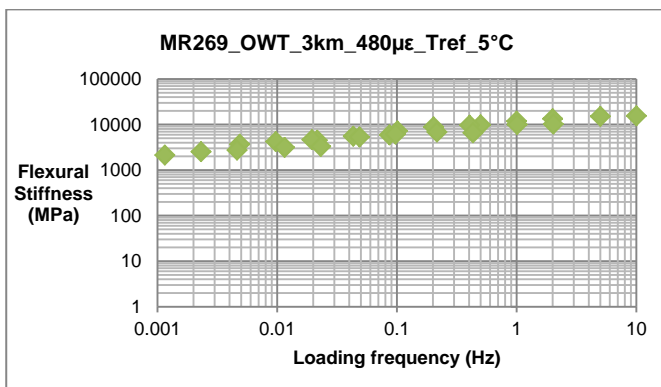
Figure 7-88: Master Curve of MR269_OWT_480µε_T$_{ref}$_5°C
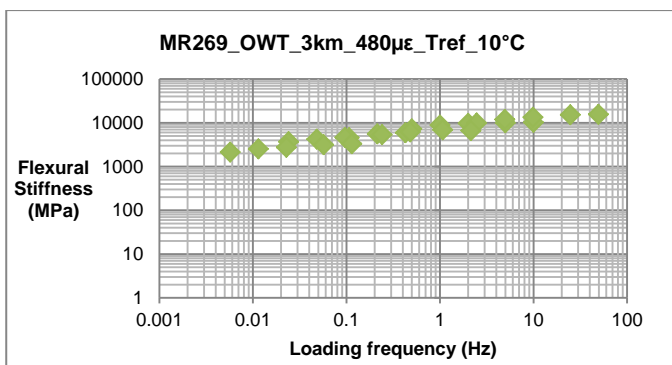
Figure 7-89: Master Curve of MR269_OWT_480µε_T_ref_10°C
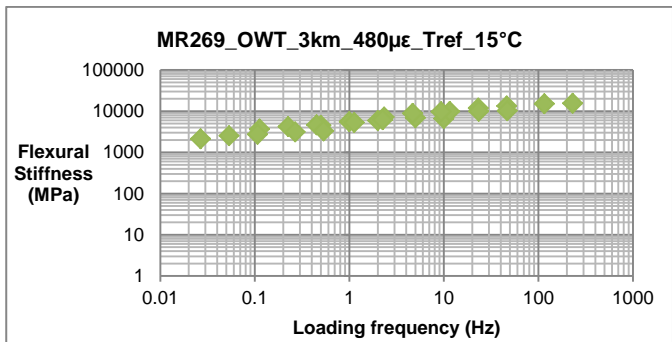
Figure 7-90: Master Curve of MR269_OWT_480µε_T_ref_15°C
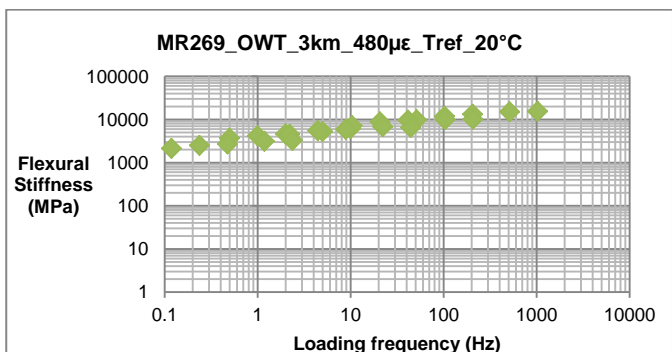
Figure 7-91: Master Curve of MR269_OWT_480µε_T_ref_20°C
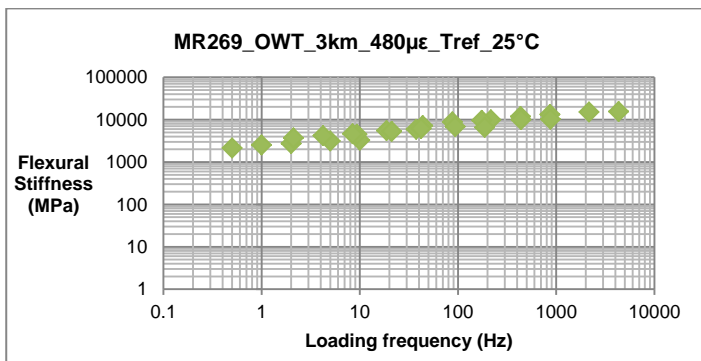
Figure 7-92: Master Curve of MR269_OWT_480µε_T_ref_25°C

213
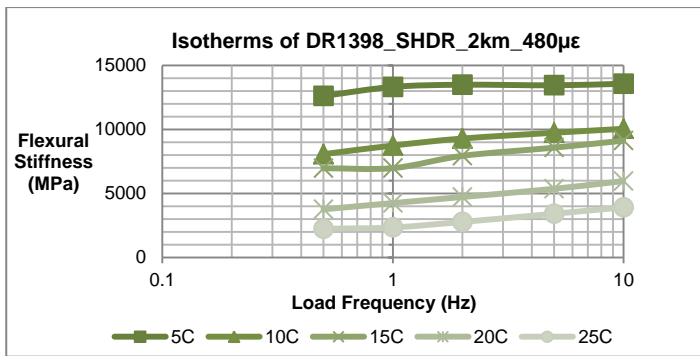
Figure 7-93: Isotherms of DR1398_SHDR_480µε
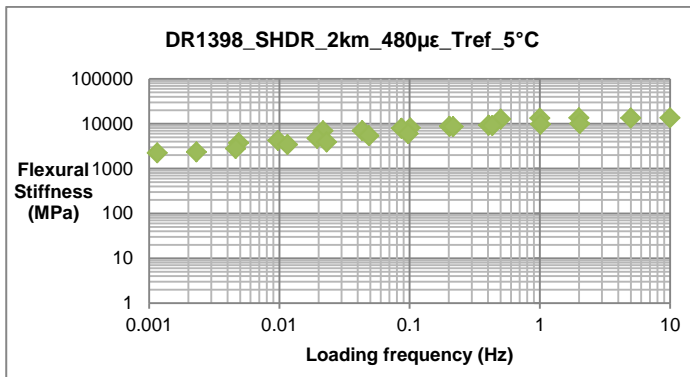
Figure 7-94: Master Curve of DR1398_SHDR_480µε_T$_{ref}$_5°C
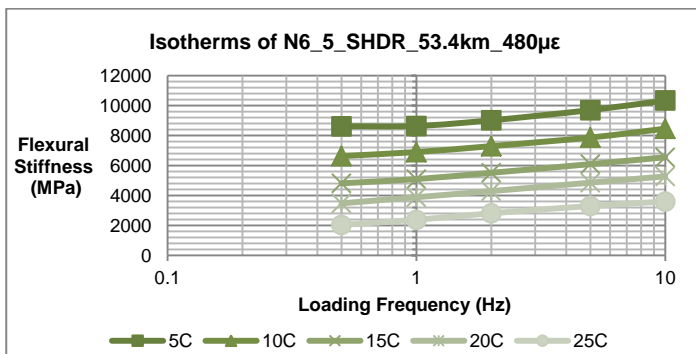
Figure 7-95: Isotherms of N6_5_SHDR_53.4km_480
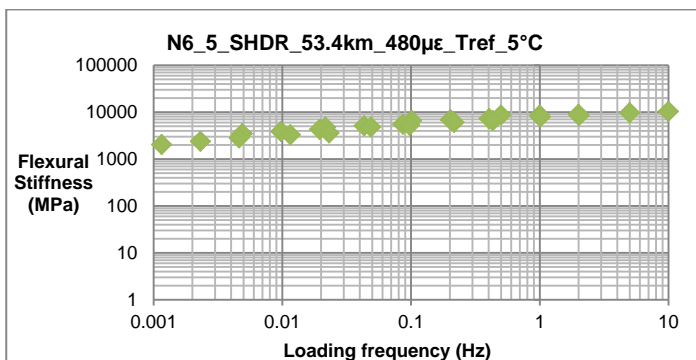
Figure 7-96: Master Curve of N6_5_SHDR_53.4km_480µε_T$_{ref}$_5°C
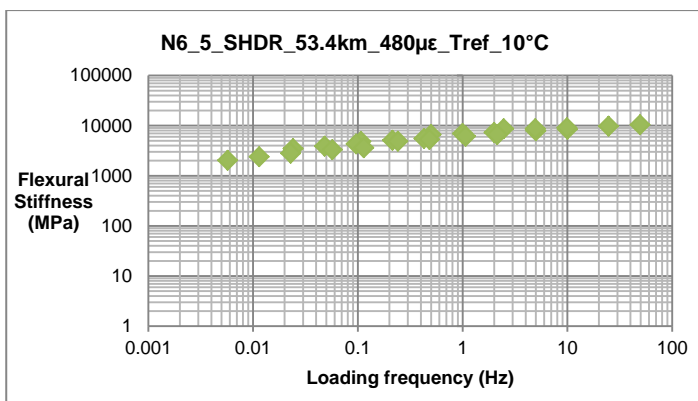
Figure 7-97: Master Curve of N6_5_SHDR_53.4km_480με_T$_{ref}$_10°C
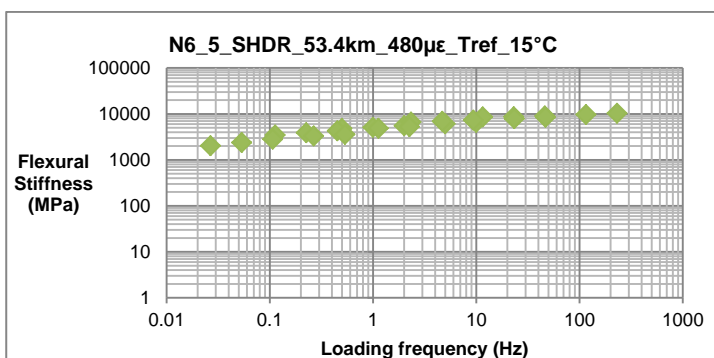
Figure 7-98: Master Curve of N6_5_SHDR_53.4km_480με_T$_{ref}$_15°C
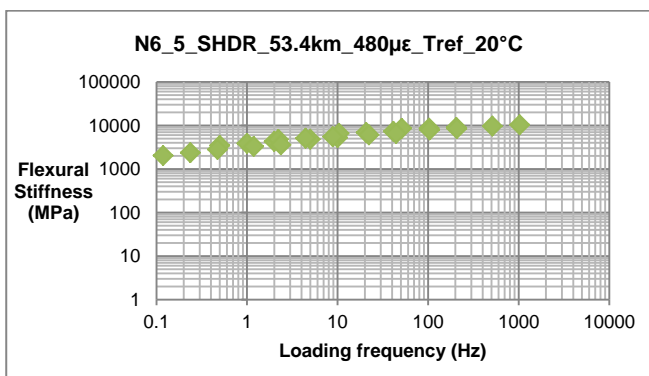
Figure 7-99: Master Curve of N6_5_SHDR_53.4km_480με_T$_{ref}$_20°C
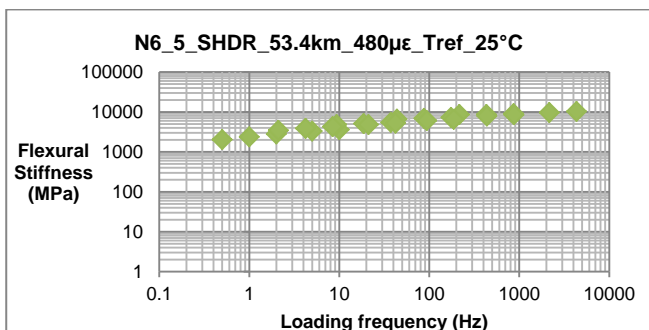
Figure 7-100: Master Curve of N6_5_SHDR_53.4km_480με_T$_{ref}$_25°C
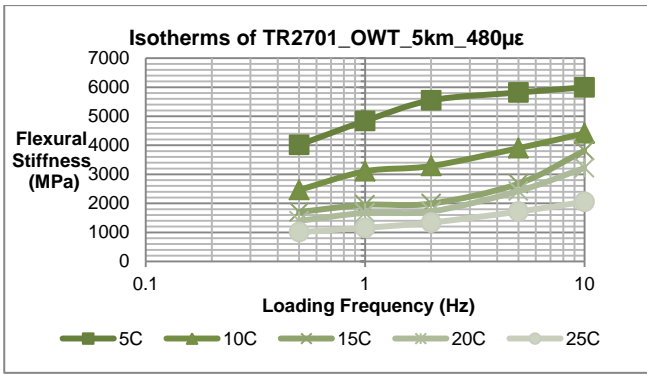
Figure 7-101: Isotherms of TR2701_OWT_5km_480µε
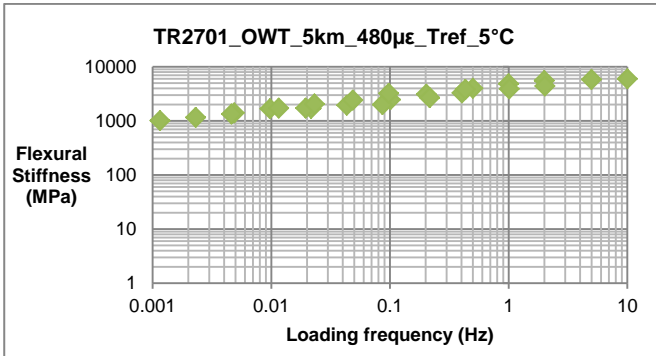
Figure 7-102: Master Curve of TR2701_OWT_5km_480µε_T$_{ref}$_5°C
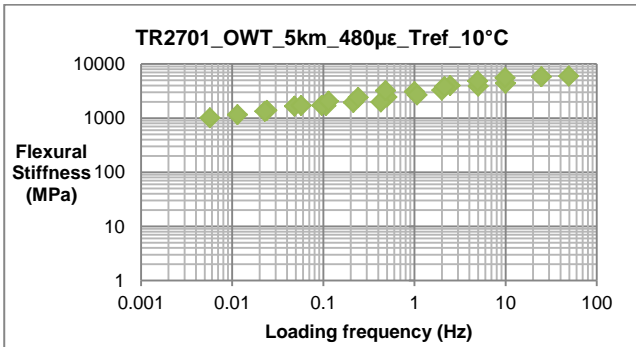
Figure 7-103: Master Curve of TR2701_OWT_5km_480µε_T$_{ref}$_10°C
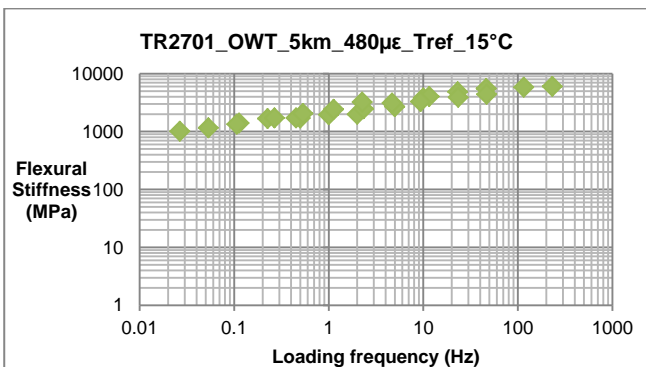
Figure 7-104: Master Curve of TR2701_OWT_5km_480µε_T$_{ref}$_15°C

216
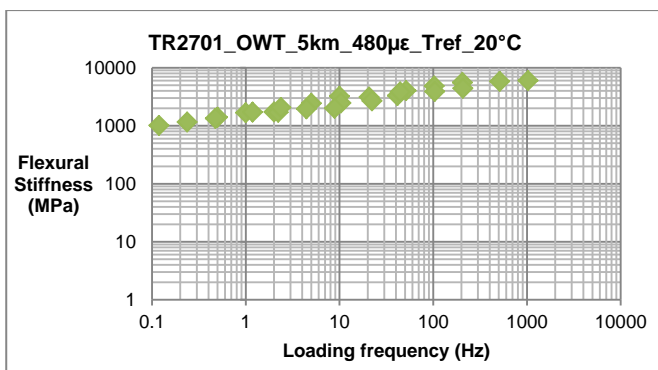
Figure 7-105: Master Curve of TR2701_OWT_5km_480µε_T_{ref}_20°C
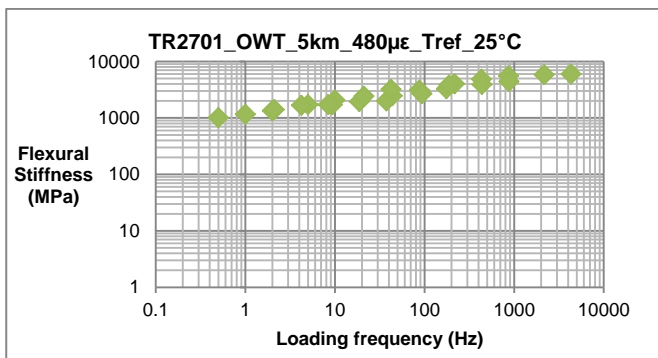
Figure 7-106: Master Curve of TR2701_OWT_5km_480µε_T_{ref}_25°C
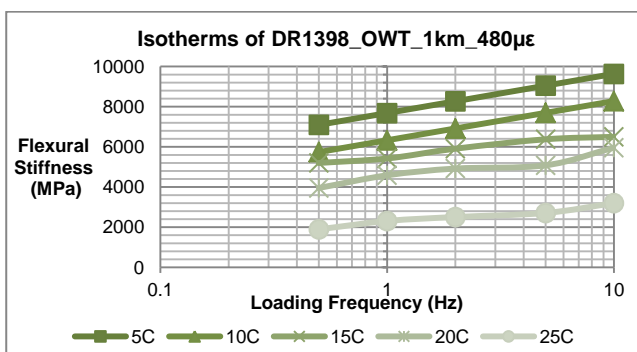
Figure 7-107: Isotherms of DR1398_OWT_480µε
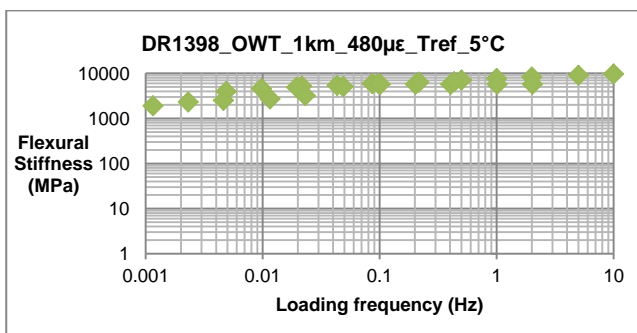
Figure 7-108: Master Curve of DR1398_OWT_1km_480µε_T_{ref}_5°C
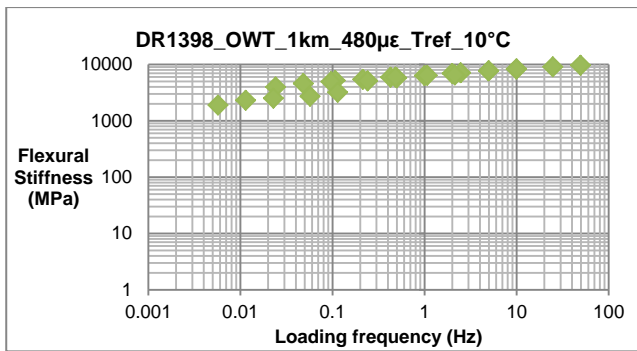
Figure 7-109: Master Curve of DR1398_OWT_1km_480µε_T$_{ref}$_10°C
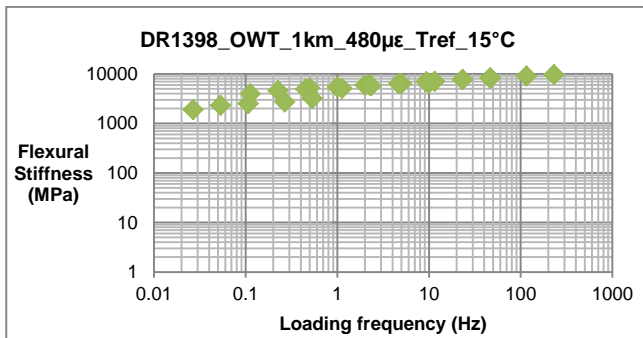
Figure 7-110: Master Curve of DR1398_OWT_1km_480µε_T$_{ref}$_15°C
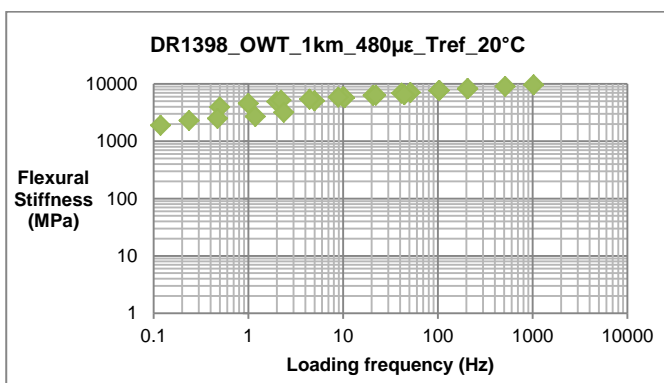
Figure 7-111: Master Curve of DR1398_OWT_1km_480µε_T$_{ref}$_20°C
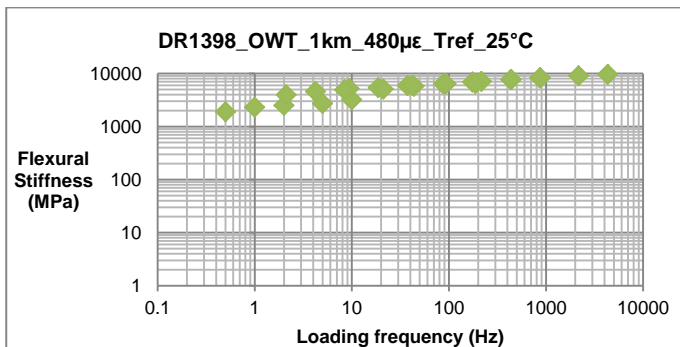
Figure 7-112: Master Curve of DR1398_OWT_1km_480µε_T$_{ref}$_25°C
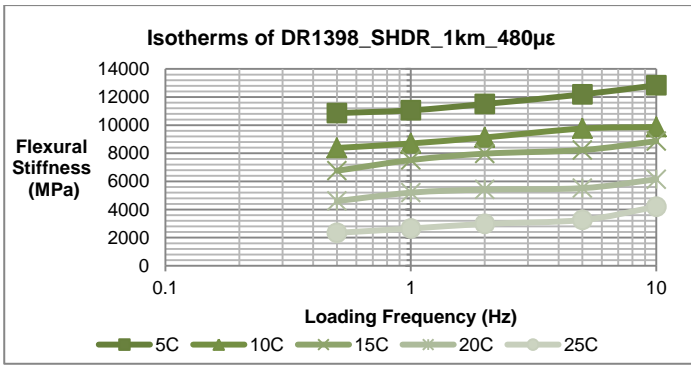
Figure 7-113: Isotherms of DR1398_SHDR_1km_480µε
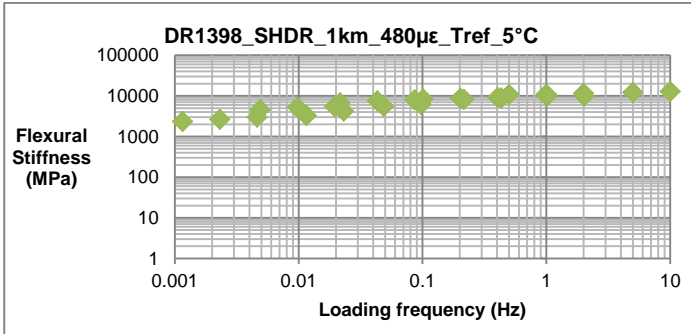
Figure 7-114: Master Curve of DR1398_ SHDR _1km_480µε_T$_{ref}$_5°C
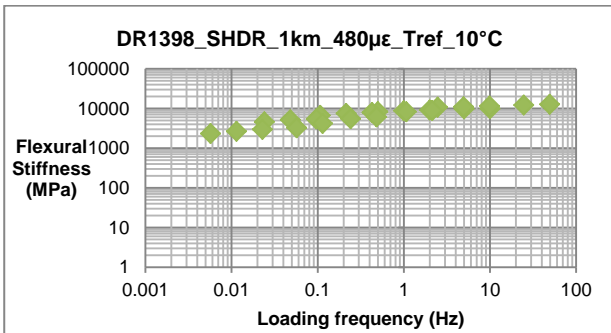
Figure 7-115: Master Curve of DR1398_ SHDR _1km_480µε_T$_{ref}$_10°C
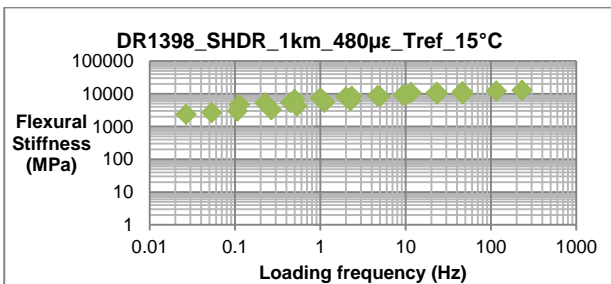
Figure 7-116: Master Curve of DR1398_ SHDR _1km_480µε_T$_{ref}$_15°C
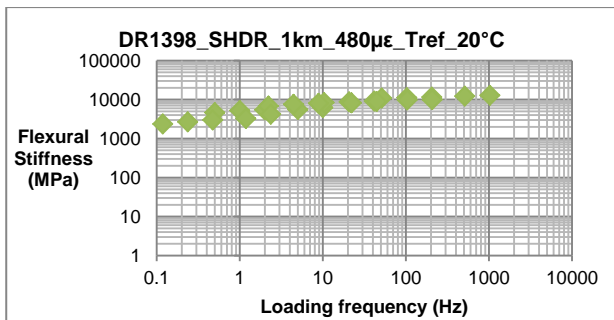
Figure 7-117: Master Curve of DR1398_SHDR_1km_480µε_T$_{ref}$_20°C
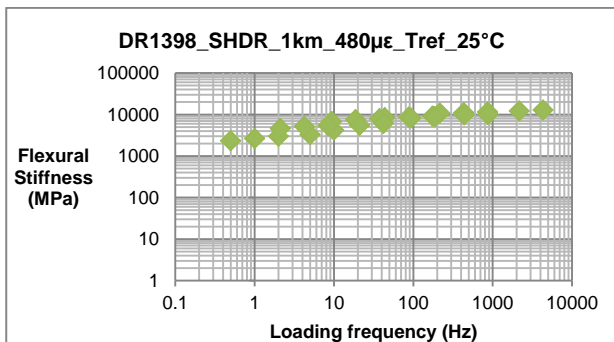
Figure 7-118: Master Curve of DR1398_SHDR_1km_480µε_T$_{ref}$_25°C
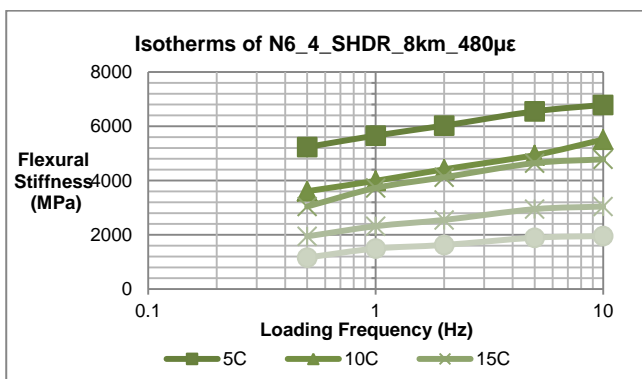
Figure 7-119: Isotherms of N6_4_SHDR_8km_480µε
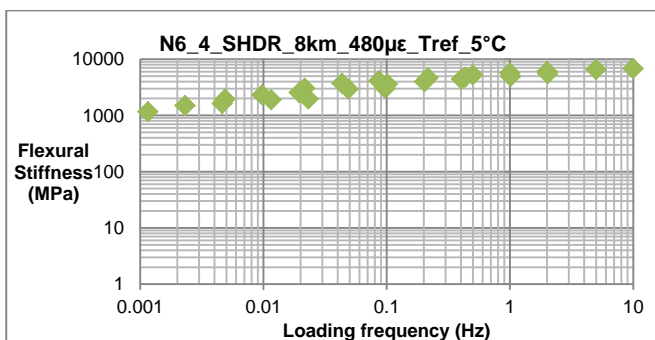
Figure 7-120: Master Curve of N6_4_SHDR_480µε_T$_{ref}$_5°C
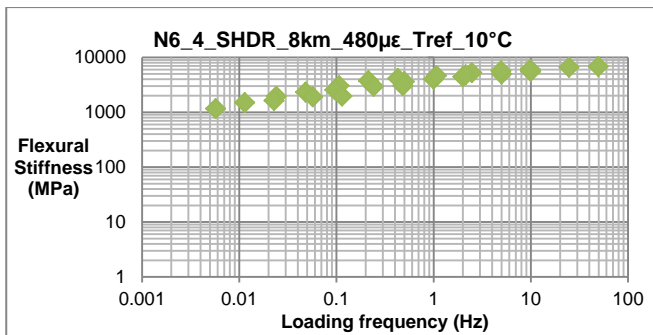
Figure 7-121: Master Curve of N6_4_SHDR_480µε_T$_{ref}$_10°C
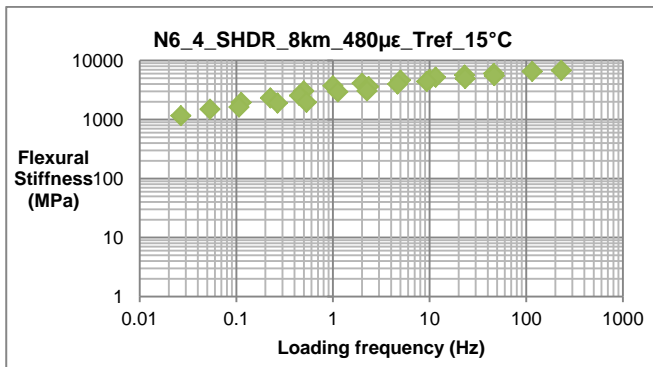
Figure 7-122: Master Curve of N6_4_SHDR_480µε_T$_{ref}$_15°C
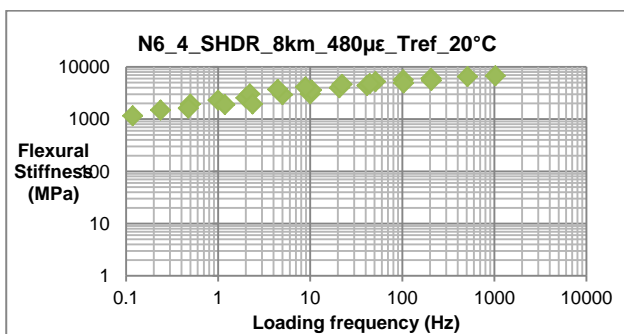
Figure 7-123: Master Curve of N6_4_SHDR_480µε_T$_{ref}$_20°C
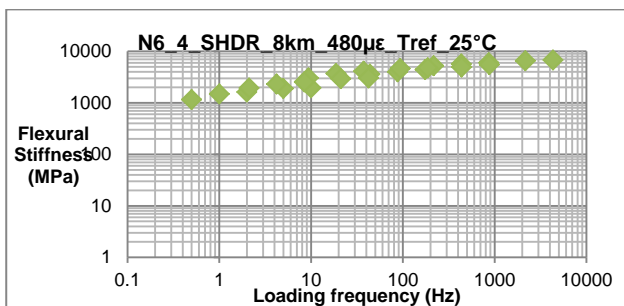
Figure 7-124: Master Curve of N6_4_SHDR_480µε_T$_{ref}$_25°C

221
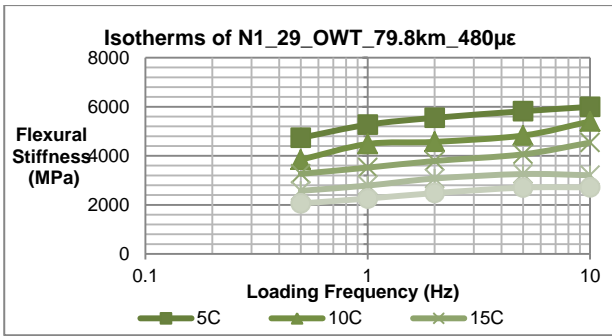
Figure 7-125: Isotherms of N1_29_OWT_79.8km_480µε
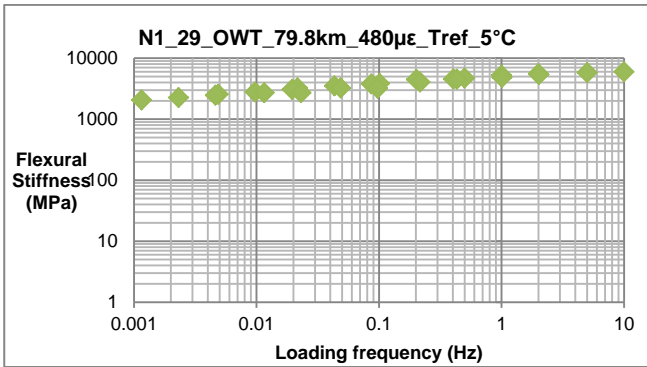
Figure 7-126: Master Curve of N1_29_OWT_79.8km_480µε_T$_{ref}$_5°C
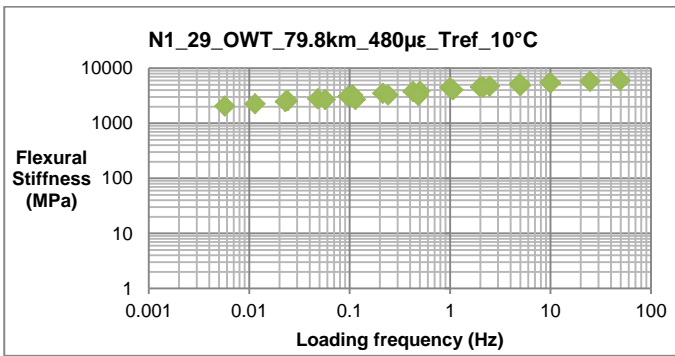
Figure 7-127: Master Curve of N1_29_OWT_79.8km_480µε_T$_{ref}$_5°C
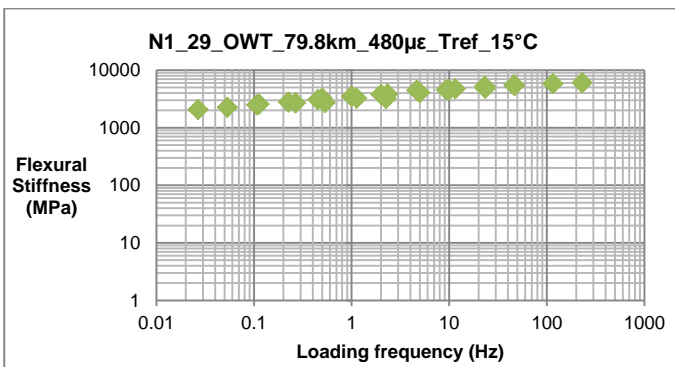
Figure 7-128: Master Curve of N1_29_OWT_79.8km_480µε_T$_{ref}$_5°C
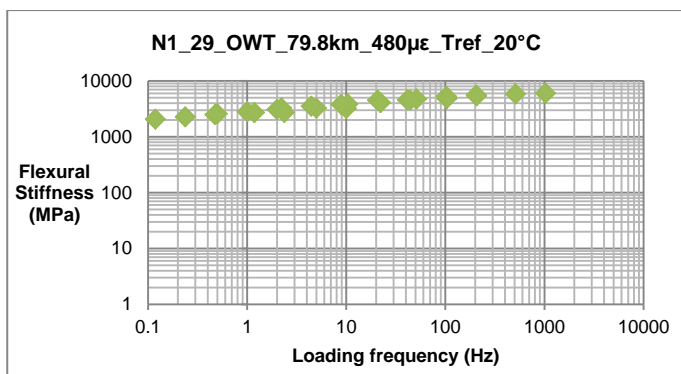
Figure 7-129: Master Curve of N1_29_OWT_79.8km_480µε_T$_{ref}$_20°C
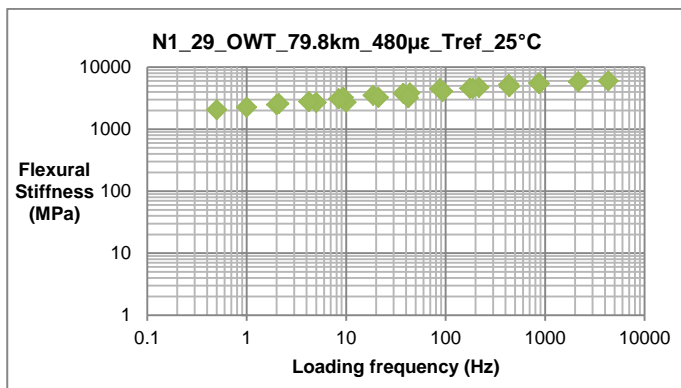
Figure 7-130: Master Curve of N1_29_OWT_79.8km_480µε_T$_{ref}$_25°C

Appendix I: Graphs of Fatigue Testing from Group 2
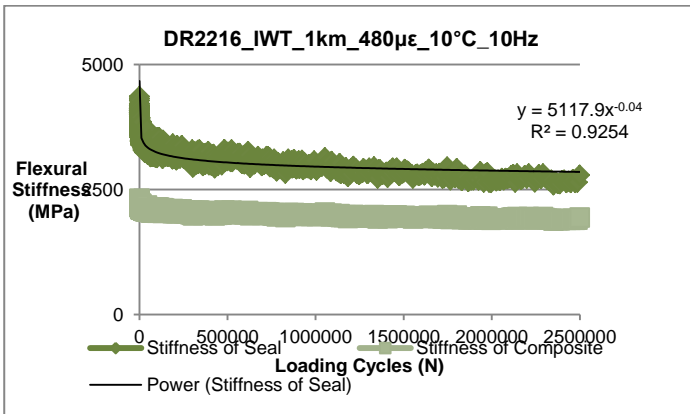
Figure 7-131: Fatigue Testing_DR2216_IWT_1km_480µε_10°C_10Hz
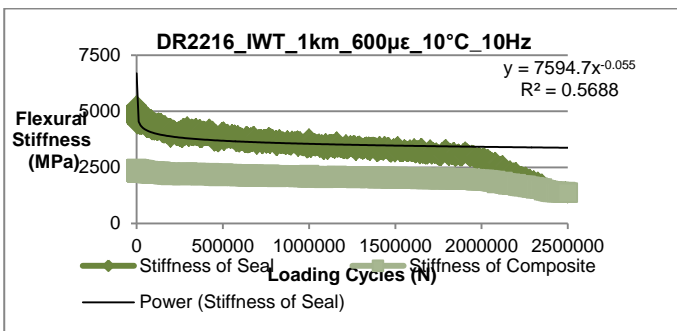
Figure 7-132: Fatigue Testing_DR2216_IWT_1km_600µε_10°C_10Hz
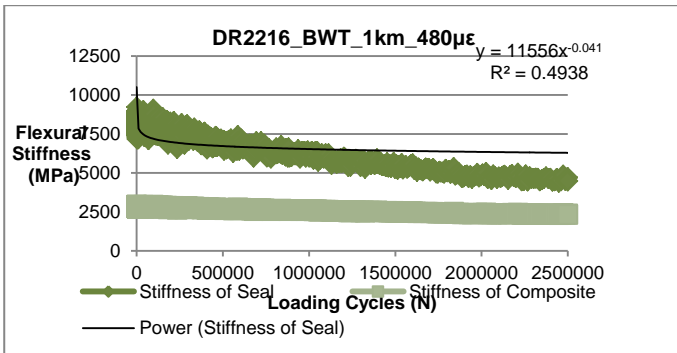
Figure 7-133: Fatigue Testing_DR2216_BWT_1km_480µε_10°C_10Hz
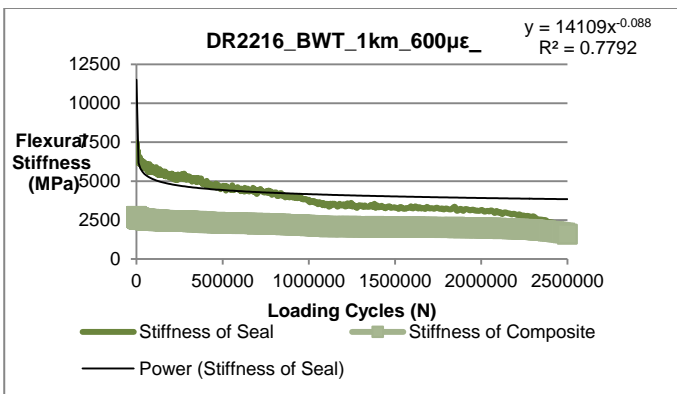
Figure 7-134: Fatigue Testing_DR2216_BWT_1km_600µε_10°C_10Hz
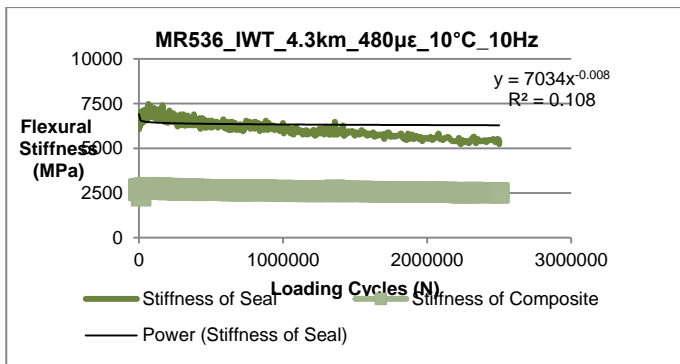
Figure 7-135: Fatigue Testing_MR536_IWT_4.3km_480με_10°C_10Hz
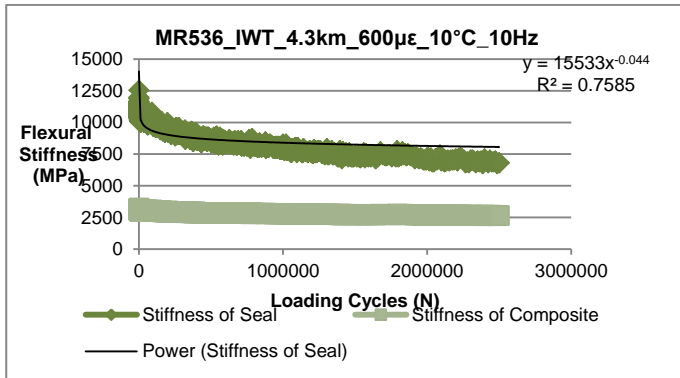
Figure 7-136: Fatigue Testing_MR536_IWT_4.3km_600με_10°C_10Hz
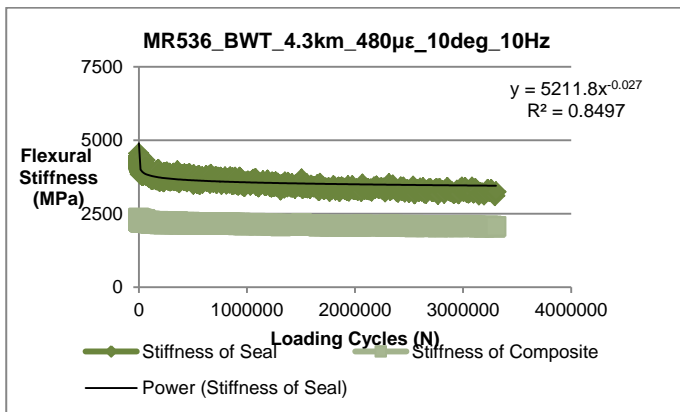
Figure 7-137: Fatigue Testing_MR536_BWT_4.3km_480με_10°C_10Hz
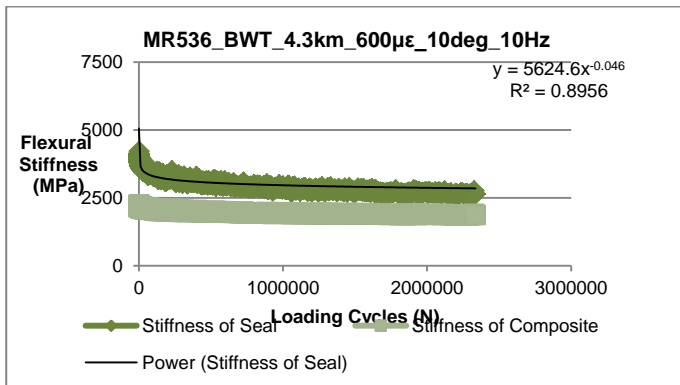
Figure 7-138: Fatigue Testing_MR536_BWT_4.3km_600με_10°C_10Hz
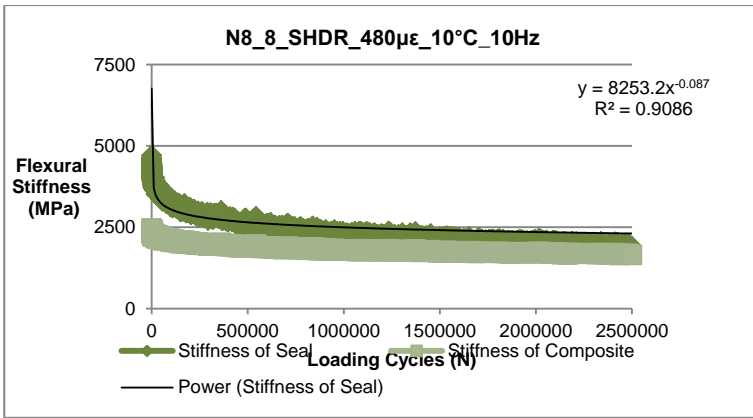
Figure 7-139: Fatigue Testing_N8_8_SHDR_5.6km_480µε_10°C_10Hz
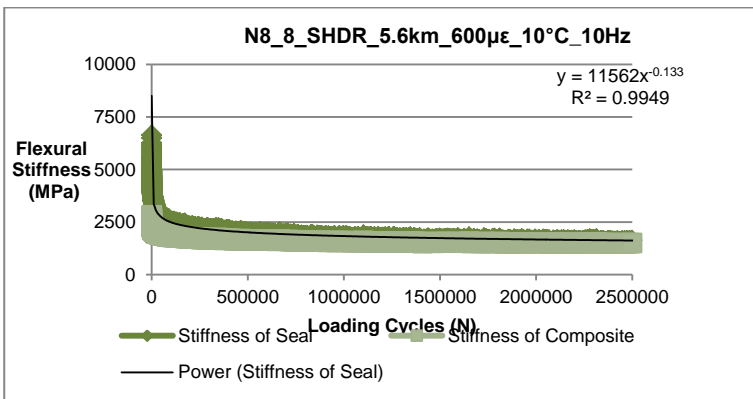
Figure 7-140: Fatigue Testing_N8_8_SHDR_5.6km_600µε_10°C_10Hz
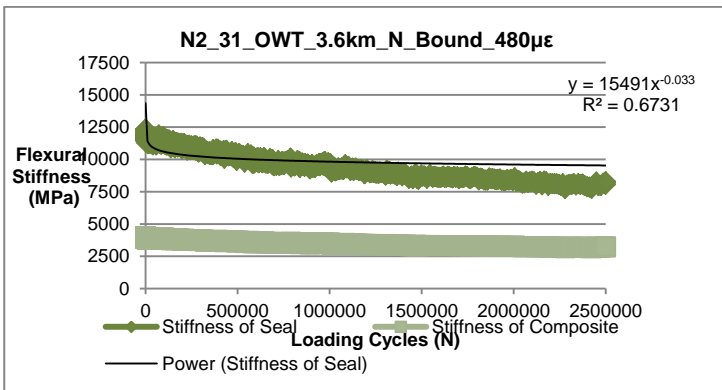
Figure 7-141: Fatigue Testing_N2_31_OWT_3.6km_N_B_480µε_10°C_10Hz
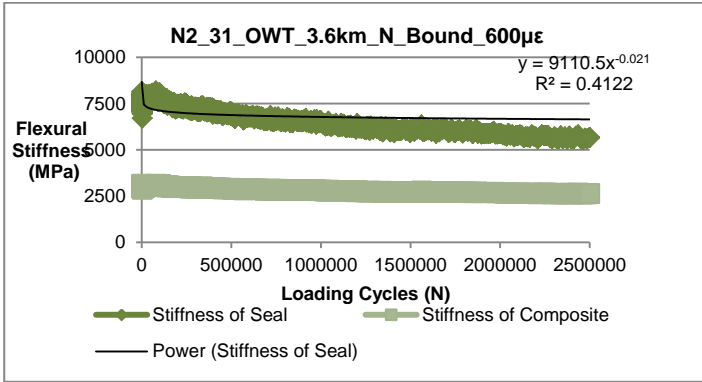
Figure 7-142: Fatigue Testing_N2_31_OWT_3.6km_N_B_600µε_10°C_10Hz
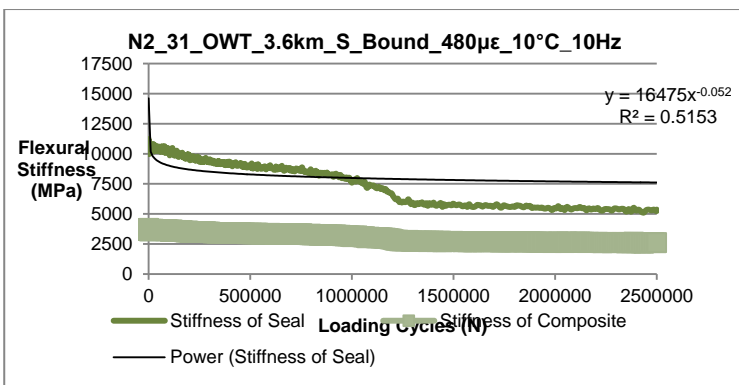
Figure 7-143: Fatigue Testing_N2_31_OWT_3.6km_S_B_480µε_10°C_10Hz
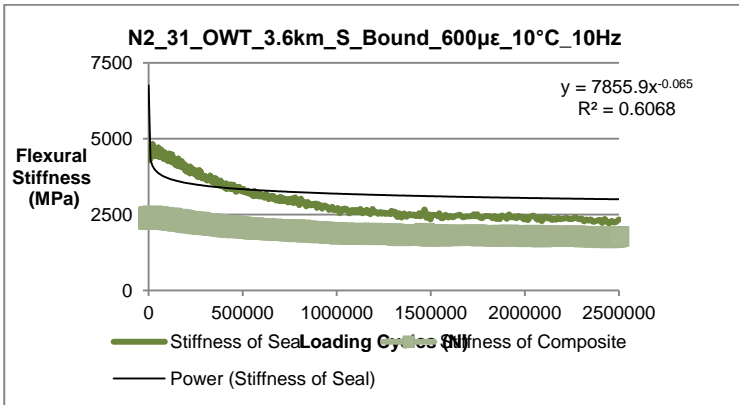
Figure 7-144: Fatigue Testing_N2_31_OWT_3.6km_S_B_600µε_10°C_10Hz

227
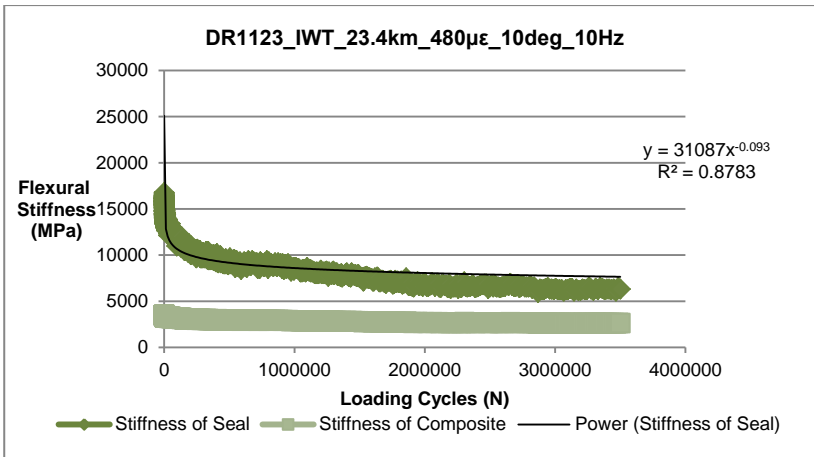
Figure 7-145: Fatigue Testing_DR1123_IWT_23.4km_480µε_10°C_10Hz
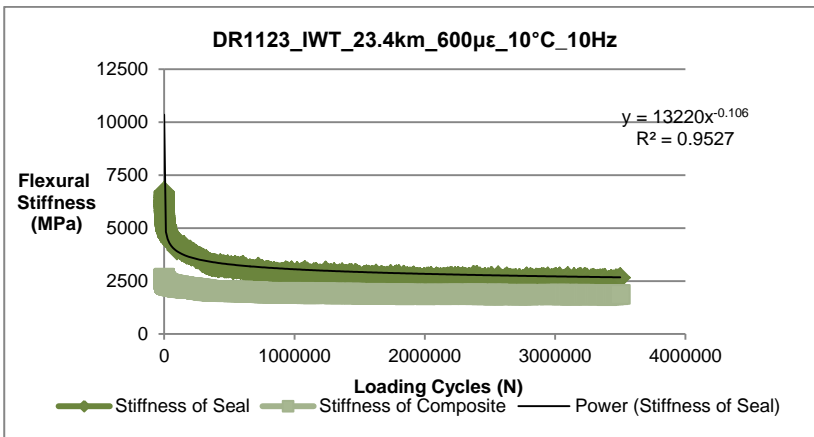
Figure 7-146: Fatigue Testing_DR1123_IWT_23.4km_600µε_10°C_10Hz
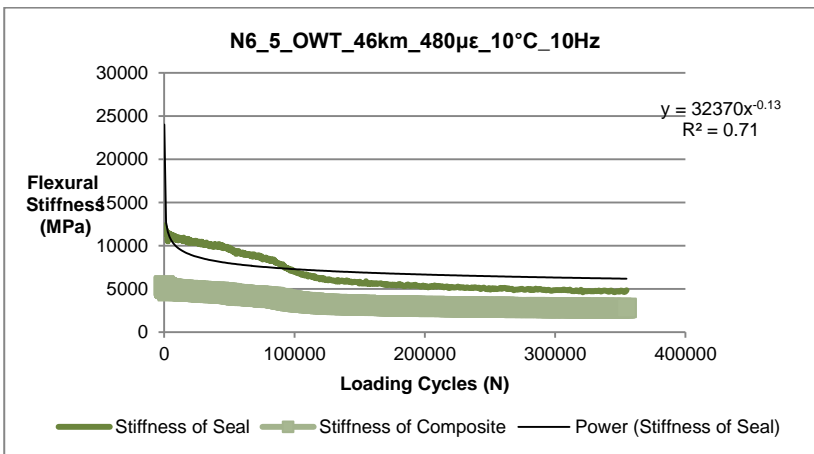
Figure 7-147: Fatigue Testing_N6_5_OWT_46km_480µε_10°C_10Hz
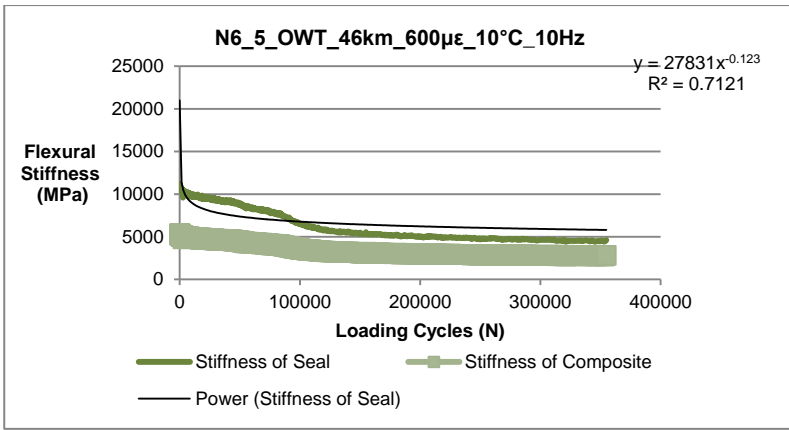
Figure 7-148: Fatigue Testing_N6_5_OWT_46km_600με_10°C_10Hz
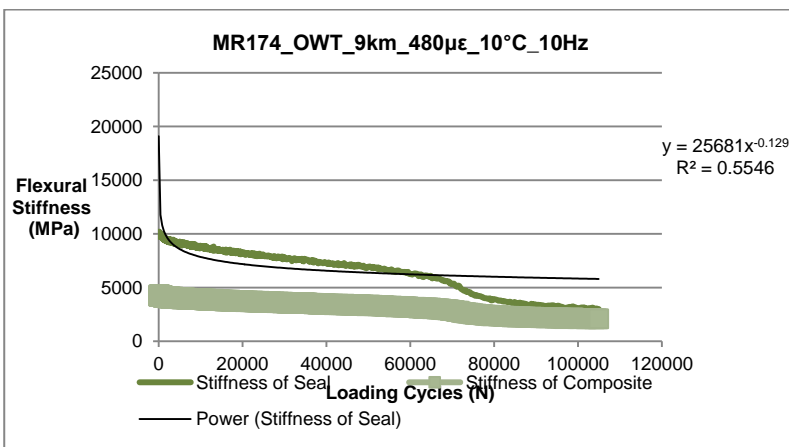
Figure 7-149: Fatigue Testing_MR174_OWT_9km_480με_10°C_10Hz
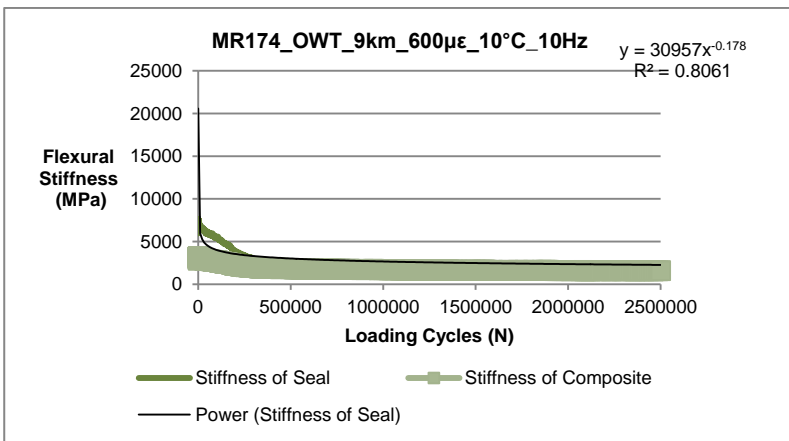
Figure 7-150: Fatigue Testing_MR174_OWT_9km_600με_10°C_10Hz

229

Appendix J: Statistical Analysis

Appendix 7 J1: Statistical Analysis of Individual Variables of Single Seals on the outcome of Fatigue

Influence on Fatigue ($N_{30\%}$):

Table 7-22: Model Summary of $N_{30\%}$_Single Seals

No.	Constant, a	R	R Squared	Adjusted R Squared	Std. Error of the Estimate
1	Age	0.451[a]	0.203	0.070	5.86
2	Climate	0.153[a]	0.023	-0.139	6.49
3	Effective Thickness	0.484[a]	0.234	0.106	5.75
4	Moment of Inertia	0.489[a]	0.239	0.113	5.72
5	Log (Strain)	0.480[a]	0.231	0.103	5.76
6	Log (Flexural Stiffness)	0.061[a]	0.004	-0.162	6.55

Table 7-23: ANOVA Summary of $N_{30\%}$_Single Seals

No.	Constant, a	Regression			Residual			Total		Significance of Regression	
		SSR	df	Mean Square	SSE	df	Mean Square	SST	df	F	Sig.
1	Age	52.51	1	52.51	205.97	6	34.33	258.48	7	1.53	0.262[b]
2	Climate	6.044	1	6.044	252.44	6	42.07	258.48	7	0.144	0.718[b]
3	Effective Thickness	60.43	1	60.43	198.05	6	33.01	258.48	7	1.83	0.225[b]
4	Moment of Inertia	61.90	1	61.90	196.58	6	32.76	258.48	7	1.889	0.218[b]
5	Log (Strain)	59.66	1	59.66	198.82	6	33.14	258.48	7	1.801	0.228[b]
6	Log(Flexural Stiffness)	0.954	1	0.954	257.53	6	42.92	258.48	7	0.022	0.886[b]

Table 7-24: Coefficient Summary of $N_{30\%}$_Single Seals

No.	Model	Unstandardized Coefficients		Standardized Coefficient	t	Sig.
		B	Std. Error	Beta		
1	Age	0.569	0.460	0.451	1.237	0.262
	Constant	0.557	6.995	-	0.080	0.939
2	Climate	379.34	1000.87	0.153	0.379	0.718
	Constant	-1509.85	4006.97	-	-0.377	0.719
3	Effective Thickness	1.06	0.785	0.484	1.353	0.225
	Constant	-11.25	14.97	-	-0.751	0.481
4	Moment of Inertia	183.67×10^6	13.36×10^6	0.489	1.375	0.218
	Constant	1.72	5.55	-	0.311	0.766
5	Log (Strain)	-56.362	42.003	-0.480	-1.342	0.228
	Constant	162.67	114.67	-	1.419	0.206
6	Log (Flexural Stiffness)	2.240	15.03	0.061	0.149	0.886
	Constant	0.717	54.41	-	0.013	0.990

- Significance of Age on Fatigue ($N_{30\%}$) in Single Seals:

Coefficient, R = 0.451, suggests that there is a weak relationship between the ages of single seals and fatigue, while the coefficient of determination, R^2 = 0.203, suggests that only 20% of the variance in the fatigue values of the single seals can be explained by the respective ages of the seals tested.

Significance, p = 0.262, meaning there is only 73.8% probability that the ages of the single seals can influence the outcome of fatigue ($N_{30\%}$). The regression model is therefore not statistically significant.

- Significance of Climate on Fatigue ($N_{30\%}$) in Single Seals:

Coefficient, R = 0.153, suggests that there is an even weaker relationship between the climate from which the single seals were sampled from and the fatigue values, than compared with the ages of the single seals. Furthermore the coefficient of determination, R^2 = 0.023, suggests that only 3% of the variance in the fatigue values can be explained by the effect of climate.

Significance, p = 0.718, meaning there is only 28.2% probability that the climate of the single seals can influence the outcome of fatigue ($N_{30\%}$). The regression model is therefore not statistically significant.

- Significance of Effective Thickness on Fatigue ($N_{30\%}$) in Single Seals:

Coefficient, R = 0.484, suggests that there exists also a weak relationship between the effective thickness of the single seals and the fatigue values. The coefficient of determination, R^2 = 0.234, suggests that only 23% of the variance in the fatigue values can be explained by the effective thickness of the single seals.

Significance, p = 0.225, meaning there is only 77.5% probability that effective thickness of the single seals can influence the outcome of fatigue ($N_{30\%}$). The regression model is therefore not statistically significant.

- Significance of Moment of Inertia on Fatigue ($N_{30\%}$) in Single Seals:

Coefficient, R = 0.489, suggests that a weak relationship exists between the moment of inertia (non-linearity of the thickness of the sampled sprayed seal) and the fatigue values. The coefficient of determination, R^2 = 0.239, furthermore suggests that only 24% of the variance in fatigue results for the single seals can attributed to the effect of the non-linearity of the thickness of the single seals.

Significance, p = 0.218, meaning there is only 78.2% probability that the moment of inertia of the cross section of the single seals can influence the outcome of fatigue ($N_{30\%}$). The regression model is therefore not statistically significant.

- Significance of Log (Strain) on Fatigue ($N_{30\%}$) in Single Seals:

Coefficient, R = 0.480, suggests that a weak relationship exists between the logarithmic value of the applied test strain and the fatigue of single seals. The coefficient of determination, R^2 = 0.231, furthermore suggests that only 23% of the variance in the fatigue values can be attributed to the effect of the logarithmic value of the applied test strain.

Significance, p = 0.228, meaning there is only 77.2% probability that the logarithmic strain applied during testing of the single seals can influence the outcome of fatigue ($N_{30\%}$). The regression model is therefore not statistically significant.

- Significance of Log (Flexural Stiffness) on Fatigue ($N_{30\%}$) in Single Seals:

Coefficient, R = 0.061, suggests that a very weak relationship exists between the logarithmic value of the flexural stiffness that was used as a direct input in the Classical Fatigue Characterisation Approach, as detailed in *Chapter 2 Literature Study.* Furthermore only 0.4% of the variance in the fatigue values can be explained by the logarithmic value of the flexural stiffness, described by the coefficient of determination, R^2 = 0.004.

Significance, p = 0.886, meaning there is only 11.4% probability that the logarithmic flexural stiffness from the flexural testing of the single seals can influence the outcome of fatigue ($N_{30\%}$). The regression model is therefore not statistically significant.

Influence on Fatigue (N$_{40\%}$):

Table 7-25: Model Summary of N$_{40\%}$_Single Seals

No.	Constant, a	R	R Squared	Adjusted R Squared	Std. Error of the Estimate
1	Age	0.395[a]	0.156	0.015	8.56
2	Climate	0.089[a]	0.008	-0.158	9.28
3	Effective Thickness	0.422[a]	0.178	0.041	8.44
4	Moment of Inertia	0.427[a]	0.182	0.046	8.42
5	Log (Strain)	0.426[a]	0.182	0.045	8.43
6	Log (Flexural Stiffness)	0.103[a]	0.011	-0.154	9.27

Table 7-26: ANOVA Summary of N$_{40\%}$_Single Seals

No.	Constant, a	Regression			Residual			Total		Significance of Regression	
		SSR	df	Mean Square	SSE	df	Mean Square	SST	df	F	Sig.
1	Age	81.05	1	81.05	439.49	6	73.25	520.54	7	1.11	0.333[b]
2	Climate	4.09	1	4.09	516.45	6	86.08	520.54	7	0.047	0.835[b]
3	Effective Thickness	92.82	1	92.82	427.72	6	71.29	520.54	7	1.302	0.297[b]
4	Moment of Inertia	94.90	1	94.90	425.63	6	70.94	520.54	7	1.34	0.291[b]
5	Log (Strain)	94.55	1	94.55	425.99	6	70.99	520.84	7	1.332	0.292[b]
6	Log(Flexural Stiffness)	5.47	1	5.47	515.07	6	85.85	520.54	7	0.064	0.809[b]

Table 7-27: Coefficient Summary of $N_{40\%}$_Single Seals

No.	Model	Unstandardized Coefficients		Standardized Coefficient	t	Sig.
		B	Std. Error	Beta		
1	Age	0.707	0.672	0.395	1.052	0.333
	Constant	0.500	10.22	-	0.049	0.963
2	Climate	311.88	1431.58	0.089	0.218	0.835
	Constant	-1237.84	5731.33	-	-0.216	0.836
3	Effective Thickness	1.316	1.153	0.422	1.141	0.297
	Constant	-14.11	22.00	-	-0.641	0.545
4	Moment of Inertia	227.42×10^6	196.62×10^6	0.427	1.157	0.291
	Constant	1.98	8.16	-	0.242	0.817
5	Log (Strain)	-70.95	61.48	-0.426	-1.154	0.292
	Constant	204.44	167.86	-	1.218	0.269
6	Log (Flexural Stiffness)	5.36	21.25	0.103	0.252	0.809
	Constant	-8.28	75.53	-	-0.110	0.916

235

- Significance of Age on Fatigue ($N_{40\%}$) in Single Seals:

Coefficient, R = 0.395, suggests that there is a weak relationship between the ages of single seals and fatigue, while the coefficient of determination, R^2 = 0.156, suggests that only 16% of the variance in the fatigue values of the single seals can be explained by the respective ages of the seals tested.

Significance, p = 0.333, meaning there is only 66.7% probability that ages of the single seals can influence the outcome of fatigue ($N_{40\%}$). The regression model is therefore not statistically significant.

- Significance of Climate on Fatigue ($N_{40\%}$) in Single Seals:

Coefficient, R = 0.089, suggests that there is an even weaker relationship between the climate from which the single seals were sampled from and the fatigue values, than compared with the ages of the single seals. Furthermore the coefficient of determination, R^2 = 0.008, suggests that only 0.8% of the variance in the fatigue values can be explained by the effect of climate.

Significance, p = 0.835, meaning there is only 16.5% probability that climate of the single seals can influence the outcome of fatigue ($N_{40\%}$). The regression model is therefore not statistically significant.

- Significance of Effective Thickness on Fatigue ($N_{40\%}$) in Single Seals:

Coefficient, R = 0.422, suggests that there exists also a weak relationship between the effective thickness of the single seals and the fatigue values. The coefficient of determination, R^2 = 0.178, suggests that only 18% of the variance in the fatigue values can be explained by the effective thickness of the single seals.

Significance, p = 0.297, meaning there is only 70.3% probability that effective thickness of the single seals can influence the outcome of fatigue ($N_{40\%}$). The regression model is therefore not statistically significant.

- Significance of Moment of Inertia on Fatigue ($N_{40\%}$) in Single Seals:

Coefficient, R = 0.427, suggests that a weak relationship exists between the moment of inertia (non-linearity of the thickness of the sampled sprayed seal) and the fatigue values. The coefficient of determination, R^2 = 0.182, furthermore suggests that only 18% of the variance in fatigue results for the single seals can attributed to the effect of the non-linearity of the thickness of the single seals.

Significance, p = 0.291, meaning there is only 70.9% probability that the moment of inertia of the cross section of single seals can influence the outcome of fatigue ($N_{40\%}$). The regression model is therefore not statistically significant.

- Significance of Log (Strain) on Fatigue ($N_{40\%}$) in Single Seals:

Coefficient, R = 0.426, suggests that a weak relationship exists between the logarithmic value of the applied test strain and the fatigue of single seals. The coefficient of determination, R^2 = 0.182, furthermore suggests that only 18% of the variance in the fatigue values can be attributed to the effect of the logarithmic value of the applied test strain.

Significance, p = 0.292, meaning there is only 70.8% probability that logarithmic strain during the flexural testing of the single seals can influence the outcome of fatigue ($N_{40\%}$). The regression model is therefore not statistically significant.

- Significance of Log (Flexural Stiffness) on Fatigue ($N_{40\%}$) in Single Seals:

Coefficient, R = 0.103, suggests that a very weak relationship exists between the logarithmic value of the flexural stiffness that was used as a direct input in the Classical Fatigue Characterisation Approach, as detailed in *Chapter 2 Literature Study.* Furthermore only 1% of the variance in the fatigue values can be explained by the logarithmic value of the flexural stiffness, described by the coefficient of determination, $R^2 = 0.011$.

Significance, p = 0.809, meaning there is only 19.1% probability that the logarithmic flexural stiffness of the single seals can influence the outcome of fatigue ($N_{40\%}$). The regression model is therefore not statistically significant.

Influence on Fatigue ($N_{50\%}$):

Table 7-28: Model Summary of $N_{50\%}$_Single Seals

No.	Constant, a	R	R Squared	Adjusted R Squared	Std. Error of the Estimate
1	Age	0.466[a]	0.217	0.086	11.01
2	Climate	0.161[a]	0.026	-0.137	12.28
3	Effective Thickness	0.497[a]	0.247	0.122	10.80
4	Moment of Inertia	0.503[a]	0.254	0.129	10.75
5	Log (Strain)	0.499[a]	0.249	0.123	10.79
6	Log (Flexural Stiffness)	0.046[a]	0.002	-0.164	12.43

Table 7-29: ANOVA Summary of N50%_Single Seals

No.	Constant, a	Regression			Residual			Total		Significance of Regression	
		SSR	df	Mean Square	SSE	df	Mean Square	SST	df	F	Sig.
1	Age	201.46	1	201.46	727.84	6	121.31	929.30	7	1.66	0.245[b]
2	Climate	23.99	1	23.99	905.31	6	150.89	929.30	7	0.159	0.704[b]
3	Effective Thickness	229.69	1	229.69	699.61	6	116.60	929.30	7	1.97	0.210[b]
4	Moment of Inertia	235.58	1	235.58	693.72	6	115.62	929.30	7	2.04	0.203[b]
5	Log (Strain)	230.97	1	230.97	698.33	6	116.39	929.30	7	1.984	0.209[b]
6	Log(Flexural Stiffness)	1.99	1	1.99	927.31	6	154.55	929.30	7	0.013	0.913[b]

Table 7-30: Coefficient Summary of $N_{50\%}$_Single Seals

No.	Model	Unstandardized Coefficients		Standardized Coefficient	t	Sig.
		B	Std. Error	Beta		
1	Age	1.115	0.865	0.466	1.289	0.245
	Constant	-2.28	13.150	-	-0.174	0.868
2	Climate	755.76	1895.39	0.161	0.399	0.704
	Constant	-3011.78	7588.19	-	-0.397	0.705
3	Effective Thickness	2.07	1.475	0.497	1.404	0.210
	Constant	-25.23	28.14	-	-0.897	0.404
4	Moment of Inertia	358.3×10^6	251.0×10^6	0.503	1.427	0.203
	Constant	0.056	10.42	-	0.005	0.996
5	Log (Strain)	-110.89	78.72	-0.499	-1.409	0.209
	Constant	316.61	214.92	-	1.473	0.191
6	Log (Flexural Stiffness)	3.26	28.78	0.064	0.113	0.913
	Constant	2.57	100.05	-	0.026	0.980

- Significance of Age on Fatigue ($N_{50\%}$) in Single Seals:

Coefficient, R = 0.466, suggests that there is a weak relationship between the ages of single seals and fatigue, while the coefficient of determination, R^2 = 0.217, suggests that only 22% of the variance in the fatigue values of the single seals can be explained by the respective ages of the seals tested.

Significance, p = 0.245, meaning there is only 75.5% probability that ages of the single seals can influence the outcome of fatigue ($N_{50\%}$). The regression model is therefore not statistically significant.

- Significance of Climate on Fatigue ($N_{50\%}$) in Single Seals:

Coefficient, R = 0.161, suggests that there is an even weaker relationship between the climate from which the single seals were sampled from and the fatigue values, than compared with the ages of the single seals. Furthermore the coefficient of determination, R^2 = 0.026, suggests that only 3% of the variance in the fatigue values can be explained by the effect of climate.

Significance, p = 0.704, meaning there is only 29.6% probability that climate of the single seals can influence the outcome of fatigue ($N_{50\%}$). The regression model is therefore not statistically significant.

- Significance of Effective Thickness on Fatigue ($N_{50\%}$) in Single Seals:

Coefficient, R = 0.497, suggests that there exists also a weak relationship between the effective thickness of the single seals and the fatigue values. The coefficient of determination, R^2 = 0.247, suggests that only 25% of the variance in the fatigue values can be explained by the effective thickness of the single seals.

Significance, p = 0.210, meaning there is only 79% probability that effective thickness of the single seals can influence the outcome of fatigue ($N_{50\%}$). The regression model is therefore not statistically significant.

- Significance of Moment of Inertia on Fatigue ($N_{50\%}$) in Single Seals:

Coefficient, R = 0.503, suggests that a weak relationship exists between the moment of inertia (non-linearity of the thickness of the sampled sprayed seal) and the fatigue values. The coefficient of determination, R^2 = 0.254, furthermore suggests that only 25% of the variance in fatigue results for the single seals can attributed to the effect of the non-linearity of the thickness of the single seals.

Significance, p = 0.203, meaning there is only 79.7% probability that moment of inertia of the cross section of the single seals can influence the outcome of fatigue ($N_{50\%}$). The regression model is therefore not statistically significant.

- Significance of Log (Strain) on Fatigue ($N_{50\%}$) in Single Seals:

Coefficient, R = 0.499, suggests that a weak relationship exists between the logarithmic value of the applied test strain and the fatigue of single seals. The coefficient of determination, R^2 = 0.249, furthermore suggests that only 25% of the variance in the fatigue values can be attributed to the effect of the logarithmic value of the applied test strain.

Significance, p = 0.209, meaning there is only 79.1% probability that logarithmic strain at which the single seals were tested can influence the outcome of fatigue ($N_{50\%}$). The regression model is therefore not statistically significant.

- Significance of Log (Flexural Stiffness) on Fatigue ($N_{50\%}$) in Single Seals:

Coefficient, R = 0.046, suggests that a very weak relationship exists between the logarithmic value of the flexural stiffness that was used as a direct input in the Classical Fatigue Characterisation Approach, as detailed in *Chapter 2 Literature Study.* Furthermore only 0.2% of the variance in the fatigue values can be explained by the logarithmic value of the flexural stiffness, described by the coefficient of determination, $R^2 = 0.002$.

Significance, p = 0.913, meaning there is only 8.7% probability that logarithmic flexural stiffness of the single seals can influence the outcome of fatigue ($N_{50\%}$). The regression model is therefore not statistically significant.

Sensitivity Analysis of Effective Thickness

Table 7-31: Influence of Effective Thickness on Fatigue ($N_{20\%}$)

Single Seals Thinner (-4.9mm)			Single Seals Thinner (-4.9mm)		
Variable	$N_{20\%}$			$N_{20\%}$		
	R	R 2	p	R	R 2	p
Log (Strain)	0.511	0.261	0.191	0.554	0.306	0.245
Log (Flexural Stiffness)	0.187	0.035	0.658	0.321	0.103	0.436
Age	0.156	0.024	0.712	0.32	0.102	0.44
Moment of Inertia	0.123	0.015	0.772	0.275	0.076	0.51
Effective Thickness	0.113	0.013	0.789	0.103	0.011	0.808
Climate	0.065	0.004	0.878	0.05	0.002	0.907

Table 7-32: Influence of Effective Thickness on Fatigue ($N_{30\%}$)

Single Seals Thinner (-4.9mm)			Single Seals Thicker (+3.1mm)		
Variable	$N_{30\%}$			$N_{30\%}$		
	R	R 2	p	R	R 2	p
Log Strain	0.576	0.332	0.135	0.545	0.297	0.262
Moment of Inertia	0.369	0.136	0.368	0.406	0.165	0.319
Effective Thickness	0.364	0.133	0.375	0.403	0.162	0.323
Age	0.324	0.105	0.433	0.362	0.131	0.378
Log (Flexural Stiffness)	0.091	0.008	0.831	0.101	0.01	0.812
Climate	0.079	0.006	0.852	0.054	0.003	0.9

Table 7-33: Influence of Effective Thickness on Fatigue ($N_{40\%}$)

Single Seals Thinner (-4.9mm)			Single Seals Thicker (+3.1mm)		
Variable	$N_{40\%}$			$N_{40\%}$		
	R	R 2	p	R	R 2	p
Log (Strain)	0.586	0.344	0.127	0.54	0.291	0.259
Moment of Inertia	0.415	0.173	0.306	0.454	0.206	0.259
Effective Thickness	0.41	0.168	0.313	0.45	0.202	0.264
Age	0.371	0.137	0.366	0.412	0.17	0.311
Climate	0.106	0.011	0.803	0.16	0.026	0.705
Log (Flexural Stiffness)	0.087	0.008	0.838	0.132	0.017	0.756

Table 7-34: Influence of Effective Thickness on Fatigue ($N_{50\%}$)

Single Seals Thinner (-4.9mm)			Single Seals Thicker (+3.1mm)		
Variable	$N_{50\%}$			$N_{50\%}$		
	R	R 2	p	R	R 2	p
Moment of Inertia	0.705	0.497	0.051	0.554	0.307	0.209
Effective Thickness	0.697	0.485	0.055	0.501	0.251	0.21
Age	0.673	0.453	0.067	0.497	0.247	0.21
Log (Strain)	0.614	0.377	0.12	0.464	0.215	0.247
Climate	0.261	0.068	0.532	0.182	0.033	0.667
Log (Flexural Stiffness)	0.207	0.043	0.622	0.15	0.022	0.723

Appendix 7 J2: Statistical Analysis of Individual Variables of Double Seals on the outcome of Fatigue:

Influence on Fatigue ($N_{20\%}$):

Table 7-35: Model Summary of $N_{20\%}$_Double Seals

No.	Constant, a	R	R Squared	Adjusted R Squared	Std. Error of the Estimate
1	Age	0.041[a]	0.002	-0.165	1.85
2	Climate	0.764[a]	0.584	0.515	1.19
3	Effective Thickness	0.192[a]	0.037	-0.124	1.82
4	Moment of Inertia	0.181[a]	0.033	-0.129	1.82
5	Log (Strain)	0.062[a]	0.004	-0.162	1.85
6	Log (Flexural Stiffness)	0.194[a]	0.038	-0.123	1.82

Table 7-36: ANOVA Summary of $N_{20\%}$_Double Seals

No.	Constant, a	Regression			Residual			Total		Significance of Regression	
		SSR	df	Mean Square	SSE	df	Mean Square	SST	df	F	Sig.
1	Age	0.034	1	0.034	20.56	6	3.43	20.59	7	0.010	0.923[b]
2	Climate	12.02	1	12.02	8.57	6	1.428	20.59	7	8.42	0.027[b]
3	Effective Thickness	0.757	1	0.757	19.83	6	3.31	20.59	7	0.229	0.649[b]
4	Moment of Inertia	0.673	1	0.673	119.92	6	3.32	20.59	7	0.203	0.668[b]
5	Log (Strain)	0.078	1	0.078	20.51	6	3.42	20.59	7	0.023	0.885[b]
6	Log(Flexural Stiffness)	0.776	1	0.776	1982	6	3.30	20.59	7	0.235	0.645[b]

Table 7-37: Coefficient Summary of N$_{20\%}$_Double Seals

No.	Model	Unstandardized Coefficients		Standardized Coefficient	t	Sig.
		B	Std. Error	Beta		
1	Age	0.017	0.168	0.041	0.100	0.923
	Constant	4.84	2.00	-	2.42	0.052
2	Climate	-0.578	0.199	-0.764	-2.90	0.027
	Constant	6.76	0.732	-	9.24	0.000
3	Effective Thickness	0.090	0.189	0.192	0.478	0.649
	Constant	2.65	5.00	-	0.529	0.616
4	Moment of Inertia	$10.2*10^6$	$22.7*10^6$	0.181	0.450	0.668
	Constant	3.98	2.42	-	1.64	0.152
5	Log (Strain)	2.04	13.49	0.062	0.151	0.885
	Constant	-0.545	36.83	-	-0.015	0.989
6	Log (Flexural Stiffness)	1.63	3.37	0.194	0.485	0.645
	Constant	-1.15	12.77	-	-0.090	0.931

- Significance of Age on Fatigue ($N_{20\%}$) in Double Seals:

Coefficient, R = 0.041, suggests that there is a very weak relationship between the ages of double seals and fatigue, while the coefficient of determination, R^2 = 0.002, suggests that only 0.2% of the variance in the fatigue values of the double seals can be explained by the respective ages of the seals tested.

Significance, p =0.923, meaning there is only 7.7% probability that ages of the double seals can influence the outcome of fatigue ($N_{20\%}$). The regression model is therefore not statistically significant.

- Significance of Climate on Fatigue ($N_{20\%}$) in Double Seals:

Coefficient, R = 0.764, suggests that there is a slightly positive relationship between the climate from which the double seals were sampled from and the fatigue values, a significant difference compared with the effect of the ages of the double seals. Furthermore the coefficient of determination, R^2 = 0.584, suggests that 58% of the variance in the fatigue values can be explained by the effect of climate.

Significance, p = 0.027, meaning there is a 97.3% probability that climate of the double seals can influence the outcome of fatigue ($N_{20\%}$). The regression model is therefore statistically significant.

- Significance of Effective Thickness on Fatigue ($N_{20\%}$) in Double Seals:

Coefficient, R = 0.192, suggests that there exists a weak relationship between the effective thickness of the double seals and the fatigue values. The coefficient of determination, R^2 = 0.037, suggests that only 4% of the variance in the fatigue values can be explained by the effective thickness of the double seals.

Significance, p = 0.649, meaning there is only 35.1% probability that effective thickness of the double seals can influence the outcome of fatigue ($N_{20\%}$). The regression model is therefore not statistically significant.

- Significance of Moment of Inertia on Fatigue ($N_{20\%}$) in Double Seals:

Coefficient, R = 0.181, suggests that a weak relationship exists between the moment of inertia (non-linearity of the thickness of the sampled sprayed seal) and the fatigue values. The coefficient of determination, R^2 = 0.033, furthermore suggests that only 4% of the variance in fatigue results for the double seals can attributed to the effect of the non-linearity of the thickness of the double seals.

Significance, p =0.668, meaning there is only 33.2% probability that moment of inertia of the cross section of the double seals can influence the outcome of fatigue ($N_{20\%}$). The regression model is therefore not statistically significant.

- Significance of Log (Strain) on Fatigue ($N_{20\%}$) in Double Seals:

Coefficient, R = 0.062, suggests that a weak relationship also exists between the logarithmic value of the applied test strain and the fatigue of double seals. The coefficient of determination, R^2 = 0.004 furthermore suggests that only 0.4% of the variance in the fatigue values can be attributed to the effect of the logarithmic value of the applied test strain.

Significance, p = 0.885, meaning there is only 11.5% probability that logarithmic strain applied during the flexural testing of the double seals can influence the outcome of fatigue ($N_{20\%}$). The regression model is therefore not statistically significant.

- Significance of Log (Flexural Stiffness) on Fatigue ($N_{20\%}$) in Double Seals:

Coefficient, R = 0.194, suggests that a weak relationship exists between the logarithmic value of the flexural stiffness that was used as a direct input in the Classical Fatigue Characterisation Approach, as detailed in *Chapter 2 Literature Study.* Furthermore only 4% of the variance in the fatigue values can be explained by the logarithmic value of the flexural stiffness, described by the coefficient of determination, $R^2 = 0.038$.

Significance, p = 0.645, meaning there is only 35.5% probability that logarithmic flexural stiffness of the double seals can influence the outcome of fatigue ($N_{20\%}$). The regression model is therefore not statistically significant.

In general, there exist a strong positive relationship plot between climate as an independent variable and the respective fatigue values ($N_{20\%}$) of the double seals, whereas a weak relationship exists for the remaining of the five (5) independent variables in the regression models. The independent single variable that best influenced the fatigue values, in descending order, are Climate, Log (Flexural Stiffness), Effective Thickness, Moment of Inertia, Log (Strain) and Age.

Influence on Fatigue (N$_{30\%}$):

Table 7-30: Model Summary of N$_{30\%}$_Double Seals

No.	Constant, a	R	R Squared	Adjusted R Squared	Std. Error of the Estimate
1	Age	0.019[a]	0.000	-0.166	2.70
2	Climate	0.741[a]	0.549	0.474	1.81
3	Effective Thickness	0.204[a]	0.042	-0.118	264
4	Moment of Inertia	0.194[a]	0.038	-0.123	2.65
5	Log (Strain)	0.068[a]	0.005	-0.161	2.69
6	Log (Flexural Stiffness)	0.201[a]	0.040	-0.120	2.64

Table 7-31: ANOVA Summary of N$_{30\%}$_Double Seals

No.	Constant, a	Regression			Residual			Total		Significance of Regression	
		SSR	df	Mean Square	SSE	df	Mean Square	SST	df	F	Sig.
1	Age	0.015	1	0.015	43.62	6	7.3	43.64	7	0.002	0.965[b]
2	Climate	23.97	1	23.97	19.66	6	3.28	43.64	7	7.32	0.035[b]
3	Effective Thickness	1.82	1	1.82	41.82	6	6.97	43.64	7	0.261	0.628[b]
4	Moment of Inertia	1.65	1	1.65	41.99	6	6.99	43.64	7	0.235	0.645[b]
5	Log (Strain)	0.200	1	0.200	43.44	6	7.24	43.64	7	0.028	0.874[b]
6	Log (Flexural Stiffness)	1.76	1	1.76	41.88	6	6.98	43.64	7	0.252	0.634[b]

Table 7-32: Coefficient Summary of N$_{30\%}$_Double Seals

No.	Model	Unstandardized Coefficients		Standardized Coefficient	t	Sig.
		B	Std. Error	Beta		
1	Age	0.011	0.245	0.019	0.046	0.965
	Constant	6.00	2.92	-	2.06	0.085
2	Climate	-0.816	0.302	-0.741	-2.71	0.035
	Constant	8.58	1.11	-	7.73	0.000
3	Effective Thickness	0.140	0.274	0.204	0.511	0.628
	Constant	2.443	7.27	-	0.336	0.748
4	Moment of Inertia	$15.9*10^6$	$32.91*10^6$	0.194	0.485	0.645
	Constant	4.48	3.52	-	1.279	0.249
5	Log (Strain)	3.26	19.63	0.068	0.166	0.874
	Constant	-2.77	53.60	-	-0.052	0.960
6	Log (Flexural Stiffness)	2.46	4.89	0.201	0.502	0.634
	Constant	.-3.04	18.28	-	-0.166	0.874

- Significance of Age on Fatigue ($N_{30\%}$) in Double Seals:

Coefficient, R = 0.019, suggests that there is a very weak relationship between the ages of double seals and fatigue, while the coefficient of determination, R^2 = 0.000, suggests that a negligible percentage (%) of the variance in the fatigue values of the double seals can be explained by the respective ages of the seals tested.

Significance, p = 0.965, meaning there is only 3.5% probability that ages of the double seals can influence the outcome of fatigue ($N_{30\%}$). The regression model is therefore not statistically significant.

- Significance of Climate on Fatigue ($N_{30\%}$) in Double Seals:

Coefficient, R = 0.741, suggests that there is a slightly positive relationship between the climate from which the double seals were sampled from and the fatigue values, a significant difference compared with the effect of the ages of the double seals. Furthermore the coefficient of determination, R^2 = 0.549, suggests that 55% of the variance in the fatigue values can be explained by the effect of climate.

Significance, p = 0.035, meaning there is 96.5% probability that climate of the double seals can influence the outcome of fatigue ($N_{30\%}$). The regression model is therefore statistically significant.

- Significance of Effective Thickness on Fatigue ($N_{30\%}$) in Double Seals:

Coefficient, R = 0.204, suggests that there exists a weak relationship between the effective thickness of the double seals and the fatigue values. The coefficient of determination, R^2 = 0.042, suggests that only 4% of the variance in the fatigue values can be explained by the effective thickness of the double seals.

Significance, p = 0.628, meaning there is only 37.2% probability that effective thickness of the double seals can influence the outcome of fatigue ($N_{30\%}$). The regression model is therefore not statistically significant.

- Significance of Moment of Inertia on Fatigue($N_{30\%}$) in Double Seals:

Coefficient, R = 0.194, suggests that a weak relationship exists between the moment of inertia (non-linearity of the thickness of the sampled sprayed seal) and the fatigue values. The coefficient of determination, R^2 = 0.038, furthermore suggests that only 4% of the variance in fatigue results for the double seals can attributed to the effect of the non-linearity of the thickness of the double seals.

Significance, p = 0.645, meaning there is only 35.5% probability that moment of inertia of the cross section of the double seals can influence the outcome of fatigue ($N_{30\%}$). The regression model is therefore not statistically significant.

- Significance of Log (Strain) on Fatigue ($N_{30\%}$) in Double Seals:

Coefficient, R = 0.068, suggests that a weak relationship also exists between the logarithmic value of the applied test strain and the fatigue of double seals. The coefficient of determination, R^2 = 0.005, furthermore suggests that only 0.5% of the variance in the fatigue values can be attributed to the effect of the logarithmic value of the applied test strain.

249

Significance, p = 0.874, meaning there is only 12.6% probability that logarithmic strain applied during flexural testing of the double seals can influence the outcome of fatigue ($N_{30\%}$). The regression model is therefore not statistically significant.

- Significance of Log (Flexural Stiffness) on Fatigue ($N_{30\%}$) in Double Seals:

Coefficient, R = 0.201, suggests that a weak relationship exists between the logarithmic value of the flexural stiffness that was used as a direct input in the Classical Fatigue Characterisation Approach, as detailed in *Chapter 2 Literature Study.* Furthermore only 4% of the variance in the fatigue values can be explained by the logarithmic value of the flexural stiffness, described by the coefficient of determination, $R^2 = 0.040$.

Significance, p = 0.634, meaning there is only 36.6% probability that logarithmic flexural stiffness of the double seals can influence the outcome of fatigue ($N_{30\%}$). The regression model is therefore not statistically significant.

Influence on Fatigue ($N_{40\%}$):

Table 7-33: Model Summary of $N_{40\%}$_Double Seals

No.	Constant, a	R	R Squared	Adjusted R Squared	Std. Error of the Estimate
1	Age	0.006[a]	0.000	-0.167	3.68
2	Climate	0.727[a]	0.528	0.449	2.53
3	Effective Thickness	0.211[a]	0.044	-0.115	3.60
4	Moment of Inertia	0.202[a]	0.041	-0.119	3.60
5	Log (Strain)	0.071[a]	0.005	-0.161	3.67
6	Log (Flexural Stiffness)	0.204[a]	0.042	-0.118	3.60

Table 7-38: ANOVA Summary of $N_{40\%}$_Double Seals

No.	Constant, a	Regression			Residual			Total		Significance of Regression	
		SSR	df	Mean Square	SSE	df	Mean Square	SST	df	F	Sig.
1	Age	0.002	1	0.002	81.17	6	13.53	81.17	7	0.000	0.990[b]
2	Climate	42.87	1	42.87	38.31	6	6.38	81.17	7	6.71	0.041[b]
3	Effective Thickness	3.61	1	3.61	77.56	6	12.93	81.17	7	0.279	0.616[b]
4	Moment of Inertia	3.29	1	3.29	77.88	6	12.98	81.17	7	0.254	0.632[b]
5	Log (Strain)	0.410	1	0.410	80.76	6	13.46	81.17	7	0.030	0.867[b]
6	Log (Flexural Stiffness)	3.37	1	3.37	77.8	6	12.97	81.17	7	0.260	0.628[b]

Table 7-39: Coefficient Summary of N$_{40\%}$_Double Seals

No.	Model	Unstandardized Coefficients		Standardized Coefficient	t	Sig.
		B	Std. Error	Beta		
1	Age	0.005	0.334	0.006	0.014	0.990
	Constant	7.35	3.98	-	1.85	0.114
2	Climate	-1.09	0.421	-0.727	-2.59	0.041
	Constant	10.67	1.55	-	6.89	0.000
3	Effective Thickness	0.197	0.374	0.211	0.529	0.616
	Constant	2.20	9.91	-	0.222	0.831
4	Moment of Inertia	$22.6*10^6$	$44.8*10^6$	0.202	0.504	0.632
	Constant	5.07	4.79	-	1.06	0.330
5	Log (Strain)	4.67	26.77	0.071	0.171	0.867
	Constant	-5.36	73.09	-	-0.073	0.944
6	Log (Flexural Stiffness)	3.40	24.47	0.204	0.510	0.628
	Constant	.-5.07	24.47	-	-0.207	0.843

- Significance of Age on Fatigue ($N_{40\%}$) in Double Seals:

Coefficient, R = 0.006, suggests that there is a very weak relationship between the ages of double seals and fatigue, while the coefficient of determination, R^2, of .000, suggests that a negligible percentage (%) of the variance in the fatigue values of the double seals can be explained by the respective ages of the seals tested.

Significance, p = 0.990, meaning there is only 1% probability that ages of the double seals can influence the outcome of fatigue ($N_{40\%}$). The regression model is therefore not statistically significant.

- Significance of Climate on Fatigue ($N_{40\%}$) in Double Seals:

Coefficient, R = 0.727, suggests that there is a slightly positive relationship between the climate from which the double seals were sampled from and the fatigue values, a significant difference compared with the effect of the ages of the double seals. Furthermore the coefficient of determination, R^2 = 0.528, suggests that 53% of the variance in the fatigue values can be explained by the effect of climate.

Significance, p = 0.041, meaning there is 95.9% probability that climate of the double seals can influence the outcome of fatigue ($N_{40\%}$). The regression model is therefore not statistically significant.

- Significance of Effective Thickness on Fatigue ($N_{40\%}$) in Double Seals:

Coefficient, R = 0.211, suggests that there exists a weak relationship between the effective thickness of the double seals and the fatigue values. The coefficient of determination, R^2 = 0.044, suggests that only 4% of the variance in the fatigue values can be explained by the effective thickness of the double seals.

Significance, p = 0.616, meaning there is only 38.4% probability that effective thickness of the double seals can influence the outcome of fatigue ($N_{40\%}$). The regression model is therefore not statistically significant.

- Significance of Moment of Inertia on Fatigue ($N_{40\%}$) in Double Seals:

Coefficient, R = 0.202, suggests that a weak relationship exists between the moment of inertia (non-linearity of the thickness of the sampled sprayed seal) and the fatigue values. The coefficient of determination, R^2 = 0.041, furthermore suggests that only 4% of the variance in fatigue results for the double seals can attributed to the effect of the non-linearity of the thickness of the double seals.

Significance, p = 0.632, meaning there is only 36.8% probability that moment of inertia of the cross section of the double seals can influence the outcome of fatigue ($N_{40\%}$). The regression model is therefore not statistically significant.

- Significance of Log (Strain) on Fatigue ($N_{40\%}$) in Double Seals:

Coefficient, R = 0.071, suggests that a weak relationship also exists between the logarithmic value of the applied test strain and the fatigue of double seals. The coefficient of determination, R^2 = 0.005, furthermore suggests that only 0.5% of the variance in the fatigue values can be attributed to the effect of the logarithmic value of the applied test strain.

Significance, p = 0.867, meaning there is only 13.3% probability that logarithmic strain applied during the flexural testing of the double seals can influence the outcome of fatigue ($N_{40\%}$). The regression model is therefore not statistically significant.

- Significance of Log (Flexural Stiffness) on Fatigue ($N_{40\%}$) in Double Seals:

Coefficient, R = 0.204, suggests that a weak relationship exists between the logarithmic value of the flexural stiffness that was used as a direct input in the Classical Fatigue Characterisation Approach, as detailed in *Chapter 2 Literature Study.* Furthermore only 4% of the variance in the fatigue values can be explained by the logarithmic value of the flexural stiffness, described by the coefficient of determination, $R^2 = 0.042$.

Significance, p = 0.628, meaning there is only 37.2% probability that the logarithmic flexural stiffness of the double seals can influence the outcome of fatigue ($N_{40\%}$). The regression model is therefore not statistically significant.

Influence on Fatigue ($N_{50\%}$):

Table 7-40: Model Summary of $N_{50\%}$_Double Seals

No.	Constant, a	R	R Squared	Adjusted R Squared	Std. Error of the Estimate
1	Age	0.003[a]	0.000	-0.167	4.84
2	Climate	0.717[a]	0.513	0.432	3.38
3	Effective Thickness	0.215[a]	0.046	-0.113	4.73
4	Moment of Inertia	0.206[a]	0.043	-0.117	4.74
5	Log (Strain)	0.073[a]	0.005	-0.160	4.83
6	Log (Flexural Stiffness)	0.206[a]	0.042	-0.117	4.74

Table 7-41: ANOVA Summary of $N_{50\%}$_Double Seals

No.	Constant, a	Regression			Residual			Total		Significance of Regression	
		SSR	df	Mean Square	SSE	df	Mean Square	SST	df	F	Sig.
1	Age	0.001	1	0.001	140.67	6	23.44	140.68	7	0.000	0.994[b]
2	Climate	72.22	1	72.22	68.45	6	11.41	140.67	7	6.33	0.046[b]
3	Effective Thickness	6.53	1	6.53	134.14	6	22.36	140.67	7	0.292	0.608[b]
4	Moment of Inertia	5.99	1	5.99	134.68	6	22.45	140.67	7	0.267	0.624[b]
5	Log (Strain)	0.755	1	0.755	139.9	6	23.3	140.67	7	0.032	0.863[b]
6	Log (Flexural Stiffness)	5.98	1	5.98	134.69	6	22.45	140.67	7	0.266	0.624[b]

Table 7-42: Coefficient Summary of N$_{50\%}$_Double Seals

No.	Model	Unstandardized Coefficients		Standardized Coefficient	t	Sig.
		B	Std. Error	Beta		
1	Age	-0.003	0.439	-0.003	-0.007	0.994
	Constant	8.93	5.23	-	1.71	0.139
2	Climate	-1.42	0.563	-0.717	-2.52	0.046
	Constant	13.15	2.07	-	6.36	0.001
3	Effective Thickness	0.265	0.491	0.215	0.540	0.608
	Constant	1.92	13.03	-	0.147	0.888
4	Moment of Inertia	30.4×10^{6}	58.9×10^{6}	0.206	0.517	0.624
	Constant	5.76	6.3	-	0.916	0.395
5	Log (Strain)	6.34	35.24	0.073	0.180	0.863
	Constant	-8.41	96.19	-	-0.087	0.933
6	Log (Flexural Stiffness)	4.53	8.77	0.206	0.516	0.624
	Constant	.-7.33	31.49	-	-0.233	0.824

- Significance of Age on Fatigue ($N_{50\%}$) in Double Seals:

Coefficient, R = 0.003, suggests that there is a very weak relationship between the ages of double seals and fatigue, while the coefficient of determination, R^2 = 0.000, suggests that a negligible percentage (%) of the variance in the fatigue values of the double seals can be explained by the respective ages of the seals tested.

Significance, p = 0.994, meaning there is only 0.6% probability that ages of the double seals can influence the outcome of fatigue ($N_{50\%}$). The regression model is therefore not statistically significant.

- Significance of Climate on Fatigue ($N_{50\%}$) in Double Seals:

Coefficient, R = 0.717, suggests that there is a slightly positive relationship between the climate from which the double seals were sampled from and the fatigue values, a significant difference compared with the effect of the ages of the double seals. Furthermore the coefficient of determination, R^2, of 0.513, suggests that 51% of the variance in the fatigue values can be explained by the effect of climate.

Significance, p = 0.046, meaning there is 95.4% probability that climate of the double seals can influence the outcome of fatigue ($N_{50\%}$). The regression model is therefore statistically significant.

- Significance of Effective Thickness on Fatigue ($N_{50\%}$) in Double Seals:

Coefficient, R = 0.215, suggests that there exists a weak relationship between the effective thickness of the double seals and the fatigue values. The coefficient of determination, R^2 = 0.046, suggests that only 5% of the variance in the fatigue values can be explained by the effective thickness of the double seals.

Significance, p = 0.608, meaning there is only 39.2% probability that effective thickness of the double seals can influence the outcome of fatigue ($N_{50\%}$). The regression model is therefore not statistically significant.

- Significance of Moment of Inertia on Fatigue ($N_{50\%}$) in Double Seals:

Coefficient, R = 0.206, suggests that a weak relationship exists between the moment of inertia (non-linearity of the thickness of the sampled sprayed seal) and the fatigue values. The coefficient of determination, R^2 = 0.043, furthermore suggests that only 4% of the variance in fatigue results for the double seals can attributed to the effect of the non-linearity of the thickness of the double seals.

Significance, p = 0.624, meaning there is only 37.6% probability that moment of inertia of the cross section of the double seals can influence the outcome of fatigue ($N_{50\%}$). The regression model is therefore not statistically significant.

- Significance of Log (Strain) on Fatigue ($N_{50\%}$) in Double Seals:

Coefficient, R = 0.073, suggests that a weak relationship also exists between the logarithmic value of the applied test strain and the fatigue of double seals. The coefficient of determination, R^2 = 0.005, furthermore suggests that only 0.5% of the variance in the fatigue values can be attributed to the effect of the logarithmic value of the applied test strain.

257

Significance, p = 0.865, meaning there is only 13.5% probability that logarithmic strain applied during flexural testing of the double seals can influence the outcome of fatigue ($N_{50\%}$). The regression model is therefore not statistically significant.

- Significance of Log (Flexural Stiffness) on Fatigue ($N_{50\%}$) in Double Seals:

Coefficient, R = 0.206, suggests that a weak relationship exists between the logarithmic value of the flexural stiffness that was used as a direct input in the Classical Fatigue Characterisation Approach, as detailed in *Chapter 2 Literature Study.* Furthermore only 4% of the variance in the fatigue values can be explained by the logarithmic value of the flexural stiffness, described by the coefficient of determination, $R^2 = 0.042$.

Significance, p = 0.624, meaning there is only 37.6% probability that logarithmic flexural stiffness of the double seals can influence the outcome of fatigue ($N_{50\%}$). The regression model is therefore not statistically significant.

Appendix 7 J3: Statistical Analysis of Individual Variables of Cape Seals on the outcome of Fatigue:

Influence on Fatigue (N$_{20\%}$):

Table 7-43: Model Summary of N$_{20\%}$_Cape Seals

No.	Constant, a	R	R Squared	Adjusted R Squared	Std. Error of the Estimate
1	Age	0.230[a]	0.053	-0.184	0.085
2	Climate	0.095[a]	0.009	-0.239	0.087
3	Effective Thickness	0.295[a]	0.087	-0.141	0.083
4	Moment of Inertia	0.283[a]	0.080	-0.105	0.084
5	Log (Strain)	0.753[a]	0.567	0.459	0.057
6	Log (Flexural Stiffness)	0.607[a]	0.369	0.211	0.069

Table 7-44: ANOVA Summary of N$_{20\%}$_Cape Seals

No.	Constant, a	Regression			Residual			Total		Significance of Regression	
		SSR	df	Mean Square	SSE	df	Mean Square	SST	df	F	Sig.
1	Age	0.002	1	0.002	0.029	4	0.007	0.030	5	0.223	0.661[b]
2	Climate	0.000	1	0.000	0.030	4	0.008	0.030	5	0.036	0.858[b]
3	Effective Thickness	0.003	1	0.003	0.028	4	0.007	0.030	5	0.380	0.571[b]
4	Moment of Inertia	0.002	1	0.002	0.028	4	0.007	0.030	5	0.348	0.587[b]
5	Log (Strain)	0.017	1	0.017	0.013	4	0.003	0.030	5	5.24	0.084[b]
6	Log (Flexural Stiffness)	0.011	1	0.011	0.019	4	0.005	0.030	5	2.34	0.201[b]

Table 7-45: Coefficient Summary of N$_{20\%}$_Cape Seals

No.	Model	Unstandardized Coefficients		Standardized Coefficient	t	Sig.
		B	Std. Error	Beta		
1	Age	-0.006	0.012	-0.230	-0.473	0.661
	Constant	4.08	0.104	-	39.31	0.000
2	Climate	-3.95	20.74	-0.095	-190	0.858
	Constant	19.85	83.02	-	0.239	0.823
3	Effective Thickness	0.005	0.008	0.295	0.617	0.571
	Constant	3.88	0.255	-	15.24	0.000
4	Moment of Inertia	$0.29*10^6$	$0.5*10^6$	0.283	0.590	0.587
	Constant	3.99	0.092	-	43.49	0.000
5	Log (Strain)	1.106	0.483	0.753	2.29	0.084
	Constant	1.017	1.32	-	0.771	0.484
6	Log (Flexural Stiffness)	-0.346	0.226	-0.607	-1.53	0.201
	Constant	5.39	0.887	-	6.08	0.004

260

- Significance of Age on Fatigue ($N_{20\%}$) in Cape Seals:

Coefficient, R = 0.230, suggests that there is a weak relationship between the ages of cape seals and fatigue, while the coefficient of determination, R^2 = 0.053, suggests that only 5.3% of the variance in the fatigue values of the cape seals can be explained by the respective ages of the seals tested.

Significance, p = 0.661, meaning there is only 33.9% probability that ages of the cape seals can influence the outcome of fatigue ($N_{20\%}$). The regression model is therefore not statistically significant.

- Significance of Climate on Fatigue ($N_{20\%}$) in Cape Seals:

Coefficient, R = 0.095, suggests that there is a weak relationship between the climate from which the cape seals were sampled from and the fatigue values. Furthermore the coefficient of determination, R^2 = 0.009, suggests that only 0.9% of the variance in the fatigue values can be explained by the effect of climate.

Significance, p = 0.858, meaning there is only 14.2% probability that climate of the cape seals can influence the outcome of fatigue ($N_{20\%}$). The regression model is therefore not statistically significant.

- Significance of Effective Thickness on Fatigue ($N_{20\%}$) in Cape Seals:

Coefficient, R = 0.295, suggests that there exists a weak relationship between the effective thickness of the cape seals and the fatigue values. The coefficient of determination, R^2 = 0.087, suggests that only 8.7% of the variance in the fatigue values can be explained by the effective thickness of the cape seals.

Significance, p = 0.571, meaning there is only 42.9% probability that the effective thickness of the cape seals can influence the outcome of fatigue ($N_{20\%}$). The regression model is therefore not statistically significant.

- Significance of Moment of Inertia on Fatigue ($N_{20\%}$) in Cape Seals:

Coefficient, R = 0.283, suggests that a weak relationship exists between the moment of inertia (non-linearity of the thickness of the sampled sprayed seal) and the fatigue values. The coefficient of determination, R^2 = 0.080, furthermore suggests that only 8% of the variance in fatigue results for the cape seals can be attributed to the effect of the non-linearity of the thickness of the cape seals.

Significance, p = 0.587, meaning there is only 41.3% probability that moment of inertia of the cross section of the cape seals can influence the outcome of fatigue ($N_{20\%}$). The regression model is therefore not statistically significant.

- Significance of Log (Strain) on Fatigue ($N_{20\%}$) in Cape Seals:

Coefficient, R = 0.753, suggests that a slightly positive relationship between the logarithmic value of the applied test strain and the fatigue of cape seals. The coefficient of determination, R^2 = 0.567, furthermore suggests that 56.7% of the variance in the fatigue values can be attributed to the effect of the logarithmic value of the applied test strain.

Significance, p = 0.084, meaning there is 91.6% probability that logarithmic strain applied during flexural testing of the cape seals can influence the outcome of fatigue ($N_{20\%}$). The regression model is however not statistically significant.

- Significance of Log (Flexural Stiffness) on Fatigue ($N_{20\%}$) in Cape Seals:

Coefficient, R = 0.607, suggests that a weak relationship exists between the logarithmic value of the flexural stiffness that was used as a direct input in the Classical Fatigue Characterisation Approach, as detailed in *Chapter 2 Literature Study.* Furthermore only 36.9% of the variance in the fatigue values can be explained by the logarithmic value of the flexural stiffness, described by the coefficient of determination, R^2 = 0.369.

Significance, p = 0.201, meaning there is only 79.9% probability that the logarithmic flexural stiffness of the cape seals can influence the outcome of fatigue ($N_{20\%}$). The regression model is therefore not statistically significant.

In general, there exist a slightly positive relationship between the logarithmic strain and fatigue ($N_{20\%}$), but with low statistical significance. Weak relationship plots exists for the remaining five (5) individual independent variables and the respective fatigue values of the cape seals, as well as low statistical significance.

The independent individual variable that best influenced the fatigue values ($N_{20\%}$), in descending order, are Log (Strain), Log (Flexural Stiffness), Effective Thickness, Moment of Inertia, Age and Climate.

Influence on Fatigue ($N_{30\%}$):

Table 7-46: Model Summary of $N_{30\%}$_Cape Seals

No.	Constant, a	R	R Squared	Adjusted R Squared	Std. Error of the Estimate
1	Age	0.791[a]	0.625	0.532	0.055
2	Climate	0.755[a]	0.570	0.463	0.059
3	Effective Thickness	0.891[a]	0.793	0.742	0.041
4	Moment of Inertia	0.881[a]	0.776	0.720	0.042
5	Log (Strain)	0.367[a]	0.135	-0.081	0.083
6	Log (Flexural Stiffness)	0.169[a]	0.029	-0.214	0.088

Table 7-47: ANOVA Summary of $N_{30\%}$_Cape Seals

No.	Constant, a	Regression			Residual			Total		Significance of Regression	
		SSR	df	Mean Square	SSE	df	Mean Square	SST	df	F	Sig.
1	Age	0.020	1	0.020	0.012	4	0.003	0.032	5	6.67	0.061[b]
2	Climate	0.018	1	0.018	0.014	4	0.003	0.032	5	5.30	0.083[b]
3	Effective Thickness	0.025	1	0.025	0.007	4	0.002	0.032	5	15.65	0.017[b]
4	Moment of Inertia	0.025	1	0.025	0.007	4	0.002	0.032	5	13.84	0.020[b]
5	Log (Strain)	0.004	1	0.004	0.028	4	0.007	0.032	5	0.624	0.474[b]
6	Log (Flexural Stiffness)	0.001	1	0.001	0.031	4	0.008	0.032	5	0.118	0.749[b]

Table 7-48: Coefficient Summary of N$_{30\%}$_Cape Seals

No.	Model	Unstandardized Coefficients		Standardized Coefficient	t	Sig.
		B	Std. Error	Beta		
1	Age	-0.020	0.008	-0.791	-2.58	0.061
	Constant	4.60	0.067	-	68.79	0.000
2	Climate	-32.2	13.98	-0.755	-2.303	0.083
	Constant	133.33	55.97	-	2.38	0.076
3	Effective Thickness	0.016	0.004	0.891	3.92	0.017
	Constant	3.96	0.124	-	31.92	0.000
4	Moment of Inertia	$0.94*10^6$	$0.25*10^6$	0.881	3.72	0.020
	Constant	4.28	0.046	-	92.35	0.000
5	Log (Strain)	0.552	0.699	0.367	0.790	0.474
	Constant	2.93	1.91	-	1.54	0.200
6	Log (Flexural Stiffness)	-0.099	0.287	-0.169	-0.343	0.012
	Constant	4.82	1.11	-	4.34	0.749

- Significance of Age on Fatigue ($N_{30\%}$) in Cape Seals:

Coefficient, R = 0.791, suggests that there is a slightly positive relationship between the ages of cape seals and fatigue, while the coefficient of determination, R^2 = 0.625, suggests that 62.5% of the variance in the fatigue values of the cape seals can be explained by the respective ages of the seals tested.

Significance, p = 0.061, meaning there is 93.9% probability that the ages of the cape seals can influence the outcome of fatigue ($N_{30\%}$). The regression model is however not statistically significant.

- Significance of Climate on Fatigue ($N_{30\%}$) in Cape Seals:

Coefficient, R = 0.755, suggests that there is a slightly positive relationship between the climate from which the cape seals were sampled from and the fatigue values. Furthermore the coefficient of determination, R^2 = 0.570, suggests that 57% of the variance in the fatigue values can be explained by the effect of climate.

Significance, p = 0.083, meaning there is 91.7% probability that the climate of the cape seals can influence the outcome of fatigue ($N_{30\%}$). The regression model is however not statistically significant.

- Significance of Effective Thickness on Fatigue ($N_{30\%}$) in Cape Seals:

Coefficient, R = 0.891, suggests that there exists a positive relationship between the effective thickness of the cape seals and the fatigue values. The coefficient of determination, R^2 = 0.793, suggests that 79.3% of the variance in the fatigue values can be explained by the effective thickness of the cape seals.

Significance, p = 0.017, meaning there is 98.3% probability that the effective thickness of the cape seals can influence the outcome of fatigue ($N_{30\%}$). The regression model is therefore statistically significant.

- Significance of Moment of Inertia on Fatigue ($N_{30\%}$) in Cape Seals:

Coefficient, R = 0.881, suggests that a positive relationship exists between the moment of inertia (non-linearity of the thickness of the sampled sprayed seal) and the fatigue values. The coefficient of determination, R^2 = 0.776, furthermore suggests that 77.6% of the variance in fatigue results for the cape seals can be attributed to the effect of the non-linearity of the thickness of the cape seals.

Significance, p = 0.020, meaning there is 98% probability that the moment of inertia of the cross section of the cape seals can influence the outcome of fatigue ($N_{30\%}$). The regression model is therefore statistically significant.

- Significance of Log (Strain) on Fatigue ($N_{30\%}$) in Cape Seals:

Coefficient, R = 0.367, suggests that a weak relationship exists between the logarithmic value of the applied test strain and the fatigue of cape seals. The coefficient of determination, R^2 = 0.135, furthermore suggests that only 13.5% of the variance in the fatigue values can be attributed to the effect of the logarithmic value of the applied test strain.

Significance, p = 0.474, meaning there is only 52.6% probability that the logarithmic strain applied during the flexural testing of the cape seals can influence the outcome of fatigue ($N_{30\%}$). The regression model is therefore not statistically significant.

- Significance of Log (Flexural Stiffness) on Fatigue ($N_{30\%}$) in Cape Seals:

Coefficient, R = 0.169, suggests that a weak relationship exists between the logarithmic value of the flexural stiffness that was used as a direct input in the Classical Fatigue Characterisation Approach, as detailed in *Chapter 2 Literature Study.* Furthermore only 2.9% of the variance in the fatigue values can be explained by the logarithmic value of the flexural stiffness, described by the coefficient of determination, $R^2 = 0.029$.

Significance, p = 0.749, meaning there is only 25.1% probability that the effective thickness of the cape seals can influence the outcome of fatigue ($N_{30\%}$). The regression model is therefore not statistically significant.

Influence on Fatigue (N$_{40\%}$):

Table 7-49: Model Summary of N$_{40\%}$_Cape Seals

No.	Constant, a	R	R Squared	Adjusted R Squared	Std. Error of the Estimate
1	Age	0.878[a]	0.771	0.741	0.070
2	Climate	0.924[a]	0.854	0.817	0.056
3	Effective Thickness	0.965[a]	0.931	0.913	0.039
4	Moment of Inertia	0.960[a]	0.921	0.901	0.041
5	Log (Strain)	0.035[a]	0.001	-2.48	0.147
6	Log (Flexural Stiffness)	0.195[a]	0.038	-0.202	0.144

Table 7-50: ANOVA Summary of N$_{40\%}$_Cape Seals

No.	Constant, a	Regression			Residual			Total		Significance of Regression	
		SSR	df	Mean Square	SSE	df	Mean Square	SST	df	F	Sig.
1	Age	0.066	1	0.066	0.020	4	0.005	0.086	5	13.48	0.021[b]
2	Climate	0.074	1	0.074	0.013	4	0.003	0.086	5	23.38	0.008[b]
3	Effective Thickness	0.080	1	0.080	0.006	4	0.001	0.086	5	53.56	0.002[b]
4	Moment of Inertia	0.079	1	0.079	0.007	4	0.002	0.086	5	46.64	0.002[b]
5	Log (Strain)	0.000	1	0.000	0.086	4	0.022	0.086	5	0.005	0.947[b]
6	Log (Flexural Stiffness)	0.003	1	0.003	0.083	4	0.021	0.086	5	0.158	0.711[b]

Table 7-51: Coefficient Summary of N$_{40\%}$_Cape Seals

No.	Model	Unstandardized Coefficients		Standardized Coefficient	t	Sig.
		B	Std. Error	Beta		
1	Age	-0.037	0.010	-0.878	-3.67	0.021
	Constant	5.19	0.086	-	60.47	0.000
2	Climate	-64.82	13.41	-0.924	-4.84	0.008
	Constant	264.36	53.66	-	4.93	0.008
3	Effective Thickness	0.028	0.004	0.965	7.32	0.002
	Constant	4.04	0.118	-	34.18	0.000
4	Moment of Inertia	1.69×10^{6}	0.25×10^{6}	0.960	6.83	0.002
	Constant	4.61	0.045	-	102.02	0.000
5	Log (Strain)	-0.087	1.24	-0.035	-.071	0.947
	Constant	5.14	3.37	-	1.52	0.202
6	Log (Flexural Stiffness)	0.187	0.470	0.195	0.398	0.711
	Constant	4.19	1.79	-	2.35	0.079

- Significance of Age on Fatigue ($N_{40\%}$) in Cape Seals:

Coefficient, R = 0.878, suggests that there is a positive relationship between the ages of cape seals and fatigue, while the coefficient of determination, R^2 = 0.771, suggests that 77.1% of the variance in the fatigue values of the cape seals can be explained by the respective ages of the seals tested.

Significance, p = 0.021, meaning there is 97.9% probability that the ages of the cape seals can influence the outcome of fatigue ($N_{40\%}$). The regression model is therefore statistically significant

- Significance of Climate on Fatigue ($N_{40\%}$) in Cape Seals:

Coefficient, R = 0.924, suggests that there is a strong positive relationship between the climate from which the cape seals were sampled from and the fatigue values. Furthermore the coefficient of determination, R^2 = 0.854, suggests that 85.4% of the variance in the fatigue values can be explained by the effect of climate.

Significance, p = 0.008, meaning there is 99.2% probability that the climate of the cape seals can influence the outcome of fatigue ($N_{40\%}$). The regression model is therefore statistically significant.

- Significance of Effective Thickness on Fatigue ($N_{40\%}$) in Cape Seals:

Coefficient, R = 0.965, suggests that there exists a strong positive relationship between the effective thickness of the cape seals and the fatigue values. The coefficient of determination, R^2 = 0.931, suggests that 93.1% of the variance in the fatigue values can be explained by the effective thickness of the cape seals.

Significance, p = 0.002, meaning there is 99.8% probability that the effective thickness of the cape seals can influence the outcome of fatigue ($N_{40\%}$). The regression model is therefore statistically significant.

- Significance of Moment of Inertia on Fatigue ($N_{40\%}$) in Cape Seals:

Coefficient, R = 0.960, suggests that a strong positive relationship exists between the moment of inertia (non-linearity of the thickness of the sampled sprayed seal) and the fatigue values. The coefficient of determination, R^2 = 0.921, furthermore suggests that 92.1% of the variance in fatigue results for the cape seals can be attributed to the effect of the non-linearity of the thickness of the cape seals.

Significance, p = 0.002, meaning there is 99.8% probability that the moment of inertia of the cross section of the cape seals can influence the outcome of fatigue ($N_{40\%}$). The regression model is therefore statistically significant.

- Significance of Log (Strain) on Fatigue ($N_{40\%}$) in Cape Seals:

Coefficient, R = 0.035, suggests that a weak relationship exists between the logarithmic value of the applied test strain and the fatigue of cape seals. The coefficient of determination, R^2 = 0.001, furthermore suggests that only 0.1% of the variance in the fatigue values can be attributed to the effect of the logarithmic value of the applied test strain.

Significance, p = 0.947, meaning there is only 5.3% probability that the logarithmic strain applied during the flexural testing of the cape seals can influence the outcome of fatigue ($N_{40\%}$). The regression model is therefore not statistically significant.

- Significance of Log (Flexural Stiffness) on Fatigue ($N_{40\%}$) in Cape Seals:

Coefficient, R = 0.195, suggests that a weak relationship exists between the logarithmic value of the flexural stiffness that was used as a direct input in the Classical Fatigue Characterisation Approach, as detailed in *Chapter 2 Literature Study*. Furthermore only 3.8% of the variance in the fatigue values can be explained by the logarithmic value of the flexural stiffness, described by the coefficient of determination, $R^2 = 0.038$.

Significance, p = 0.711, meaning there is only 28.9% probability that the effective thickness of the cape seals can influence the outcome of fatigue ($N_{40\%}$). The regression model is therefore not statistically significant.

Influence on Fatigue ($N_{50\%}$):

Table 7-52: Model Summary of $N_{50\%}$_Cape Seals

No.	Constant, a	R	R Squared	Adjusted R Squared	Std. Error of the Estimate
1	Age	0.838^a	0.702	0.627	0.129
2	Climate	0.916^a	0.839	0.798	0.095
3	Effective Thickness	0.910^a	0.829	0.786	0.098
4	Moment of Inertia	0.908^a	0.824	0.780	0.099
5	Log (Strain)	0.212^a	0.045	-0.194	0.231
6	Log (Flexural Stiffness)	0.340^a	0.116	-0.105	0.222

Table 7-53: ANOVA Summary of $N_{50\%}$_Cape Seals

No.	Constant, a	Regression			Residual			Total		Significance of Regression	
		SSR	df	Mean Square	SSE	df	Mean Square	SST	df	F	Sig.
1	Age	0.157	1	0.157	0.067	4	0.017	0.223	5	9.41	0.037^b
2	Climate	0.187	1	0.187	0.036	4	0.009	0.223	5	20.80	0.010^b
3	Effective Thickness	0.185	1	0.185	0.038	4	0.010	0.223	5	19.33	0.012^b
4	Moment of Inertia	0.184	1	0.184	0.039	4	0.010	0.223	5	18.78	0.012^b
5	Log (Strain)	0.010	1	0.010	0.213	4	0.053	0.223	5	0.188	0.687^b
6	Log (Flexural Stiffness)	0.026	1	0.026	0.197	4	0.049	0.223	5	0.523	0.510^b

Table 7-54: Coefficient Summary of N$_{50\%}$_ Cape Seals

No.	Model	Unstandardized Coefficients		Standardized Coefficient	t	Sig.
		B	Std. Error	Beta		
1	Age	-0.057	0.019	-0.838	-3.07	0.037
	Constant	5.90	0.158	-	37.374	0.000
2	Climate	-103.40	22.67	-0.916	-4.56	0.010
	Constant	419.31	90.74	-	4.62	0.010
3	Effective Thickness	0.042	0.010	0.910	4.39	0.012
	Constant	4.14	0.299	-	13.86	0.000
4	Moment of Inertia	$2.58*10^6$	$0.59*10^6$	0.908	4.33	0.012
	Constant	5.01	0.109	-	46.171	0.000
5	Log (Strain)	-0.843	1.95	-0.212	-0.434	0.687
	Constant	7.75	5.31	-	1.46	0.218
6	Log (Flexural Stiffness)	0.523	0.726	0.340	0.723	0.510
	Constant	3.49	2.69	-	1.29	0.265

- Significance of Age on Fatigue ($N_{50\%}$) in Cape Seals:

Coefficient, R = 0.838, suggests that there is a positive relationship between the ages of cape seals and fatigue, while the coefficient of determination, R^2 = 0.702, suggests that 70.2% of the variance in the fatigue values of the cape seals can be explained by the respective ages of the seals tested.

Significance, p = 0.037, meaning there is 96.3% probability that the ages of the cape seals can influence the outcome of fatigue ($N_{50\%}$). The regression model is therefore statistically significant

- Significance of Climate on Fatigue ($N_{50\%}$) in Cape Seals:

Coefficient, R = 0.916, suggests that there is a strong positive relationship between the climate from which the cape seals were sampled from and the fatigue values. Furthermore the coefficient of determination, R^2 = 0.839, suggests that 83.9% of the variance in the fatigue values can be explained by the effect of climate.

Significance, p = 0.010, meaning there is 99% probability that the climate of the cape seals can influence the outcome of fatigue ($N_{50\%}$). The regression model is therefore statistically significant.

- Significance of Effective Thickness on Fatigue ($N_{50\%}$) in Cape Seals:

Coefficient, R = 0.910, suggests that there exists a strong positive relationship between the effective thickness of the cape seals and the fatigue values. The coefficient of determination, R^2 = 0.829, suggests that 82.9% of the variance in the fatigue values can be explained by the effective thickness of the cape seals.

Significance, p = 0.012, meaning there is 98.8% probability that the effective thickness of the cape seals can influence the outcome of fatigue ($N_{50\%}$). The regression model is therefore statistically significant.

- Significance of Moment of Inertia on Fatigue ($N_{50\%}$) in Cape Seals:

Coefficient, R = 0.908, suggests that a strong positive relationship exists between the moment of inertia (non-linearity of the thickness of the sampled sprayed seal) and the fatigue

values. The coefficient of determination, R^2 = 0.824, furthermore suggests that 82.4% of the variance in fatigue results for the cape seals can be attributed to the effect of the non-linearity of the thickness of the cape seals.

Significance, p = 0.012, meaning there is 98.8% probability that the moment of inertia of the cross section of the cape seals can influence the outcome of fatigue ($N_{50\%}$). The regression model is therefore statistically significant.

- Significance of Log (Strain) on Fatigue ($N_{50\%}$) in Cape Seals:

Coefficient, R = 0.212, suggests that a weak relationship exists between the logarithmic value of the applied test strain and the fatigue of cape seals. The coefficient of determination, R^2 = 0.045, furthermore suggests that only 4.5% of the variance in the fatigue values can be attributed to the effect of the logarithmic value of the applied test strain.

Significance, p = 0.687, meaning there is only 31.3% probability that the logarithmic strain applied during the flexural testing of the cape seals can influence the outcome of fatigue ($N_{50\%}$). The regression model is therefore not statistically significant.

- Significance of Log (Flexural Stiffness) on Fatigue ($N_{50\%}$) in Cape Seals:

Coefficient, R = 0.340, suggests that a weak relationship exists between the logarithmic value of the flexural stiffness that was used as a direct input in the Classical Fatigue Characterisation Approach, as detailed in *Chapter 2 Literature Study.* Furthermore only 11.6% of the variance in the fatigue values can be explained by the logarithmic value of the flexural stiffness, described by the coefficient of determination, $R^2 = 0.116$.

Significance, p = 0.510, meaning there is only 49% probability that the effective thickness of the cape seals can influence the outcome of fatigue ($N_{50\%}$). The regression model is therefore not statistically significant.

Appendix 7 J4: Statistical Analysis of Combination of Variables on the outcome of Fatigue:

Single Seals_N$_{50\%}$

Table 7-55: Model Summary of N$_{50\%}$_Single Seals

No.	Constant, a	R	R Squared	Adjusted R Squared	Std. Error of the Estimate
1	Moment of Inertia, Log (Strain), Effective Thickness, Age	0.700[a]	0.490	-0.191	12.57
2	Moment of Inertia, Log (Strain), Age	0.696[a]	0.485	0.098	10.94
3	Log (Strain), Effective Thickness, Age	0.692[a]	0.479	0.088	11.00
4	Moment of Inertia, Effective Thickness, Age	0.614[a]	0.377	-0.090	12.03
5	Moment of Inertia, Log (Strain), Effective Thickness	0.698[a]	0.487	0.102	10.92

Table 7-56: ANOVA Summary of N$_{50\%}$_Single Seals

No.	Constant, a	Regression			Residual			Total		Significance of Regression	
		SSR	df	Mean Square	SSE	df	Mean Square	SST	df	F	Sig.
1	Moment of Inertia, Log (Strain), Effective Thickness, Age	455.05	4	113.76	474.26	3	158.09	929.30	7	0.72	0.632[b]
2	Moment of Inertia, Log (Strain), Age	450.41	3	150.14	478.89	4	.119.72	929.30	7	1.25	0.402[b]
3	Log (Strain), Effective Thickness, Age	445.08	3	148.36	484.22	4	121.06	929.30	7	1.23	0.409[b]
4	Moment of Inertia, Effective Thickness, Age	350.52	3	116.84	578.78	4	144.69	929.30	7	0.81	0.552[b]
5	Moment of Inertia, Log (Strain), Effective Thickness	452.48	3	150.83	476.82	4	119.21	929.30	7	1.27	0.399[b]

Table 7-57: Coefficient Summary of N50%_ Single Seals

No.	Model	Unstandardized Coefficients		Standardized Coefficient	t	Sig.
		B	Std. Error	Beta		
1	Moment of Inertia	3337.8×10^6	13292.3×10^6	4.69	0.251	0.818
	Log (Strain)	-89.87	110.52	-0.404	-0.813	0.476
	Effective Thickness	-14.67	85.62	-3.52	-0.171	0.875
	Age	-1.66	13	-0.692	-0.127	0.907
	Constant	431.55	1061.22	-	0.407	0.712
2	Moment of Inertia	11.38×10^6	2982.3×10^6	1.59	0.381	0.722
	Log (Strain)	-90.62	96.1	-0.407	-0.943	0.399
	Age	-2.69	10.02	-1.12	-0.269	0.802
	Constant	256.39	247.38	-	1.04	0.359
3	Log (Strain)	-94.92	95.09	-0.427	-0.998	0.375
	Effective Thickness	6.11	19.32	1.47	0.316	0.768
	Age	-2.38	11.09	-0.994	-0.214	0.841
	Constant	192.14	407.82	-	0.471	0.662

Table 7-58: Continuation of Coefficient Summary of N50%_ Single Seals

No.	Model	Unstandardized Coefficients		Standardized Coefficient	t	Sig.
		B	Std. Error	Beta		
4	Moment of Inertia	$5305.7*10^6$	$2504.8*10^6$	7.45	0.424	0.693
	Effective Thickness	-17.44	81.85	-4.19	-0.213	0.842
	Age	-6.65	10.97	-2.78	-0.606	0.577
	Constant	235.19	988.65	-	0.238	0.824
5	Moment of Inertia	$3712.9*10^6$	$11255.8*10^6$	5.22	0.33	0.758
	Log (Strain)	-95.52	84.59	-0.434	-1.14	0.318
	Effective Thickness	-19.74	65.84	-4.47	-0.3	0.779
	Constant	506.96	764.82	-	0.663	0.544

- Significance of the Combination of Moment of Inertia, Log (Strain), Effective Thickness and Age on Fatigue ($N_{50\%}$) in Single Seals:

Coefficient, R = 0.466, suggests that there is a weak relationship between the combination of moment of inertia, log (strain), effective thickness and ages of single seals and fatigue, while the coefficient of determination, R^2 = 0.490, suggests that only 49% of the variance in the fatigue values of the single seals can be explained by this particular combination of variables.

Significance, p = 0.632, meaning there is only 36.8% probability that this combination of variables can influence the outcome of fatigue ($N_{50\%}$). The regression model is therefore not statistically significant.

- Significance of the Combination of Moment of Inertia, Log (Strain) and Age on Fatigue ($N_{50\%}$) in Single Seals:

Coefficient, R = 0.696, suggests that there is a weak relationship between the combination of moment of inertia, log (strain) and ages of the single seals and the fatigue values. Furthermore the coefficient of determination, R^2 = 0.485, suggests that only 48.5% of the variance in the fatigue values can be explained by this particular combination of variables.

Significance, p = 0.402, meaning there is only 59.8% probability that this particular combination of variables of the single seals can influence the outcome of fatigue ($N_{50\%}$). The regression model is therefore not statistically significant.

- Significance of the Combination of Log (Strain), Effective Thickness and Age on Fatigue ($N_{50\%}$) in Single Seals:

Coefficient, R = 0.692, suggests that there exists a weak relationship between the combination of log (strain), effective thickness and the ages of the single seals and the fatigue values. The coefficient of determination, R^2 = 0.479, suggests that only 47.9% of the variance in the fatigue values can be explained by this particular combination of variables.

Significance, p = 0.409, meaning there is only 59.1% probability that this particular combination of variables of the single seals can influence the outcome of fatigue ($N_{50\%}$). The regression model is therefore not statistically significant.

- Significance of the Combination of Moment of Inertia, Effective Thickness and Age on Fatigue ($N_{50\%}$) in Single Seals:

Coefficient, R = 0.614, suggests that a weak relationship exists between the combination of moment of inertia (non-linearity of the thickness of the sampled sprayed seal), effective thickness and ages and the fatigue values. The coefficient of determination, R^2 = 0.377, furthermore suggests that only 37.7% of the variance in fatigue results for the single seals can be attributed to this particular combination of variables.

Significance, p = 0.552, meaning there is only 44.8% probability that this particular combination of variables can influence the outcome of fatigue ($N_{50\%}$). The regression model is therefore not statistically significant.

- Significance of the Combination of Moment of Inertia, Log (Strain) and Effective Thickness on Fatigue ($N_{50\%}$) in Single Seals:

Coefficient, R = 0.698, suggests that a weak relationship exists between the combination of moment of inertia, log (strain) and effective and the fatigue of single seals. The coefficient of determination, R^2 = 0.487, furthermore suggests that only 48.7% of the variance in the fatigue values can be attributed to this particular combination of variables.

Significance, p = 0.399, meaning there is only 60.1% probability that this particular combination of variables can influence the outcome of fatigue ($N_{50\%}$). The regression model is therefore not statistically significant.

Double Seals_$N_{20\%}$

Table 7-59: Model Summary of $N_{20\%}$_Double Seals

No.	Constant, a	R	R Squared	Adjusted R Squared	Std. Error of the Estimate
1	Climate, Log (Flexural Stiffness), Effective Thickness, Moment of Inertia	0.768[a]	0.590	0.044	1.68
2	Climate, Log (Flexural Stiffness), Effective Thickness	0.768[a]	0.590	0.283	1.45
3	Climate, Log (Flexural Stiffness), Moment of Inertia	0.768[a]	0.590	0.282	1.45
4	Log (Flexural Stiffness), Effective Thickness, Moment of Inertia	0.528[a]	00.278	-0.263	1.93
5	Climate, Effective Thickness, Moment of Inertia	0.768[a]	0.590	0.283	1.45

Table 7-60: ANOVA Summary of $N_{20\%}$_Double Seals

No.	Constant, a	Regression			Residual			Total		Significance of Regression	
		SSR	df	Mean Square	SSE	df	Mean Square	SST	df	F	Sig.
1	Climate, Log (Flexural Stiffness), Effective Thickness, Moment of Inertia	12.15	4	3.04	8.44	3	2.81	20.59	7	1.08	0.495[b]
2	Climate, Log (Flexural Stiffness), Effective Thickness	12.15	3	4.05	8.44	4	2.11	20.59	7	1.92	0.268[b]
3	Climate, Log (Flexural Stiffness), Moment of Inertia	12.15	3	4.05	8.44	4	2.11	20.59	7	1.92	0.268[b]
4	Log (Flexural Stiffness), Effective Thickness, Moment of Inertia	5.73	3	1.91	14.86	4	3.72	20.59	7	0.51	0.694[b]
5	Climate, Effective Thickness, Moment of Inertia	12.15	3	4.05	8.44	4	2.11	20.59	7	1.92	0.268[b]

Table 7-61: Coefficient Summary of N$_{20\%}$_Double Seals

No.	Model	Unstandardized Coefficients		Standardized Coefficient	t	Sig.
		B	Std. Error	Beta		
1	Climate	-0.567	0.375	-0.749	-1.51	0.228
	Log (Flexural Stiffness)	-0.012	4.92	-0.001	-0.002	0.998
	Effective Thickness	0.153	6.29	0.324	0.024	0.982
	Moment of Inertia	-1462.8	$750.9*10^6$	-0.245	-0.018	0.986
	Constant	4.18	93.03	-	0.045	0.967
2	Climate	-0.57	0.296	-0.753	-1.93	0.127
	Log (Flexural Stiffness)	-0.017	4.26	-0.002	-0.004	0.997
	Effective Thickness	0.037	0.228	0.078	0.161	0.88
	Constant	5.83	21.5	-	0.271	0.8
3	Climate	-0.571	0.293	-0.755	-1.95	0.123
	Log (Flexural Stiffness)	-0.022	4.25	-0.003	-0.005	0.996
	Moment of Inertia	$4.4*10^6$	$27.2*10^6$	0.077	0.16	0.881
	Constant	6.38	18.79	-	0.339	0.751

Table 7-62: Coefficient Summary of N$_{20\%}$_Double Seals

No.	Model	Unstandardized Coefficients		Standardized Coefficient	t	Sig.
		B	Std. Error	Beta		
4	Log (Flexural Stiffness)	3.95	0.79	0.47	0.826	0.455
	Effective Thickness	4.27	6.53	9.04	0.654	0.549
	Moment of Inertia	-51187.4	785.6*10^6	-8.55	-0.615	0.572
	Constant	-73.37	89.64	-	-0.807	0.465
5	Climate	-0.566	0.275	-0.749	-2.06	0.108
	Effective Thickness	0.154	5.43	0.326	0.028	0.979
	Moment of Inertia	-1473.4	649.3*10^6	-0.247	-0.021	0.984
	Constant	4.11	76.47	-	0.054	0.96

- Significance of the Combination of Climate, Log (Flexural Stiffness), Effective Thickness and Moment of Inertia on Fatigue ($N_{20\%}$) in Double Seals:

Coefficient, R = 0.768, suggests that there is a slightly positive relationship between the combination of climate, log (flexural stiffness), effective thickness and moment of inertia of double seals and fatigue, while the coefficient of determination, R^2 = 0.590, suggests that only 59% of the variance in the fatigue values of the double seals can be explained by this particular combination of variables.

Significance, p = 0.454, meaning there is only 50.5% probability that this particular combination of variables of the double seals can influence the outcome of fatigue ($N_{20\%}$). The regression model is therefore not statistically significant.

- Significance of the Combination of Climate, Log (Flexural Stiffness and Effective Thickness on Fatigue ($N_{20\%}$) in Double Seals:

Coefficient, R = 0.768, suggests that there is a slightly positive relationship between the combination of climate, log (flexural stiffness and effective thickness of the double seals and the fatigue values. Furthermore the coefficient of determination, R^2 = 0.590, suggests that 59% of the variance in the fatigue values can be explained by this particular combination of variables.

Significance, p = 0.268 meaning there is a 73.2% probability that this particular combination of variables of the double seals can influence the outcome of fatigue ($N_{20\%}$). The regression model is therefore statistically significant.

- Significance of the Combination of Climate, Log (Flexural Stiffness) and Moment of Inertia on Fatigue ($N_{20\%}$) in Double Seals:

Coefficient, R = 0.768, suggests that there exists a slightly positive relationship between the combination of climate, log (flexural stiffness) and moment of inertia of the double seals and the fatigue values. The coefficient of determination, R^2 = 0.590, suggests that only 59% of the variance in the fatigue values can be explained this particular combination of variables of the double seals.

Significance, p = 0.268, meaning there is a 73.2% probability that this particular combination of variables the double seals can influence the outcome of fatigue ($N_{20\%}$). The regression model is therefore not statistically significant.

- Significance of the Combination of Log (Flexural Stiffness), Effective Thickness and Moment of Inertia on Fatigue ($N_{20\%}$) in Double Seals:

Coefficient, R = 0.528, suggests that a weak relationship exists between the combination of log (flexural stiffness), effective thickness and moment of inertia and the fatigue values. The coefficient of determination, R^2 = 0.278, furthermore suggests that only 27.8% of the variance in fatigue results for the double seals can attributed to this particular combination of variables of the double seals.

Significance, p = 0.694, meaning there is only 30.6% probability that this particular combination of variables of the double seals can influence the outcome of fatigue ($N_{20\%}$). The regression model is therefore not statistically significant.

- Significance of the Combination of Climate, Effective Thickness and Moment of Inertia on Fatigue ($N_{20\%}$) in Double Seals:

Coefficient, R = 0.768, suggests that a slightly positive relationship exists between the combination of climate, effective thickness and moment of inertia and the fatigue of double seals. The coefficient of determination, R^2 = 0.590, furthermore suggests that only 59% of the variance in the fatigue values can be this particular combination of variables.

Significance, p = 0.268, meaning there is a 732% probability that this particular combination of variables of the double seals can influence the outcome of fatigue ($N_{20\%}$). The regression model is therefore not statistically significant.

Cape Seals_N$_{40\%}$

Table 7-63: Model Summary of N$_{40\%}$_Cape Seals

No.	Constant, a	R	R Squared	Adjusted R Squared	Std. Error of the Estimate
1	Effective Thickness , Moment of Inertia, Climate , Age	0.965[a]	0.931	0.828	0.054
2	Effective Thickness , Climate , Age	0.965[a]	0.931	0.828	0.054
3	Moment of Inertia, Climate , Age	0.966[a]	0.934	0.834	0.053
4	Effective Thickness , Moment of Inertia, Age	0.965[a]	0.931	0.886	0.044
5	Effective Thickness , Moment of Inertia, Climate	0.965[a]	0.931	0.828	0.055

Table 7-64: ANOVA Summary of N$_{40\%}$_Cape Seals

No.	Constant, a	Regression			Residual			Total			Significance of Regression	
		SSR	df	Mean Square	SSE	df	Mean Square	SST	df	F		Sig.
1	Effective Thickness , Moment of Inertia, Climate , Age	0.08	3	0.027	0.027	2	0.003	0.086	5	9.05		0.101[b]
2	Effective Thickness , Climate , Age	0.08	3	0.027	0.006	2	0.003	0.086	5	9.05		0.101[b]
3	Moment of Inertia, Climate , Age	0.08	3	0.027	0.006	2	0.003	0.086	5	9.39		0.098[b]
4	Effective Thickness , Moment of Inertia, Age	0.08	2	0.040	0.006	3	0.002	0.086	5	20.3		0.018[b]
5	Effective Thickness , Moment of Inertia, Climate	0.08	3	0.027	0.006	2	0.003	0.086	5	8.99		0.102[b]

Table 7-65: Coefficient Summary of N$_{40\%}$_Cape Seals

No.	Model	Unstandardized Coefficients		Standardized Coefficient	t	Sig.
		B	Std. Error	Beta		
1	Effective Thickness	0.028	0.027	0.989	1.05	0.404
	Climate	-2.39	46.01	-0.034	-0.813	0.476
	Age	0.003	0.022	0.062	0.119	0.916
	Constant	13.58	184.94	-	0.073	0.948
	Moment of Inertia	Excluded	0.842 Partial Correlation 1.8*10^{-5} Collinearity Tolerance	51.996[b]	1.56	0.362
2	Effective Thickness	0.028	0.027	0.989	1.05	0.404
	Climate	-2.39	46.01	-0.034	-0.052	0.963
	Age	0.003	0.022	0.062	0.119	0.916
	Constant	13.58	184.94	-	0.073	0.948
3	Moment of Inertia	2.2*10^{6}	2.0*10^{6}	1.27	1.09	0.386
	Climate	-163	44.83	-0.023	-0.036	0.974
	Age	0.015	0.031	0.35	0.485	0.676
	Constant	10.94	179.89	-	0.061	0.957

Table 7-66: Continuation of Coefficient Summary of $N_{40\%}$_Cape Seals

No.	Model	Unstandardized Coefficients		Standardized Coefficient	t	Sig.
		B	Std. Error	Beta		
4	Effective Thickness	0.03	0.011	1.03	2.6	0.077
	Age	0.003	0.016	0.073	0.186	0.864
	Constant	3.96	0.472	-	8.39	0.004
	Moment of Inertia	Excluded	0.780 Partial Correlation $2.3*10^{-5}$ Collinearity Tolerance	45.31^{b}	1.76	0.22
5	Effective Thickness	0.03	0.078	1.05	0.384	0.738
	Moment of Inertia	-24.38	$4.2*10^{6}$	-0.129	-0.054	0.962
	Climate	-3.54	46.49	-0.05	-0.076	0.946
	Constant	18.17	187.24	-	0.097	0.932

287

- Significance of the Combination of Effective Thickness, Moment of Inertia, Climate and Age on Fatigue ($N_{40\%}$) in Cape Seals:

Coefficient, R = 0.965, suggests that there is a strong positive relationship between the combination of effective thickness, moment of inertia, climate, age and fatigue, while the coefficient of determination, R^2 = 0.931, suggests that 93.1% of the variance in the fatigue values of the cape seals can be explained by this particular combination of variables.

Significance, p = 0.101, meaning there is only 89.8% probability that this particular combination of variables of the cape seals can influence the outcome of fatigue ($N_{40\%}$). The regression model is therefore not statistically significant

- Significance of the Combination of Effective Thickness, Climate and Age on Fatigue ($N_{40\%}$) in Cape Seals:

Coefficient, R = 0.965, suggests that there is a strong positive relationship between the combination of effective thickness, climate, age and the fatigue values. Furthermore the coefficient of determination, R^2 = 0.931, suggests that 93.1% of the variance in the fatigue values can be explained by this particular combination of variables.

Significance, p = 0.101, meaning there is only 89.9% probability that this particular combination of variables of the cape seals can influence the outcome of fatigue ($N_{40\%}$). The regression model is therefore not statistically significant.

- Significance of the Combination of Moment of Inertia, Climate and Age on Fatigue ($N_{40\%}$) in Cape Seals:

Coefficient, R = 0.966, suggests that there exists a strong positive relationship between the combination of moment of inertia, climate, age and the fatigue values. The coefficient of determination, R^2 = 0.934, suggests that 93.4% of the variance in the fatigue values can be explained by this particular combination of variables.

Significance, p = 0.098, meaning there is only 90.2% probability that this particular combination of variables of the cape seals can influence the outcome of fatigue ($N_{40\%}$). The regression model is therefore not statistically significant.

- Significance of the Combination of Effective Thickness, Moment of Inertia and Age on Fatigue ($N_{40\%}$) in Cape Seals:

Coefficient, R = 0.965, suggests that a strong positive relationship exists between the combination of effective thickness, moment of inertia, age and the fatigue values. The coefficient of determination, R^2 = 0.931, furthermore suggests that 93.1% of the variance in fatigue results for the cape seals can be attributed to this particular combination of variables of the cape seals.

Significance, p = 0.018, meaning there is 98.2% probability that to this particular combination of variables of the cape seals can influence the outcome of fatigue ($N_{40\%}$). The regression model is therefore statistically significant.

- Significance of the Combination of Effective Thickness, Moment of Inertia and Climate on Fatigue ($N_{40\%}$) in Cape Seals:

Coefficient, R = 0.965, suggests that a strong relationship exists between the combination of effective thickness, moment of inertia, climate and the fatigue of cape seals. The coefficient of determination, R^2 = 0.931, furthermore suggests that 93.1% of the variance in the fatigue values can be attributed to this particular combination of variables.

Significance, p = 0.102, meaning there is only 89.9% probability that to this particular combination of variables of the cape seals can influence the outcome of fatigue ($N_{40\%}$). The regression model is therefore not statistically significant.

Appendix 7 J5: Statistical Analysis of Interaction between Variables on the outcome of Fatigue:

Single Seals_N$_{50\%}$

Table 7-67: Model Summary of N$_{50\%}$_Single Seals

No.	Constant, a	R	R Squared	Adjusted R Squared	Std. Error of the Estimate
1	Moment of Inertia, Log (Strain), Effective Thickness, Age, intageht	0.771[a]	0.595	-0.418	13.72
2	Moment of Inertia, Log (Strain), Age, intageht	0.724[a]	0.525	-0.109	12.13
3	Log (Strain), Effective Thickness, Age, intageht	0.694[a]	0.482	-0.208	12.66
4	Moment of Inertia, Effective Thickness, Age, intageht	0.771[a]	0.594	0.054	11.21
5	Moment of Inertia, Log (Strain), Effective Thickness, intageht	0.767[a]	0.588	0.039	11.29

Table 7-68: ANOVA Summary of N$_{50\%}$_Single Seals

No.	Constant, a	Regression			Residual			Total			Significance of Regression	
		SSR	df	Mean Square	SSE	df	Mean Square	SST	df	F	Sig.	
1	Moment of Inertia, Log (Strain), Effective Thickness, Age, intageht	552.7	5	110.6	376.6	2	188.3	929.3	7	0.58	0.727[b]	
2	Moment of Inertia, Log (Strain), Age, intageht	487.6	4	121.9	441.7	3	147.2	929.3	7	0.83	0.586[b]	
3	Log (Strain), Effective Thickness, Age, intageht	448.1	4	112.0	481.2	3	160.4	929.3	7	0.69	0.642[b]	
4	Moment of Inertia, Effective Thickness, Age, intageht	552.4	4	138.1	376.9	3	125.6	929.3	7	0.11	0.489[b]	
5	Moment of Inertia, Log (Strain), Effective Thickness, intageht	546.5	4	136.6	382.9	3	127.6	929.3	7	1.07	0.498[b]	

Table 7-69: Coefficient Summary of N$_{50\%}$_Single Seals

No.	Model	Unstandardized Coefficients		Standardized Coefficient	t	Sig.
		B	**Std. Error**	**Beta**		
1	Moment of Inertia	23502.1*10^6	31528.9*10^6	33.03	0.745	0.534
	Log (Strain)	7.38	181.04	0.033	0.041	0.971
	Effective Thickness	-72.42	123.12	-17.39	-0.588	0.616
	Age	17.16	29.73	7.17	0.577	0.622
	intageht	-1028.2	13.5*10^6	-22.3	-0.72	0.546
	Constant	547.16	1169.2	-	0.468	0.686
2	Moment of Inertia	6524.4*10^6	11215.9*10^6	9.17	0.582	0.602
	Log (Strain)	-46.47	138.11	-0.209	0-.336	0.759
	Age	4.21	17.67	1.76	0.238	0.827
	intageht	-482.3	9.0*10^6	-10.44	-0.503	0.65
	Constant	-12.41	601.03	-	-0.021	0.985
3	Log (Strain)	-89.49	116.33	-0.402	-0.769	0.498
	Effective Thickness	11.61	45.71	2.79	0.254	0.816
	Age	-1.21	15.35	-0.504	-0.079	0.942
	intageht	-83.74	5.7*10^6	-1.81	-0.138	0.899
	Constant	84.09	914.2	-	0.092	0.933

Table 7-70: Continuation of Coefficient Summary of N50%_Single Seals

No.	Model	Unstandardized Coefficients		Standardized Coefficient	t	Sig.
		B	Std. Error	Beta		
4	Moment of Inertia	$22579.2*10^6$	$17929.1*10^6$	31.73	1.26	0.297
	Effective Thickness	-69.88	86.76	-16.78	-0.805	0.48
	Age	16.55	20.96	6.91	0.79	0.487
	intageht	-985.8	$7.3*10^6$	-21.35	-1.27	0.294
	Constant	549.44	956.96	-	0.576	0.605
5	Moment of Inertia	$20423.6*10^6$	$22690.3*10^6$	28.69	0.9	0.434
	Log (Strain)	54.39	196.43	0.245	0.277	0.8
	Effective Thickness	-27.02	68.65	-6.49	-0.394	0.72
	intageht	-23553.2	$258.9*10^6$	-21.71	-0.858	0.454
	Constant	53.51	951.55	-	0.056	0.959

- Significance of the Interaction between Moment of Inertia, Log (Strain), Effective Thickness and Age on Fatigue ($N_{50\%}$) in Single Seals:

Coefficient, R = 0.771, suggests that there is a slightly positive relationship between the interaction between moment of inertia, log (strain), effective thickness and ages of single seals and fatigue, while the coefficient of determination, R^2 = 0.595, suggests that only 59.5% of the variance in the fatigue values of the single seals can be explained by this particular interaction of variables.

Significance, p = 0.727, meaning there is only 27.3% probability that this interaction between variables can influence the outcome of fatigue ($N_{50\%}$). The regression model is therefore not statistically significant.

- Significance of the Interaction between Moment of Inertia, Log (Strain) and Age on Fatigue ($N_{50\%}$) in Single Seals:

Coefficient, R = 0.724, suggests that there is a slightly positive relationship between the interaction between moment of inertia, log (strain), ages of the single seals and the fatigue values. Furthermore the coefficient of determination, R^2 = 0.525, suggests that only 52.5% of the variance in the fatigue values can be explained by this particular interaction between variables.

Significance, p = 0.586, meaning there is only 41.4% probability that this particular interaction between variables of the single seals can influence the outcome of fatigue ($N_{50\%}$). The regression model is therefore not statistically significant.

- Significance of the Combination of Log (Strain), Effective Thickness and Age on Fatigue ($N_{50\%}$) in Single Seals:

Coefficient, R = 0.694, suggests that there exists a weak relationship between the interaction of log (strain), effective thickness and the ages of the single seals and the fatigue values. The coefficient of determination, R^2 = 0.482, suggests that only 48.2% of the variance in the fatigue values can be explained by this particular interaction between variables.

Significance, p = 0..642, meaning there is only 35.8% probability that this interaction between variables of the single seals can influence the outcome of fatigue ($N_{50\%}$). The regression model is therefore not statistically significant.

- Significance of the Combination of Moment of Inertia, Effective Thickness and Age on Fatigue ($N_{50\%}$) in Single Seals:

Coefficient, R = 0.771, suggests that a slightly positive relationship exists between the interaction between of moment of inertia (non-linearity of the thickness of the sampled sprayed seal), effective thickness and ages and the fatigue values. The coefficient of determination, R^2 = 0.594, furthermore suggests that only 59.4% of the variance in fatigue results for the single seals can be attributed to this particular combination of variables.

Significance, p = 0.489, meaning there is only 51.1% probability that this particular interaction between variables can influence the outcome of fatigue ($N_{50\%}$). The regression model is therefore not statistically significant.

- Significance of the Combination of Moment of Inertia, Log (Strain) and Effective Thickness on Fatigue ($N_{50\%}$) in Single Seals:

Coefficient, R = 0.767, suggests that a slightly positive relationship exists between the interaction between moment of inertia, log (strain) and effective and the fatigue of single seals. The coefficient of determination, R^2 = 0.588, furthermore suggests that only 58.8% of the variance in the fatigue values can be attributed to this particular interaction between variables.

Significance, p = 0.489, meaning there is only 51.1% probability that this particular interaction between variables can influence the outcome of fatigue ($N_{50\%}$). The regression model is therefore not statistically significant.

Double Seals_N$_{20\%}$

Table 7-71: Model Summary of N$_{20\%}$_Double Seals

No.	Constant, a	R	R Squared	Adjusted R Squared	Std. Error of the Estimate
1	Climate, Log (Flexural Stiffness), Effective Thickness, Moment of Inertia, intageht	0.873[a]	0.762	0.167	1.56
2	Climate, Log (Flexural Stiffness), Effective Thickness, intageht	0.829[a]	0.687	0.269	1.47
3	Climate, Log (Flexural Stiffness), Moment of Inertia, intageht	0.864[a]	0.747	0.409	1.32
4	Log (Flexural Stiffness), Effective Thickness, Moment of Inertia, intageht	0.515[a]	0.265	-0.287	1.95
5	Climate, Effective Thickness, Moment of Inertia, intageht	0.856[a]	0.733	0.377	1.35

Table 7-72: ANOVA Summary of N$_{20\%}$_Double Seals

No.	Constant, a	Regression			Residual			Total		Significance of Regression	
		SSR	df	Mean Square	SSE	df	Mean Square	SST	df	F	Sig.
1	Climate, Log (Flexural Stiffness), Effective Thickness, Moment of Inertia, intageht	15.69	5	3.14	4.89	2	2.45	20.59	7	1.28	0.493[b]
2	Climate, Log (Flexural Stiffness), Effective Thickness, intageht	14.14	4	3.53	6.45	3	2.15	20.59	7	1.64	0.356[b]
3	Climate, Log (Flexural Stiffness), Moment of Inertia, intageht	15.38	4	3.84	5.21	3	1.74	20.59	7	2.21	0.270[b]
4	Log (Flexural Stiffness), Effective Thickness, Moment of Inertia, intageht	5.45	3	1.82	15.14	4	3.79	20.59	7	0.48	0.713[b]
5	Climate, Effective Thickness, Moment of Inertia, intageht	15.09	4	3.77	5.50	3	1.83	20.59	7	2.06	0.290[b]

Table 7-73: Coefficient Summary of N$_{20\%}$_Double Seals

No.	Model	Unstandardized Coefficients		Standardized Coefficient	t	Sig.
		B	Std. Error	Beta		
1	Climate	8.27	7.35	10.93	1.12	0.378
	Log (Flexural Stiffness)	4.56	5.96	0.543	0.765	0.524
	Effective Thickness	-3.02	6.44	-6.39	-0.469	0.686
	Moment of Inertia	-77931.2	$937.5*10^6$	13.02	0.784	0.515
	intageht	-826.8	$0.65*10^6$	-12.35	-1.2	0.352
	Constant	-9.89	87.57	-	-0.113	0.92
2	Climate	9.14	10.09	12.08	0.905	0.432
	Log (Flexural Stiffness)	3.98	5.98	0.474	0.666	0.553
	Effective Thickness	1.32	1.35	2.79	0.975	0.402
	intageht	-0.097	0.101	-12.5	-0.962	0.407
	Constant	-44.19	56.31	-	-0.784	0.49
3	Climate	9.04	7.06	11.96	1.28	0.29
	Log (Flexural Stiffness)	4.7	5.18	0.559	0.907	0.431
	Moment of Inertia	$355.7*10^6$	$258.9*10^6$	6.3	1.37	0.263
	intageht	-2469.8	$17.1*10^6$	-13.04	-1.36	0.266
	Constant	6.38	18.79	-	-1.12	0.344

Table 7-74: Continuation of Coefficient Summary of N$_{20\%}$_Double Seals

No.	Model	Unstandardized Coefficients		Standardized Coefficient	t	Sig.
		B	Std. Error	Beta		
4	Log (Flexural Stiffness)	12.25	14.82	0.1.46	0.826	0.455
	Effective Thickness	3.07	5.16	6.51	0.594	0.584
	intageht	-286.2	$4.8*10^6$	-5.42	-0.545	0.614
	Constant	-93.95	139.19	-	-0.675	0.537
	Moment of Inertia	Excluded	-0.519 Partial Correlation $3.6*10^{-6}$ Collinearity Tolerance	-233.33[b]	-1.05	0.371
5	Climate	10.51	8.75	13.89	1.2	0.316
	Effective Thickness	0.208	5.07	0.442	0.041	0.97
	Moment of Inertia	$422.8*10^6$	$696.6*10^6$	7.49	0.607	0.587
	intageht	-371	$2.8*10^6$	-15.65	-1.27	0.295
	Constant	-46.49	81.72	-	-0.569	0.609

297

- Significance of the Interaction between Climate, Log (Flexural Stiffness), Effective Thickness and Moment of Inertia on Fatigue ($N_{20\%}$) in Double Seals:

Coefficient, R = 0.873, suggests that there is a positive relationship between the interaction between climate, log (flexural stiffness), effective thickness and moment of inertia of double seals and fatigue, while the coefficient of determination, R^2 = 0.762, suggests that only 76.2% of the variance in the fatigue values of the double seals can be explained by this particular interaction between variables.

Significance, p = 0.493, meaning there is only 50.7% probability that this particular interaction between variables of the double seals can influence the outcome of fatigue ($N_{20\%}$). The regression model is therefore not statistically significant.

- Significance of the Combination of Climate, Log (Flexural Stiffness and Effective Thickness on Fatigue ($N_{20\%}$) in Double Seals:

Coefficient, R = 0.829, suggests that there is a positive relationship between the interaction between climate, log (flexural stiffness and effective thickness of the double seals and the fatigue values. Furthermore the coefficient of determination, R^2 = 0.687, suggests that 68.7% of the variance in the fatigue values can be explained by this particular interaction between variables.

Significance, p = 0.356 meaning there is a 64.4% probability that this particular interaction between variables of the double seals can influence the outcome of fatigue ($N_{20\%}$). The regression model is therefore not statistically significant.

- Significance of the Combination of Climate, Log (Flexural Stiffness) and Moment of Inertia on Fatigue ($N_{20\%}$) in Double Seals:

Coefficient, R = 0.864, suggests that there exists a positive relationship between the interaction between climate, log (flexural stiffness) and moment of inertia of the double seals and the fatigue values. The coefficient of determination, R^2 = 0.747, suggests that only 74.7% of the variance in the fatigue values can be explained this particular interaction between variables of the double seals.

Significance, p = 0.270, meaning there is a 73% probability that this particular interaction between variables the double seals can influence the outcome of fatigue ($N_{20\%}$). The regression model is therefore not statistically significant.

- Significance of the Combination of Log (Flexural Stiffness), Effective Thickness and Moment of Inertia on Fatigue ($N_{20\%}$) in Double Seals:

Coefficient, R = 0.515, suggests that a weak relationship exists between the interaction between log (flexural stiffness), effective thickness and moment of inertia and the fatigue values. The coefficient of determination, R^2 = 0.265, furthermore suggests that only 26.5% of the variance in fatigue results for the double seals can attributed to this particular interaction between variables of the double seals.

Significance, p = 0.713, meaning there is only 28.7% probability that this particular interaction between variables of the double seals can influence the outcome of fatigue ($N_{20\%}$). The regression model is therefore not statistically significant.

- Significance of the Combination of Climate, Effective Thickness and Moment of Inertia on Fatigue ($N_{20\%}$) in Double Seals:

Coefficient, R = 0.856, suggests that a positive relationship exists between the interaction between climate, effective thickness and moment of inertia and the fatigue of double seals. The coefficient of determination, R^2 = 0.733, furthermore suggests that only 73.3% of the variance in the fatigue values can be this particular interaction between variables.

Significance, p = 0.268, meaning there is a 71% probability that this particular interaction between variables of the double seals can influence the outcome of fatigue ($N_{20\%}$). The regression model is therefore not statistically significant.

Cape Seals_N$_{40\%}$

Table 7-75: Model Summary of N$_{40\%}$_Cape Seals

No.	Constant, a	R	R Squared	Adjusted R Squared	Std. Error of the Estimate
1	Effective Thickness , Moment of Inertia, Climate , Age, intageht	0.965[a]	0.932	0.830	0.054
2	Effective Thickness , Climate , Age, intageht	0.965[a]	0.931	0.828	0.054
3	Moment of Inertia, Climate , Age, intageht	0.966[a]	0.933	0.833	0.054
4	Effective Thickness , Moment of Inertia, Age, intageht	0.965[a]	0.932	0.887	0.044
5	Effective Thickness , Moment of Inertia, Climate, intageht	0.965[a]	0.931	0.828	0.055

Table 7-76: ANOVA Summary of N$_{40\%}$_Cape Seals

No.	Constant, a	Regression			Residual			Total		Significance of Regression	
		SSR	df	Mean Square	SSE	df	Mean Square	SST	df	F	Sig.
1	Effective Thickness , Moment of Inertia, Climate , Age, intageht	0.08	3	0.027	0.006	2	0.003	0.086	5	9.15	0.100[b]
2	Effective Thickness , Climate , Age, intageht	0.08	3	0.027	0.006	2	0.003	0.086	5	9.05	0.101[b]
3	Moment of Inertia, Climate , Age, intageht	0.08	3	0.027	0.006	2	0.003	0.086	5	9.29	0.099[b]
4	Effective Thickness , Moment of Inertia, Age, intageht	0.08	2	0.040	0.006	3	0.002	0.086	5	20.6	0.018[b]
5	Effective Thickness , Moment of Inertia, Climate, intageht	0.08	3	0.027	0.006	2	0.003	0.086	5	8.99	0.102[b]

Table 7-77: Coefficient Summary of $N_{40\%}$_Cape Seals

No.	Model	Unstandardized Coefficients		Standardized Coefficient	t	Sig.
		B	Std. Error	Beta		
1	Climate	-1.34	46.32	-0.019	-0.029	0.98
	Age	-0.034	0.023	-0.804	-1.51	0.271
	intageht	1472.59	1383.95	0.396	1.06	0.399
	Constant	10.3	185.39	-	0.056	0.961
	Effective Thickness	Excluded	-.328 Partial Correlation $1.6*10^{-5}$ Collinearity Tolerance	-21.20^{b}	-0.347	0.787
	Moment of Inertia	Excluded	0.961 Partial Correlation $6.6*10^{-6}$ Collinearity Tolerance	96.98^{b}	3.48	0.178
2	Effective Thickness	0.028	0.023	0.962	1.21	0.35
	Climate	-2.46	46.08	-0.035	-0.053	0.962
	intageht	$1.73*10^{-5}$	0	0.039	0.115	0.919
	Constant	13.89	185.11	-	0.075	0.947
	Age	Excluded	0.988 Partial Correlation $1.46*10^{-6}$ Collinearity Tolerance	214.00^{b}	6.42	0.098
3	Moment of Inertia	$1.67*10^{6}$	$1.1*10^{6}$	0.945	1.46	0.281
	Climate	-1.83	45.42	-0.026	-0.04	0.971
	intageht	13663.3	29489.9	0.105	0.463	0.689
	Constant	11.88	182.04	-	0.065	0.954
	Age	Excluded	0.992 Partial Correlation $1.21*10^{-6}$ Collinearity Tolerance	73.77^{b}	8.04	0.079

Table 7-78: Continuation of Coefficient Summary of $N_{40\%}$_Cape Seals

No.	Model	Unstandardized Coefficients		Standardized Coefficient	t	Sig.
		B	Std. Error	Beta		
4	Age	-0.035	0.006	-0.818	-5.38	0.013
	intageht	6028.19	2261.62	0.406	2.67	0.076
	Constant	4.96	0.105	-	47.28	0
	Effective Thickness	Excluded	-0.275 Partial Correlation $2.5*10^{-5}$ Collinearity Tolerance	-14.41^{b}	-0.404	0.725
	Moment of Inertia	Excluded	0.519 Partial Correlation $2.16*10^{-5}$ Collinearity Tolerance	29.06^{b}	0.858	0.481
5	Effective Thickness	0.029	0.058	0.999	0.499	0.667
	Climate	-3.58	46.58	-0.051	-0.077	0.946
	intageht	-864.87	17068.19	-0.084	-0.051	0.964
	Constant	18.37	187.45	-	0.098	0.931
	Moment of Inertia	Excluded	-0.711 Partial Correlation $5.07*10^{-8}$ Collinearity Tolerance	-829.95	.-1.01	0.496

- Significance of the Interaction between Effective Thickness, Moment of Inertia, Climate and Age on Fatigue ($N_{40\%}$) in Cape Seals:

Coefficient, R = 0.965, suggests that there is a strong positive relationship between the interaction between effective thickness, moment of inertia, climate, age and fatigue, while the coefficient of determination, R^2 = 0.932, suggests that 93.2% of the variance in the fatigue values of the cape seals can be explained by this particular interaction between variables.

Significance, p = 0.100, meaning there is only 90% probability that this particular interaction between variables of the cape seals can influence the outcome of fatigue ($N_{40\%}$). The regression model is therefore not statistically significant

- Significance of the Combination of Effective Thickness, Climate and Age on Fatigue ($N_{40\%}$) in Cape Seals:

Coefficient, R = 0.965, suggests that there is a strong positive relationship between the interaction between effective thickness, climate, age and the fatigue values. Furthermore the coefficient of determination, R^2 = 0.931, suggests that 93.1% of the variance in the fatigue values can be explained by this particular interaction between variables.

Significance, p = 0.101, meaning there is only 89.9% probability that this particular interaction between variables of the cape seals can influence the outcome of fatigue ($N_{40\%}$). The regression model is therefore not statistically significant.

- Significance of the Combination of Moment of Inertia, Climate and Age on Fatigue ($N_{40\%}$) in Cape Seals:

Coefficient, R = 0.966, suggests that there exists a strong positive relationship between the interaction between moment of inertia, climate, age and the fatigue values. The coefficient of determination, R^2 = 0.933, suggests that 93.3% of the variance in the fatigue values can be explained by this particular interaction between variables.

Significance, p = 0.099, meaning there is only 90.1% probability that this particular interaction between variables of the cape seals can influence the outcome of fatigue ($N_{40\%}$). The regression model is therefore not statistically significant.

- Significance of the Combination of Effective Thickness, Moment of Inertia and Age on Fatigue ($N_{40\%}$) in Cape Seals:

Coefficient, R = 0.965, suggests that a strong positive relationship exists between the interaction between effective thickness, moment of inertia, age and the fatigue values. The coefficient of determination, R^2 = 0.932, furthermore suggests that 93.2% of the variance in fatigue results for the cape seals can be attributed to this particular interaction between variables of the cape seals.

Significance, p = 0.018, meaning there is 98.2% probability that to this particular interaction between variables of the cape seals can influence the outcome of fatigue ($N_{40\%}$). The regression model is therefore statistically significant.

- Significance of the Combination of Effective Thickness, Moment of Inertia and Climate on Fatigue ($N_{40\%}$) in Cape Seals:

Coefficient, R = 0.965, suggests that a strong relationship exists between the interaction between effective thickness, moment of inertia, climate and the fatigue of cape seals. The coefficient of determination, R^2 = 0.931, furthermore suggests that 93.1% of the variance in the fatigue values can be attributed to this particular interaction between variables.

Significance, p = 0.102, meaning there is only 89.9% probability that to this particular interaction between variables of the cape seals can influence the outcome of fatigue ($N_{40\%}$). The regression model is therefore not statistically significant.